Miocene-Pliocene-Pleistocene paleoclimate and glacial history of the western Dry Valleys region, Antarctica

David R. Marchant

The University of Edinburgh
Department of Geography
Edinburgh, Scotland

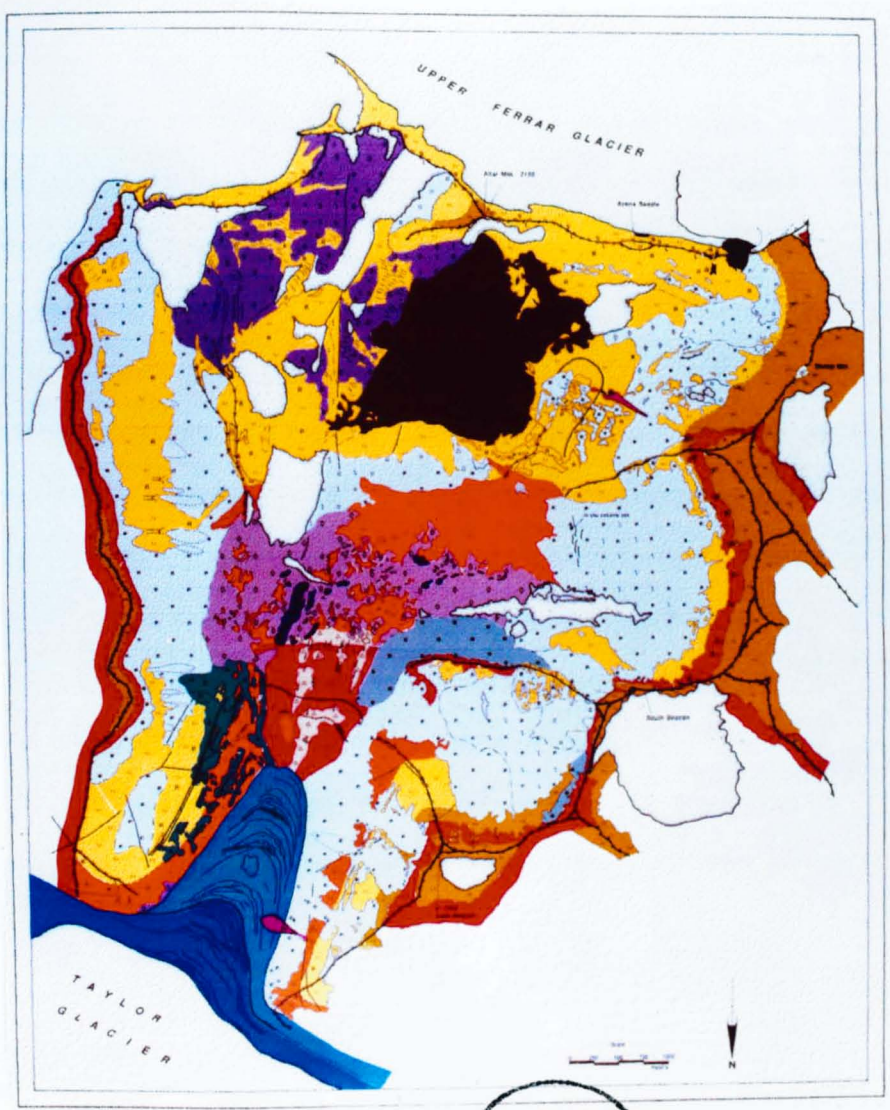

PAGE

NUMBERING

AS ORIGINAL


BEAUFORT
SPECIALLY PROTEC
Trespass or overflight
ternational agreement.
ZONE SPECIALEMEN
No. 5. Violation de la
interdit par accord inter
Allan Hills
Coombs Hills
Mt Brooke
Carapace Nunatak
Staten Island Heights
Mt Razorback
Alatna Val
Mount Morrison
Mount Woolnough
Mt Gran
Gateway Nunatak
Pegtop Mtn
Detour Nunatak
Mt Dearborn
Shapeless Mtn
Mt Fleming
Mt Thor
Depot Nunatak
Finger Mtn
Pyramid Mtn
Tabular Mtn
Mt Crean
Lashly Mts
Mt Feather
Flagship Mtn
Mount Whitcombe
Tiger
Lion I
Gregory I
Cape Archer
Point Retreat
Mt Marston
Discovery Bluff
The Flatiron
Mt Suess
Mt England
Cape Roberts
Cape Ross
Granite Harbor
Glacier
Wilson Piedmont Glacier
Victoria Lower Glacier
Victoria Valley
Wright Lower Glacier
Wright Valley
Wright Upper Glacier
Dunlop I
Spike Cape
Land aerodrome (no facilities)
Gneiss Pt
Marble Pt
Cape Bernacchi
Cape Bird
Adélie penguin rookeries
Romanes Beach
Wohlschlag Bay
MCMURDO SOUND
Cape Royds
Adélie penguin rookeries
SHACKLETON
Cape Evans
SCOTT
Dellbridge Islands
Butter Pt
NEW HARBOR
The Strand Moraines
Dailey Islands
MCMURDO STATION (US)
Cape Chocolate
Williams Pt
Garwood Val
Brania I
Brown Pen
Cape Hodgson
Black Island
Mt Aurora
Hahn I
Heald I
Miers Val
Mt Lister
Mt Rucker
Mt Huggins
Mt Kempe
Mount Dremedary
KEETELZ GLACIER
MOUNT DISCOVERY
Minna Saddle
Minna Bluff
Mason Spur
East Ice Piedmont
Mount Morning
Mt Tricouni
Mt Cocks
Clem Nunatak
Eastface Nunatak
Northcliffe Pk
Ant Hill
Mt Speyer
Shults Pen
Fishtail Pt
Cape Timberlake
Teall Island
Cape Teall
WORCESTER RANGE
MULOCK GLACIER
SKELTON NEVE
Boomerang Range
Warren Range
Escalade Pk
Swartz Nunataks
Mt Harmsworth
Mt Marvel
Mt Metschel
Angino Buttress
Stepaside Spur
Halfway Nunatak
The Spire
Rampart Ridge
The Portal
Portal Mtn
Pivot Pk
Ugolini Pk
Table Mtn
Knobhead
Cavendish Rocks
New Mtn
Cathedral Rocks
Bettle Pk
Taylor Valley
Taylor Hills
LAKE BONNEY HUT
Mt Barnes
Mt Coleman
Mt Odin
Mt Doorly
Mt Insel
Mt Aeolus
Mt Cerberus
King Pin
HUT (NZ)
MESERVE GLACIER CAMP (US)
Dais
Hut Pt
Northwest Mtn
Round Mtn
Finlay Hills
Apocalypse Peaks
Barwick Val
Balham Val
McKelvey Val
Insel Range
Willett Range
Claire Range
Mt Mahony
Skew Pk
Sponsors Pk
St Johns Range
Siaeffler Ridge
Conville and Caius Range
Olympus Range
Asgard Range
Prentice Glacier
Lashly Glacier
Crevasses
Airstrip
Icefalls
Beaufort
Cape Ross
Cape Roberts
Cape Bird
Cape Evans
Cape Royds
Cape Chocolate
Cape Hodgson
Cape Timberlake
Fishtail Pt
Cape Teall
Point Retreat
Butter Pt
Dellbridge Islands
Romanes Beach
Wohlschlag Bay
Minna Saddle
Minna Bluff
Mason Spur
Brania I
Brown Pen
Garwood Val
Miers Val
Heald I
Hahn I
Black Island
Mt Aurora
Dailey Islands
The Strand Moraines
Williams Pt
Marble Pt
Gneiss Pt
Land aerodrome (no facilities)
Dunlop I
Spike Cape
Adélie penguin rookeries
Romanes Beach
Wohlschlag Bay
Cape Royds
Adélie penguin rookeries
Dellbridge Islands
Butter Pt
Cape Evans
Cape Bernacchi
Cape Bird
Cape Ross
Cape Roberts
Point Retreat
Cape Archer
Gregory I
Lion I
Tiger
Mount Whitcombe
Mount Morrison
Mount Woolnough
Mt Gran
Mt Razorback
Staten Island Heights
Alatna Val
Coombs Hills
Mt Brooke
Carapace Nunatak
Allan Hills
Gateway Nunatak
Pegtop Mtn
Detour Nunatak
Mt Dearborn
Shapeless Mtn
Mt Fleming
Mt Thor
Depot Nunatak
Finger Mtn
Pyramid Mtn
Tabular Mtn
Mt Crean
Lashly Mts
Mt Feather
Flagship Mtn
Mt Suess
Mt England
The Flatiron
Discovery Bluff
Granite Harbor
Glacier
Wilson Piedmont Glacier
Victoria Lower Glacier
Victoria Valley
Wright Lower Glacier
Wright Valley
Wright Upper Glacier
Dunlop I
Spike Cape
Land aerodrome (no facilities)
Gneiss Pt
Marble Pt
Cape Bernacchi
Cape Bird
Adélie penguin rookeries
Romanes Beach
Wohlschlag Bay
MCMURDO SOUND
Cape Royds
Adélie penguin rookeries
SHACKLETON
Cape Evans
SCOTT
Dellbridge Islands
Butter Pt
NEW HARBOR
The Strand Moraines
Dailey Islands
MCMURDO STATION (US)
Cape Chocolate
Williams Pt
Garwood Val
Brania I
Brown Pen
Cape Hodgson
Black Island
Mt Aurora
Hahn I
Heald I
Miers Val
Mt Lister
Mt Rucker
Mt Huggins
Mt Kempe
Mount Dremedary
KEETELZ GLACIER
MOUNT DISCOVERY
Minna Saddle
Minna Bluff
Mason Spur
East Ice Piedmont
Mount Morning
Mt Tricouni
Mt Cocks
Clem Nunatak
Eastface Nunatak
Northcliffe Pk
Ant Hill
Mt Speyer
Shults Pen
Fishtail Pt
Cape Timberlake
Teall Island
Cape Teall
WORCESTER RANGE
MULOCK GLACIER
SKELTON NEVE
Boomerang Range
Warren Range
Escalade Pk
Swartz Nunataks
Mt Harmsworth
Mt Marvel
Mt Metschel
Angino Buttress
Stepaside Spur
Halfway Nunatak
The Spire
Rampart Ridge
The Portal
Portal Mtn
Pivot Pk
Ugolini Pk
Table Mtn
Knobhead
Cavendish Rocks
New Mtn
Cathedral Rocks
Bettle Pk
Taylor Valley
Taylor Hills
LAKE BONNEY HUT
Mt Barnes
Mt Coleman
Mt Odin
Mt Doorly
Mt Insel
Mt Aeolus
Mt Cerberus
King Pin
HUT (NZ)
MESERVE GLACIER CAMP (US)
Dais
Hut Pt
Northwest Mtn
Round Mtn
Finlay Hills
Apocalypse Peaks
Barwick Val
Balham Val
McKelvey Val
Insel Range
Willett Range
Claire Range
Mt Mahony
Skew Pk
Sponsors Pk
St Johns Range
Siaeffler Ridge
Conville and Caius Range
Olympus Range
Asgard Range
Prentice Glacier
Lashly Glacier
Crevasses
Airstrip
Icefalls
Victoria Land Traverse 1958-59 1959-60

UNIVERSITY OF EDINBURGH

ABSTRACT OF THESIS (Regulation 3.5.10)

Name of Candidate....David Roland Marchant.....

Address.....

Degree...PhD..... *Date...September 30, 1993*.....

Title of Thesis...Miocene-Pliocene-Pleistocene paleoclimate and glacial history of the western Dry Valleys region, Antarctica.....

No. of words in the main text of Thesis.....

A case is made for the stability of the polar East Antarctic Ice Sheet since middle-Miocene time from landscape development and surficial sediments in the western Dry Valleys region, southern Victoria Land. The alternate hypothesis that calls for repeated Miocene and Pliocene growth and decay of wet-based ice sheets across East Antarctica requires atmospheric temperatures 20°C above present values and late Pliocene ice-sheet overriding of the Transantarctic Mountains. The geomorphological and sedimentological results suggest that these conditions were not met in the western Dry Valleys. Rather, mean annual atmospheric temperatures during the last 13.6 Ma were at most only 3° to 5°C above present values; ice-sheet overriding occurred in middle Miocene time (> 13.6 Ma); and Pliocene glacier expansion was limited. These conclusions are based on field studies in the western Asgard Range and in the Quartermain Mountains. The chronology comes from $^{40}Ar/^{39}Ar$ laser fusion analyses on individual volcanic crystals and glass shards removed from in-situ volcanic ashes that occur in stratigraphic association with unconsolidated diamictons in the western Dry Valleys region. The combined geomorphological and sedimentological evidence indicates that slope evolution in the western Dry Valleys was severely restricted since at least the middle Miocene. The implication is that most of the landscape is relict and that it reflects ancient erosion under semi-arid climate conditions prior to middle-Miocene time.

PREFACE

This work was jointly funded by The University of Edinburgh and the University of Maine. It forms part of a large research effort, with Antarctic centers in both Edinburgh and Maine. The results given below represent my scientific contributions to these research groups during the last 8 years. Because the scope of this project is extremely large and involves a number of subdisciplines (geology, geomorphology, stratigraphy, glaciology, geochronology) several of the results presented here reflect the contributions of outside experts. However, I wrote the early drafts of each chapter and am fully responisble for all the implications for glacial history/ stratigraphy, volcanic ash stratigraphy, and paleoclimate history are based solely on my own work in the field. I accept full responsiblity for the conclusions given at the end of this manuscript and throughout the text. However, I would like to indentify the efforts of several individuals who made each chapter possible. Chapter Two: Dr. Carl Swisher completed 18 individual $^{40}Ar/^{39}Ar$ laser-fusion analyses on the Arena Valley Ash at the Berkeley Geochronology Center, Berkeley California. David P. West and Daniel R. Lux dated the Arena Valley Ash using standard K/Ar dating techniques at the University of Maine. In the latter case, I completed all the necessary labwork leading up to irradiation and mass spectroscopy. Chapters 3, 4, and 5: Dr. Carl Swisher dated the ash deposits using $^{40}Ar/^{39}Ar$ laser-fusion analyses. Chapter 6: Dr. James Bockhiem and Dr. Scott Wilson analyzed the geochemistry of the Taylor drifts and generated Tables 1, 3, and 4. Dr. Andrew Kerr assisted in modeling the Taylor Glacier and in the preperation of Figure 9. In all other cases, the laboratory analyses and field work were completed by the author.

ACKNOWLEDGMENTS

This work has been several years in the making and in the process I have received the support and encouragement of many whose help has been invaluable. I am deeply grateful to Professor David Sugden for the opportunity to conduct research in Edinburgh and in Maine and all the support, encouragement, and advice he has given me in the field and at home. My studies at Edinburgh benefitted greatly from discussions with Andrew Dugmore, Michael Summerfield, Andy Kerr, Mike Bentley, Nick Hulton, and Jane Boygle. Many thanks to Norma Henderson and Nicola Exly for helping me with photographs and drawings. I am deeply indebted to the members of the Institute for Quaternary Studies at the University of Maine for all the help they have given to me over the years. Marty Yates assisted tremendously with SEM and microprobe analyses of volcanic ashes. Terry Hughes provided invaluable insight on ice dynamics. Dan Belknap provided much needed space in his sediment laboratory. Lynn Tremblay and Nancy Keahiler have always provided kind words and encouragement throughout the years. I am also indebted to Carl Swisher, without whose volcanic ash dates this thesis would not have been possible.

I owe a special debt to all those who helped so untiringly in the field. In particular, I wish to thank Scott Wilson, Christopher Grallert, Charles Lagerbom, Mark Dubois, John Florek, Tom Fenn, Garth Hirsch, Steve Hinshaw, and Thom Wilch and the New Zealand surveyors, Pat Sole and Garth Falloon.

George Denton has assisted in so many ways that it is impossible to mention them all here. However, without his constant help and attention, none of this would have been possible. He has provided all of the logistic support to work in Antarctica, and for this I am very grateful. I am also grateful for the long discussions we have had over the years on Antarctic research. I feel extremely fortunate to have been able to work with Professor Sugden and Professor Denton in Antarctica.

I wish to thank my family and friends. It seemed that at times my home town of Wayland Massachusetts seemed farther away than Antarctica, Edinburgh, or Maine. But no matter where I was during the years of work that lead to this manuscript, I could always count on support and encouragement from my family, and it is to them that I dedicate this thesis. Finally, for her patience, kindness, and undying understanding I am most grateful to Rebecca.

Declaration of Originality

This is to declare that the undersigned is fully responsible for the material in this thesis and that it was written by him during the pursuit of a PhD from Edinburgh University.

David R. Marchant October 1993

TABLE OF CONTENTS

CHAPTER ONE: Introduction

The Problem

A basic problem of global change involves the response of the Antarctic Ice Sheet to warmer-than-present polar climate. This problem can be attacked by developing numerical models based on the dynamics of the present ice sheet. But insights can also come from examining the geological record of ice-sheet behaviour during past intervals of warmer-than-present climate. The most recent such intervals occurred during the Pliocene Epoch. A knowledge of ice-sheet response to excess Pliocene warmth is particularly relevant, because increasing atmospheric carbon dioxide is predicted to warm the planet to levels last experienced in the Pliocene. Depending on how different were Pliocene and present-day boundary conditions, this knowledge should afford a firm framework for understanding the Antarctic response to this carbon-dioxide-induced greenhouse warming.

Repeated intervals of warmer-than-present Pliocene climate occurred prior to 2.9 Ma ago, when large ice sheets were restricted to Antarctica. The last Pliocene warm interval occurred about 3.0 Ma ago, when high-latitude air and sea-surface temperatures in the Northern Hemisphere were elevated due to increased meridional oceanic heat transport (Dowsett et al., 1992). Evidence for Pliocene warmth during this and earlier intervals comes from numerous paleoclimatic indicators, including European flora (van der Hammen et al., 1971; Grube et al., 1986); the lack of significant ice-rafted detritus in North Atlantic Ocean cores (Ruddiman and Raymo, 1988); terrestrial plant fossils in the Arctic (Funder et al., 1985; Matthews, 1989); African pollen assemblages (Bonnefille, 1976, 1983), micromammals (Wesselman, 1985), and Bovids (Vrba, 1988a, 1988b); molluscs along the western margin of the North Atlantic (Stanley, 1985); diatoms, radiolaria, and silicoflagellates from the Pacific and Southern Oceans (Hays and Opydyke, 1967; Ciesielski and Weaver, 1974); Andean flora (Hooghiemstra, 1993); and some interpretations of the marine oxygen-isotope record (Shackleton, 1993; Prentice and Denton, 1988).

A major question of Pliocene ice-sheet dynamics is whether the huge terrestrial East Antarctic Ice Sheet ($14 \times 10^6 km^2$; $30 \times 10^6 km^3$; 60 m sea-level equivalent: Drewry, 1982, 1983) responded to Pliocene warmth by meltdown resulting in catastrophic deglaciation (Fig. 1). Until recently the prevailing view was of a persistent and robust polar ice sheet in East Antarctica since about 14 Ma ago (Kennett, 1982). The implication is of Pliocene ice-sheet stability; hence the origin of the **Pliocene stability hypothesis**. But a new concept that a dynamic temperate ice sheet persisted in East Antarctica until late Pliocene/ early Pleistocene time has now become the prevailing view of the evolution of polar ice sheets (Webb et al., 1984). The implication is of massive meltdown during Pliocene warm intervals (Barrett et al., 1992); hence the origin of the **Pliocene deglaciation hypothesis**. The overall problem involves not

only the evolution of polar ice sheets and Antarctic sensitivity to global warming, but also another fundamental question of Antarctic science - namely, the evolution of the Transantarctic Mountains. This is because critical terrestrial evidence (geomorphic, rock, and fossil) of past ice sheets can be interpreted only in the context of landscape development.

The Controversy

The Pliocene deglaciation hypothesis is dependent on the age and inferred origin of reworked marine diatoms in the Sirius Group, which crops out as semi-lithified glacigenic deposits along the crest of the Transantarctic Mountains (Mercer, 1968; Webb et al., 1984; Harwood, 1986). The Pliocene deglaciation hypothesis is anchored on the assumption that Sirius Group diatoms originated in marine basins in East Antarctica (now covered by as much as 4 km of glacier ice) during ice-sheet meltdown. The diatoms were subsequently stripped from the basins and transported to the Transantarctic Mountains during the buildup of the present-day East Antarctic Ice Sheet after 3.0 Ma (Barrett et al., 1992). Because Nothofagus fossil wood occurs within Sirius Group deposits now at 1800 m elevation near Beardmore Glacier at 85°S latitude, the ice sheet is inferred to have advanced into Transantarctic scrub vegetation (Webb et al., 1987; Webb and Harwood, 1987; McKelvey et al., 1987, 1991; Webb and Harwood, 1991; Carlquist, 1987; Hill et al., 1991). The postulated growth of Nothofagus implies late Pliocene/ early Pleistocene atmospheric warming up to 20°-25°C above present temperatures (Barrett, 1991, p. 46), a value also suggested for early Pliocene time (Webb and Harwood, 1991, p. 215). The diatom flora in the Sirius Group include species that today colonize relatively warm subantarctic seas (2°-5°C) (Harwood, 1986; Webb and Harwood, 1987). The critical species *Thalassiosira insigna* and *T. vulnifica* were initially assigned ages from early to late Pliocene from stratigraphic ranges in sub-Antarctic deep-sea cores (Harwood, 1986). Isotopic dating of a volcanic ash associated with these diatoms in the CIROS-2 core in the Ferrar Glacier trough has confirmed an age of about 3.0 Ma for these diatoms and thus affords a maximum age for the Sirius Group deposits and hence also for the Nothofagus fossil wood at Beardmore Glacier (Barrett et al., 1992). Another component of the deglaciation hypothesis is that late Pliocene overriding of the Transantarctic Mountains involved a relatively thin ice sheet because the Transantarctic Mountains are assumed to have been lower in Pliocene time than they are now (Webb and Harwood, 1987). Pliocene-Pleistocene mountain uplift of 1000-3000 m is inferred from faulting of Sirius Group deposits and from the current high elevation of Nothofagus fossil wood at Beardmore Glacier (Webb et al., 1986; Webb and Harwood, 1987), as well as from the "youthful-appearing" rift shoulder scarp along the mountain front (Behrendt and Cooper, 1991). Pliocene uplift of much less magnitude is inferred from benthic foraminifers in DVDP cores 10 and 11 in eastern Taylor Valley (Ishman and Rieck, 1992). Overall mountain uplift is credited with forcing late Pliocene climatic deterioration and thus transforming the Antarctic Ice Sheet from temperate to polar (Behrendt and Cooper, 1991).

Warm Antarctic environmental conditions are also inferred from early-to-mid-Pliocene benthic foraminifers in cores from DVDP sites 10 and 11 in eastern Taylor Valley (Ishman and Rieck, 1992); from early Pliocene diatoms and silicoflagellates in the subantarctic Southern Ocean (Ciesielski and Weaver, 1974; Abelman et al., 1990); and from microfossils in raised marine deposits in the Vestfold Hills (Pickard et al., 1988). Also, the Pagadroma tillite in the Prince Charles Mountains contains Pliocene fossils and may be a counterpart of the Sirius Group of the Transantarctic Mountains (McKelvey and Stevenson, 1990).

The postulated Pliocene collapse of the East Antarctic Ice Sheet has been used to explain a variety of diverse geologic phenomena. High sea levels (35 $\pm$ 18 m) of mid-Pliocene age (~3.0-3.5 Ma ago) on the Atlantic coastal plain (Orangeburg, Chippenham, and Thornburg Scarps) have been related to melting of the East Antarctic Ice Sheet (Krantz, 1991; Dowsett and Cronin, 1990). Wide oscillations of a dynamic East Antarctic Ice Sheet are used to explain fluctuations in the marine-oxygen isotope record and in biogenic productivity noted in some deep-sea cores (Krantz, 1991; Abelmann et al., 1990; Ishman and Rieck, 1992). A multi-disciplinary study (PRISM) designed to assess the Pliocene warm peak at 3.0 Ma ago (Cronin and Dowsett, 1991) has incorporated East Antarctic ice-sheet collapse into an emerging global reconstruction (Dowsett et al., 1992).

The contrasting Pliocene stability hypothesis of a robust polar East Antarctic Ice Sheet since middle Miocene time, with only modest fluctuations, is anchored on interpretations of the marine-oxygen isotope record, which shows a major sustained increase in $d0^{18}$ values at about 14.0 Ma ago attributed to ice buildup on Antarctica (Shackleton and Kennett, 1975; Savin et al., 1975; Kennett, 1982; Miller et al., 1987). Corollaries of this hypothesis are minimal Pliocene-Pleistocene uplift of the Transantarctic Mountains and persistent cold-desert climatic conditions through the Pliocene. The implications are that relatively modest global Pliocene warmth was not leveraged by up to 20°C in Antarctica to cause ice-sheet meltdown, that high Pliocene sea levels can not be ascribed to East Antarctic deglaciation, and that future collapse of the East Antarctic Ice Sheet is unlikely for greenhouse warming of the magnitude achieved in the Pliocene.

The Strategy

The purpose of this thesis is to test from geological data the conflicting hypotheses of Pliocene East Antarctic Ice Sheet stability. In this regard, I mapped the bedrock morphology and stratigraphy of surficial sediments in the western Dry Valleys region of the Transantarctic Mountains. The Dry Valleys region is the largest tract of ice-free terrain in the Transantarctic Mountains and lies adjacent to the East Antarctic Ice Sheet. It contains an extensive surficial glacial stratigraphy that extends back to at least middle Miocene time. It features an array of large-scale bedrock landforms that reflect landscape evolution and ice-sheet mountain overriding. Most important, the Dry Valleys are adjacent to numerous late Cenozoic volcanoes. Repeated eruptions have produced a suite of ashfall deposits that occur interbedded with Dry Valleys surficial sediments. These ashes are dated reliably using new

laser-fusion $^{40}Ar/^{39}Ar$ technology. The resulting absolute chronology of surficial stratigraphic units and of landscape evolution allows two fundamental tests of the divergent hypotheses of Pliocene ice-sheet dynamics. These tests form the core of this thesis. The first test is to determine if Pliocene marine diatoms in high-elevation Sirius Group outcrops in the western Dry Valleys region could indeed have been emplaced by the East Antarctic Ice Sheet, a requirement for the Pliocene deglaciation hypothesis. The second test is to determine if Pliocene climate in the Dry Valleys region remained polar, with mean annual temperatures well below 0°C (a requirement for polar ice-sheet stability), or whether atmospheric temperatures rose by as much as 20°C above present values (a requirement for ice-sheet meltdown).

The Organization

The thesis is arranged in five chapters. Each chapter forms a separate paper that has been accepted for publication in a refereed international journal (Boreas (1), Geografiska Annaler (2), Paleoclimatology, Paleoecology, Paleogeography (1), and Science (1)). Because chapters 2 through 6 represent free-standing papers, there is inevitably some repetition in each introduction. However, the main text of the various chapters is arranged first to describe the Miocene-to-Pleistocene paleoclimate of the Dry Valleys and then to give evidence for coeval East Antarctic ice sheet fluctuations. In this regard, Chapter 2 presents the paleoclimatic implications of an in-situ Pliocene ashfall deposit in Arena Valley of the Quartermain Mountains. This chapter specifically addresses the proposition that scrub Nothofagus colonized parts of the Transantarctic Mountains during Pliocene time (Webb and Harwood, 1987). Chapter 3 provides the evidence for a paleoclimate record for the Dry Valleys that extends back to at least 11.3 Ma ago. Chapters 4, 5, and 6 highlight the evidence for Miocene-to-Pleistocene fluctuations of the East Antarctic Ice Sheet as recorded in the Dry Valleys. These chapters are also arranged to give the stratigraphy of surficial sediments in chronological order. Chapter 4 presents the stratigraphy and sedimentology of Miocene-age surficial sediments in the western Asgard Range; Chapter 5 gives the Miocene, Pliocene, and Pleistocene stratigraphy of surficial deposits in Arena Valley; and Chapter 6 addresses implications for Quaternary dynamics of the East Antarctic Ice Sheet from an interpretation of the youngest glacial deposits in Arena Valley. Finally, Chapter 7 highlights the main conclusions that bear on the Pliocene stability/instability of the East Antarctic Ice Sheet.

REFERENCES

Abelmann, A., Gersonde, R. & Spiess, V. 1990: Pliocene-Pleistocene paleooceanography in the Weddell Sea-siliceous microfossil evidence. In *Geological History of the Polar Oceans: Arctic Versus Antarctic, (U. Bleil and J. Theide eds.)*, Kluwer Academic Publishers, 729-759.

Barrett, P.J. 1991. Antarctica and global climatic change: a geological perspective. In *Antarctica and Global Climatic Change (C. Harris and B. Stonehouse eds.)*: 35-50.

Barrett, P.J., Adams, C.J., McIntosh, W.C., Swisher III, C.C. & Wilson, G.S. 1992: Geochronological evidence supporting Antarctic deglaciation three million years ago. *Nature* 359: 816-818.

Behrendt, J.C. & Cooper, A.K. 1991: Evidence of rapid Cenozoic uplift of the shoulder escarpment of the Cenozoic West Antarctic Rift system and a speculation on possible climate forcing. *Geology* 19: 315-319.

Bonnefille R. 1976: Palynological evidence for an important change in the vegetation of the Omo Basin between 2.5 and 2.0 million years ago. In *"Earliest man and environments in the Lake Rudolph Basin." (Y. Coopens, F.C. Howell, G.L. Isaac and R.E.F. Leakey, eds.)*: 421-431. University of Chicago Press, Chicago.

Bonnefile, R. 1983. Evidence for a cooler and drier climate in Ethiopia uplands towards 2.5 Myr ago. *Nature* 303, 487-491.

Carlquist, S. 1987: Upper Pliocene-lower Pleistocene Nothofagus wood from the Transantarctic Mountains. *Aliso* 11: 571-583.

Ciesielski, P.F. & Weaver, F.M. 1974: Early Pliocene temperature changes in the Antarctic Seas. *Geology* 2: 511-15.

Cronin, T.M. & Dowsett, H.J. (eds.) 1991: Pliocene Climates. *Quaternary Science Reviews* 10(2/3).

Dowsett, H.J., Cronin, T.M., Poore, R.Z., Thompson, R.S., Whately, R.C. & Wood, A.M. 1992: Micropaleontological Evidence for Increased Meridional Heat Transport in the North Atlantic Ocean During the Pliocene. *Science* 258: 1133-35.

Dowsett, H.J. & Cronin, T.M. 1990: High eustatic sea level during the middle Pliocene: Evidence from the southeastern U.S. Atlantic Coastal Plain. *Geology* 18: 435-38.

Drewry, D.J., Jordan, S.R., & Jankowski, E. 1982: *Measured properties of the Antarctic Ice Sheet: surface configuration, ice thickness, volume, and bedrock characteristics. Annals of Glaciology* 3: 83-91.

Drewry, D.J. (ed.) 1983: *Antarctica: Glaciological and Geophysical Folio*. Scott Polar Research Institute, Cambridge.

Funder, S., Abrahamsen, N., Bennike, O. & Feyling-Hanssen, R.W. 1985: Forested Artic: Evidence from North Greenland. *Geology*, 13: 542-46.

Grube, F., Christensen, S. & Vollmer, T. 1986. Glaciations in Northwest Germany. *Quat. Sci. Rev.* 5: 347-358.

Harwood, D. M. 1986: Diatom biostratigraphy and paleoecology and a Cenozoic history of Antactic ice sheets. PhD dissertation, Ohio State University, Columbus Ohio.

Hays, J.D. & Opdyke, N.D. 1967: Antarctic radiolaria, magnetic reversal and climate change. *Science* 158, 1001-11.

Hill, R.S., Harwood, D.M. & Webb, P.N. 1991: Last remnant of Antarctica's Cenozoic flora: Pliocene Nothofagus of the Sirius Group, Transantarctic Mountains. In *Eig'ith Gondwana Subcommission Symposium*, Hobart, Australia. (Abstract).

Ishman, S.E. & Rieck, H.J. 1992: A Late Neogene Antarctic Glacio-eustatic Record, Victoria Land Basin Margin, Antarctica. In *The Antactic Paleoenvironment: A perspective on Global Change, Part One (J.P. Kennett and D.A. Warnke, eds.)*, Antarctic Research Series, A.G.U., Washington D.C.

Kennett, J.P. 1982: *Marine Geology*. Prentice-Hall, Englewood Cliffs, New Jersey.

Krantz, D.E. 1991: A chronology of Pliocene sea-level fluctuations: The U.S. Middle Atlantic coastal plain record. *Quaternary Science Reviews* 10: 163-174.

Matthews, J.V. 1989: Late Tertiary Arctic Environments: a Vision of the Future. *GEOS*, 18(3): 14-18.

McKelvey, B.C., Webb, P.N., Harwood, D.M. & Mabin, M.C.G. 1987: The Dominion Range Sirius Group: a late Pliocene-early Pleistocene record of the ancestral Beardmore Glacier. In *Fifth International Symposium on Antarctic Earth Sciences*. Cambridge. (Abstract 97).

McKelvey, B.C., Webb, P.N., Harwood, D.M. & Mabin, M.C.G. 1991. The Dominion Range Sirius Group: a record of the late Pliocene-early Pleistocene Beardmore Glacier. In *Geological Evolution of Antarctica* (M.R.A. Thomson, J.A. Crane and J.W. Thomson, eds.): 675-682. Cambridge University Press, Cambridge.

Mercer, J.H. 1968: Glacial geology of the Reedy Glacier area, Antarctica. *Geol. .Soc. of Amer. Bull.* 79: 471-86.

Miller, K.G., Fairbanks, R.G., & Mountain, G.S. 1987: Tertiary oxygen isotope synthesis, sea level history, and continental margin erosion. *Paleoceanography* 2 (1), 1-19.

Pickard, J., Adamson, D.A., Harwood, D.M., Miller, G.H., Quilty,P.G. & Dell, R.K. 1988: Early Pliocene marine sediments, coastline and climate of East Antarctica. *Geology* 16: 158-161.

Prentice, M.L. & Denton, G.H. 1988: The deep-sea oxygen isotope record, the global ice sheet system and hominid evolution. In *Evolutionary History of the Robust Australopithecines. (F. Grine, ed.)*, Aldine de Gruyter, New York: 383-403.

Savin, S.M., Douglas, R.G., & Stehli, F.G. 1975: Tertiary marine paleotemperatures. *Geol. Soc. Amer. Bull.* 86: 1499-1510.

Shackleton, N.J. & Kennett, J.P. 1975: Paleotemperature history of the Cainozoic and the initiation of Antarctic glaciation: oxygen and carbon analysis in DSDP sites 277, 279 and 281. In *Initial Reports of the Deep Sea Drilling Project (Kennett, J.P. and Houtz, R., eds.)* 29: 743-755.

Shackleton, N.J. 1993: New Data on the Evolution of Pliocene Climatic Variability (abs.). In *Conference on Palaeoclimate and Evolution with Emphasis on Human Origins*, Airlie Conference Center, Virginia (May 17- May 21, 1993).

Stanley, S.M. 1985: Climatic cooling and Plio-Pleistocene mass extinction of molluscs around the margins of the Atlantic. *South African Journal of Science* 81(5): 266.

Van der Hammen, T., Wijmstra, T.A. & Zagwijn, W.H. 1971: The floral record of the late Cenozoic of Europe. In *Late Cenozoic glacial ages (K.K. Turekian, ed.)*, Yale University Press: 391-424.

Vrba, E.S. 1988a: The environmental context of the evolution of early hominids and their culture. In *Bone modification (R. Bonnichsen and M.H. Sorg, eds.)*, Center for the Study of Early Man :27-42.

Vrba, E.S. 1988b: *Late Pliocene climatic events and hominid evolution. In Evolutionary history of the Robust Australopithecines (F. Grine, ed.)*, Aldine de Gruyter, NY: 383-403.

Webb, P.N., Harwood, D.M., McKelvey, B.C., Mercer, J.H. & Stott, L.D. 1984: Cenozoic marine sedimentation and ice-volume variation on the East Antarctic craton. *Geology* 12: 287-291.

Webb, P.N. & Harwood, D.M. 1987. Terrestrial flora of the Sirius Formation: Its significance for late Cenozoic glacial history. *Antarctic Journal of the United States 22(4): 7-11.*

Webb, P.N., McKelvey, B.C., Harwood, D.M., Mabin, M.C.G. and Mercer, J.H. 1987: Sirius Formation of the Beardmore Glacier region. *Antarctic Journal of the United States* 22(1): 8-13.

Webb, P.N. & Harwood, D.M. 1991: Late Cenozoic glacial history of the Ross Embayment, Antarctica. *Quat. Sci. Revs.* 10: 215-23.

Wesselman, H.B. 1985.: Fossil micromammals as indicators of climatic change about 2.4 Myr ago in the Omo Valley, Ethiopia. *South African Journal of Science* 81: 260-261.

CHAPTER TWO

Pliocene Paleoclimate and East Antarctic Ice Sheet history from surficial ash deposits

ABSTRACT

The preservation, age, and stratigraphic relation of an in-situ ashfall layer with an underlying desert pavement in Arena Valley, southern Victoria Land indicate that a cold-desert climate has persisted in Arena Valley since at least 4.3 Ma. Our climatic reconstruction indicates that the present East Antarctic Ice Sheet has endured for at least the last 4.3 Ma, and that the maximum potential Pliocene warming in Arena Valley was less than 3° C above present values. One implication is that collapse of the East Antarctic Ice Sheet due to "greenhouse" warming is unlikely, even if global atmospheric temperatures rise to levels last experienced during mid-Pliocene times.

INTRODUCTION

Two divergent hypotheses have been developed with regard to Pliocene paleoclimate and East Antarctic Ice Sheet dynamics. The first hypothesis, based on the ecology of warm-water marine diatoms and Nothofagus (Southern Beech) wood within Sirius Group glacial deposits in the Transantarctic Mountains, postulates that East Antarctic ice-sheet deglaciation occurred around 3.0 Ma (Webb et al., 1984; Webb and Harwood, 1987, 1991; Barrett et al., 1992). This hypothesis relies on two fundamental assumptions. The first is that reworked marine diatoms within the Sirius Group originated in ocean basins in the interior of East Antarctica and were subsequently transported into the forested Transantarctic Mountains by an expanded East Antarctic ice sheet. The second assumption is that the biostratigraphy of sub-Antarctic deep sea cores applies to far southern regions of interior Antarctica and hence can be used to apply confining ages to the Sirius Group. The latter assumption has apparently been confirmed by independent dating of volcanic ash in association with marine diatoms in the CIROS-2 core, southern Victoria Land (Barrett et al., 1992). In sharp contrast, the second hypothesis postulates that the East Antarctic Ice Sheet has been relatively stable under persistent cold-desert conditions since around 14 Ma (Shackelton and Kennet, 1975; Savin et al., 1975; Miller et al., 1987; Kennet, 1982). This latter hypothesis is based on interpretation of the marine-oxygen isotope record which shows little change around 3.0 Ma. To evaluate these contradictory hypotheses, we examined Pliocene surficial sediments in Arena Valley, southern Victoria Land, for physical evidence of either warmer-than-present climates, including traces of meltwater (rills, stream channels, mudflows, levees), or persistent cold-desert conditions similar to the present climate (desert pavements, ultraxerous soils, sand-wedges).

The Dry Valleys region of southern Victoria Land features about 4000 km^2 of predominantly ice-free, mountainous desert between the McMurdo Sound sector of the Ross Sea and the East Antarctic polar plateau (Fig. 1). Arena Valley, which lies at an average elevation of 1400 m in the Quartermain Mountains along the western margin of

the Dry Valleys region, is 70 km^2 in area and predominantly ice-free. A cold-based peripheral lobe of the upper Taylor Glacier extends 0.5 km into lower Arena Valley (Robinson, 1984). Mean annual temperatures in Arena Valley are about -30°C and precipitation is less than 45 mm water equivalent (Schwedtfegger, 1984; Bockheim, 1982; Keys, 1980). Under such climatic conditions ablation of Taylor Glacier at the valley mouth is entirely by sublimation (Robinson, 1984). Glacial drifts, hummocky moraines, talus cones, and colluvial deposits cover part of the floor and walls of Arena Valley. Conspicuously absent are geomorphic features indicative of liquid water, such as mudflows, levees, rills, lacustrine deposits, and stream channels, although they are common at elevations below about 800 m in the western Dry Valleys.

The Arena Valley Ash crops out on an extensive colluvial deposit with an average slope of 20°. The colluvium exhibits a well-developed ultraxerous soil profile and indurated salt pan suggesting persistent desert conditions (Bockheim, 1990). The Arena Valley Ash deposit is about 25 cm thick and covers a circular area with a radius of about 10 m. It rests on a well-developed in-situ desert pavement formed of an interlocking mosaic of gravel-sized ventifacts of Ferrar Dolerite, Beacon Supergroup sandstone, and orthoquartzite (Fig. 2). The ventifacts are commonly pitted and bear siliceous crusts and 5-10 mm thick quartz rinds, suggesting long-term subaerial exposure in a desert environment (Weed and Norton, 1991). A similar desert pavement now overlies the Arena Valley Ash and prevents erosion by wind deflation.

The Arena Valley Ash includes a lower basal unit and an upper ash-rich diamicton. The lower unit is structureless and consists of a thin layer (0.5 cm to 1.0 cm) of coarse-grained (0.5 mm to 1.0 mm), angular glass shards and volcanic crystals. The upper unit, approximately 20-25 cm thick, is composed of about 95% vesicular glass shards and volcanic crystals, 1-2% weathered quartz and dolerite sand-sized grains, and about 3% gravel-sized ventifacts of Beacon Supergroup sandstones and Ferrar Dolerite. Both units within the Arena Valley Ash contain less than 2.5% clay-sized grains. Glass shards are angular and unweathered and volcanic crystals lack evidence of chemical etching (Fig. 3). X-Ray microprobe analyses (MAC 400 Microprobe) indicate that the glass fraction (about 95% of the tephra by volume) is phonolitic. The crystal component includes anorthoclase, aegerine, sub-calcic augite, and magnetite. Mount Discovery, 110 km to the SE (Fig. 1), is largely phonolitic in composition (Kyle, 1990), and is the most likely source for the Arena Valley Ash.

The pure composition of the lower unit and the preservation of the underlying in-situ desert pavement indicate airfall deposition. The admixture of sand grains, ventifacts, and ash in the upper unit suggests penecontemporaneous slumping of adjacent oversteepened colluvial deposits on top of the airfall ash. The desert pavement overlying the Arena Valley Ash most probably formed by deflation of the upper ash-rich diamicton and the resulting concentration of enclosed ventifacts onto the ash surface.

The age of the Arena Valley Ash was determined both by $^{40}Ar/^{39}Ar$ dating of bulk anorthoclase separates and by laser-fusion $^{40}Ar/^{39}Ar$ dating of single anorthoclase crystals. Analyses of bulk anorthoclase separates yielded a slightly U-shaped spectrum with a plateau age of 4.69 $\pm$ 0.10 Ma (Fig. 4). Similarly, 18 separate $^{40}Ar/^{39}Ar$ dates on single crystals of anorthoclase yielded an average age of 4.34 $\pm$ 0.025 Ma (SEM) (Table 1). We attribute the slightly older age of the bulk separate date to differences in calibration between the two laboratories, rare contamination from older detrital feldspar, or excess argon as suggested by the U-shaped $^{40}Ar/^{39}Ar$ spectrum (McDougal and Harrison, 1988; Lo Bello et al., 1987).

The age and stratigraphic relation of the Arena Valley Ash with the underlying ventifact pavement indicate that a desert climate existed in Arena Valley at 4.3 Ma. We suggest that a cold desert (as opposed to a hot desert) prevailed in Arena Valley at 4.3 Ma and has persisted to the present time for two reasons. First, landscape analysis indicates that surficial sediments that are coeval and older than the Arena Valley ash (which includes most of the Arena Valley surficial stratigraphy) lack geomorphic evidence of liquid water. For example, there are no mudflow deposits, levees, rills, lacustrine deposits, or stream channels, although such features today are common elsewhere below an elevation of about 800 m in western Dry Valleys region. The mean annual air temperature at 800 m elevation is about -27°C (based on a recorded mean annual temperature of -19.8°C at about 100 m elevation at nearby Lake Vanda (Schwedtfegger, 1984), and an average lapse rate of 1°C/100 m elevation rise (Robin, 1988). In addition, advances of Taylor Glacier into lower Arena Valley during at least the last 2.1 Ma lack evidence of basal or surface melting even during periods of global interglaciations (Marchant et al., 1994; Brook et al., 1993). The preservation of the Arena Valley Ash and underlying in-situ ventifact pavement, together with the lack of geomorphic evidence for liquid water anywhere on the surface of unconsolidated sediments in Arena Valley, implies persistent cold desert conditions and strongly suggests that mean annual temperatures in Arena Valley failed to rise above about -27°C during at least the last 4.3 Ma. Second, the absence of clay-sized grains in the Arena Valley Ash is consistent with persistent cold-desert conditions since ash deposition. This is because the rate at which surficial ash deposits alter to clay minerals is largely a function of atmospheric temperature and/or the presence or absence of pore waters (with increased rates due to higher atmospheric temperatures and higher pore-water pressures (Lowe, 1986; Lowe and Nelson, 1983). For example, under humid temperate conditions in New Zealand, which are compatible with growth of Nothofagus, tephras older than about 50,000 yr have >60% clay (Birrel and Pullar, 1973; Lowe and Nelson, 1983; Lowe, 1986).

Pliocene deglaciation would almost certainly require extensive surface-melting ablation zones, analogous to the melting margins of terrestrial Northern Hemisphere ice sheets during the last termination (Denton and Hughes, 1981; Huybrechts, 1993). Such ablation zones would demand a dramatic rise of the 0°C isotherm, which now lies at an equivalent of 600 m below sea level in the vicinity of Arena Valley (Robin, 1988). A 2200 m rise in the 0°C isotherm, necessary to initiate a narrow band of surface melting up to 1600 m elevation near Arena Valley (Fig.

1), would require an atmospheric temperature rise of 11°C to 31°C over Antarctica, assuming lapse rates of 0.5°C and 1.4°C per 100 m elevation rise, respectively (Fortuin and Oerlemans, 1990). This estimate agrees with those of ice-sheet models which show that deglaciation of Antarctica requires an increase of mean annual surface temperatures by 17°C to 20°C above present values (Oerlemans, 1982; Huybrechts, 1993). Our estimate for maximum Pliocene warmth in Arena Valley since 4.3 Ma is about 3°C above present values. This is well below the minimum temperature rise necessary for either East Antarctic surface-melting ablation zones or ice-sheet collapse predicted by numerical models.

Postulated Nothofagus growth in the Transantarctic Mountains bears on the question of ice-sheet collapse. If verified, the growth of Nothofagus in the Transantarctic Mountains during Pliocene time would contribute strong evidence for East Antarctic deglaciation because today, north of the Antarctic Convergence, such trees occur in association with active glaciers possessing extensive surface-melting ablation zones. But Nothofagus, which today does not inhabit Antarctica, has strict ecological requirements. Nothofagus cannot survive mean annual temperatures below 5°C or minimum temperatures below -19° C for even a few hours (Sakai, 1981). In view of the paleoclimatic inferences associated with the Arena Valley Ash, we argue that Nothofagus was eliminated from the Transantarctic Mountains before 4.3 Ma. Nothofagus cannot migrate long distances across salt-water and its seeds are not aerodynamic (Sakai, 1981). As such, Nothofagus could not re-colonize Antarctica after 4.3 Ma, even if atmospheric temperatures in the Transantarctic Mountains had warmed since 4.3 Ma. We conclude that postulated Nothofagus growth subsequent to 4.3 Ma in the Transantarctic Mountains is incorrect and cannot be used to support the warming necessary for surface-melting ablation zones required for ice-sheet collapse.

The geomorphological evidence presented here argues strongly for continuous cold and dry climatic conditions in Arena Valley for at least the last 4.3 Ma. Such a view agrees with interpretations of the oceanic record (Shackelton and Kennet, 1975; Savin et al., 1975) and points to the stability of the East Antarctic ice sheet under climatic warming of a few degrees. It is difficult at present to reconcile this conclusion with the hypothesis of Pliocene ice-sheet deglaciation (Webb et al., 1984; Webb and Harwood, 1991; Barrett et al., 1992). Perhaps it is possible that the Sirius Group antedates 3.0 Ma and that its enclosed diatoms have been emplaced by some mechanism other than glacier ice (Sugden, 1992).

REFERENCES

Barrett, P.J., Adams, C.J., McIntosh, W.C., Swisher III, C.C. and Wilson, G.S. 1992. Geochronological evidence supporting Antarctic deglaciation three million years ago. Nature 359, 816-818.

Birrell, K.S. and Pullar, W.A. 1973. Weathering of paleosols in Holocene and late Pleistocene tephras in central North Island, New Zealand. New Zealand Jour. of Geol. and Geophys. 16, 687-702.

Bockheim, J.G. 1982. Properties of a chronosequence of ultraxerous soils in the Trans-Antarctic Mountains. Geoderma, 28, pp. 239-255.

Bockheim, J.G. 1990. Soil development rates in the Transantarctic Mountains. Geoderma, 47, p.59-77.

Brook, E.J., Kurz, M.D., Ackert, R.P. Jr, Denton. G.H., Brown, E.T., Raisbeck G.M., Yiou, F. 1993. Chronology of Taylor Glacier advances in Arena Valley, Antarctica, using in-situ cosmogenic ^{3}He and ^{10}Be. Quaternary Research 39, 11-23.

Cebula, G.T., Kunk, M.J., Mehnert, H.H., Naeser, C.W., Obradovich, J.O., and Sutter, J.F. 1986. Terra Cognita 6(2), 139-146.

Dalrymple, G.B. 1979. Geology 7, 558.

Denton, G.H, and Hughes, T.J. 1981. The last Great Ice Sheets. Wiley Interscience, New York.

Fortuin, J.P.F. and Oerlemans, J. 1990. Parameterization of the annual surface temperature and mass balance of Antarctica. Ann. of Glac. 14, 78-84.

Huybrechts, Ph. 1993. Glaciological and climatological aspects of a stabilist versus dynamic view of the late Cenozoic glacial history of East Antarctica. Geographiska Annaler in press.

Kennett, J.P. 1982. Marine Geology Prentice-Hall, Englewood Cliffs, New Jersey.

Keys, J.R. 1980. Air temperature, wind, precipitation and atmospheric humidity in the McMurdo region. Antarctic Data Series. no. 9, Victoria University of Wellington, No. 17.

Kyle, P.R. 1990. McMurdo Volcanic Group - western Ross Embayment. In Volcanoes of the Antarctic Plate and southern oceans. American Geophysical Union, Washington, DC. pp 19-134.

Lo Bello, Ph. et al. 1987. Chemical Geology 66, 61-81.

Lowe, D.J. 1986. Controls on the rates of weathering and clay mineral genesis in airfall tephras: a review and New Zealand case study. In S.M. Colman and D.P. Dethier Eds., Rates of chemical weathering of rocks and minerals. Academic Press, Inc., New York. pp 265-330.

Lowe, D.J., and Nelson, C.S. 1983. Occas. Rep. 11. Department of Earth Scicences, University of Waikato, Hamilton, New Zealand.

Marchant, D.R., Denton, G.H., Bockheim, J.G., Wilson, S.C. and Kerr, A.R. 1994. Quaternary ice-level changes of upper Taylor Glacier, Antarctica: Implications for paleoclimate and ice-sheet dynamics. Boreas, in press.

McDougall and Harrison. Geochronology and Thermochronology by the $^{40}Ar/^{39}Ar$ Method. Oxford Univ. Press New York, 212 p. (1988).

Miller, K.G., Fairbanks, R.G., and Mountain, G.S. 1987. Tertiary oxygen isotope synthesis, sea level history, and continental margin erosion. Paleoceanography 2 (1), 1-19.

Oerlemans, J. 1982. A model of the Antarctic Ice Sheet. Nature 297, 550-553.

Robin, G. de Q. 1988. The Antarctic ice sheet, its history and response to sea level and climatic changes over the past 100 million years. Paleogeography, Paleoclimatology, Paleoecology 67, 31-50.

Robinson, P.H. 1984. Ice dynamics and thermal regime of Taylor Glacier, south Victoria Land, Antarctica. Jour. of Glaciology 30, 153-160.

Sakai, A. 1981. Freezing resistance of trees of the south temperate zone, especially subalpine species of Australia. Ecological Society of America 62, 563-570.

Samson, S.D., and Alexander, E.C. 1987. Chem. Geol. Isot. Geosci. 66, 27.

Savin, S.M., Douglas, R.G., and Stehli, F.G. 1975. Tertiary marine paleotemperratures. Geol. Soc. Amer. Bull. 86, 1499

Schwerdtfeger, W. 1984. Weather and climate of the Antarctic. In Developments in Atmospheric Science 15. Elsevier Publishing Company, Amsterdam.

Shackleton, N.J. and Kennet, J.P. 1975. Paleotemperature history of the Cainozoic and the initiation of Antarctic glaciation: oxygen and carbon analysis in DSDP sites 277, 279 and 281. In Kennet< J.P. and Houtz, R. (eds.), Initial Reports of the Deep Sea Drilling Project, 29, 743-755.

Steiger, R.H., and Jager E. 1977. EPSL 36, 359.

Sugden, D.E. 1992. Antarctic ice sheets at risk? Nature 359, 776-777.

Webb, P.N., Harwood, D.M., McKelvey, B.C., Mercer, J.H. and Stott, L.D. 1984. Cenozoic marine sedimentation and ice-volume variation on the East Antarctic craton. Geology 12, 287-291.

Webb, P.N. and Harwood, D.M. 1987. Terrestrial flora of the Sirius Formation: Its significance for late Cenozoic glacial history. Antarctic Journal of the U.S. 22(4), 7-11.

Webb, P.N. and Harwood, D.M. 1991. Late Cenozoic glacial history of the Ross Embayment, Antarctica. Quaternary Science Reviews 10, 215-223.

Weed, R., and Norton, S.A. 1991. Sileceous crusts, quartz rinds and biotic weathering of sandstones in the cold desert of Antarctica. In Proceedings of the International Symposium on Environmental Biogeochemistry, pp. 327-339. Elsevier Publishers.

FIGURE CAPTIONS

FIG. 1. Location map of Arena Valley, southern Victoria Land, Antarctica. Hatch marks represent the areal extent of surface-melting ablation zones in East Antarctica that we calculate would occur with a 22°C rise in atmospheric temperature over Antarctica. We suggest that Pliocene deglaciation of the East Antarctic Ice Sheet from elevated atmospheric temperatures would require a rise of the 0° isotherm to at least 1600 m elevation (hatch marks on map), or about 200 m elevation above the Arena Valley Ash deposit. We note that outside Antarctica, sediments that lie at or near the 0°C isotherm show a dynamic surficial stratigraphy. The preservation of in-situ Pliocene-age Arena Valley surficial deposits (including the Arena Valley Ash and underlying ventifact pavement), unmarked by erosion from liquid water, strongly suggests that the 0° isotherm never advanced up to 1600 m in Arena Valley during late Pliocene time (see discussion below).

FIG. 2. Photograph of the surficial volcanic ash deposit in west central Arena Valley. The vertical face of the Arena Valley Ash has been cut back to expose the underlying buried desert pavement. A weathered, relict colluvial deposit (devoid of volcanic material) underlies the ash.

FIG. 3. Scanning electron microscope images of glass shards and anorthoclase crystals from the Arena Valley Ash. Plates (a), (b), and (c) show unweathered anorthoclase crystals at about 100, 200, and 700 magnification, respectively. Plates (d), (e), and (f) show part of the vitric component of the ash at about 100, 150, and 700 magnification. Glass shards removed from the middle unit of the Arena Valley ash show evidence of slight wind abrasion. Note the absence of etched crystals and authigenic minerals within the Pliocene-age, surficial Arena Valley Ash deposit.

FIG. 4. Conventional $^{40}Ar/^{39}Ar$ release spectrum diagram from a bulk sample of anorthoclase separated from the Arena Valley Ash. The minimum age represents the mean of the 5 lowest age increments (which comprise 25 % of the total ^{39}Ar released). The total gas age is a weighted average of all the increments based on the amount of ^{39}Ar in each increment. The saddle-shaped release spectrum suggests excess argon and/or xenocrystic contamination (McDougall and Harrison, 1988; Lo Bello et al., 1987). The incremental-heating experiment was carried out at the Department of Geological Sciences, University of Maine, laboratory on a Nuclide 6-60-SGA 1.25 mass spectrometer. The anorthoclase was irradiated at the Phoenix Reactor, University of Michigan, using FCT-3 biotite with an age of 27.68 as a monitor mineral. Anorthoclase crystals were removed from the Arena Valley Ash using standard magnetic density mineral separation techniques. Approximately 100 grams of the ash yielded about 0.1 gram of feldspar.

TABLE 1. Laser total fusion $^{40}Ar/^{39}Ar$ analyses of individual anorthoclase crystals from the Arena Valley Ash, carried out by the Institute of Human Origins Geochronology Center. Pristine euhedral crystals of anorthoclase were hand-picked from the Arena Valley Ash using a binocular microscope, treated with 7% hydrofluoric acid in an ultrasonic cleaner for 5 minutes to remove any altered clays and/or attached glass, followed by 10 minutes in distilled water, and then irradiated in the hydraulic rabbit core of the Omega West research reactor at Los Alamos National Laboratory for four hours. The calculated mean age of 4.343 $\pm$ 0.108 Ma (SD, one standard deviation), $\pm$ 0.025 Ma (SEM, standard error of the mean) is based on 18 separate single - crystal analyses measured on a Mass Analyzer Product 215 noble-gas mass spectrometer, calibrated with monitor minerals Fish Canyon Sanidine and MMhb-I, with published ages of 27.84 Ma (modified from Cebula et al. 1986) and 520.4 Ma (31), respectively. Decay constants are those recommended by Steiger and Jager (1977) and Dalrymple (1979); Ca and K corrections used in this study as determined from laboratory salts are: (36/37)Ca= $2.557 \times 10^{-4} \pm 4.6 \times 10^{-6}$, (39/37)Ca = $6.608 \times 10^{-4} \pm 2.53 \times 10^{-5}$ and (40/39)K = $2.4 \times 10^{-3} \pm 7.0 \times 10^{-4}$.

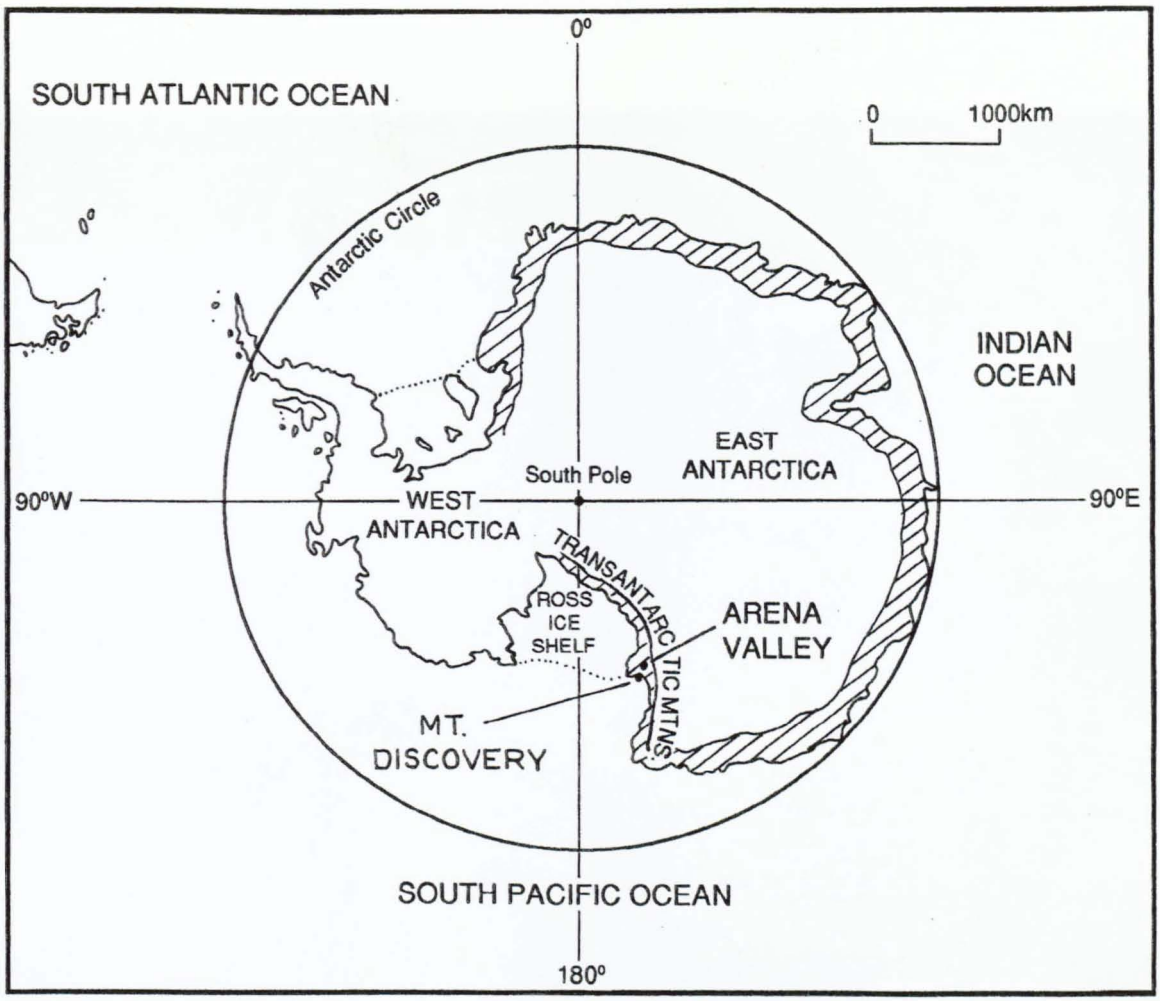

Figure 1

Figure 2

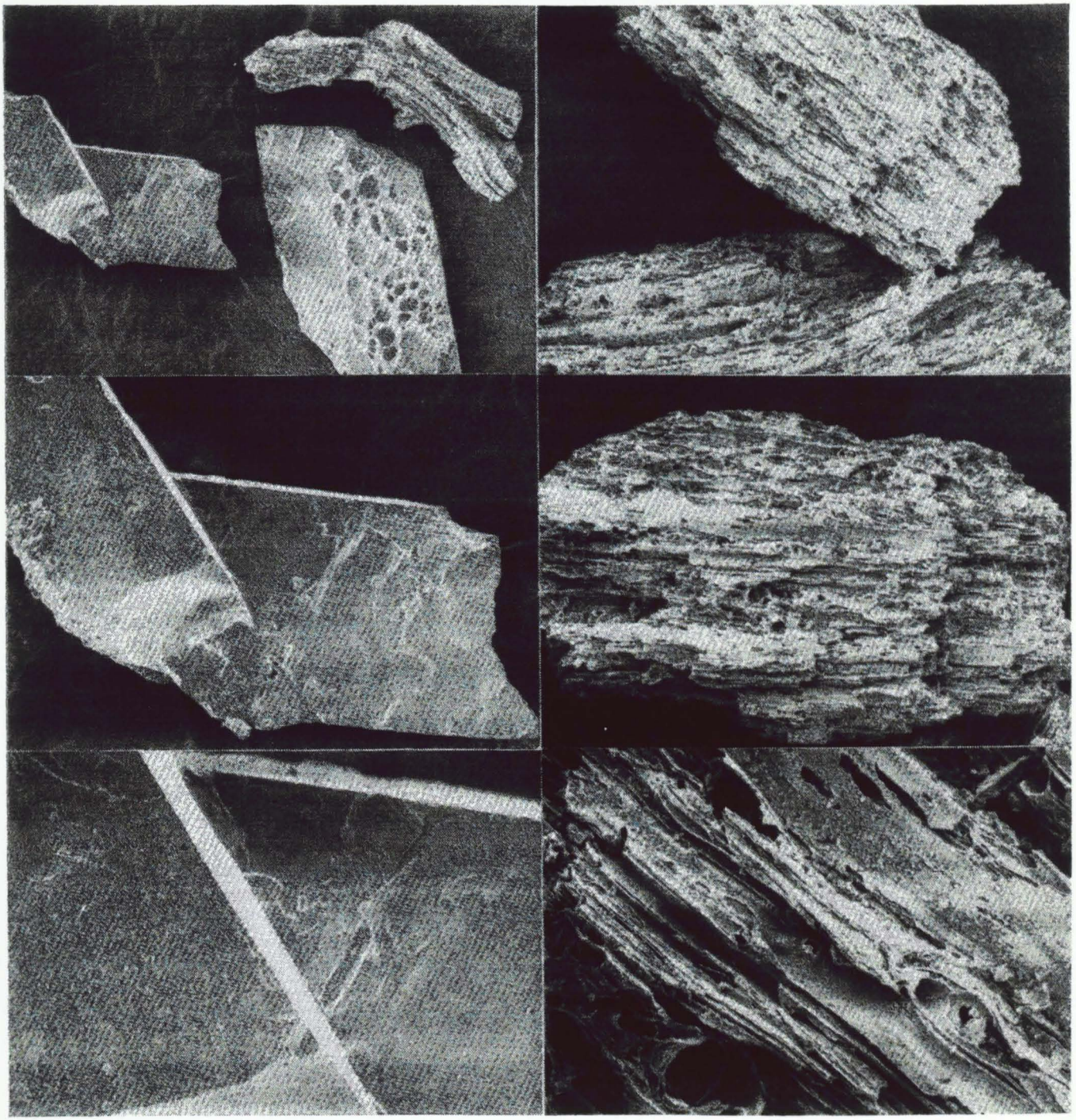

Figure 3

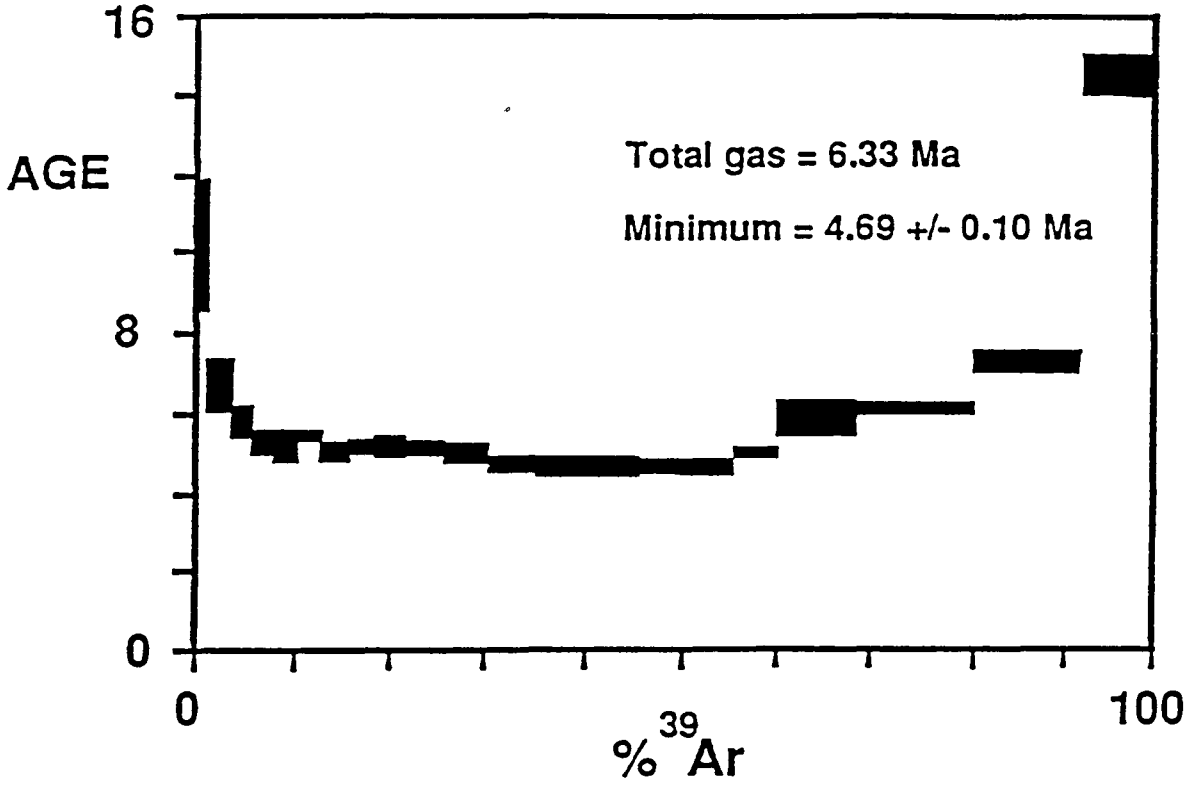

Figure 4

Table 1. $^{40}Ar/^{39}Ar$ laser total fusion analyses of selected anorthoclase from the Arena Valley Ash

L#	$^{37}Ar/^{39}Ar$	$^{36}Ar/^{39}Ar$	$^{40}Ar^*/^{39}Ar$	$\%^{40}Ar^*$	Age (Ma)	± 1σ	± SEM
5075-01	0.03024	0.000228	0.81768	92.4	4.191	0.203	
5075-02	0.03814	0.000202	0.82572	93.3	4.232	0.237	
5075-03	0.04851	0.000014	0.86715	99.7	4.444	0.250	
5075-04	0.01887	0.000325	0.82006	89.4	4.203	0.239	
5075-05	0.02662	0.000519	0.82769	84.3	4.242	0.278	
5075-06	0.03051	0.000187	0.88239	94.1	4.522	0.554	
5075-07	0.02588	0.000054	0.86973	98.2	4.457	0.422	
5075-08	0.02000	0.000151	0.85239	94.9	4.368	0.283	
5075-09	0.03349	0.000274	0.82778	91.1	4.242	0.418	
5075-10	0.03700	0.000314	0.83205	90.0	4.264	0.528	
5075-11	0.03884	0.000126	0.86479	96.0	4.432	0.271	
5075-12	0.03493	0.000233	0.84062	92.5	4.308	0.293	
5075-13	0.04068	0.000183	0.85403	94.1	4.377	0.334	
5075-14	0.02144	0.000206	0.82717	93.1	4.239	0.495	
5075-15	0.04436	0.000025	0.88435	99.3	4.532	0.366	
5075-16	0.03135	0.000090	0.85779	97.0	4.396	0.169	
5075-17	0.03072	0.000082	0.85375	97.2	4.375	0.359	
5075-18	0.01180	0.000247	0.84824	91.9	4.347	0.409	
			Mean of 18 analyses	=	4.343	0.108	0.025

* = radiogenic

$\lambda\varepsilon + \lambda\varepsilon' = 0.581 \times 10^{-10} yr^{-1}$; $\lambda\beta = 4.962 \times 10^{-10} yr^{-1}$; $^{40}K/^{40}K_{total} = 1.167 \times 10^{-4}$

CHAPTER THREE

Late Cenozoic Antarctic paleoclimate reconstructed from volcanic ashes in the Dry Valleys region, south Victoria Land

ABSTRACT

We report here laser-fusion $^{40}Ar/^{39}Ar$ dates of volcanic ashes from the Dry Valleys sector of the Transantarctic Mountains that range from 4.3 to 15.0 Ma in age. The Arena Valley ash (4.343±0.108 Ma) rests in situ on the surface of a well-developed desert pavement and ultraxerous soil profile at 1410 m elevation; lack of geomorphic evidence of liquid water on surficial sediments coeval and older than the Arena Valley ash, together with the pristine condition of volcanic crystals, indicate a cold desert at and since 4.3 Ma ago. The Beacon Valley Ash (10.4 Ma), the Koenig Valley Ash (13.648±0.060), and the Nibelungen Valley Ash (15.014±0.024) fill the upper half of relict sand wedge troughs formed in cold desert conditions. The absence of numerous authigenic clay-sized minerals in these ash deposits, along with preservation of sharp lateral contacts with surrounding sand-and-gravel deposits, suggest that frozen conditions have persisted in Beacon, Koenig, and Nibelungen Valleys since ash deposition. Ash avalanche deposits that rests on rectilinear slopes contain matrix ash dated to 7.422±0.037 Ma ago in upper Arena Valley and 11.28±0.05 Ma ago in lower Arena Valley. Little slope development has occurred since emplacement of these ash avalanche deposits; such slope stability is consistent with cold-desert conditions. Taken together, these ash deposits point to persistent cold-desert conditions since at least 15.0 Ma ago at elevations above 1400 m in the western Dry Valleys region. This is not compatible with the development of the widespread surface melting zones necessary for East Antarctic ice sheet deglaciation during Pliocene time.

INTRODUCTION

There are two widely divergent hypotheses concerning late Tertiary paleoclimate and coeval East Antarctic Ice Sheet dynamics. The first hypothesis, based on the ecology of warm-water marine diatoms and Nothofagus (Southern Beech) wood within glacial deposits (Sirius Group) in the Transantarctic Mountains, postulates atmospheric temperatures 15-20°C above present values, with extensive East Antarctic ice-sheet deglaciation as recently as 3.0 Ma (Webb et al., 1984, 1986; Harwood, 1985; Webb and Harwood, 1991; Barrett et al., 1992). The second hypothesis, based predominantly on interpretations of the marine-oxygen isotope record, postulates an enduring East Antarctic Ice Sheet since around 14 Ma (Shackelton and Kennett, 1975; Savin et al., 1975; Miller et al., 1987; Robin, 1988).

Surficial sediments in the Dry Valleys region of southern Victoria Land bear directly on these hypotheses. Dry Valleys sediments reveal one of the most extensive and well-preserved late Cenozoic sedimentary records in Antarctica. Until now this record has remained largely untapped, mostly because it has lacked an absolute

chronology. We report here the discovery of numerous in-situ to near in-situ volcanic ash deposits that appear to provide an internally consistent absolute glacial chronology for the Dry Valleys region. Laser-fusion $^{40}Ar/^{39}Ar$ dates of Dry Valleys ashes interbedded with glacial and non-glacial deposits record a history of surficial sedimentation that, in places, extends back into middle Miocene time. Such a record reveals the timing of Antarctic Ice Sheet fluctuations, along with inferred coeval paleoclimates, and permits comparison of such records with Tertiary sea-level curves and marine oxygen-isotope records (Miller et al., 1987; Prentice and Mathews, 1989; Kennett, 1985; Krantz, 1991).

Our preliminary results favor an enduring East Antarctic Ice Sheet since at least late Miocene time. We find no evidence for warmer-than-present air temperatures leading to mid-Pliocene ice-sheet collapse, or late Pliocene temperate-glacial overriding of the Dry Valleys region. Instead, cold-desert conditions (with mean annual temperatures well below 0°C) have persisted in the Dry Valleys region (at least at elevations above 1100 m) for the last 15.0 Ma and much of the Dry Valleys bedrock morphology is relict and predates late Miocene time (see also Sugden et al., 1994; Denton et al., 1993).

PHYSICAL SETTING

THE TOPOGRAPHY

The Dry Valleys of southern Victoria Land occur along the margin of a major crustal suture that separates the Transantarctic Mountains from down-faulted rift basins in the Ross Sea (Fitzgerald et al., 1986). Cenozoic volcanism, associated in part with active crustal thinning and extension along rift margins (Kyle, 1990), occurs in and adjacent to the Dry Valleys region.

The Dry Valleys region includes about 4000 km^2 of predominantly ice-free mountainous desert topography between the McMurdo Sound sector of the Ross Sea and the East Antarctic polar plateau (Fig. 1). Volcanic landforms within this region range from isolated basaltic cinder cones (McCraw, 1962; Kyle, 1990; Wilch, 1991) to large stratovolcanoes nearly 3800 m in elevation along the southeastern border of the Dry Valleys region. Such volcanic centers comprise part of the McMurdo Volcanic Group (see below) (Kyle, 1990).

Major east-west trending troughs (formerly occupied by expanded East Antarctic outlet glaciers) transect the Dry Valleys region and separate intervening sandstone mountain blocks. The Quartermain Mountains, the Asgard Range, and the Olympus Range are three such mountain blocks. In the western Dry Valleys these mountain blocks reach 2400-2600 m elevation and prevent overflow of inland ice into the Dry Valleys region. Isolated névés along mountain divides feed small alpine glaciers that descend along the flanks of Taylor, Wright, and Victoria Valley troughs. Large piedmont glaciers, fed by local precipitation, occupy the mouths of Wright and Victoria Valleys.

THE CLIMATE

The Dry Valleys feature a cold-desert climate. Mean annual temperature and precipitation (recorded at about 100 m elevation near Lake Vanda in central Wright Valley) approaches -20°C and 80 mm water equivalent, respectively (Schwerdtfeger, 1984). Assuming a lapse rate of 1°C per 100 m elevation rise (Robin, 1988) the mean annual temperature within the Asgard Range, Olympus Range, and Quartermain Mountains approaches -30°C to -35°C. High-velocity katabatic winds drain across intervalley mountain blocks and are channeled through deep valley troughs towards the Ross Sea. Under such climatic conditions, sublimation is the dominant form of ablation (Chinn, 1980), although some melting (<10% of ablation) occurs in places below about 1200-1400 m elevation. The evidence for surface melt in the Dry Valleys region is based on direct observation and on landscape analyses of geomorphological features indicative of liquid water. For example, rills, mudflows, levees, stream channels, and lacustrine sediments form only where meltwater is present. Such features are common up to 800 m elevation in the extreme western Dry Valleys region (Quartermain Mountains) and up to 1200-1400 m elevation nearer to the coast (eastern and central Asgard Range). This apparent rise in elevation may reflect the combined effects of reduced katabatic winds, which are more persistent in the western Dry Valleys, and enhanced maritime climates towards the coast.

THE GLACIERS

The polar glaciers in the Dry Valleys of southern Victoria Land are cold and predominantly dry based (Chinn, 1980). They contrast with temperate glaciers of mid-latitude regions, which are composed of ice at (or just below) 0°C (Sugden and John, 1976). This thermal contrast is manifested in (1) the character of glacial deposits, and in (2) the areal distribution and mechanism of ice accumulation and ablation on temperate and polar glaciers. For example, temperate glaciers show distinct accumulation and ablation zones, providing well-defined equilibrium line altitudes (ELA's) that can be plotted for glaciological study (Paterson, 1981; Sugden and John, 1976) and that can be reconstructed for late Quaternary glaciers (Porter, 1975). In most cases, the ELA on temperate glaciers corresponds to the geographic distribution of the 0° isotherm (Robin, 1988). Temperate glaciers also possess extensive surface-melting ablation zones, with meltwater run-off concentrated in supra- and englacial channels. Such ablation zones are commonly covered with thick supraglacial debris and are associated with ice-contact heads, kame terraces, eskers, and stratified outwash trains (Brodzikowski and van Loon, 1991). Temperate glaciers (in mass balance equilibrium) also require high precipitation rates in the accumulation area to compensate for excess surface melting in the ablation zone (Nye, 1960).

In sharp contrast, the polar glaciers of the Dry Valleys region lack well-defined accumulation zones, show little to no surface melting, and are nowhere associated with widespread outwash sediments. Dry Valleys glaciers are strikingly free of surficial and basal debris and are nearly everywhere frozen to their bed. The geographic distribution of their accumulation and ablation zones is governed solely by local wind patterns and the resulting

concentration of transient snow drifts in topographically favored areas and sporadic blue-ice sublimation patches in windswept zones (Chinn, 1980). This is very different from the situation on temperate glaciers where excess precipitation and extensive surface-melting zones control glacier accumulation and ablation. Hence, polar glaciers lack well defined equilibrium lines and, if present, such lines reflect only local wind patterns. They are not related to the position of the 0°C isotherm. In fact, the Taylor Glacier equilibrium line, as defined by the irregular geographic boundary between dry snow and blue ice on the glacier surface (Muller, 1962; Robinson, 1984), lies at about 2000 m elevation, 2600 m above the 0°C isotherm, where mean annual temperatures approach -35°C (Fig. 1).

SURFICIAL DEPOSITS OF THE DRY VALLEYS

Widespread glacial drifts, hummocky moraines, talus cones, and thin colluvial sheets cover most of the ice-free valley floors and walls of the Dry Valleys region. Such deposits record fluctuations of local alpine glaciers (Nichols, 1966, 1971; Bull, 1962; Calkin and Bull, 1972; Denton et al., 1971, 1989), East Antarctic outlet glaciers (Hendy et al., 1979; Denton et al., 1989; Wilch, 1991; Ackert, 1990; Marchant et al., 1993a, 1993b, 1993c, 1994) grounded ice in the Ross Sea (Nichols, 1961; Denton et al., 1989), and ice-free periods (Marchant et al., 1993a, 1993b). Most of these deposits feature ventifact pavements (Weed and Norton, 1991), ultraxerous to subxerous soil profiles (Campbell and Claridge, 1969; Bockheim, 1982; Marchant et al., 1993b), extensive polygonal ground (Berg and Black, 1966), and in places, small saline ponds with local evaporite deposits (Calkin and Nichols, 1972; Nichols, 1966).

VOLCANIC ASHES IN THE DRY VALLEYS

DEPOSITIONAL SETTINGS

At least 50 different ash sites (possibly representing 50 different volcanic ashes) occur within Dry Valleys surficial sediments. Ten are described here. These ashes are preserved only when volcanic ashfall is buried rapidly or incorporated into glacial ice. Otherwise, high-velocity katabatic winds would quickly disperse unprotected surficial ash deposits that rest on exposed surfaces. Given these constraints, it is unlikely that continuous ash layers occur within Dry Valleys sediments, although such layers exist in local névés (Keys et al., 1977) and within the East Antarctic Ice Sheet (see below). Rather, Dry Valleys ashes occur either as individual glass shards disseminated in fine-grained sediments or as lenses, pods, and wedges of concentrated ash in at least five characteristic settings. Ashfall deposits occur draped on top of, or buried within (1) desert pavements, (2) sand wedges (tesselations of Péwé, 1959), (3) ash avalanche deposits, (4) supraglacial deposits (including ice-marginal and pro-glacial pond/lacustrine deposits), and (5) subglacial tills.

I. Buried Desert Pavements

Ashfall deposits on desert pavements rest conformably and with sharp planar contacts on pre-existing in-situ

ventifacts. The basal sections of such ash deposits show graded bedding and lack non-volcanic contamination, whereas the upper sections may show increasing amounts of detrital contamination and deformed bedding. One example is the Arena Valley Ash.

Arena Valley Ash. The Arena Valley Ash crops out in central Arena Valley on the surface of an extensive colluvial deposit (1410 m elevation) exhibiting a well-developed desert pavement and ultraxerous soil profile. The Arena Valley Ash is about 25 cm thick and covers a circular area with a radius of about 10 m. It rests with a sharp planar contact on a well-developed in-situ desert pavement formed of an interlocking mosaic of gravel-sized ventifacts (Fig. 2). The ventifacts are commonly pitted and exhibit silicious crusts and 5-10 mm quartz rinds suggesting long-term subaerial exposure in a desert environment (Weed and Norton, 1991). A similar desert pavement now overlies the Arena Valley Ash and prevents erosion by wind deflation.

The Arena Valley Ash includes a lower basal unit, a middle cross-bedded unit, and an upper ash-rich diamicton. The lower unit is structureless and consists of a thin lens (0.5 cm to 1.0 cm) of coarse-grained (0.5 mm to 1.0 mm) glass shards and volcanic crystals. The middle unit ranges between 5 and 10 cm thick and, in places, shows alternating cross-bedded layers of fine (0.01 mm to 0.31 mm) and very-coarse grained (0.5 mm to 2.0 mm) ash. The upper unit, about 15 cm thick, is composed of nearly 95% ash, 3% detrital sand grains, and 2% gravel-sized ventifacts of Beacon Supergroup sandstones and Ferrar Dolerite. All units within the Arena Valley Ash contain less than 2.5% clay-size sediment. Glass shards, which show a bimodal grain-size distribution, are angular and unweathered (Fig. 3).

The pure composition of the lower unit, the angular glass shards, and the preservation of the underlying in-situ desert pavement suggest primary ashfall deposition with little (if any) post-depositional reworking. The admixture of sand grains, ventifacts, and ash in the upper unit suggests slight post-depositional reworking and/or penecontemporaneous slumping of adjacent colluvial deposits on top of the airfall ash. The cross-bedding in the middle unit represents slight aeolian transport during initial ashfall deposition. The desert pavement overlying the Arena Valley Ash probably formed by deflation of the upper ash-rich diamicton and the resulting concentration of the enclosed ventifacts onto the ash surface.

We postulate that the Arena Valley Ash represents only a very small portion of a formerly extensive ash layer that once covered Arena Valley. High-velocity katabatic winds (common in the Dry Valleys) most likely dispersed this ash. We suggest that ash was preserved only where it was quickly buried.

II. Sand Wedges

Sand wedges are vertically stratified sand-and-gravel deposits that infill thermal contraction cracks in perennially frozen ground (Péwé, 1959; Svensson, 1988; Watson, 1981; Black, 1976; Berg and Black, 1966). We distinguish between active and relict sand wedges. Active sand wedges lie beneath surficial V-shaped troughs that are visible on the land surface. Intersecting troughs delineate networks of interlocking surface polygons. The largest sand-wedge troughs that we know of in the Dry Valleys region are 2.0 to 3.0 m deep (in Beacon Valley), but most average between 35 and 95 cm deep. In sharp contrast, relict sand wedges lack overlying troughs and are visible only in stratigraphic section. This is because inactive troughs (no longer associated with thermal contraction of the frozen ground below) are quickly infilled with slumped gravel- and cobble-sized ventifacts and coarse-grained aeolian sand. (It is well-known that the loci of thermal contraction sites vary over time, and that sand wedges pass through growth cycles (Berg and Black, 1966), but the exact mechanism of wedge migration is not fully understood).

Sand wedges (relict or active) rarely contain volcanic ash. If present, ash occurs in narrow veins or within wide V-shaped wedges between infilled sand-and-gravel layers. Thick ash deposits are concentrated in the upper half of sand wedges (towards the land surface), whereas thin ash veins generally occur at depth. Ash wedges may reach thicknesses of up to 50 cm. One example is the Beacon Valley Ash.

Beacon Valley Ash. The Beacon Valley Ash is enclosed within the upper half of a relict sand wedge at about 1300 m elevation in east-central Beacon Valley (Fig. 4). The ash rests with sharp planar contacts between conformable layers of stratified sand and gravel. The ash wedge is about 45 cm thick and dips about 75° to the south. A single layer of interlocking gravel-sized ventifacts now overlies the ash and prevents erosion by wind deflation.

The Beacon Valley Ash is composed predominantly of poorly sorted and angular pumice. Individual glass shards show intact bubble vesicles. The ash is bimodal, with a maximum grain-size of about 1.5 mm. The Beacon Valley Ash contains about 5% detrital-quartz sand grains and about 1 to 2% gravel ventifacts. Ventifacts occur predominantly along ash margins and show a preferred near-vertical orientation.

The high concentration of volcanic ash (95% ash and 5% detrital sands), intact bubble vesicles, and sharp planar contacts with surrounding sediments all suggest primary ashfall deposition. The poor sorting within the Beacon Valley Ash is consistent with ashfall deposition and implies limited aeolian transport (see also below).

The deposit morphology (including ash wedge and adjacent stratified sand and gravel) strongly suggests that ashfall occurred into an open sand-wedge trough that has since been infilled with aeolian sand and slumped ventifacts (eg Péwé, 1959; Berg and Black, 1966). We postulate that slumped gravel clasts produced the protective ventifact

pavement that now overlies the Beacon Valley Ash. Figure 5 shows two additional sand wedges with enclosed volcanic ash.

III. Ash Avalanche Deposits

Ash avalanche deposits are lobate in plan view and occur on the surface of steep slopes in excess of 25°. They show poorly sorted mixtures of ash, ventifacts, local bedrock, and sand. These deposits are similar to pumice flows first described by Kuno (1940).

A well-preserved lobate avalanche deposit occurs on the steep (28° to 33°), rectilinear bedrock wall of lower Arena Valley (Fig. 6). The avalanche deposit heads in a cliffed bedrock couloir and terminates two-thirds of the way down the valley wall at about 1100 m elevation. It overlies stratified colluvial sediments (devoid of volcanic ash) and contains a chaotic internal assemblage of gravel-sized ventifacts, detrital quartz-sand grains, local bedrock fragments, and about 40% angular-to-subangular ash in the matrix (<2.0 mm) fraction. A similar ash avalanche deposit occurs on the rectilinear bedrock wall of upper Arena Valley.

The geomorphic setting, deposit form, poor sorting, and chaotic internal stratigraphy suggest rapid emplacement of avalanche deposits over pre-existing stratified-slope sediments. We suggest that ash avalanches originate from collapse of unstable accumulations of volcanic ash on either over-steepened valley slopes or in narrow bedrock couloirs. Collapse of such ash deposits initiates avalanches which flow down valley walls and incorporate pre-existing colluvial sediments.

Ash avalanche deposits probably form at or near times of volcanic eruptions because (1) high-velocity katabatic winds would most likely disperse unprotected surficial volcanic ash, and (2) hanging-ash deposits trapped in bedrock couloirs probably avalanched shortly after initial containment. We note that rapid emplacement of airfall ash within avalanche deposits prevents ash dispersal by katabatic winds and preserves high volcanic concentrations by enclosing glass shards within a protective shield of admixed ventifacts and detrital sands.

IV. Supraglacial Deposits

Ash-rich supraglacial deposits commonly contain folded and faulted layers of well-stratified volcanic ash. This ash may be interbedded with flow tills, lodgement tills, lacustrine deposits, sediment-gravity flows, and deltaic sediments.

Rhone Ash. A well-preserved sediment complex (about 2.5 m thick) including waterlain deposits, subglacial till(s), and coarse-grained ash occurs at about 1000 m elevation along the north wall of central Taylor Valley near Rhone

Glacier (Wilch, 1991). Layers of stratified ash (here termed Rhone Ash) are interbedded with a quartz-rich silty diamicton that shows well-developed climbing ripples (delineated by individual volcanic-ash laminae (each about 1 mm thick)), drop stones, and gravel lenses (Fig. 7). The sediment complex is deformed with numerous faults, overturned bedding, and recumbent folds. A subglacial lodgement till (devoid of volcanic ash) interfingers with these folded and faulted ash-rich sediments (Wilch, 1991).

The Rhone Ash reaches up to 40 cm in thickness and shows alternating lenses of light- and dark-colored pumice. Individual ash layers contain less than 4% clay. This ash is coarse grained (containing 86% sand sized pumice, Fig. 8) and glass shards are subangular-to-rounded. Granite gruss and detrital quartz-sand layers occur interbedded with ash layers.

The entire sediment package, which includes ice-rafted detritus (drop-stones), small-scale sediment gravity flows (sand-and-gravel layers), subglacial lodgement till, and volcanic ash layers, most likely represent deposition along a former ice margin. Wilch (1991) concluded that such features indicate deposition alongside an expanded Taylor Glacier. Faults and folds within this sediment complex most likely reflect extensional and compressional stresses common alongside fluctuating ice margins (Drewry, 1986; Brodzikowski and van Loon, 1991).

The absence of volcanic glass within the lodgement till at this site argues strongly against subglacial transport and deposition of the Rhone Ash. Rather, the data are consistent with supraglacial transport and deposition of volcanic ashfall on top of the Taylor Glacier ablation surface. The high-volcanic concentration and sub-angular grain morphology of some pumice shards within the Rhone ash deposit implies limited glacial transport consistent with deposition from nearby supraglacial sources.

V. Subglacial Deposits

Ash-bearing subglacial tills generally contain from 3 to 10% pumice disseminated in the <2.0 mm fraction. Glass shards are rounded-to-subrounded and commonly hold detrital silts within open pipe vesicles. We postulate that ash disseminated in basal tills reflects either primary airfall ash onto a former accumulation surface (with subsequent dispersal during englacial or basal transport) or basal entrainment of pre-existing ash deposits. As such, isotopic dates from glass shards disseminated in basal tills yield maximum ages for the drift.

RADIOISOTOPIC DATING AND CHRONOLOGY

Laser $^{40}Ar/^{39}Ar$ total fusion and incremental-heating analyses of individual anorthoclase crystals and volcanic glass shards separated from ashes in the Dry Valleys region were carried out at the Institute of Human Origins Geochronology Center. Following washing and screening to remove fine clays, pristine euhedral crystals of anorthoclase and/or sanidine along with angular volcanic glass shards were hand-picked under a binocular

microscope, treated with 7% hydrofluoric acid in an ultrasonic cleaner for 5 minutes to remove any attached altered clays and/or attached glass, followed by 10 minutes in distilled water. The samples were then irradiated in the hydraulic rabbit core facility of the Omega West Research Reactor at Los Alamos National Laboratory.

Following irradiation, single crystals of the monitor mineral, single crystals of the Dry Valleys sanidines, and multiple shards of the volcanic glass were loaded into individual 2-mm-diameter wells of a copper sample disk and then placed within the sample chamber of the extraction system and baked out at 200^0 for eight hours. Total fusion and incremental heating of the samples and monitor mineral were accomplished with a 6W Coherent Ar ion laser. The released gases were purified by two Zr-Fe V getters operated at approximately 150^0C, and condensable gases were collected on a cold-trap operated at -45^0C. Argon was measured in an on-line Mass Analyzer Product 215 noble-gas mass spectrometer operated in the static mode using automated data collection techniques. Laser heating, gas purification, and mass spectrometry were completely automated following computer programmed schedules (1).

The low blank $^{40}Ar/^{39}Ar$ laser system at GC permitted the analysis of extremely small amounts of the Dry Valleys samples. For the sanidines the laser beam was focused to fuse individual crystals while for the glass shards the beam was defocused to heat evenly the 2mm- diameter sample wells and incrementally heated for 45 seconds by stepwise increasing output from the Ar-ion laser. The $^{40}Ar/^{39}Ar$ ages of the Dry Valleys samples were calculated using a J value (see Table 1) determined from replicate analyses of individual grains of the co-irradiated monitor mineral Fish Canyon Tuff sanidine (FC) with a reference age of 27.84 Ma intercalibrated in-house with Minnesota hornblende MMhb-I with a published age of 520.4 Ma (2).

The calculated weighted mean ages and accompanying standard error (SE) for the sanidines are based on multiple total fusion analyses of individual crystals (3). The plateau ages are calculated as the weighted (by inverse variances) mean of all increments defining the plateau, and the uncertainties that accompany the plateau ages are standard errors (SE). The spectra are essentially flat; the plateaus consist of more than three contiguous increments that overlap the mean at the 2σ level and compose over 50% of the total ^{39}Ar released (4).

Table 1 shows laser total fusion $^{40}Ar/^{39}Ar$ analyses of volcanic crystals and glass shards from the Dry Valleys ash deposits described above. The results indicate that each deposit is composed of a single volcanic ash. Ashes of different isotopic ages are not mixed together in Dry Valleys sediments. Ashes range from mid Miocene to mid Pliocene age. The Paleozoic ages listed in Table 1 represent analyses of non-volcanic contaminants.

Notes

(1) Analytical procedures follow Swisher *et al*al. [Science 257: 954-958 (1992)] and references *therein ie.* A. Deino and R. Potts [J. Geophysical Res. 95, 8453 (1990)], A. Deino, L. Tauxe, M. Monaghan, and R. Drake [*J. Geol.* 98, 567 (1990)], C.C. Swisher and D.R. Prothero [*Science* 249, 760 (1990)], P.R. Renne

and A.R. Basu [*Science* **253**, 176 (1991)] and Swisher *et al.* [*Science* **257**: 954-958 (1992)]. Decay constants are those recommend by Steiger, R.H. and E. Jager [*Earth Planet. Sci. Lett.*, **36**, 359 (1977) and G.B. Dalrymple, *Geology* **7**, 558 (1979)].

(2) The age of the Fish Canyon sanidine adopted in this study (27.84 Ma) is similar to that recommended by G.T. Cebula, et al., TERRA *Cognita* **6**, 139 (1986) but slightly modified as a result of in-house intercalibration at the Geochronology Center with MMhb-I with a published age of 520.4 $\pm$ 1.7 Ma by S.D. Samson and E.C. Alexander, *Chem. Geol. Isot. Geosci. Sect.* **66**, 27 (1987).

(3) The uncertainties associated with the individual incremental apparent ages are 2σ errors, while those that accompany the calculated weighted mean ages of the plateau increments and weighted means of the replicate analyses are standard errors (SE) following J.R. Taylor, *An Introduction to Error Analysis* (Oxford Univ. Press, 1982).

(4) Plateau definition follows that of R.J. Fleck *et al.*, *Geochim. Cosmochim. Acta* **41**, 15 (1977).

SOURCE AREAS

Primary Sources

The chemical composition, grain-size, and age of Dry Valleys ashes permit identification of potential volcanic source areas. Table 2 and Figure 8 show the chemical composition and grain-size distribution of the Dry Valleys ashes. For comparison, we also show various grain-size and geochemical data of glass shards from volcanic horizons within the Byrd (Palais, 1985; Kyle et al., 1981) and Dome Circe (Kyle et al., 1981, 1982) ice cores, as well as ash from the surface ice near the Allan Hills in southern Victoria Land and near the Yamato Mountains in Queen Maud Land (Nishio et al., 1984, 1985; Katsushima et al., 1984). With the exception of the Allan Hills ash, all pyroclastic debris now found within the East Antarctic Ice Sheet is significantly finer than the relatively coarse-grained Dry Valleys ashes. Figure 9 shows an SiO_2 - Na_20 + K_20 diagram, which plots the composition of glass shards from several Dry Valleys ashes along with compositional fields of volcanic rocks from the McMurdo Volcanic Group, Marie Byrd Land, and the south Sandwich Islands (LeMasurier and Thomson, 1990).

Our results indicate that Dry Valleys ashes are geochemically similar to alkaline volcanic rocks found either in the McMurdo Volcanic Group (Kyle et al., 1990) or in Marie Byrd Land (LeMasurier and Thomson, 1990). The coarse texture and bimodal grain-size distribution of Dry Valleys ashes, both of which independently suggest deposition close to volcanic regions (Carey and Sigurdsson, 1982; Fisher and Schmincke, 1984), limit potential source areas to eruptive centers in the McMurdo Volcanic Group. The McMurdo Group includes all volcanic rocks within the Melbourne, Hallet, and Erebus Volcanic Provinces (Kyle, 1990).

The most likely source areas within the McMurdo Volcanic Group are the numerous alkali volcanoes of the Erebus

Volcanic Province (Fig. 1). The Erebus Volcanic Province contains at least 27 individual eruptive centers (Kyle, 1990), which range from small cinder cones to large shield and stratovolcanoes. The oldest volcanic rocks yet dated from the McMurdo Group come from Mount Morning, which shows a subvolcanic complex between about 12 and 19 Ma (Armstrong, 1978; Muncy, 1979; Kyle, 1990). Our present geochemical data cannot single out particular volcanic sources for each ash deposit, but they indicate that most of the ashes described above are probably related to large stratovolcanoes situated just east of the Dry Valleys region (Fig. 1).

Our isotopic-age data on volcanic ash deposits, together with K/Ar dates on McMurdo Group volcanics (Kyle, 1990), afford a limited history of volcanism in the Erebus Province and helps constrain the number of potential source areas for some Dry Valleys ashes. For example, because Mount Erebus is relatively young (<1.0 Ma, Kyle, 1990)), it could not have produced the Pliocene-age ashes described above. Likewise, because Mt. Discovery is <6.0 Ma (Kyle, 1990), it is not a possible source for mid-to-late Miocene-age Dry Valleys ashes.

Secondary Sources

Because the Dry Valleys are located adjacent to the East Antarctic Ice Sheet, it is reasonable to suggest that some ashes may have been trapped beneath (or locked within) East Antarctic ice for several thousand years (or much longer) before final deposition in the Dry Valleys region. Although this scenario seems possible for ash disseminated in some glacial deposits, we suggest that it is highly unlikely for concentrated, coarse-grained , poorly sorted (bimodal) ash deposits exhibiting angular glass shards. This is because such characteristics reflect primary ashfall with limited transport (Fisher and Schmincke, 1984). We suggest that aeolian transport of ash formerly buried within East Antarctic ice and now exposed in lenses at the ice-sheet surface (i.e. the Allan Hills ash and ash near Yamato Mountains (Nishio et al., 1984, 1985; Katsushima et al., 1984) would disperse the ash, introduce a non-volcanic component, abrade individual glass shards, and almost surely mix together ashes of different isotopic ages. Because none of the concentrated ash deposits in the Dry Valleys show these characteristics, we argue that such deposits reflect primary ashfall and do not represent retransported ashes formerly locked in East Antarctic ice. Similarly, we consider it highly unlikely that concentrated Dry Valleys ashes represent reworked and retransported ashes from pre-existing Dry Valleys deposits.

In support of this conclusion we show below that concentrated ash trapped in sand wedges must have been deposited at the time of volcanic eruptions. Granulometric analyses show that sand wedges are composed almost entirely of sand-and-gravel sized clasts. They essentially lack non-volcanic silt-sized grains (Table 3). Because silt is a common constituent of Dry Valleys deposits (many sand wedges truncate diamictons containing up to 30% silt and clay), we argue that sand wedges are ineffective aeolian traps for silt-sized (and finer-grained) sediments. We postulate (1) that any detrital silt- and clay-sized grains eroded from glacial tills and other mud-rich deposits are

transported by wind in suspension, well above (and isolated from) sand wedges, and (2) that only sand-sized grains and small gravel clasts transported by saltation fall readily into active sand wedges (excluding slumped ventifacts).

During large volcanic eruptions there is most probably sufficient ash to mantle the land surface and fill open sand-wedge furrows in the fall-out zone (see for example, Fisher and Schmincke, 1984; Kuno, 1940). Ash that falls in areas outside sand wedges (or other suitable geomorphic ash traps) is eventually carried away in suspension by high-velocity katabatic winds. This ash, transported in suspension, is probably mixed with detrital silt-sized grains, sorted on the basis of hydraulic equivalency, combined with other ash deposits, and abraded so that individual pumice shards become rounded and glass vesicles shattered (Fisher and Schmincke, 1984). Hence, concentrated ash deposits exhibiting bimodal grain-size distributions and angular glass shards (with intact bubble vesicles) almost certainly represent primary ashfall. The uniform isotopic ages and geochemical compositions of glass shards within individual sand wedges (Table 1) indicate no aeolian mixing of volcanic ashes, consistent with primary ashfall deposition in active sand wedges.

DISCUSSION

Isotopically dated, in-situ ashfall deposits provide minimum ages for the surfaces on which they rest, and yield additional paleoclimatic data when associated with sand wedges, desert pavements, or glacial tills (Table 4). In addition, because the rate at which surficial volcanic glass alters to clay minerals is largely a function of atmospheric temperature (with increasing rates due to rising atmospheric temperatures; Lowe, 1986 and references therein), the percentage of clay minerals within Dry Valleys ashes provides a crude (order of magnitude) estimate for possible atmospheric warming. We describe below the implications for Dry Valleys ashes on regional paleoclimate and paleogeography.

Arena Valley Ash

The age and stratigraphic relationship of the Arena Valley Ash (Table 1) with the underlying ventifact pavement indicate that a desert climate existed in Arena Valley at 4.3 Ma. We suggest that cold desert prevailed in Arena Valley at 4.3 Ma and has persisted to the present time for two reasons. First, landscape analysis indicates that surficial sediments coeval and older than the Arena Valley Ash (which includes most of the Arena Valley surficial stratigraphy (Marchant, 1993c; Denton et al., 1993) lack geomorphic evidence of liquid water (Bockheim, 1982). For example, there are no mudflow deposits, levees, rills, lacustrine deposits, or stream channels, although such features today are common below about 800 m elevation elsewhere in the Dry Valleys region. The mean annual temperature at 800 m elevation is about -27°C (based on a recorded mean annual temperature of -19.8°C at about 100 m elevation at nearby Lake Vanda (Schwerdtfeger, 1984) and an average lapse rate of 1°C/100 m elevation rise (Robin, 1988). We conclude that mean annual temperatures in Arena Valley failed to rise above about -27°C during at least the last 4.3 Ma. In fact, we see no evidence in Arena Valley for warmer-than-present temperatures during

the last 4.3 Ma. Second, the absence of etched volcanic crystals and authigenic clay-sized minerals within the Arena Valley Ash, common in most pre-Quaternary surficial ash deposits (Lowe, 1986), indicates limited chemical alteration, consistent with a continuous cold and dry climate. We note that under humid temperate conditions in New Zealand (suitable for Nothofagus growth), tephras older than about 50,000 yr have >60% clay (Lowe, 1986; Birrell and Pullar, 1973).

Beacon Valley Ash

The age and stratigraphic relationship of the Beacon Valley ash (Table 1) with surrounding sand-and-gravel deposits indicate airfall deposition into an open sand-wedge trough at 10.4 Ma. Péwé (1959, 1966) and Romanovskij (1973) argued that sand wedges form only in dry, cold conditions, similar to the present Dry Valleys climate. As such we suggest that cold desert conditions existed in Beacon Valley as early as 10.4 Ma. The absence of numerous authigenic clay-sized minerals in the Beacon Valley Ash (< 7.0% clay-sized sediment) and the preservation of sharp lateral contacts with surrounding sand-and-gravel deposits suggest that frozen conditions have persisted in Beacon Valley since ash deposition. Similar sand wedges occur in the western Asgard Range and indicate that here cold desert conditions existed at 15.0 Ma (Nibelungen Valley) and 13.6 Ma (Koenig Valley).

Ash Avalanche Deposits

The age and geomorphic setting of Arena Valley ash avalanche deposits (Table 1) suggest that the morphologic evolution of Arena Valley bedrock walls and rectilinear slopes (Selby, 1971, 1974) predates late Miocene time. In fact, the preservation of surficial avalanche deposits on valley walls indicates that here no slope development has occurred since ash deposition. Otherwise, the ash would be buried beneath younger colluvial sediments or the morphologic form of each avalanche deposit would be destroyed, which we here show is not the case. Our interpretation implies that subaerial (non-glacial) slope development in the Dry Valleys region (at least at elevations above 1000 m in Arena Valley) has proceeded at a much slower rate than hitherto imagined (eg Selby, 1971, 1974; Agustinus and Selby, 1990). Such long-term slope stability is consistent with persistent cold-desert conditions in Arena Valley during the last 11.3 Ma.

CONCLUSIONS

(1) Volcanic ash occurs within surficial sediments in the Dry Valleys region. Ashes are preserved only when volcanic airfall is buried rapidly or incorporated into glacial ice. Dry Valleys ashes occur draped on top of, or buried within desert pavements, sand wedges, ash avalanche deposits, supraglacial deposits (including ice-marginal and pro-glacial pond/lacustrine deposits), and subglacial tills. Laser-fusion $^{40}Ar^{39}Ar$ dates on individual crystals and

glass shards from Dry Valleys ashes indicate that each deposit is composed of a single ash. Dated ashes range from middle-Miocene to mid-Pliocene in age.

(2) The chemical composition, grain-size, and age of the Dry Valleys ashes suggest volcanic source areas within the McMurdo Group. The most likely candidates are the numerous alkali volcanoes of the Erebus Volcanic Province. Concentrated ash deposits with little detrital contamination (<7%), uniform isotopic ages and geochemical compositions, bimodal grain-size distributions, and angular glass shards with intact bubble vesicles represent direct ashfall from volcanic sources. We consider it highly unlikely that such ashes represent reworked and retransported ashes from either debris in East Antarctic ice or from pre-existing Dry Valleys ash deposits.

(3) Isotopically dated in-situ ashfall deposits provide minimum ages for the surfaces on which they rest and yield additional paleoclimatic data when the deposits are associated with sand wedges, desert pavements, and glacial tills. The age and stratigraphic relationship of the Arena Valley Ash with an underlying desert pavement indicate that a desert climate existed in Arena Valley at 4.3 Ma. We suggest that a dry and cold climate prevailed in Arena Valley at 4.3 Ma and has persisted to the present time because surficial sediments that are coeval and older than the Arena Valley ash lack warm desert geomorphic features. The Beacon Valley ash represents volcanic airfall into an active sand-wedge trough. The isotopic age of this ash indicates that cold-desert conditions existed in the Beacon Valley at 10.4 Ma. The inferred age and geomorphic setting of Arena Valley avalanche deposits suggests that the morphologic evolution of underlying rectilinear slopes predate late Miocene time. We conclude that such slope stability (no talus development or erosion of colluvium) strongly suggests persistent cold-desert conditions in Arena Valley since 11.3 Ma. The low percentage of clay-sized sediment (<7.0 %) in all Dry Valleys ashes indicates little chemical weathering. We suggest that such limited weathering of surficial volcanic ash deposits (of alkali to basic compositions) implies persistent cold-desert conditions since ash deposition. In New Zealand, surficial ashes alter to >60% clay in about 50,000 years.

(4) Persistent cold-desert conditions since late Miocene time in the Dry Valleys region preclude development of extensive Pliocene-age surface-melting ablation zones and coeval Nothofagus growth in the Transantarctic Mountains. If correct, this conclusion implies an enduring East Antarctic Ice Sheet throughout Pliocene time, and makes it difficult to ascribe late Pliocene sea-level fluctuations to large-scale ice-volume variations on the East Antarctic craton.

REFERENCES

Armstrong, R.L. 1978. K-Ar dating: late Cenozoic McMurdo Group and Dry Valley glacial history, Victoria Land, Antarctica. New Zealand Jour. Geol. and Geophys. 21 (6), 685-698.

Augustinus, P.C. and Selby, M.J. 1990. Rock slope development in McMurdo oasis, Antarctica, and implications for interpretations of glacial history. Geogr. Ann. 72 A (1), 55-62.

Ackert, R.P., Jr. 1990. Surficial geology and geomorphology of Njord Valley and adjacent areas of the western Asgard Range, Antarctica: Implications for late Tertiary glacial history. Unpublished MSc Thesis, University of Maine, Orono, ME. 147 pp.

Barrett, P.J., Adams, C.J., McIntosh, W.C., Swisher III, C.C. and Wilson, G.S. 1992. Geochronological evidence supporting Antarctic deglaciation three million years ago. Nature 359, 816-818.

Berg, T.E. and Black, R.F. 1966. Preliminary measurements of growth of nonsorted polygons, Victoria Land, Antarctica. In Antarctic Soils and Soil Forming Processes, J. C. F. Tedrow, Ed. Antarctic Res. Ser. No. 8., 61-108. Washington, D.C.

Birrell, K.S. and Pullar, W.A. 1973. Weathering of paleosols in Holocene and late Pleistocene tephras in central North Island, New Zealand. New Zealand Jour. of Geol. and Geophys. 16, 687-702.

Black, R.F. 1976. Periglacial features idicative of permafros: ice and soil wedges. Quaternary Research 6, 3-26.

Bockheim, J.G. 1982. Properties of a chronosequence of ultraxerous soils in the Transantarctic Mountains. Geoderma 28, 239-255.

Brodzikowski, K. and van Loon, A.J. 1991. Glacigenic Sediments. Developments in Sedimentology 49. Elsevier Press, Amsterdam, 674 pp.

Bull, C. 1962. Quaternary glaciations in southern Victoria Land, Antarctica. Jour. of Glaciology 4 (32), 240-241.

Calkin, P.E. and Nichols, R.L. 1972. Quaternary studies in Antarctica. In Antarctic Geology and Geophysics. Raymond J. Adie, Ed. Universitetsforlaget, Oslo. pp 625-644.

Calkin, P.E. and Bull, C. 1972. Interaction of the East Antarctic Ice Sheet, alpine glaciation, and sea level in the Wright Valley area, southern Victoria Land. In Antarctic Geology and Geophysics. Raymond J. Adie, Ed. Universitetsforlaget, Oslo. pp 435-440.

Campbell, I.B. and Claridge, G.G.C. 1969. A classification of frigic soils - The zonal soils of the Antarctic continent. Soil Science 107, 75-85.

Carey , S.N. and Sigurdsson, H. 1982. Influence of particle aggregation on deposition of distal tephra from the May 18, 1980, eruption of Mount St. Helens Volcano. Jour. of Geophys. Res. 87, B8, 7061-7072.

Chinn, T.J. 1980. Glacier balances in the Dry valleys area, victoria Land, Antarctica. In Proceedings of the Riederlap Workshop, September 1978. IAHS-AISH Publ. no. 126, 237-247.

Denton, G.H. Armstrong, R.L. and Stuiver, M. 1971. The late Cenozoic glacial history of Antarctica. In The late Cenozoic Glacial Ages. K.K. Turekian, Ed., Yale University Press, New Haven CT., pp 267-306.

Denton, G.H., Bockheim, J.G., Wilson, S.C. and Stuiver, M. 1989. Late Wisconsin and early Holocene glacial

history inner Ross Embayment, Antarctica. Quaternary Research 31, 151-182.

Denton, G.H., Sugden, D.E., Marchant, D.R., Wilch, T.I., and Hall, B.E. 1993. East Antarctic Ice Sheet sensitivity from a Dry Valleys prespective. Geographiska Annaler in press.

Drewry, D.J. 1986. Glacial Geologic Processes. Edward Arnold, London.

Fisher, R.V. and Schmincke, H.U. 1984. Pyroclastic Rocks. Springer-Verlag, New York.

Fitzgerald, P.G., Sandiford, M., Barrett, P.J. and Gleadow, A.J.W. 1986. Asymmetric extension associated with uplift and subsidence in the Transantarctic Mountains and Ross Embayment. Earth and Planetary Science Letters 81, 67-78.

Harwood, D.M. 1985. Late Neogene climatic fluctuations in the southern high latitudes: implications of a warm Pliocene deglaciated Antarctic continent. South African Journal of Science 81, 239-241.

Hendy, C.H., Healy, T.R., Rayner, E.M., Shaw, J. and Wilson, A.T. 1979. Late Pleistocene glacial chronology of the Taylor Valley, Antarctica, and the global climate. Quaternary Research 11, 172-184.

Katsushima, T., Nishio, F., Ohmae, H., Ishikawa, M. and Takahashi, S. 1984. Composition of dirt layers in the bare ice areas near the Yamato Mountains in Queen Maud Land and the Allan Hills in Victoria Land, Antarctica. In Memoirs of National Institute of Polar Research, Special Issue No. 34, 147-187. (Proceedings of the sixth symposium onpolar meteorology and glaciology, K.Kusunoki, Ed. Printed by Tokyo Press Co., Ltd.)

Kennett, J.P. 1985. Neogene paleooceanography and planktonic evolution. South African Journal of Science 81, 251-253.

Keys, J.R., Anderton, P.W. and Kyle, P.R. 1977. Tephra and debris layers in the Skelton Névé and Kempe Glacier, south Victoria Land, Antarctica. New Zealand Jour. of Geol. and Geophys. 20, No. 3, 971-1002.

Krantz, D. 1991. A chronology of Pliocene sea-level fluctuations: The U.S. middle Atlantic Coastal Plain record. Quat. Sci. Rev. 10, 163-174.

Kuno, H. 1940. Characteristics of deposits formed by pumice flows and those by ejected pumice. Tokyo Daigaku Earthquake Inst. Bull. 19, 144-149.

Kyle, P.R., Jezek, P.A., Mosley-Thompson, E. and Thompson, L.G. 1981. Tephra layers in the Byrd Station ice core and the Dome C ice core, Antarctica and their climatic importance. Jour. of Volc. and Geotherm. Res. 11, 29-39.

Kyle, P., Palais, J. and Delmas, R. 1982. The volcanic record of Antarctic ice cores: Preliminary results and potential for future investigations. Ann. of Glaciology 3, 172-177.

Kyle, P.R. 1990. McMurdo Volcanic Group - western Ross Embayment. In Volcanoes of the Antarctic Plate and southern oceans. American Geophysical Union, Washington, DC. pp 19-134.

LeMasurier, W.E. and Thomson, J.W. 1990. Volcanoes of the Antarctic Plate and southern oceans. American Geophysical Union, Washington, DC.

Lowe, D.J. 1986. Controls on the rates of weathering and clay mineral genesis in airfall tephras: a review and New Zealand case study. In S.M. Colman and D.P. Dethier Eds., Rates of chemical weathering of rocks and minerals. Academic Press, Inc., New York. pp 265-330.

Marchant, D.R., Swisher, C.C. III, Lux, D.R., West, D.P., Jr., and Denton, G.H. 1993a. Pliocene paleoclimate and East Antarctic Ice-Sheet history from surficial ash deposits. Science 260, 667-670.

Marchant, D.R., Denton, G.H., Sugden, D.E., and Swisher, C.C. III. 1993b. Miocene glacial stratigraphy and landscape evolution of the western Asgard Range, Antarctica. Geographiska Annaler, in press.

Marchant, D.R., Denton, G.H., Sugden, D.E., and Swisher, C.C. III. 1993c. Miocene-Pliocene-Pleistocene stratigraphy and landscape evolution of Arena Valley, Quartermain Mountains, Antarctica. Geographiska Annaler, in press.

Marchant, D.R., Denton, G.H., Bockheim, J.G., Wilson, S.C. and Kerr A.J. 1994. Quaternary changes in level of the upper Taylor Glacier, Antarctica: implications for paleoclimate and ice-sheet dynamics. Boreas, submitted.

McCraw, J.D. 1962. Volcanic detritus in Taylor Valley, Victoria Land, Antarctica. N.Z. Jour. of Geol. and Geophys. 5, 740-745.

Miller, K.G., Fairbanks, R.G. and Mountain, G.S. 1987. Tertiary oxygen isotope synthesis, sea level history, and continental margin erosion. Paleoceanography 2 (1), 1-19.

Muller, F. 1962. Zonation in the accumulation area of the glaciers of Axel Heiberg Island, N.W.T., Canada. Journal of Glaciology 4, No. 33, 302-311.

Muncy, H.L. 1979. Geologic history and petrogenesis of alkaline volcanic rocks, Mount Morning, Antarctica. M.S. Thesis, Ohio State University, Columbus.

Nichols, R.L. 1966. Geomorphology of Antarctica. In Antarctic Soils and Soil Forming Processes, J. C. F. Tedrow, Ed. Antarctic Res. Ser. No. 8., 61-108. Washington, D.C.

Nichols, R.L. 1971. Glacial geology of the Wright Valley, McMurdo Sound. In Research in the Antarctic, L.O. Quam Ed. American Association for the advancement of Science, Washington, DC. pp 293-340.

Nishio, F., Katsushima, T., Ohmae, H., Ishikawa, M. and Takahashi, S. 1984. Dirt layers and atmospheric transportation of volcanic glass in the bare ice areas near the Yamato Mountains in Queen Maud Land and the Allan Hills in Victoria Land, Antarctica In Memoirs of National Institute of Polar Research, Special Issue No. 34, 160-173. (Proceedings of the sixth symposium onpolar meteorology and glaciology, K.Kusunoki, Ed. Printed by Tokyo Press Co., Ltd.)

Nishio, F., Katsushima, T., Ohmae, H. 1985. Volcanic ash layers in bare ice areas near the Yamato Mountains, Dronning Maud Land and the Allan Hills, Victoria Land, Antarctica. Ann. of Glaciology 7, 34-41.

Nye, J.F. 1960. The response of glaciers and ice-sheets to seasonal and climatic change Proc. Roy. Soc. A. Vol. 256, 559-584.

Palais, J.M. 1985. Particle morphology, composition and associated ice chemistry of tephra layers in the Byrd ice

core: evidence for hydrovolcanic eruptions. Ann. of Glaciology 7, 42-48.

Paterson, W.S.B. 1981. The physics of glaciers. Pergamon Press, London. 250 pp.

Péwé, T.L. 1959. Sand-wedge polygons (tesselations) in the McMurdo Sound, region, Antarctica - a progress report. Am. Jour. Sci. 257 No. 8, 545-552.

Péwé, T. L. 1966. Paleoclimatic significance of fossil ice wedges. Biuletyn Peryglacjalny 15, 65-73.

Porter, S.C. 1975. Equilibrium-line altitudes of the late Quaternary glaciers in the southtern Alps, New Zealand. Quaternary Research 5, 27-47.

Prentice, M.L. and Mathews, R.K. 1989. Cenozoic ice volume history: development of a composite oxygen isotope record. Geology 16, 963-966.

Robin, G. de Q. 1988. The Antarctic Ice Sheet, its history and response to sea level and climatic changes over the past 100 million years. Paleo. Paleo. Paleo 67, 31-50.

Robinson, P.H. 1984. Ice dynamics and thermal regime of Taylor Glacier, south Victoria Land, Antarctica. Jour. of Glaciology 30, 153-160.

Romanovskij, N.N. 1973. Regularities in the formation of frost-fissures and development of frost-fissure polygons. Biuletyn Peryglacjalny 23, 237-277.

Savin, S.M., Douglas, R.G., and Stehli, F.G. 1975. Tertiary marine paleotemperratures. Geol. Soc. Amer. Bull. 86, 1499

Shackleton, N.J. and Kennet, J.P. 1975. Paleotemperature history of the Cainozoic and the initiation of Antarctic glaciation: oxygen and carbon analysis in DSDP sites 277, 279 and 281. In Kennet, J.P. and Houtz, R. (eds.), Initial Reports of the Deep Sea Drilling Project, 29, 743-755.

Schwerdtfeger, W. 1984. Weather and climate of the Antarctic. In Developments in Atmospheric Science 15. Elsevier Publishing Co., Amsterdam.

Selby, M.J. 1971. Slopes and their development in an ice-free, arid area of Antarctica. Geographiska Annaler 53(a), 235-245.

Selby, M.J. 1974. Slope evolution in an Antarctic oasis. New Zealand Geographer 30, 18-34.

Sugden, D.E. and John, B.S. 1976. Glaciers and Landscape. John Wiley and Sons, New York, NY.

Sugden D.E., Denton, G.H. and Marchant, D.R. 1991. Subglacial meltwater channel systems and ice sheet overriding, Asgard Range, Antarctica. Geografisha Annaler 73 A, 109-121.

Sugden, D.E., Denton, G.H. and Marchant, D.R. 1994. Landscape evolution of the Dry Valleys, Transantarctic Mountains. Journal of Geophysical Research, submitted.

Svensson, H. 1988. Ice-wedge casts and relict polygonal patterns in Scandinavia. Journal of Quaternary Science 3, 57-67.

Watson, E. 1981. Characteristics of ice-wedge casts in central Wales. Biuletyn Peryglacjalny 28, 163-167.

Webb, P.N., Harwood, D.M., McKelvey, Mercer, J.H. and Stott, L.D. 1984. Cenozoic marine sedimentation and ice-volume variation on the East Antarctic craton. Geology 12, 287-291.

Webb, P.N. and Harwood, D.M. 1991. Late Cenozoic glacial history of the Ross Embayment, Antarctica. Quaternary Science Reviews 10, 215-223.

Webb, P.N., Harwood, D.M., McKelvey, B.C., Mabin, M.G.C. and Mercer, J.H. 1986. Late Cenozoic tectonic and glacial history of the Transantarctic Mountains. Ant. Jour. of the United States 21, 99-100.

Weed, R. and Norton, S.A. 1991. Siliceous crusts, quartz rinds and biotic weathering of sandstones in the cold desert of Antarctica. In Proc. Intern. Symp. Environ. Biogeochem. Elsevier Publishers, Nancy, France. pp 327-340.

Wilch, T. 1991. $^{39}Ar/^{40}Ar$ chronology of volcanic rocks interbedded with glacial drifts, Taylor Valley, Antarctica: implications for Pliocene behavior of the East Antarctic Ice Sheet. Unpublished MS thesis, University of Maine, Orono, ME.

FIGURE CAPTIONS

Figure 1. Index map for the Dry Valleys region of southern Victoria Land showing location generalized ages for the major volcanic centers within the Erebus Volcanic Province (McMurdo Volcanic Group) (adapted from Kyle, 1990, p. 85).

Figure 2. The Arena Valley Ash deposit in west central Arena Valley. The vertical face of the ash has been cut back to expose the underlying buried desert pavement. A weathered, relict colluvial deposit (devoid of volcanic material) underlies the ash.

Figure 3. Scanning electron microscope images of glass shards and anorthoclase crystals from the Arena Valley Ash. Plates show unweathered anorthoclase crystals and glass shards at about 100, 200, and 700 magnification, respectively. Glass shards removed from the middle unit of the Arena Valley ash show evidence of slight wind abrasion. Note the absence of etched crystals and authigenic minerals within the Pliocene-age, surficial Arena Valley Ash deposit.

Figure 4. Volcanic ash enclosed within the relict sand wedge in Beacon Valley. The ash is about 45 cm thick.

Figure 5. Volcanic ash enclosed within sand wedges in the western Asgard Range. (A) narrow wedge of volcanic ash (10 cm wide) situated at the center of a relict sand-wedge in Koenig Valley. Note the stratified sand-and-gravel layers adjacent to the ash wedge. (B) concentrated volcanic ash enclosed within a relict sand wedge in Nibelungen Valley. Volcanic ash occurs concentrated along wedge margin.

Figure 6. Oblique aerial view of lower Arena Valley showing avalanche deposit on steep rectilinear bedrock wall of lower Arena Valley. Ash avalanche deposit is overlain by Taylor IVb drift and moraines, associated with former fluctuations of Taylor Glacier, Marchant et al., 1993c; 1994). Note that the geomorphic form of the avalanche deposit is preserved beneath this drift.

Figure 7. The Rhone Ash deposit. (A) Stratified layers of volcanic ash showing numerous normal and reverse faults. Ash overlies a coarse-grained unconsolidated diamicton devoid of volcanic ash. (B) Well-preserved climbing ripples delineated by individual volcanic ash laminae.

Figure 8. Grain-size distribution of some Dry Valleys ashes. For comparison, we also show various grain-size data of glass shards from volcanic horizons within the Byrd (Palais, 1985; Kyle et al., 1981) and Dome Circe (Kyle et al., 1981, 1982) ice cores, as well as ash from the surface ice near the Allan Hills in southern Victoria Land and near the Yamato Mountains in Queen Maud Land (Nishio et al., 1984, 1985; Katsushima et al., 1984).

Figure 9. Summary total alkali versus silica diagram showing Dry Valleys ashes as well as compositional fields for volcanic rocks from the McMurdo Group, Marie Byrd Land, and South Sandwich Islands (adapted from LeMasurier and Thomson, 1990 p. 7).

TABLES

Table 1a. $^{40}Ar/^{39}Ar$ laser fusion analyses of sanadine from selected ash deposits in the Dry Valleys region. Sample RAS84-343 is from the matrix of an ash avalanche deposit that mantles a rectilinear slope in the western Asgard Range. Sample TWS87-142C is from the Rhone ash. Sample DMS86-131 is from the matrix of an ash avalanche deposit that mantles a rectilinear slope in upper Arena Valley. Sample DMS87-113 is from the matrix of an ash avalanche deposit that mantles a rectilinear slope in lower Arena Valley. Sample DMS86-86B is the Arena Valley ash.

Table 1b. $^{40}Ar/^{39}Ar$ incremental laser heating analyses of glass shards from selected ash deposits in the Dry Valleys region. Sample DMS86-113 (see Table 1a) is from the matrix of an ash avalanche deposit that mantles a rectilinear slope in lower Arena Valley. Sample DMF86-141 is from the same ash avalanche deposit as DMS86-131 in Table 1a. Sample NPS84-327 is the Beacon Valley ash and was collected from a sand wedge in Beacon Valley.

Table 2. Major element analyses (MAC 400 microprobe) of glass shards from selected Dry Valleys ashes.

Table 3. Grain-size of Dry Valleys ashes and detrital infill of relict sand wedge deposits.

Table 4. Summary of Dry Valleys ash deposits.

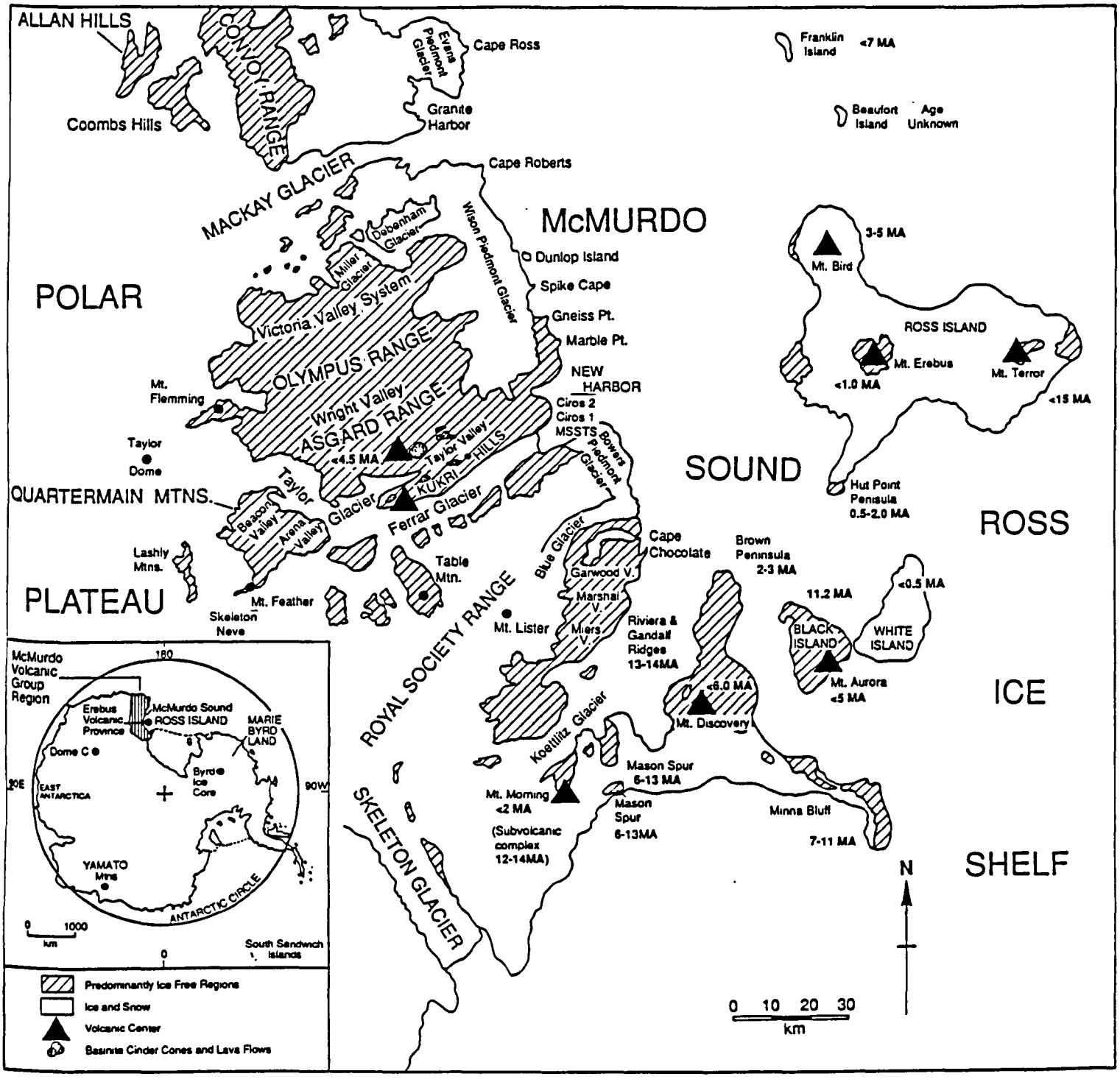
ALLAN HILLS
CONO RANGE
Coombs Hills
Evans Piedmont Glacier
Cape Ross
Granite Harbor
Franklin Island <7 MA
Beaufort Island Age Unknown
MACKAY GLACIER
Cape Roberts
McMURDO
Debenham Glacier
Miller Glacier
Wilson Piedmont Glacier
Dunlop Island
POLAR
Spike Cape
Victoria Valley System
Gneiss Pt.
OLYMPUS RANGE
Marble Pt.
Wright Valley
ASGARD RANGE
NEW HARBOR
Mt. Flemming
Ciros 2
Ciros 1
MSSTS
Taylor Valley
HILLS
Bowers Piedmont Glacier
Taylor Dome
<4.5 MA
KUKRI
QUARTERMAIN MTNS.
Taylor Glacier
Beacon Valley
Arena Valley
Ferrar Glacier
SOUND
Hut Point Peninsula 0.5-2.0 MA
ROSS
Lashly Mtns.
Table Mtn.
Blue Glacier
Cape Chocolate
Brown Peninsula 2-3 MA
Garwood V.
PLATEAU
Mt. Feather
Skeleton Neve
Marshal V.
Mt. Lister
Miers V.
ROYAL SOCIETY RANGE
Riviera & Gandalf Ridges 13-14MA
11.2 MA
<0.5 MA
BLACK ISLAND
WHITE ISLAND
Mt. Aurora <5 MA
ICE
<6.0 MA
Mt. Discovery
Koettlitz Glacier
Mason Spur 6-13 MA
Mt. Morning <2 MA
(Subvolcanic complex 12-14MA)
Mason Spur 6-13MA
Minna Bluff
7-11 MA
SKELETON GLACIER
SHELF
N
0 10 20 30
km
McMurdo Volcanic Group Region
180
Erebus Volcanic Province
McMurdo Sound
ROSS ISLAND
MARIE BYRD LAND
Dome C
Byrd Ice Core
90E
EAST ANTARCTICA
90W
YAMATO Mtns
ANTARCTIC CIRCLE
0 1000 km
0
South Sandwich Islands
Predominantly Ice Free Regions
Ice and Snow
Volcanic Center
Basinite Cinder Cones and Lava Flows

FIGURE 1

Fig. 2. Photograph of the surficial volcanic ash deposit in west central Arena Valley. The vertical face has been cut back to expose the underlying buried desert pavement. A weathered, relict colluvial deposit (devoid of volcanic material) underlies the ash.

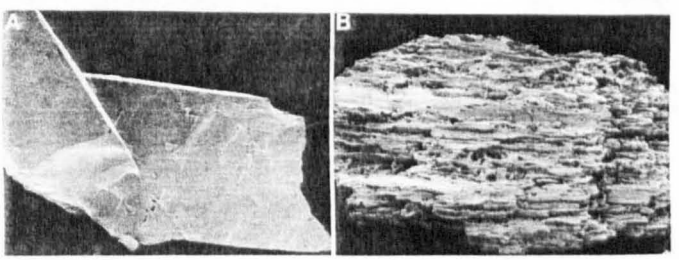

Fig. 3. Scanning electron microscope images of glass shards and anorthoclase crystals from the Arena Valley Ash. (**A**) shows an unweathered anorthoclase crystal (field of view is about 0.23 mm) (**B**) shows part of the vitric component of the ash (field of view is 0.30 mm). Glass shards removed from the upper unit of the Arena Valley ash show evidence of slight wind abrasion. Note the absence of etched crystals and authigenic minerals in the Pliocene-age, surficial Arena Valley Ash deposit.

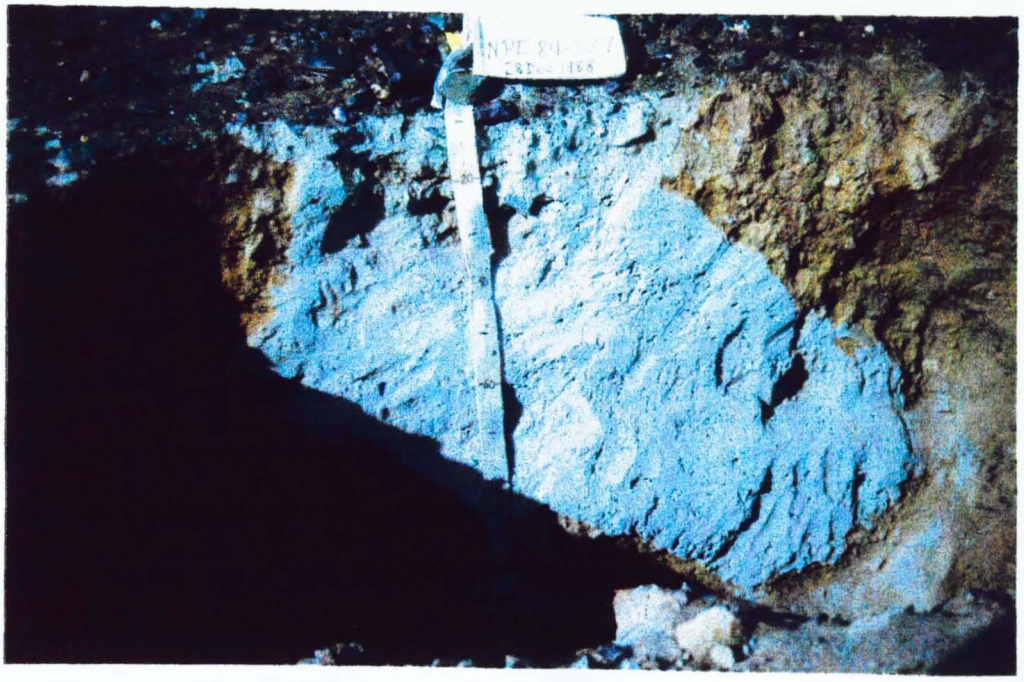

Figure 4

Figure 5

Figure 5 (b)

Figure 6

Figure 7 (a)

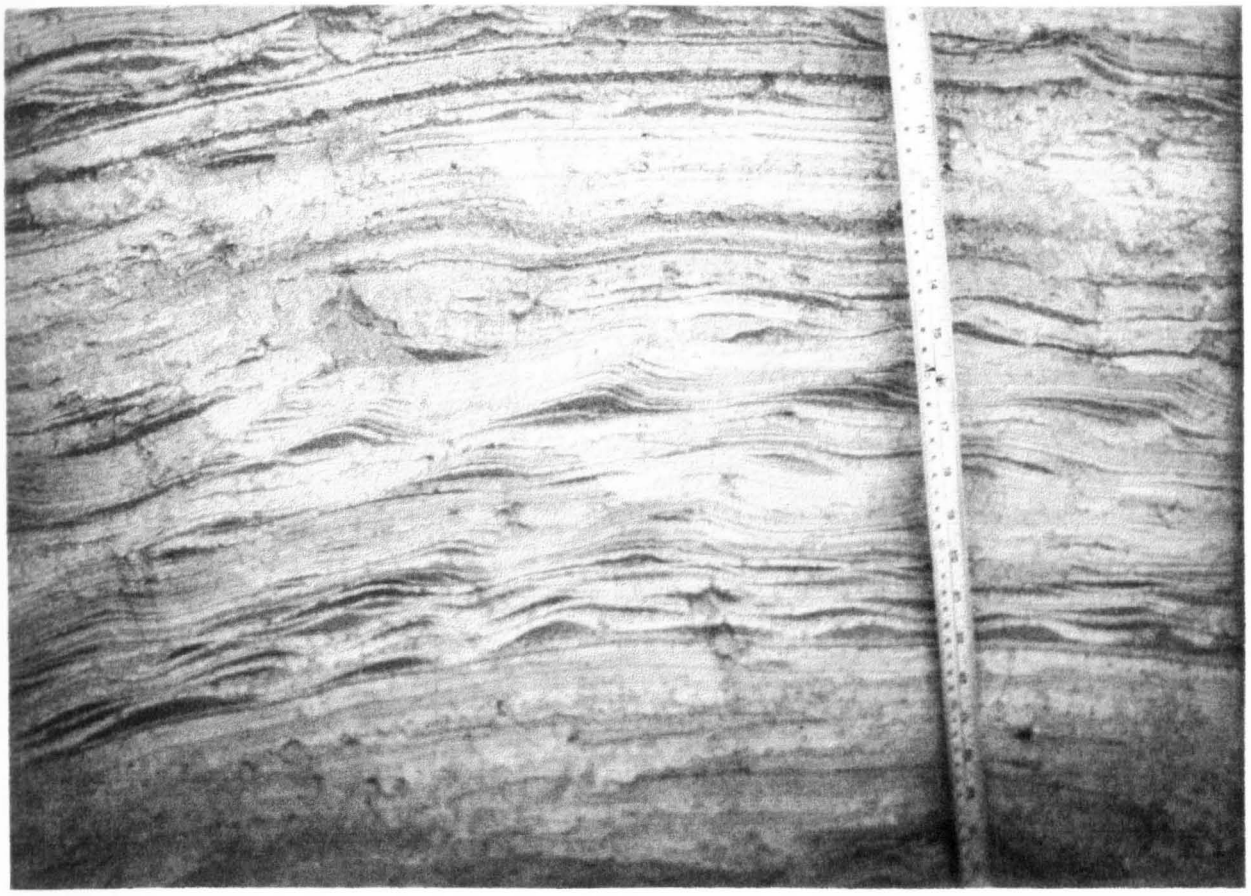

Figure 7 (b)

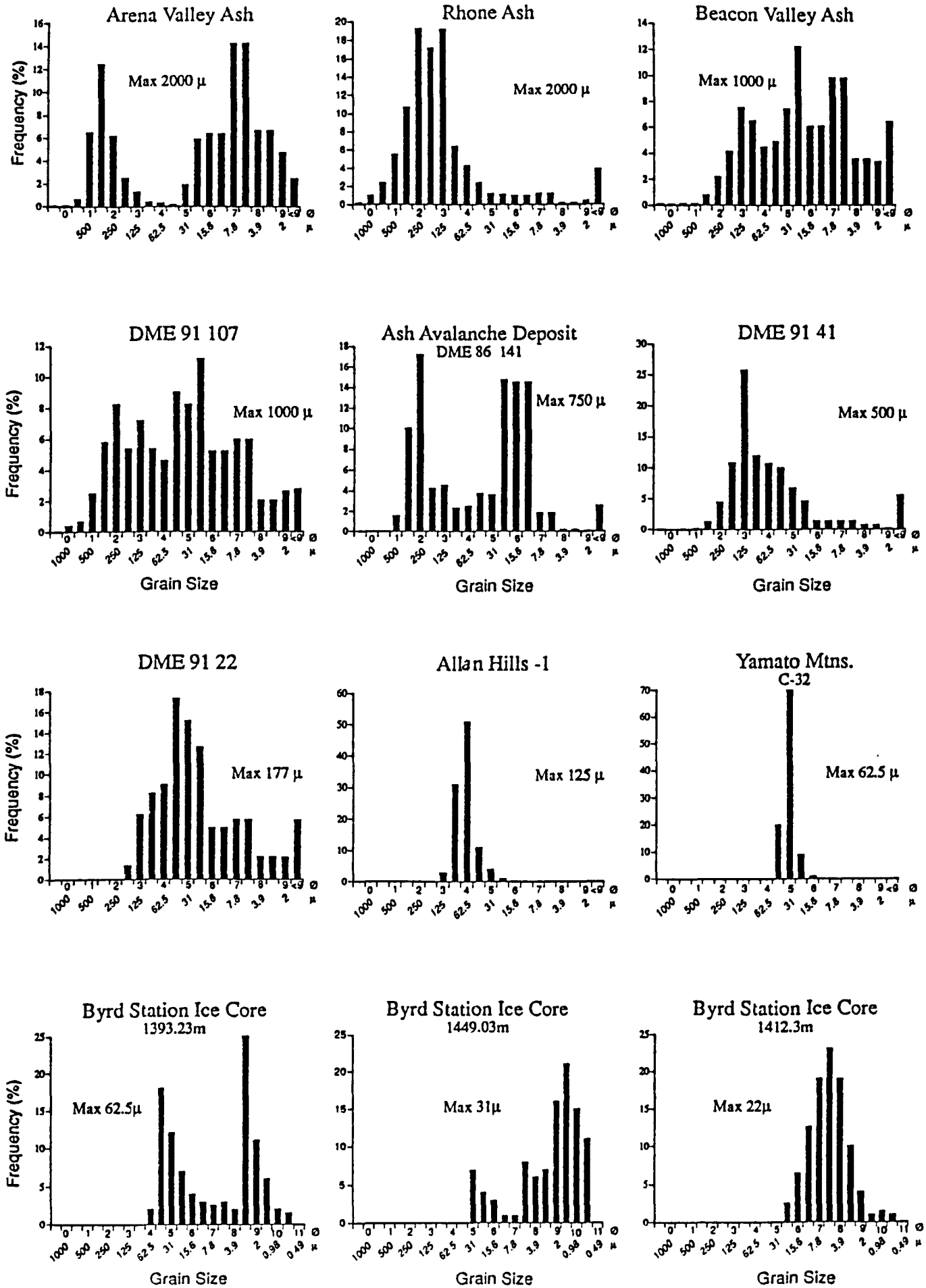
Arena Valley Ash
Max 2000 µ
Rhone Ash
Max 2000 µ
Beacon Valley Ash
Max 1000 µ
DME 91 107
Max 1000 µ
Ash Avalanche Deposit
DME 86 141
Max 750 µ
DME 91 41
Max 500 µ
DME 91 22
Max 177 µ
Allan Hills -1
Max 125 µ
Yamato Mtns.
C-32
Max 62.5 µ
Byrd Station Ice Core
1393.23m
Max 62.5µ
Byrd Station Ice Core
1449.03m
Max 31µ
Byrd Station Ice Core
1412.3m
Max 22µ
Frequency (%)
Grain Size

Figure 8

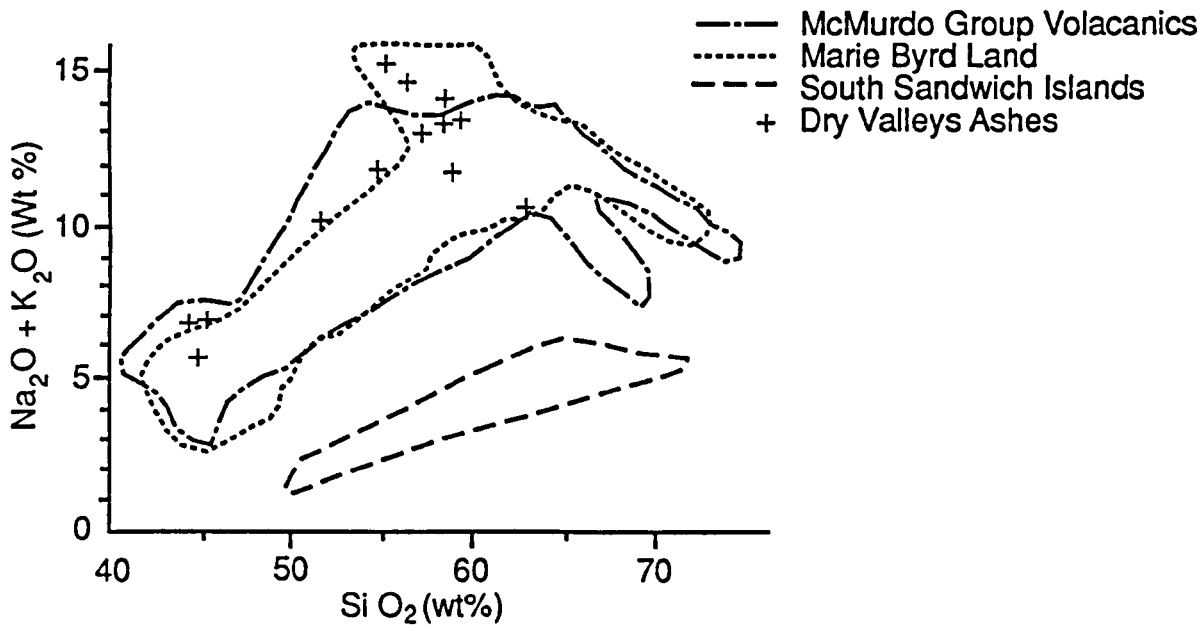
McMurdo Group Volacanics
Marie Byrd Land
South Sandwich Islands
Dry Valleys Ashes
15
10
5
0
40
50
60
70
$Na_2O + K_2O$ (Wt %)
Si O_2 (wt%)

Figure 9

Table 1a. *$^{40}Ar/^{39}Ar$ laser fusion analyses of sanadine from selected ash deposits in the Dry Valleys region.* Sample RAS84-343 is from the matrix of an ash avalanche deposit that mantles a rectilinear slope in the western Asgard Range. Sample TWS87-142C is from the Rhone ash. Sample DMS86-131 is from the matrix of an ash avalanche deposit that mantles a rectilinear slope in upper Arena Valley. Sample DMS87-113 is from the matrix of an ash avalanche deposit that mantles a rectilinear slope in lower Arena Valley. Sample DMS86-86B is the Arena Valley ash.

Sample L#	$^{40}Ar/^{39}Ar$	$^{37}Ar/^{39}Ar$	$^{36}Ar/^{39}Ar$	$^{40}Ar^*/^{39}Ar$	$\%^{40}Ar^*$	Age (Ma)	SD (1σ)	
RAS84-343								
1791-01	5.4036	0.17331	0.00084	5.1686	95.6	13.270	0.167	
1791-02	5.5404	0.06532	0.00106	5.2295	94.4	13.426	0.192	
1791-02B	5.4468	0.03839	0.00067	5.2493	96.4	13.476	0.202	
1791-03	5.3843	0.04879	0.00059	5.2120	96.8	13.381	0.164	
1791-03B	5.2480	0.07228	0.00127	4.8763	92.9	12.522	0.226	
1791-04B	5.8670	0.12315	0.00278	5.0529	86.1	12.974	0.453	
1791-05	5.2995	0.01855	0.00094	5.0228	94.8	12.897	0.091	
1791-06	5.3632	0.06930	0.00086	5.1127	95.3	13.127	0.082	
1791-07	5.3417	0.05382	0.00061	5.1645	96.7	13.259	0.078	
1791-08	5.3663	0.09238	0.00052	5.2178	97.2	13.396	0.082	
1791-09	5.5718	0.08725	0.00221	4.9240	88.4	12.644	0.166	
1791-10	5.5636	0.13972	0.00103	5.2692	94.7	13.527	0.103	
			Weighted Mean		=	**13.212**	**0.034**	**SE**
TWS87-142C								
1796-01	3.1755	0.11376	0.00130	2.7994	88.1	7.199	0.052	
1796-04	3.1682	0.09562	0.00141	2.7579	87.0	7.093	0.095	
1796-05	3.1430	0.10361	0.00126	2.7769	88.3	7.142	0.093	
1796-06	3.1026	0.13082	0.00119	2.7606	89.0	7.100	0.079	
1796-07	3.0357	0.12588	0.00092	2.7737	91.4	7.133	0.059	
1796-08	3.0782	0.11693	0.00101	2.7864	90.5	7.166	0.077	
1796-09	3.0914	0.16183	0.00129	2.7219	88.0	7.000	0.137	
1796-10	3.1762	0.08127	0.00136	2.7779	87.5	7.144	0.113	
			Weighted Mean		=	**7.144**	**0.027**	**SE**
DMS86-131								
5113-02	1.4679	0.04481	0.00000	1.4809	100.0	7.444	0.676	
5113-03	1.4668	0.03782	0.00009	1.4396	98.1	7.237	1.051	
5113-05	1.7351	0.04352	0.00086	1.4823	85.4	7.451	0.489	
5113-06	1.9447	0.03215	0.00140	1.5301	78.7	7.691	0.761	
5113-07	1.6257	0.04128	0.00070	1.4200	87.3	7.138	0.787	
			Weighted Mean		=	**7.422**	**0.037**	**SE**
Detrital grains?								
5113-04	1.8072	0.00043	0.00013	1.7669	97.8	8.878	0.637	
5113-01	2.0091	0.00958	0.00012	1.9729	98.2	9.910	0.335	
DMS87-113								
1794-01	4.7513	0.11444	0.00175	4.2405	89.2	10.894	0.104	
1794-02	4.7750	0.12648	0.00102	4.4810	93.8	11.510	0.085	
1794-08	4.6351	0.04320	0.00078	4.4076	95.1	11.322	0.088	
1794-03	78.0796	0.01741	0.00738	75.8994	97.2	185.690	0.334	
1794-04	58.7546	0.06432	0.00416	57.5321	97.9	142.476	0.576	
1794-05	99.6740	0.03651	0.00238	98.9741	99.3	238.553	0.799	
1794-06	58.4763	0.03399	0.00262	57.7051	98.7	142.888	0.440	
1794-07	106.5401	0.03132	0.01340	102.5835	96.3	246.683	0.846	
1794-09	88.5037	0.01762	0.00358	87.4462	98.8	212.337	0.365	

Sample L#	$^{40}Ar/^{39}Ar$	$^{37}Ar/^{39}Ar$	$^{36}Ar/^{39}Ar$	$^{40}Ar^*/^{39}Ar$	$\%^{40}Ar^*$	Age (Ma)	SD (1σ)	
DMS8686B								
5075-01	0.8850	0.0302	0.00023	0.8177	92.4	4.191	0.203	
5075-02	0.8845	0.0381	0.00020	0.8257	93.3	4.232	0.237	
5075-03	0.8697	0.0485	0.00001	0.8672	99.7	4.444	0.250	
5075-04	0.9169	0.0189	0.00032	0.8201	89.4	4.203	0.239	
5075-05	0.9814	0.0266	0.00052	0.8277	84.3	4.242	0.278	
5075-06	0.9377	0.0305	0.00019	0.8824	94.1	4.522	0.554	
5075-07	0.8860	0.0259	0.00005	0.8697	98.2	4.457	0.422	
5075-08	0.8978	0.0200	0.00015	0.8524	94.9	4.368	0.283	
5075-09	0.9083	0.0335	0.00027	0.8278	91.1	4.242	0.418	
5075-10	0.9242	0.0370	0.00031	0.8320	90.0	4.264	0.528	
5075-11	0.9013	0.0388	0.00013	0.8648	96.0	4.432	0.271	
5075-12	0.9090	0.0349	0.00023	0.8406	92.5	4.308	0.293	
5075-13	0.9072	0.0407	0.00018	0.8540	94.1	4.377	0.334	
5075-14	0.8887	0.0214	0.00021	0.8272	93.1	4.239	0.495	
5075-15	0.8905	0.0444	0.00003	0.8844	99.3	4.532	0.366	
5075-16	0.8843	0.0314	0.00009	0.8578	97.0	4.396	0.169	
5075-17	0.8779	0.0307	0.00008	0.8538	97.2	4.375	0.359	
5075-18	0.9226	0.0118	0.00025	0.8482	91.9	4.347	0.409	
			Mean Age		=	**4.343**	**0.025**	**SE**
			Weighted Mean		=	**4.329**	**0.068**	**SE**

$^{40}Ar^*$ = radiogenic ^{40}Ar
J (Irr. 20) = 0.001428 ± 0.000001
(Irr. 61B) = 0.002792 ± 0.000002 (for DMS86-131 only)
(Irr. 61A2) = 0.002844 ± 0.000006 (for DMS86-86B only)
D = 1.0059 ± 0.0021
Ca $^{39}Ar/^{37}Ar$ = 0.00067 ± 0.00003
Ca $^{36}Ar/^{37}Ar$ = 0.0002582 ± 0.000006
K $^{40}Ar/^{39}Ar$ = 0.002A ± 0.0001

Table 1b. $^{40}Ar/^{39}Ar$ incremental laser heating analyses of glass shards from selected ash deposits in the Dry Valleys region. Sample DMS86-113 (see Table 1a) is from the matrix of an ash avalanche deposit that mantles a rectilinear slope in lower Arena Valley. Sample DMF86-141 is from the same ash avalanche deposit as DMS86-131 in Table 1a. Sample NPS84-327 is the Beacon Valley ash and was collected from a sand wedge in Beacon Valley.

Sample L# / Step	$^{40}Ar/^{39}Ar$	$^{37}Ar/^{39}Ar$	$^{36}Ar/^{39}Ar$	$^{40}Ar^*/^{39}Ar$	$\%^{39}Ar$	$\%^{40}Ar^*$	Age (Ma)	SD (1σ)
DMS86-113								
5089-01A	3.0750	0.2980	0.00081	2.8567	0.5	92.9	14.718	3.439
5089-01B	2.7218	0.1209	0.00079	2.4965	22.1	91.7	12.869	0.146
5089-01C	2.5905	0.1142	0.00031	2.5066	54.4	96.8	12.920	0.060
5089-01D	2.4890	0.1366	0.00005	2.4822	20.8	99.7	12.795	0.141
5089-01E	2.3416	0.0000	-0.01444	6.6057	0.1	282.1	33.852	23.501
5089-01F	2.5887	0.4047	0.00079	2.3834	2.0	92.0	12.287	2.688
DMF86-141								
5088-01A	3.2438	0.1069	0.00612	1.4407	4.2	44.4	7.437	1.544
5088-01B	2.0309	0.0873	0.00208	1.4215	23.2	70.0	7.338	0.260
5088-01C	1.8110	0.0882	0.00121	1.4568	33.4	80.4	7.520	0.288
5088-01D	1.7661	0.0899	0.00112	1.4396	18.5	81.5	7.431	0.239
5088-01E	2.2530	0.0933	0.00288	1.4074	17.8	62.5	7.266	0.287
5088-01F	1.6796	5.0740	0.00278	1.2476	2.9	74.0	6.442	1.517
NPS84-327								
5076-01A	13.5296	0.2821	0.03843	2.1939	0.8	16.2	11.313	1.329
5076-01B	8.7710	0.0741	0.02266	2.0775	15.3	23.7	10.715	0.282
5076-01C	19.3280	0.0943	0.05868	1.9919	14.9	10.3	10.275	0.679
5076-01D	51.2231	0.1087	0.16705	1.8652	14.5	3.6	9.623	1.929
5076-01E	47.7520	0.0914	0.15566	1.7592	10.1	3.7	9.078	1.772
5076-01F	29.4940	0.1180	0.09248	2.1730	44.5	7.4	11.206	0.984

$^{40}Ar^*$ = radiogenic ^{40}Ar
J (Irr. 61A) = 0.00287 ± 0.0000058
D = 1.0059 ± 0.0021
Ca $^{39}Ar/^{37}Ar$ = 0.00067 ± 0.00003
Ca $^{36}Ar/^{37}Ar$ = 0.0002582 ± 0.000006
K $^{40}Ar/^{39}Ar$ = 0.0024 ± 0.0007

Table 2. **Major element analyses (MAC 400 microprobe) of glass shards from selected Dry Valleys ashes.**

MAJOR ELEMENT ANALYSES (WT %) OF VOLCANIC GLASS FROM DRY VALLEYS ASHES								
ASH/ LOCALITY	ARENA VALLEY ASH	BEACON VALLEY ASH	AVALANCHE DEPOSIT	RHONE ASH	QUARTER-MAIN ASH	BEACON VALLEY	ARENA VALLEY	ASGARD RANGE
SAMPLE	87032	87031	DMS-86-131	87024-3	DMS-87-26	DMS-91-107	DMS-86-100B	DMS-91-41
N	6	5	5	6	6	6	6	6
SiO_2	57.3	58.2	57.38 (0.68)	59.6	60.59 (1.96)	53.54 (0.71)	45.60 (1.2)	60.00 (0.66)
TiO_2	0.3	0.3	0.14 (0.02)	0.5	0.00	2.53 (0.36)	4.59 (0.21)	0.72 (0.04)
Al_2O_3	20.1	19.9	19.83 (0.36)	16.5	17.20 (0.68)	18.47 (0.56)	15.79 (0.55)	15.51 (0.19)
FeO	4.3	4.5	6.24 (0.11)	6.1	6.79 (0.47)	8.07 (0.71)	11.49 (0.21)	6.96 (0.34)
MnO	0.3	0.2	0.42 (0.03)	0.3	0.38 (0.05)	0.28 (0.04)	0.22 (0.04)	0.38 (0.02)
MgO	0.3	0.3	0.09 (0.03)	0.3	0.18 (0.05)	2.51 (0.37)	5.07 (0.22)	0.48 (0.05)
CaO	1.5	1.2	0.64 (0.02)	1.7	0.68 (0.07)	4.19 (0.21)	9.47 (0.22)	0.87 (0.03)
Na_2O	7.9	8.7	7.23 (1.3)	8.0	8.22 (0.71)	6.39 (0.16)	4.49 (0.11)	6.71 (0.37)
K_2O	5.0	5.7	3.60 (0.26)	5.1	3.96 (0.36)	2.92 (0.14)	1.80 (0.11)	4.68 (0.16)
TOTAL	96.7	99.0	95.59	98.1	98.08	98.90	98.53	96.33

Total Fe as FeO. N= Number of samples analyzed. Value in parenthesis represents one standard deviation. Analyses of Arena Valley Ash, Beacon Valley Ash (87031), and Rhone Ash kindly provided by W.C. McIntosh.

MAJOR ELEMENT ANALYSES (WT %) OF VOLCANIC GLASS FROM DRY VALLEYS ASHES (CONT.) AND COMPARATIVE ANALYSES OF GLASS IN THE BRYD AND DOME CIRCE ICE CORES, AND IN SURFACE ICE NEAR THE ALLAN HILLS AND YAMATO MOUNTAINS.

ASH/ LOCALITY	ASGARD RANGE	ASGARD RANGE	BYRD STATION ICE CORE[1]	BYRD STATION ICE CORE[2]	DOME CIRCE ICE CORE[3]	ALLAN	YAMATO
SAMPLE	DMS-91-38B	DMS-91-22				ASH[4]	ASH[4]
N	5	6	21	101	16	12	14
SiO_2	58.55 (0.79)	60.98 (0.83)	63.61 (0.59)	61.90 (0.40)	61.67 (0.64)	44.23 (2.25)	57.92 (0.71)
TiO_2	0.41 (0.05)	0.64 (0.30)	0.37 (0.07)	0.54 (0.66)	0.52 (0.04)	3.76 (0.47)	1.00 (0.09)
Al_2O_3	15.25 (0.51)	15.36 (0.30)	15.46 (0.51)	15.01 (0.25)	14.11 (0.38)	16.29 (1.37)	13.98 (0.82)
FeO	8.22 (0.94)	7.25 (0.05)	6.81 (0.91)	7.90 (0.25)	8.79 (0.36)	10.19 (0.78)	11.03 (0.44)
MnO	0.46 (0.05)	0.40 (0.03)	0.20 (0.03)	na	na	0.22 (0.06)	0.23 (0.07)
MgO	0.22 (0.05)	0.23 (0.03)	0.02 (0.01)	0.12 (0.05)	0.06 (0.03)	4.06 (1.02)	2.81 (0.37)
CaO	0.66 (0.10)	1.02 (0.05)	0.91 (1.14)	1.28 (0.13)	1.21 (0.07)	9.91 (2.37)	7.57 (0.25)
Na_2O	7.41 (0.91)	5.67 (0.49)	9.65 (0.22)	7.83 (0.23)	6.58 (0.76)	4.29 (0.86)	2.71 (0.25)
K_2O	4.22 (0.54)	4.09 (0.16)	4.84 (0.13)	4.51 (0.06)	4.40 (0.16)	2.95 (0.50)	0.39 (0.06)
P_2O_5	na	na	na	0.09 (0.02)	0.07 (0.03)	1.57 (0.24)	0.12 (0.07)
Cr_2O_3	na	na	na	na	na	0.01 (0.01)	0.01 (0.01)
NiO	na	na	na	na	na	0.03 (0.03)	0.05 (0.05)
TOTAL	95.41	95.66	99.86	99.18	97.41	97.51	97.82

[1] Ash layer at 1436 m depth (Tube No. 915). Data from Palais (1985).
[2] Mean of analyses from 6 ash layers (788 m, 1457 m, 1487 m, 1500 m, 1594 m, and 1711 m). Original data from Kyle et al. (1981). Adapted from Palais (1985).
[3] Ash layer at 726 m depth. Data from Kyle et al. (1981).
[4] Data from Katsushima et al. (1984).
Total Fe as FeO. N= Number of samples analyzed. Value in parenthesis represents one standard deviation.

Table 3. Grain-size of Dry Valleys ashes and detrital infill of relict sand wedge deposits.

GRAIN-SIZE ANALYSES OF DRY VALLEYS ASHES AND SAND-WEDGE DEPOSITS												
	DRY VALLEYS ASHES							SAND-WEDGE DEPOSITS				
SAMPLE	91-107	91-22	91-41	91-353	86-141	N-347	86-86B	189C	128C	60B	147D	151C
% SAND	39.7	24.8	66.1	86.1	42.3	26.3	30.1	91.7	93.5	96.0	94.6	96.5
% SILT	57.5	69.6	28.4	10.0	55.2	67.3	67.5	5.9	3.7	2.0	2.9	2.0
% CLAY	2.8	5.6	5.5	3.9	2.5	6.4	2.4	2.4	2.8	2.0	2.5	1.5

Sample 86-86B is from the middle unit of the Arena Valley Ash. N-347 is from the Beacon Valley Ash (data kindly provided by N. Potter, Jr.). All sand-wedge deposits are from localities in the Asgard Range.

SUMMARY OF DRY VALLEYS ASH DEPOSITS

DEPOSIT	DESCRIPTION	INTERPRETATION	AGE[1]	SIGNIFICANCE
ARENA VALLEY ASH	30 cm thick ash layer overlying in-situ ventifact pavement.	In-situ airfall ash deposited over pre-existing desert pavement.	**4.34**	Cold-desert conditions in Arena Valley at 4.34 Ma. Central Arena Valley morphology antedates 4.34 Ma.
BEACON VALLEY ASH	Inclined ash wedge (about 50 cm thick) enclosed within relict sand-wedge trough.	In-situ airfall ash deposited within open sand-wedge trough.	**10.4**	Cold-desert conditions in Beacon Valley at 10.4 Ma. Cental Beacon Valley morphology antedates 10.4 Ma.
ARENA VALLEY ASH AVALANCHES	Ash-rich debris tongues overlying steep, rectilinear valley walls.	Penecontemporaneous airfall deposition and mass wasting on steep valley slopes.	**7.4** **13.0**	No slope development since ash deposition. Implies no significant atmospheric warming in Arena Valley since at least late-Miocene time.
RHONE ASH	Stratified and deformed layers of volcanic ash mixed with waterlain sediment, flow till, and lodgement till.	Supraglacial deposition of ash that fell on Taylor Glacier ablation surface.	**7.1**	Taylor Glacier expansion at 7.1 Ma. Morphology of central Taylor Valley at ash site antedates 7.1 Ma.

[1] Laser fusion $^{40}Ar/^{39}Ar$ dates from Table 1. Mean ages in millions of years.

CHAPTER FOUR

Miocene Glacial Stratigraphy and Landscape Evolution of the Western Asgard Range, Antarctica

ABSTRACT

$^{40}Ar/^{39}Ar$ dated in-situ volcanic ashfall deposits indicate that the surficial stratigraphy of the western Asgard Range in the Dry Valleys region extends back at least to 15.0 Ma. The preservation of Miocene and Pliocene colluvium and drift on valley slopes shows that major bedrock landforms are relict and that little slope evolution has occurred during at least the last 15.0 Ma. Major bedrock landforms can be compared directly with buttes, mesas, box canyons, and escarpments of platform deserts. Although glaciers played a role in shaping the present topography of the western Asgard Range, the main landforms were probably cut by progressive scarp retreat, propagation of embayments with theater-shaped heads, and isolation of buttes and mesas prior to 15.0 Ma.

We also recognize a phase of wet-based alpine glacier expansion in theater-headed embayments prior to 15.0 Ma ago, along with a late-Miocene phase of northeast-flowing ice-sheet overriding between 14.8/ 15.2 Ma and 13.6 Ma. However, there is no evidence for notable glacier expansion during the last 13.6 Ma. Instead, in-situ ashfall deposits indicate persistent hyper-arid, cold-desert conditions with only minor advance (less than 2.5 km) of rock glaciers and glacierets at valley heads. Our results are consistent with Pliocene stability rather than meltdown of the adjacent East Antarctic Ice Sheet.

INTRODUCTION

Antarctica contains 90% of the ice on Earth, encompassed in a marine West Antarctic and a terrestrial East Antarctic Ice Sheet. Extensive Antarctic deglaciation would raise eustatic sea level, modify global energy budgets, affect planetary albedo, and alter ocean-and-atmosphere dynamics. Thus the response of Antarctic ice to global warming is a problem that could affect nearly all disciplines.

Particularly relevant to this problem is the behavior of the huge East Antarctic Ice Sheet during intervals of Pliocene warmth when global atmospheric temperatures slightly exceeded present values (Dowsett et al., 1992). Did the ice sheet expand, as might be expected if snowfall intensified over Antarctica while climate warmed only moderately (Huybrechts, 1992; Oerlemans, 1982)? Did the ice sheet undergo surface meltdown from dramatic Pliocene warming of 20°-25°C (Webb et al., 1984; Barrett, 1991)? Or did it remain essentially unchanged, with Pliocene warming in some parts of Antarctica restricted to less than 3°C (Marchant et al., 1993a)? The answers to these questions afford insights on future sea-level change and ocean dynamics, because postulated greenhouse warming is expected to raise atmospheric temperatures to levels last experienced during mid-Pliocene time.

At present, two hypotheses have been advanced with regard to East Antarctic Ice Sheet dynamics. The traditional view (the stability hypothesis) is that the present polar East Antarctic Ice Sheet developed during middle-Miocene time and has since experienced only modest fluctuations in size (Kennett, 1982). This stability hypothesis is based predominantly on the marine oxygen-isotope record, which shows a major and sustained increase in dO^{18} values beginning at about 14 Ma ago that is interpreted to represent ice buildup on Antarctica (Shackleton and Kennett, 1975; Savin et al., 1975, Kennett, 1982; Miller et al., 1987). An alternate view (the deglaciation hypothesis) is of a dynamic temperate ice sheet that waxed and waned repeatedly across East Antarctica, with the most recent deglacial episode occurring around 3.0 Ma ago (Webb et al., 1984; Barrett et al., 1992). The deglaciation hypothesis is based primarily on interpretations of reworked marine diatoms and in-situ fossil *Nothofagus* wood (Southern Beech) within Sirius Group outcrops high in the Transantarctic Mountains (Webb and Harwood, 1987; Webb et al., 1984). The latter deposit is comprised of glacial tills and stratified diamictons deposited by wet-based glaciers. Proponents of the deglaciation hypothesis argue that the marine diatoms inhabited relatively warm (2°-5°C) and open seaways in interior East Antarctica (Harwood, 1986). They were subsequently stripped from these basins and redeposited within Sirius Group outcrops by an expanded East Antarctic Ice Sheet that overtopped the Transantarctic Mountains, which at the time supported growth of Nothofagus scrub vegetation (Barrett et al., 1992).

These hypotheses are mutually contradictory and each has testable predictions. One fundamental test of the deglaciation hypothesis is whether the Transantarctic Mountains were overridden by a wet-based ice sheet shortly after 3.0 Ma ago. Such Pliocene expansion is required to emplace Sirius Group deposits with reworked marine diatoms at high elevations in the Transantarctic Mountains (Webb et al., 1984; Webb and Harwood, 1991; Barrett et al., 1992). A second test involves an analysis of the physical characteristics of Miocene-to-Pliocene age sediments exposed alongside the East Antarctic Ice Sheet in terms of paleoclimate. If the stability hypothesis is correct, then such Miocene-Pliocene age sediments should reflect persistent cold-desert conditions by exhibiting frozen-ground contraction cracks (sand-wedges), desert pavements, ventifacts, ultraxerous soil, and tills deposited by cold-based glaciers. On the other hand, if the deglaciation hypothesis is correct, then Pliocene-age sediments should show evidence for climate warming in the form of glacial outwash, lacustrine deposits, mudflows, levees, stream channels, and tills deposited by wet-based, temperate glaciers.

To conduct these definitive tests, and in a larger context to define the history of late Cenozoic ice-sheet fluctuations and paleoclimate in the Ross Sea region, we mapped the surficial deposits and geomorphology of the western Asgard Range in the Dry Valleys region of southern Victoria Land (Fig. 1). This mountain range is ideal for recording ice-sheet fluctuations and paleoclimate change because it is adjacent to the East Antarctic Ice Sheet and because it exhibits widespread drift and colluvium, along with glacial erosional features. $^{40}Ar/^{39}Ar$ analyses of in-situ volcanic ash deposits derived from offshore volcanoes afford chronologic control (e.g., Marchant et al., 1993a; 1993b).

The combination of butte-and-mesa bedrock landscape, glacial erosional features, and widespread diamictons in the western Asgard Range attest to a long and varied history of landscape evolution. Our goal here is to bring together all aspects of this assemblage to explain the landscape evolution and late Cenozoic glacial history. We start with a description of the geographic setting and morphology of the western Asgard Range. We then describe surficial sediments that rest on this morphology and finish with an analysis that ties together the bedrock morphology and stratigraphy of the surficial deposits.

GEOGRAPHIC SETTING

Transantarctic Mountains. The Transantarctic Mountains, which expose part of the uplifted and tilted shoulder of the West Antarctic Rift System (Behrendt and Cooper, 1990, 1991), trend nearly across the continent and commonly rise to 1500-2500 m elevation (less commonly to 2500-4000 m elevation). These mountains exhibit a steep, high front adjacent to the Ross Embayment and are submerged by the present-day East Antarctic Ice Sheet on the inland flank. Most transverse valleys that trend through the mountains carry outlet glaciers of the East Antarctic Ice Sheet. Only in the Dry Valleys region are transverse valleys largely free of ice.

The Dry Valleys region includes 4000 km^2 of mountainous desert topography between the McMurdo Sound sector of the Ross Sea and the East Antarctic polar plateau (Fig. 1). A basement complex of lower Paleozoic igneous and metamorphic rocks is overlain by nearly flat-lying Devonian-to-Triassic sandstones, siltstones, and conglomerates of the Beacon Supergroup. These are all intruded by Jurassic-age Ferrar Dolerite and Cenozoic volcanics. Cenozoic volcanism occurs in and adjacent to the Dry Valleys region (Kyle, 1990). The main transverse valleys (Taylor, Wright, and Victoria System) are separated by the Asgard and Olympus Ranges. These ranges are sandstone-and-dolerite capped mountain blocks that trend east-west and rise above 1500 m elevation.

Alpine glacierets and permanent ice fields in the western Asgard Range are essentially restricted to topographic areas that collect windblown snow (Fig. 2). Under the present cold-desert, hyper-arid climate, such small glaciers are cold-based, non-erosive (Holdsworth and Bull, 1970), and lack surface-melting ablation zones. To estimate mean annual atmospheric temperature in the western Asgard Range, we must refer to measurements taken beside Lake Vanda at 123 m elevation in central Wright Valley. Here mean annual temperature is -19.8°C (Schwerdtfeger, 1984) and annual precipitation is equivalent to less than 10 mm of water (Keys, 1980). Assuming an average lapse rate of 1°C/100 m elevation rise (Robin, 1988; Marchant et al., 1993a), mean annual temperature in the western Asgard Range valleys, at an elevation of 1400 to 1500 m, is about -35°C.

WESTERN ASGARD MORPHOLOGY

Background. The morphology of the Dry Valleys region, and in particular the western Asgard and Olympus

Ranges, has been studied by several workers over the last 20 years (Selby, 1971, 1974; Selby and Wilson, 1971; Augustinus and Selby, 1990; Shaw and Healy, 1977; Chinn, 1980; Calkin, 1974; Wilson, 1973; Denton et al., 1984, this volume; Sugden et al., 1994). Individual landforms were variously interpreted as arising from temperate cirque glaciation, along with salt weathering, nivation, and wind deflation in a cold-desert environment, or from some combination of these processes. The dominant denudational process was postulated to have been cirque glaciation under temperate climatic conditions, followed by extensive backwearing and development of rectilinear slopes in a rainless desert environment. On the basis of continental drift and paleomagnetic data, Wilson (1973) suggested that the last time the Dry Valleys region could have been warm enough for temperate cirque glaciation was in early Oligocene time.

Mayewski (1975), Denton et al. (1984), and Webb et al. (1984) concluded independently that during late Neogene time much of the Transantarctic Mountains was overridden by an expanded East Antarctic Ice Sheet. Denton et al. (1984) postulated that in the Dry Valleys region a suite of stossed slopes, lee troughs, breached mountain divides, bedrock striations, subglacial meltwater channels, and irregular till patches reflect bedrock erosion beneath northeast-flowing overriding ice. On the basis of available chronologic data, Denton et al. (1984) concluded that the most recent overriding episode postdated middle Miocene time and was most probably mid-to-late Pliocene in age. By the end of the 1980s the overall morphology of the western Asgard Range was inferred to represent the culmination of early cirque glaciation, a long interval of salt weathering and wind deflation, and erosion beneath overriding glacier ice.

Sugden et al. (1994) and Denton et al. (1994) presented a new synthesis of Antarctic landscape evolution that includes spatial analyses of all major landforms in the Dry Valleys region. They recognized that the valley systems are integrated to form a graded, arborescent valley network incised into high-level erosional planation surfaces. The overall pattern is atypical of alpine glacial landscapes, but instead closely resembles the morphologic distribution of valleys and planation surfaces associated with stream dissection and backwearing of scarps to form an escarpment landscape similar to that of platform deserts in semi-arid environments elsewhere in the world (Mabbutt, 1977). The recent discovery of in-situ Pliocene and Miocene ashfall deposits on valley slopes and floors (Marchant et al., 1993a, 1993b, 1994) indicates that most large-scale bedrock landforms in the Dry Valleys region are relict and that weathering and wind deflation have caused only limited modification of the Dry Valleys landscape during the last 15.0 Ma. These discoveries led to an interpretation of relict landforms in terms of ancient erosion under semi-arid or highly seasonal climate conditions along a passive continental margin, beginning with renewed rifting in the Ross Sea basin about 55 Ma ago. This long-term landscape development is tied into the tectonic evolution of the Transantarctic Mountains.

A current task for geomorphologists is to test the various hypotheses of Dry Valleys landscape development by examining the morphology of individual mountain ranges. Our goal here is to assess the relative importance of glacial erosion, semi-arid(?) erosion (scarp backwearing by stream dissection, groundwater sapping and other processes), salt weathering, and wind deflation in the development of the western Asgard topography.

Macro-morphology

The western Asgard Range consists of a high-elevation tableland dissected by theater-headed valleys of constant width, flat floors, and a few stubby tributaries (Figs. 2 and 3). The high-elevation (2000 m) tableland extends westward beneath the East Antarctic Ice Sheet and is bounded on its eastern margin by a sharp escarpment, which represents the marker feature of the landscape (Fig. 3). The upper surface of this dolerite-capped tableland is conformable with the upper surface of dissected dolerite-capped plateaus that fringe valleys in the Quartermain Mountains and in the Olympus Range. Small, north- and south-facing valleys, which are nearly free of ice, are cut either into this tableland or into the sinuous divide that separates upper Taylor and Wright Valleys. These valleys grade from well-developed box canyons in the west to elongate through valleys in the east. The floors of north-facing valleys grade from 1600 m elevation in the west to 1400 m in the east. In contrast, all south-facing valleys (collectively known as the Inland Forts) lie at about 1350 m elevation. At Inland Forts, narrow saddles connect north- and south-facing valleys and give way to gently sloping terraces that merge with wide, flat valley floors. With one exception, valley floors are incised into Altar Mountain Sandstone and Arena Sandstone. The one exception is where granite and dolerite bedrock crop out in central and lower Nibelungen Valley.

Drainage divides in the western Asgard Range show progressive dissection with distance eastward from the interior tableland. The divides also show an overall decrease in summit elevation (Fig. 3). Divides at the western margin of the range are capped by thick dolerite sills, the tops of which average 2000 m in elevation. Farther to the east, the divides are lower and are cut in sandstone. Here flat-topped buttes, mesas, and needles, comprised predominantly of sandstone bedrock surmounted by small dolerite caps, rise to elevations between 1600 and 1800 m. Smooth sandstone platforms at 1600 m elevation separate Nibelungen Valley from adjacent valleys to the east and west. Similar platforms separate two unnamed valleys in Inland Forts (East and West Groins in Fig. 2).

Well-developed rectilinear slopes (inclined 28° to 36°), with alternating bare-bedrock and debris-covered segments beneath near-vertical cliff faces, dominate the western Asgard Range. The cliff faces range from 25 to 175 m in height and are composed of thick, horizontal sills of jointed dolerite bedrock and resistant Beacon Heights Orthoquartzite. The rectilinear slopes beneath these free faces lack gullies, rills, and channels and are incised in Arena Sandstone bedrock.

Meso-morphology

Superimposed on valley floors, headwalls, divides, and rectilinear slopes in the western Asgard Range is a suite of channels, basins, and stoss-and-lee forms. These features are integrated to form a well-developed landform system. Stoss-and-lee forms grade downvalley into channel-and-pothole systems, which in turn grade into wide basins that truncate surface sediments and expose unweathered sandstone bedrock.

Stoss-and-lee slopes. The tops of saddles at the heads of Njord, Folkvangar, and Sessrumnir Valleys show smooth, convex south-facing slopes and angular, concave north-facing slopes. For the most part, the slopes below the saddles are rectilinear and unmodified by stoss-and-lee topography. The resultant form at the top of saddles is similar to that of a roche moutonnée. The stossed saddles at the heads of Sessrumnir and Njord Valleys are bare bedrock and grade downvalley into elongate tracts of exposed sandstone bedrock. In Njord Valley, a shallow basin that exposes Arena Sandstone bedrock extends northward from the stossed saddle at the valley head for a distance of 1.5 km and cuts through a variety of unconsolidated sediments. Closed bedrock depressions as much as 30 m across and 15 m deep occur at the crest of saddles in upper Njord and Folkvangar Valleys.

Stoss-and-lee slopes are best developed where valley headwalls are below 1700 m elevation. They do not occur in sandstone bedrock at the heads of either the westernmost valleys (where the tableland rises to 2000 m elevation) or the easternmost valleys (where Round Mountain and St. Pauls Mountain both rise above 2000 m elevation). Stripping and erosion of unconsolidated sediments to bare bedrock is best developed in the lee of stossed valley headwalls. A striking example of this is the difference between stripped sediments in Njord Valley on the one hand and continuous unconsolidated deposits in adjacent valleys on the other (Fig. 2). Remnants of unconsolidated sediments within and beside stripped zones commonly show sharp edges that stand 0.5 m to 1.5 m in relief above weathered sandstone bedrock.

Channel systems. A system of anastomosing channels and potholes is incised along the western and northern margins of the dolerite-capped sandstone ridge that separates Sessrumnir and Folkvangar Valleys (Sugden et al., 1991). The channel system begins at about 1700 m elevation at the base of a rectilinear slope on the lee side of the stossed bedrock saddle at the headwall of Sessrumnir Valley. It falls northward for about 2.5 km, truncates widespread outcrops of Asgard and Jotunheim tills (see below), and grades into a wide, sandstone-floored basin at about 1500 m elevation. The main channel, which runs down the western margin of the ridge, shows a stepped long profile interrupted by potholes, rock bars, and reverse gradient slopes. Tributary channels (each as much as 20 m deep and 75 m across) trend obliquely across the western and northern flanks of the ridge and join the main channel in ever increasing numbers to the north. Potholes commonly occur at the confluence of one or more tributary channels, at sharp corners within individual channels, and on the surface of smooth platforms between

channels. The channel system lacks debris except for ice-cemented sand dunes that occur within the largest potholes and along the north-facing flank of east-west trending tributary channels.

A second and less-extensive channel system covering 300 m^2 occurs on top of the smooth sandstone platform between Nibelungen and Jotunheim Valleys. This second system begins at the foot of a horseshoe-shaped bedrock step (nearly 20 m in height) that opens northward onto a wide, smooth bedrock basin. Channels about 1.0 m deep are incised along the western margin of this basin. Potholes occur at the base of the bedrock step and at the confluence of two or more channels. Two isolated sandstone bedrock mesas, each 3 to 5 m in height, punctuate the otherwise smooth center of the basin floor.

Streamlined forms. Widespread bedrock outcrops on the high-elevation tableland at the western edge of the Asgard Range are free of overlying debris and show streamlined rock-drumlin and whaleback forms with a relief of 10 to 30 m. The overall linear ridge-and-groove topography generally trends northeast-southwest and extends westward beneath East Antarctic ice. Streamlined whaleback forms are best developed on resistant igneous rocks near the eastern edge of the tableland.

Basins. Basins are incised into surficial sediments and sandstone bedrock in the western Asgard Range. Basins between 1 and 10 m deep, 10 and 150 m wide, and as much as 500 m long cut through all unconsolidated units that are stratigraphically older than the rock glacier deposits at valley heads. The basins are deepest and best developed where they are incised into Altar Mountain Sandstone and Arena Sandstone bedrock. In upper Nibelungen Valley, the margin of a large sandstone basin also cuts into granite and dolerite bedrock. In upper Njord Valley and at the mouth of Sessrumnir Valley, basins converge laterally to form wide areas of exposed bedrock (Fig. 2). The boundaries of such composite basins are irregular in plan view. Unconsolidated deposits that are cut by these basins show sharp, serrated edges.

The floors of some depressions are unconsolidated diamictons rather than sandstone bedrock. For example, in central Koenig Valley a particularly well-developed, horseshoe-shaped depression cuts obliquely through a variety of deposits (Asgard till, Koenig colluvium, and Sessrumnir till, see below), exposing only a small area of sandstone bedrock at the northern end ($< 10\%$ of the total area of the basin floor).

STRATIGRAPHY OF SURFICIAL DEPOSITS

Figures 4 and 5 show the distribution of mapped units in the western Asgard Range. Table 1 summarizes the physical characteristics, areal distribution, stratigraphic position, and isotopic age of each mapped unit. The

dominant feature of the maps is that unconsolidated deposits exhibit highly irregular outcrops such that isolated till and colluvial patches of different relative and isotopic ages merge at the surface without relief. The overall pattern shows small, disjointed, and irregularly shaped outcrops (between 20 m^2 and 2 km^2) that create an intricate surface mosaic. In stratigraphic section, unconsolidated deposits show sharp contacts and many units contain inclined beds that are truncated at the present ground surface. The general impression is that surficial sediments in the western Asgard Range have been stripped to create smooth surface transitions across disjointed and irregularly shaped outcrops. The one exception is rock-glacier deposits at several valley heads, which are complete and show considerable surface relief.

Areally Extensive Drifts

Sessrumnir till. The stratigraphically lowest unit is termed the Sessrumnir till. This unit crops out at the base of slight topographic depressions in Koenig, Sessrumnir, and Nibelungen Valleys and at the surface of wide plains at the mouths of Koenig and Nibelungen Valleys (Figs. 4 and 5). It also rests on rectilinear sandstone bedrock walls in lower Nibelungen Valley.

Sessrumnir till is an unsorted, unstratified, and unconsolidated sandy diamicton with numerous striated and molded dolerite clasts. The till contains siltstone clasts (some of which are striated) but lacks sandstone clasts, even though in most places Sessrumnir till rests on weathered sandstone bedrock or on sandstone residuum. The siltstone clasts come from the Aztec Siltstone Formation, which occurs just above Beacon Heights Orthoquartzite in stratigraphic section. Remnants of Aztec Siltstone nearest Nibelungen, Sessrumnir, and Koenig Valleys occur in the westernmost Asgard Range at Mt. Fleming and in the Quartermain Mountains, about 30 km southwest of the western Asgard Range.

Bedrock striations occur beneath Sessrumnir till at two localities. One occurs in upper Nibelungen Valley, where a thin veneer of Sessrumnir till overlies dolerite bedrock. Here, striations trend N 10° E to N 25° E, diverging around the north faces of bedrock rises. Striated bedrock knobs and small-scale roches moutonnées are preferentially smoothed on south-facing flanks, indicating downvalley ice flow. The second striation locality occurs in central Sessrumnir Valley, where Sessrumnir till up to 1.5 m thick overlies slightly displaced sandstone bedrock slabs, each about 5 to 10 m in diameter. The slabs show two sets of cross-cutting striations, the older set trending N 20° E and the younger set N 5° W. Fabric analyses, measured from rocks at the surface and within hand-dug till sections, show trends consistent with underlying bedrock striations (N 5° E to N 45° E). In stratigraphic section, the Sessrumnir till is overlain by highly oxidized Koenig colluvium.

The striated and molded dolerite clasts, unsorted texture, and glacial striations beneath Sessrumnir till indicate an origin beneath wet-based ice. If enclosed siltstone clasts represent far-travelled erratics, then glacier ice must have flowed across the Asgard Range from southwest to northeast. At present, we can not be sure if Aztec Siltstones capped valley headwalls above Beacon Heights Orthoquartzite during deposition of Sessrumnir till, and have since been removed by erosion. Therefore it is still possible that Sessrumnir till represents local alpine glaciation of the western Asgard Range.

Inland Forts till. A silt-rich and unconsolidated diamicton mantles the floor of Inland Forts at 1300 m to 1400 m elevation between East Groin and Round Mountain (Ackert, 1990). The deposit extends from the two small alpine glaciers at the head of Inland Forts to permanent snow banks alongside the margin of upper Taylor Glacier (Fig. 2). The till shows a smooth surface and thins to feather edges along rectilinear bedrock slopes at East Groin. Inland Forts till is structureless and massive. It is composed predominantly of sandstone (both in the matrix and gravel fractions) with less than 10% dolerite clasts. There are no erratic lithologies. Nearly 6% of the sandstone clasts show well-developed striations and glacial molding.

Inland Forts till rests on striated sandstone bedrock at two localities. One is near the base of Round Mountain, where exposed striated bedrock shows well-developed quartz rinds and siliceous crusts, suggestive of long-term exposure in a desert environment (Weed and Norton, 1991). Here, striations trend about S 20° W to S 40° W; this is consistent with trends derived from bullet boulders measured nearby at the till surface (Ackert, 1990). The second striation locality occurs near the base of East Groin beneath a thin veneer of Inland Forts till. Striation trends are consistent with those near Round Mountain and range from S 25° W to S 35° W. At both striation localities the steep side of well-developed concentric fractures faces to the north, indicating an ice-flow direction from north to south. Typical stoss-and-lee forms also occur in association with the striated bedrock pavement. Smoothed bedrock surfaces face northeast, whereas rough, angular cliffs face southwest. Such forms are consistent with ice-flow from north to south.

The striated bedrock, glacially molded and striated clasts, bullet boulders, and poor sorting all indicate that Inland Forts till was deposited beneath wet-based glacier ice. Crescentic bedrock gouges, stoss-and-lee bedrock molding, and the absence of far-travelled erratics show that Inland Forts till was deposited by a southward flowing, wet-based glacier that occupied Inland Forts. The preservation of rectilinear slopes beneath Inland Forts till implies that glacial ice, although wet-based and erosive at valley bottoms, failed to eradicate pre-existing bedrock landforms.

Asgard till. A silt-rich and unconsolidated diamicton containing granite erratics and striated sandstone and dolerite clasts occurs in the mouths of north-facing valleys in the western Asgard Range alongside Wright Valley (Figs. 2,

4, and 5). This diamicton crops out either as widespread sheets, the surface expression of which forms a lobate pattern that projects southward into the Asgard Range valleys, or as discontinuous and irregularly shaped patches. It overlies rectilinear slopes at the mouth of Sessrumnir Valley. The unit was informally termed the Asgard till (Ackert, 1990), because it represents the most widespread surface deposit in the western Asgard Range. The upper limit of exposed Asgard till decreases eastward, from 1650 m in Sessrumnir Valley to 1450 m at the mouth of Jotunheim Valley. The only ice-marginal feature associated with Asgard till is a small, arcuate moraine segment (75 m long, 10 m wide, and 2 m high) that opens toward Wright Valley and the mouth of Sessrumnir Valley.

Asgard till everywhere shows a complex internal stratigraphy composed of inclined and near-horizontal lenses of well-stratified sands, silts, and gravels interbedded with a boulder-rich diamicton. Sand layers inclined between 10° and 45° are truncated at the ground surface (Fig. 6). Deformation structures, such as folds, faults, and flames, occur in about 5% of the hand-dug sections and are best developed within, and at the contact between, fine sand-and-silt layers. In places, narrow lenses of silt 3 to 10 cm thick are draped over and around cobbles.

About 5% of the sandstone and 10% of the dolerite clasts within Asgard till show glacial molding and striated facets. Erratics include cobbles of the Lawson Formation and the Feather Conglomerate. Lawson Granodiorite crops out on the south wall of Wright Valley about 200 m in elevation below the lip of the Asgard Range valleys, whereas the Feather Conglomerate crops out along the north face of Mt. Fleming, in the westernmost Asgard Range (McKelvey et al., 1972). Conspicuously absent from Asgard till are erratics of Aztec Siltstone (which occur within Sessrumnir till), Vanda Granite (an alkali-rich granite that crops out in central Wright Valley), and meta-igneous rocks of the basement complex (which occur in eastern Wright Valley).

Surface boulders embedded within the Asgard and Sessrumnir tills are aligned in parallel rows in lower Nibelungen Valley (Fig. 7). These boulder rows, spaced 1 to 2 m apart, trend about N 5° E and extend downvalley from a large basin that exposes dolerite and granite bedrock. The boulders overlie eroded till remnants that are stripped and planed smooth. Individual rows are about 500 m long. Boulders are composed of sandstone and dolerite, with dolerite boulders overlying Sessrumnir till and sandstone boulders resting on Asgard till.

Asgard till overlies weathered Koenig colluvium in hand-dug stratigraphic sections in Koenig, Sessrumnir, Njord, and Nibelungen Valleys. Stratigraphic contacts range from sharp to gradational. Sharp contacts generally occur at elevations above 1500 m. Wherever a sharp contact is exposed in section, a buried cobble and boulder pavement separates Asgard till from underlying Koenig colluvium. At 1600 m elevation in central Sessrumnir Valley a relict, buried sand wedge projects down into Koenig colluvium. The morphologic form of this wedge is preserved in detail and is infilled with overlying Asgard till. Isolated dolerite ventifacts, presumably derived from erosion of underlying Koenig colluvium, occur in hand-dug sections at the base of Asgard till below 1450 m elevation at the

mouths of Sessrumnir and Nibelungen Valleys.

The striated and molded clasts, internal stratification, poor sorting, lobate outcrop pattern, and erratic lithologies within Asgard till together suggest glacial deposition beneath ice lobes that spilled southward into the Asgard Range valleys from an outlet glacier that filled Wright Valley. A current analogue is the Taylor Glacier, which feeds lobes that project southward into the mouths of north-facing valleys in the Quartermain Mountains. We suggest an inland source for the ice which deposited Asgard till on the basis of the provenance of erratics (for example, the Feather Conglomerate), the absence of Vida Granite and meta-igneous erratics of the basement complex (which crops out in eastern Wright Valley), and the decrease in elevation from west to east. In-situ ventifact pavements and sand-wedges preserved above 1500 m elevation beneath Asgard till indicate that ice tongues above 1500 m elevation were probably cold-based. Wet-based glacial conditions required to produce striated and molded clasts most probably occurred beneath thick ice at elevations below 1500 m, for example at the base of Wright Valley.

Colluvium

Koenig colluvium. A highly oxidized (5YR 8/4) and poorly sorted diamicton, composed predominantly of well-developed ventifacts set within a sandy matrix, crops out in isolated patches throughout ice-free valleys of the western Asgard Range (Figs. 4 and 5). This deposit is easily identifiable by its bright orange color and well-developed ventifacts. Koenig colluvium reaches its maximum observed thickness of 95 cm at the base of rectilinear slopes. Oxidation occurs uniformly everywhere to the base of the deposit. Ventifacts within Koenig colluvium are faceted on all sides and are composed predominantly of Arena Sandstone, Ferrar Dolerite, Beacon Heights Orthoquartzite, and Altar Mountain Sandstone. Sandstone clasts bear siliceous crusts and quartz rinds from 2 to 10 mm thick. Development of such weathering features requires long-term subaerial exposure in a desert environment (Weed and Norton, 1991). Dolerite cobbles within Koenig colluvium are commonly pitted. There are no striated, molded, or glacially polished clasts in Koenig colluvium. Where it crops out adjacent to granite bedrock in upper Nibelungen Valley, Koenig colluvium contains 75% weathered granite (in the >2 mm gravel fraction). The matrix (< 2.0 mm fraction) is predominantly oxidized quartz sand grains, weathered dolerite grus, and (in Nibelungen Valley) weathered granite grus. Koenig colluvium lacks discernible waterlain structures.

In hand-dug stratigraphic sections, Koenig colluvium overlies unoxidized or, in at least one locality, slightly oxidized Sessrumnir till. In most places the basal contact is sharp such that in hand-dug sections the transition from colluvium to underlying till occurs over a vertical distance of 1 to 2 cm. In central Sessrumnir Valley, where the basal contact is slightly gradational, the transition from Koenig colluvium to Sessrumnir till occurs over 5 to 15 cm. Most of these stratigraphic contacts are not parallel with, and are truncated by, the present surface topography. The overall impression is that sediment has been planed at the surface. Ventifacts within Koenig colluvium are oriented

preferentially such that long axes lie parallel with underlying stratigraphic contacts.

Koenig colluvium represents the products of minor hillslope degradation and subaerial weathering in a desert climate. We postulate that hillslope erosion was minor during this interval because the maximum thickness of Koenig colluvium in hand-dug sections is only 60 to 95 cm, and because Sessrumnir till, which directly underlies Koenig colluvium in stratigraphic section, still mantles rectilinear valley walls in Nibelungen and Sessrumnir Valleys. Hence, we infer that most of the bedrock morphology of the western Asgard Range predates deposition of Koenig colluvium. We also infer that desert conditions existed during the Koenig non-glacial interval because the ventifacts and extent of oxidation imply subaerial weathering in a dry climate.

Undifferentiated colluvium. About 85% of the rectilinear valley walls in the western Asgard Range are covered by a thin veneer (10-75 cm) of moderately weathered, poorly sorted, gravel-rich colluvium (Figs 4 and 5). This undifferentiated colluvium extends downslope from exposed bedrock outcrops and/or bedrock regolith. The undifferentiated colluvium is composed entirely of local bedrock. It lacks striated and molded clasts. The a-axes of gravel- and cobble-sized clasts are aligned parallel to the present surface slope. Nearly 80% of the clasts bear desert varnish. The matrix fraction is composed of weathered dolerite grus and coarse-grained quartz sand. Undifferentiated colluvium overlies Koenig colluvium and Asgard till in hand-dug stratigraphic sections.

Areally Restricted Drifts

Nibelungen till. A clast-supported and unconsolidated diamicton crops out on the floor of east-central Nibelungen Valley in thin (<75 cm) discontinuous patches near the downvalley edge of an oblong basin (200 m long, 125 m wide, and 3 m deep). This basin cuts through Sessrumnir till and Koenig colluvium and into local Arena Sandstone and granite bedrock (Fig. 8). Unconsolidated deposits at the edge of the basin have not slumped appreciably onto the bedrock floor. Nibelungen till displays a chaotic mixture of unweathered, angular gravels and poorly sorted sands. Clast lithologies are identical to bedrock now exposed within the adjacent basin. Gravel clasts within Nibelungen till lack desert varnish, ventifaction, pitting, siliceous crusts, and quartz rinds, indicating that they were not long exposed at the surface. The till surface shows a well-developed surface pavement composed primarily of sandstone ventifacts and secondarily of weathered granite clasts and granite grus. The percentage of granite clasts, both at the surface and within Nibelungen till, is highest downvalley (northeast) from granite bedrock exposed in the hollow.

In hand-dug stratigraphic sections, Nibelungen till overlies a buried in-situ desert pavement. This pavement, in turn, overlies highly weathered and oxidized Koenig colluvium. From top to bottom, the complete stratigraphic sequence of unweathered Nibelungen till, in-situ desert pavement, and oxidized Koenig colluvium occurs in several hand-dug

excavations along the northern margin of Nibelungen till.

The geometric relations and lithologic similarities between Nibelungen till and the closed bedrock hollow; the sharp, planar contact with the underlying ventifact pavement; and the absence of weathered and varnished clasts all suggest that Nibelungen till is derived from unweathered bedrock removed from the nearby basin. We explain the areal pattern of Nibelungen till and associated upvalley basin by a combination of subglacial quarrying/ plucking and deposition. We postulate that glacier ice produced the basin and deposited the material immediately downvalley from this basin.

Jotunheim till. Jotunheim till is an unconsolidated and unstructured gravel-rich diamicton (95% dolerite, 5% sandstone, see Table 1). It crops out in linear patches that trend northeast-southwest. These linear till patches (hereafter called till tongues) commonly occur downvalley from dolerite-rich colluvium, dolerite bedrock, and/or rock glaciers. Jotunheim till is best exposed in the lee of Round Mountain/ St. Pauls Mountain, where it extends northward continuously for a distance of 4 km and nearly covers the floor of Jotunheim Valley. Prominent tongues of Jotunheim till also occur in upper Nibelungen, Sessrumnir, and Koenig Valleys (Figs. 2, 4, and 5).

The northern margins of individual till tongues thin to feather edges. Till tongues are smooth and nearly everywhere merge evenly with the surface of adjacent diamictons. In lower Jotunheim Valley, the northern till of an extensive till tongue is highly eroded and serrated, such that Asgard till and Jotunheim till are exposed at the surface in an intricate areal pattern (Figs. 2 and 4). The average length-to-width ratio of Jotunheim till tongues measured along the deposit surface is about 8:1. Surface gradients average less than 10°. The till lacks erratic lithologies. Dolerite clasts are angular to subangular and generally bear desert varnish. Sandstone clasts commonly show quartz rinds and siliceous crusts. There are no striated, molded, or glacially polished clasts within Jotunheim till. Oxidation is moderate (10YR 5/6) and uniform to the base of the deposit (Table 1).

Jotunheim till overlies a variety of unconsolidated deposits. In lower Jotunheim Valley, dissected till tongues overlie Asgard till with a sharp, planar contact. In upper Nibelungen Valley, the till is wrapped around a bedrock high and overlies Sessrumnir till with a gradational contact. Elsewhere, Jotunheim till is overlain by unweathered diamictons that are contiguous with rock glaciers at valley heads (Ackert, 1990).

The areal distribution of Jotunheim till strongly suggests transport and deposition by northeast-flowing ice. We know of no other mechanism that creates such linear, unsorted, and unstructured deposits that thin to feather edges. In particular, till tongues extend for 2 to 3 km and occupy nearly horizontal or gently sloping valley floors. Because the clasts within Jotunheim till bear desert varnish and lack glacial molding/striations, we infer that Jotunheim till

represents reworked colluvial deposits, rock glacier deposits, and/or reworked dolerite regolith entrained beneath northeast-flowing glacier ice.

Rock-Glacier Deposits

Alpine glaciers, 0.5 km to 1.0 km long, occur at the heads of Koenig, Sessrumnir, and Nibelungen Valleys (Figs. 2, 4, and 5). These glaciers are nearly free of debris, but they grade northward into debris-covered rock glaciers that extend 2 to 3 km downvalley. The rock-glacier debris, which overlies clean glacier ice, is composed of a chaotic mixture of angular, unweathered dolerite gravels, cobbles, and boulders. Quartz sands and dolerite grus partially fill voids between adjacent boulders and cobbles. There are no striated/ molded clasts or erratic lithologies present in these rock-glacier deposits.

The rock glaciers show well-developed, arcuate ridges and terminate in steep-sided lobes that rise 3 to 4 m in relief. Rock-glacier debris thickness increases downvalley to a maximum in excess of 2 to 3 m. Rock-glacier deposits overlie Sessrumnir till (in upper Nibelungen Valley), Jotunheim till (in upper Sessrumnir and Nibelungen Valleys), and Asgard till (in upper Koenig Valley). Thin layers of volcanic ash (0.5 to 1.0 cm) occur between 25 and 35 cm depth within the outermost rock-glacier deposit in Koenig Valley. Undifferentiated colluvium overlies most rock glacier debris at valley heads.

Volcanic Ashes

Volcanic ashes, both reworked and in-situ, occur within glacial and non-glacial sediments of the western Asgard Range (Marchant et al., 1993b). In-situ ashfall deposits occur in sand wedges (frozen-ground contraction cracks, Péwé, 1959; 1966; Berg and Black, 1966; Black, 1976), in waterlain deposits, or rest on buried ventifact pavement. In-situ ashfall deposits are uncontaminated (with $<1\%$ non-volcanic components) and glass shards show intact bubble vesicles and delicate spires. Reworked ashes are mixed within glacial diamictons. Glass shards are abraded and pipe vesicles commonly hold detrital silt grains. None of the ashes of the western Asgard Range is weathered extensively. In-situ ashes contain less than 5% secondary clays (Marchant et al., 1993a, 1993b). We postulate that ash disseminated in glacial tills/ rock-glacier deposits (or restricted to thin, wispy layers in such deposits) reflects either primary ashfall onto the glacier accumulation surface (with subsequent dispersal during englacial or basal transport) or basal entrainment of pre-existing ash deposits.

Ash-filled sand wedges. Sand wedges, relict and active, cut down into, and therefore postdate, the surfaces of all unconsolidated deposits in the western Asgard Range. The isotopic age of in-situ ashes in such sand wedges thus afford minimum ages of these deposits. About 10% of all relict sand wedges exposed in stratigraphic section contain volcanic ash; active sand wedges lack volcanic ash. Ash in relict sand wedges most commonly occurs in

vertical layers between stratified sand-and-gravel deposits (Marchant et al., 1993b). Ash layers are commonly 5 to 10 cm wide at the surface, but in some cases are as much 35-50 cm wide. Ash-filled sand wedges cut down into undifferentiated colluvium in lower Nibelungen Valley (DMS-90-36 B; DMS-90-38 B), Asgard till in central Koenig Valley (DME-91-41), Jotunheim till in central Sessrumnir Valley (DMS-89-132 B), Sessrumnir till in upper Nibelungen Valley (DMS-91-22), and Inland Forts till near Round Mountain (DMS-89-143 B; see Table 2 and Fig. 9).

Waterlain ash deposits. A well-stratified ash that shows folded laminations, flame structures, normal and reverse faults, and small drop stones (3-5 cm across) occurs at the upper margin of Asgard till in central Njord Valley (DMS-89-211 B, Table 2) . This ash deposit, which covers an area of about 20 m^2 and reaches a maximum thickness of 35 cm, is overlain and protected from wind deflation by a coarse gravel-and-cobble lag (2 to 5 cm thick). The ash grades downward into a silty, undifferentiated diamicton that rests directly on weathered sandstone bedrock (Ackert, 1990). A sandstone-floored basin, which cuts through a variety of unconsolidated deposits (including the ash), occurs at the southern margin of the ash deposit. The well-developed stratification, penecontemporaneous deformation, drop stones, and underlying silt-rich diamicton all point to volcanic ashfall into a small pond or lake. The limited areal distribution of ash at the margin of Asgard till allows the possibility that deposition occurred within an ice-marginal pond or lake.

Ash layer on a buried pavement. Volcanic ashfall deposits that rest on buried pavements in the Dry Valleys region commonly occur as stringers concentrated in cracks between irregularly shaped, cobble-sized ventifacts, and less commonly as thick, continuous layers draped over ventifact pavements. In the western Asgard Range, volcanic ashfall rests on the buried pavement that separates Koenig colluvium from Nibelungen till in central Nibelungen Valley. This ash, phonolitic in composition, is concentrated in voids between sandstone ventifacts that form a protective cover over Koenig colluvium (DMS-90-124 B). No ash occurs within Koenig colluvium.

Chronology of Surficial Deposits

Relative chronology. Any interpretation of the glacial history of the western Asgard Range rests on a detailed relative chronology of surficial deposits in the north- and south-facing Asgard Range valleys. The relative chronology presented here is based on the map patterns of surficial deposits displayed in Figures 4 and 5, along with the sedimentologic and stratigraphic data for individual units given in the previous section and in Tables 1 and 2.

The stratigraphically lowest units in north- and south-facing Asgard Range valleys are the Sessrumnir and Inland Forts tills, respectively; both overlie striated Arena Sandstone bedrock. Sessrumnir till is overlain by Koenig

colluvium in Nibelungen, Sessrumnir, and Koenig Valleys. This colluvium shows the highest degree of oxidation for any unit in the western Asgard Range (5YR 8/4). All stratigraphically younger units show significantly less oxidation (Table 1). This contrast marks the largest break in soil development within the western Asgard Range. Asgard and Nibelungen tills both overlie Koenig colluvium in central Nibelungen Valley. In addition, Asgard till overlies Koenig colluvium with sharp stratigraphic contacts in Njord, Sessrumnir, and Koenig Valleys. Jotunheim till is the next-highest unit in the stratigraphic sequence; it overlies Asgard till in Jotunheim, Sessrumnir, and Koenig Valleys. Little-weathered, dolerite-rich rock-glacier deposits, which stratigraphically reflect the youngest glacial deposits the western Asgard Range, overlie Jotunheim till at the heads of Nibelungen, Sessrumnir and Koenig Valleys. Finally, undifferentiated colluvium overlies all units in the Asgard Range.

Absolute chronology. Our absolute chronology of surficial sediments in the Asgard Range is based on isotopic dating of in-situ ash deposits. Volcanic crystals (sanidine and anorthoclase) and glass shards extracted from the matrix of ashfall deposits were dated at the Berkeley Geochronology Center (BGC). The BGC employs a fully automated laser-fusion $^{40}Ar/^{39}Ar$ dating system that allows analysis of single volcanic crystals ($<$ 1 mm in size) and individual pumice shards.

Isotopic data presented in Table 2 and Appendix I indicate that surficial sediments in the western Asgard Range extend back to middle-Miocene time. With the exception of areally restricted rock-glacier deposits at valley heads, all surficial units in the western Asgard Range Valleys antedate 10.0 to 12.0 Ma. Sessrumnir till and Koenig colluvium antedate 14.8/ 15.2 Ma ago, based on the isotopic date of a buried ashfall layer that rests on Koenig colluvium (DMS-90-124 B). This isotopic date also affords a minimum age for Nibelungen till, which stratigraphically overlies this ash layer and Koenig colluvium in central Nibelungen Valley. Asgard till is older than 13.6 Ma, on the basis of the isotopic date of in-situ ash within a sand-wedge deposit in central Koenig Valley (DME-91-41). Likewise, isotopically dated ash in sand wedges that penetrate Sessrumnir, Inland Forts, and Jotunheim tills afford maximum drift ages of 15.0 Ma (DMS-91-22), 13.5 Ma (DMS-89-143 B), and 10.5 Ma (DMS-89-132 B), respectively. The outermost rock glacier deposit in upper Koenig Valley shows ash concentrated in thin lenses (0.5 to 1.0 cm) at the deposit margin; the ash is buried beneath 25 cm of coarse sand-and-gravel layers. The isotopic date of this ash, which is 12.5 Ma (DMS-91-46), affords a maximum age for the rock-glacier deposit. Finally, ash in two separate sand wedges that cut down into undifferentiated colluvium on the east wall of lower Nibelungen Valley are dated at 10.0 Ma (DMS-90-36 B) and 12.0 Ma (DMS-90-38 B); these dates afford a maximum age for undifferentiated colluvium.

DISCUSSION

Glacial History

Sessrumnir till, Inland Forts till, and alpine glaciation. The Sessrumnir and Inland Forts tills reflect an early episode of alpine glaciation in the western Asgard Range. Both tills were deposited by local wet-based alpine glaciers that occupied north- and south-facing western Asgard Range valleys, although the presence of Aztec Siltstone in Sessrumnir till allows the possibility of a component of far-travelled ice. We assign these tills to a single phase of alpine glaciation because both represent the stratigraphically lowest units in north- and south-facing valleys, both overlie striated and molded bedrock pavements indicating downvalley ice flow, both show similar surface and internal weathering, and both are derived from local sandstone and dolerite bedrock. The glaciation responsible for the Sessrumnir and Inland Forts tills antedates 15.0 Ma.

Asgard till, Jotunheim till, Nibelungen till, and ice-sheet overriding. A key problem of Miocene glacial history concerns the significance of Asgard, Jotunheim, and Nibelungen tills. Interpretation of the Asgard till is relatively straightforward. For reasons given above, it reflects ice lobes that spilled southward into valleys of the Asgard Range from an outlet glacier that filled Wright Valley. The problem occurs, however, in interpreting the Jotunheim and Nibelungen tills, which show the same degree of weathering and oxidation as Asgard till. Furthermore, there is no evidence in stratigraphic section for subaerial exposure between the tills where they are juxtaposed. We thus infer that the three tills are approximate age equivalents.

Asgard till lacks surface morphology and has been eroded into remnant patches. The result is that vast exposures of bare-bedrock terrain and anastomosing channels alternate with dissected patches of Asgard till. Channels and bare-bedrock terrain that dissect the Asgard till can be traced continuously up the Asgard valleys to stoss-and-lee topography at the crest of low-lying saddles. A spectacular example is the channel system in Sessrumnir Valley.

We think that the best explanation for the origin and spatial distribution of stoss-and-lee topography, erosional basins, channels, bare-bedrock tracts, and dissected till patches involves variations in the basal thermal regime of northeast-flowing ice that overrode the western Asgard Range. In this regard, abrasion is associated with wet-melting ice, stripping and plucking with wet-freezing ice, and the preservation of unconsolidated sediments with frozen ice. We postulate that wet-melting conditions occurred on south-facing headwalls and where ice velocity was greatest. Thus, extensive abrasion was concentrated along low-lying saddles at the head of Njord and Sessrumnir Valleys, which channeled northeast-flowing ice. Following mechanisms described by Nye (1973), Rothlisberger (1972), Shreve (1972, 1985), and Sugden and John (1976), we infer that the channels along the eastern divide of Sessrumnir Valley reflect erosion from meltwater produced on the upglacier side of the Arena Valley headwall. Bedrock basins at the northern end of this channel system probably reflect freezing-on of debris and meltwater

beneath wet-freezing ice. Such stripping would also explain the patchy areal distribution of unconsolidated sediments in the western Asgard Range, the bare-bedrock terrain in upper Njord Valley, and the fact that deposits interfinger at the surface without relief.

A key problem is whether the interconnected array of erosional and depositional features reflect basal conditions beneath an overriding ice sheet or a local alpine glacier. We favor an origin beneath thick overriding ice for several reasons. One is that south-facing stossed bedrock headwalls (with north-facing concave slopes and cliffed potholes) suggest ice flow across valley headwalls from south to north. A second is that the highest elevation of the main channel between Sessrumnir and Folkvangar Valleys is about 100 m above the stossed bedrock headwalls. This last relationship suggests that ice overtopped valley headwalls and was thus much thicker than local cirque glaciers (Sugden et al., 1991). Third, tributary meltwater channels that feed the main channel in Sessrumnir Valley trend obliquely across bedrock slopes, rather than directly downslope. The distribution of such channels closely resembles the pattern predicted to occur beneath overriding ice on the basis of reconstructed equipotentials for subglacial meltwater flow (Sugden et al., 1991). Fourth, channels and potholes on the divide between Jotunheim and Nibelungen Valleys imply that ice filled these valleys and merged across the divide. Fifth, overriding by thick ice is consistent with high-elevation (2000 m) whaleback forms that trend northeast-southwest on the tableland immediately west of the Asgard Range valleys. Sixth, scouring at the base of northeast-flowing ice explains the suite of aligned boulders that cuts across dissected outcrops of Asgard and Sessrumnir tills in lower Nibelungen Valley.

If we are correct in our reconstruction, then overriding ice involved two steps. First, Asgard till probably represents the initial stages of ice-sheet buildup. Second, Nibelungen and Jotunheim tills represent the culmination of overriding and were subsequently deposited by thick, northeast-flowing ice that engulfed the western Asgard Range.

Ice-sheet overriding of the western Asgard Range was completed prior to 10.5 Ma ago and probably occurred between 13.6 Ma and 14.8/ 15.2 Ma ago. The maximum age for overriding is based on an isotopically dated ashfall deposit that underlies Nibelungen till. A minimum age of 10.5 Ma comes from isotopically dated colluvium that overlies Asgard till in lower Nibelungen Valley. It is also probable that glacial overriding antedated 13.6 Ma, because of the isotopic age of in-situ ash in a sand wedge that postdates Asgard till (DME-91-41; Fig. 9).

Regional events. It is possible to correlate our map units in the western Asgard Range with surficial deposits in central Wright Valley. The surficial stratigraphy of central Wright Valley is dominated by Peleus till from about 125 m elevation on the floor of central Wright Valley up to 1100 m elevation beside Conrow Glacier (Prentice et al., 1993; Hall et al., 1994). Peleus till commonly has a patchy distribution, with individual outcrops separated by

weathered granite and metamorphic bedrock, and the upper limit is generally irregular, except near Conrow and Bartley Glaciers. Peleus till shows thick salt pans and advanced soil development (Stage 5 of Campbell and Claridge, 1975). A reinterpretation of the stratigraphy at Prospect Mesa (Denton et al., this volume) indicates that Peleus till is older than Prospect Mesa Gravels, which contain *Chlamys tuftsensis* shells dated by the $^{87}Sr/^{86}Sr$ technique at about 5.4 Ma (Prentice et al., 1993). This indicates an age in excess of 5.4 Ma for Peleus till and is in accord with a minimum age of 4.2 Ma for the Peleus till based on $^{40}Ar/^{39}Ar$ dates on reworked basalt clasts in alpine drifts that unconformably overlie Peleus till in east-central Wright Valley (Hall et al., 1994). On the basis of areal distribution and clast lithologies, Peleus till is taken to represent the most recent expansion of East Antarctic ice through Wright Valley (Prentice et al., 1993; Hall et al., 1994). From a consideration of surface-weathering characteristics, soil development, outcrop patterns, inferred ice-flow direction, and the accordance of upper till limits, we tentatively correlate Peleus till in central Wright Valley with Asgard till in the western Asgard Range. If correct, this correlation implies a minimum age of 13.6 Ma for Peleus till.

Paleoclimatic Implications

Late Cenozoic paleoclimate of the western Asgard Range can be inferred from the physical character of surficial deposits, from slope stability, and from the thermal regime of former glaciers. The results all point to persistent cold-desert, hyper-arid conditions during at least the last 13.6 Ma.

Glacier thermal regimes. The Sessrumnir and Inland Forts tills, which both predate 15.0 Ma ago, must represent a climate warmer than that of today. This is because the present-day mean annual temperature of -35°C, along with hyper-arid conditions, preclude wet-based alpine glaciers in the western Asgard Range. If it is assumed that there has been no surface uplift since till deposition, then development of wet-based alpine glaciers in the western Asgard Range requires temperatures about 35°C above present values. On the other extreme, the Asgard Range conceivably could have been close to sea-level (where mean annual temperature is now -14°C, Schwerdtfeger, 1984) during the alpine glacial episode prior to 15.0 Ma ago, if indeed late Cenozoic uplift was of the magnitude postulated by Behrendt and Cooper (1991). In that case, wet-based alpine glaciation would have required only a 14°C rise in atmospheric temperature. These extremes yield a range of 14°C to 35°C warmer than at present for mean atmospheric temperature in the western Asgard Range during deposition of Sessrumnir and Inland Forts till.

Ice-sheet overriding. From arguments given above, Asgard till represents the initial ice buildup that culminated in the overriding of the western Asgard Range between 14.8/ 15.2 Ma and 13.6 Ma. Asgard till was deposited from thin, cold-based ice lobes that projected southward into the mouths of the Asgard Range valleys. Therefore basal thermal conditions of these lobes represent a crude estimate of atmospheric temperature. Hence, the fact that basal Asgard ice was frozen carries with it the implication that mean annual temperature in the western Asgard Range

was below 0°C when Asgard till was deposited between 13.6 Ma and 14.8/ 15.2 Ma ago. The presence of well-preserved sand wedges directly beneath Asgard till is consistent with this interpretation, because sand wedges form only in cold-desert environmental conditions (Péwé, 1959, 1966).

The absence of glacial outwash, kame terraces, ice-marginal channels, and lacustrine deposits associated with the demise of middle-Miocene ice in the western Asgard Range probably reflects ice dissipation under cold-desert climatic conditions, where the dominant form of ablation is sublimation. A simple observation shows the maximum allowable mean annual temperature during dissipation of overriding ice. Surficial sediments in the western Asgard Range are unmarked by rills, levees, stream channels, lacustrine deposits or other geomorphic features indicative of liquid water. However, small ice-marginal lakes and surficial geomorphic features characteristic of liquid water (rills, levees, gullies, mudflows, and stream channels) are common below 1000 m elevation near the western Asgard Range. The mean annual temperature at 1000 m elevation in the western Dry Valleys region is now about -30°C. The implication is that mean annual temperatures during middle-Miocene dissipation of overriding ice most probably did not rise above -30°C in the western Asgard Range.

Two key points emerge from this discussion. First, atmospheric temperatures during buildup to ice-sheet overriding were not significantly different from present values. This is consistent with the observation that alpine glaciers failed to expand at the head of the Asgard Range valleys and merge with ice in the Wright Valley trough during this buildup. If alpine glaciers had expanded, then southward flowing ice lobes could not have advanced into the Asgard Range valleys to deposit Asgard till. Second, decay of overriding ice from the western Asgard Range most likely occurred by sublimation under cold-desert conditions, with mean-annual temperatures below -30°C. These observations bear on the origin and demise of glacial overriding. Most important, ice buildup did not necessarily result from warm climatic conditions fostering high accumulation rates. Nor did ice recession result from excessive climatic warming.

Hyper-aridity and cold-desert conditions. Isotopically dated, in-situ ashfall deposits that rest within well-preserved sand-wedge deposits indicate ice-free, cold-desert conditions in Nibelungen Valley at 15.0 Ma (DMS-91-22), 12.0 Ma (DMS-90-38 B), and 10.0 Ma (DMS-90-36 B); in Koenig Valley at 13.6 Ma (DME-91-41); in Inland Forts at 13.5 Ma (DMS-89-143); and in Sessrumnir Valley at 10.5 Ma (DMS-89-132 B). In-situ ash overlying a well-developed ventifact pavement on top of Koenig colluvium in Nibelungen Valley indicates dry, and most likely cold, conditions at about 14.8/ 15.2 Ma (DMS-90-124 B, see also Table 2 and Appendix I). Sand wedges form only in cold and dry climates, where mean annual temperatures are well below 0°C (Péwé, 1959, 1966). Colluviation during the present cold-desert climate has been minor and essentially restricted to north-facing dolerite bedrock slopes. Rock glaciers have expanded at most 2.5 km from valley headwalls during the last 12.5 to 13.5 Ma. This

age is based on $^{40}Ar/^{39}Ar$ analyses of volcanic ash within the outermost rock glacier deposit in upper Koenig Valley (DMS-91-46, Table 2).

Implications for Landscape Evolution

A major implication of the volcanic ash chronology is that the present landscape of the western Asgard Range was largely in place before middle-Miocene time. This conclusion is based on the chronology of in-situ ashes and unconsolidated deposits on bedrock slopes and valley floors. If either post-Miocene valley cutting by wet-based glaciers or rectilinear slope development from progressive backwearing of weathering-limited slopes under ice-free conditions had occurred, then Miocene-age tills, colluvium, and in-situ to near in-situ volcanic ashes would not be preserved now on valley walls. It follows that the Asgard Range valleys are inherited from an ancient environmental regime that predates the onset of the hyper-arid, cold-desert conditions more than 13.6 Ma ago.

The frontal scarp, tableland, rectilinear slopes, terraces, buttes, mesas, and flat-floored valleys of the western Asgard Range have nearly identical counterparts in cuestaform landscapes of platform deserts in semi-arid regions around the world (Sugden et al., 1994; Denton et al. 1994). In this regard, the basic morphology of the western Asgard Range resembles the desert morphology of the Colorado Plateau, which feature dissected valleys, box canyons, buttes, mesas, and rectilinear slopes at the margin of a prominent escarpment. In sandstone terrain, box canyons with theater-shaped heads, gently sloping pediments, buttes, mesas, and spires (all in association with rectilinear slopes) reflect progressive backwearing and parallel retreat of weathering-limited slopes and scarps (Cooke et al., 1993). Backwearing occurs by a combination of overland flow, slope wash, creep, spring sapping from groundwater, salt weathering, and granulation (Mabbutt, 1977; Laity and Malin, 1985; Howard and Kochel, 1988; Schmidt, 1989; Young, 1985; Oberlander, 1977). We suggest that the overall morphology of the western Asgard Range also formed largely by backwearing and parallel retreat of weathering limited slopes and scarps.

Erosion by wet-based alpine glaciers and an overriding ice sheet clearly played a role in sculpting the present western Asgard morphology. Subglacial channels, stoss-and-lee slopes, basins, and dissected unconsolidated deposits point to two episodes of glacial erosion in the western Asgard Range (alpine and ice-sheet overriding). Erosion from both glacial episodes was relatively minor (although concentrated in places), as illustrated by the preservation of relict landforms and deposits.

CONCLUSIONS

In-situ volcanic ashfall deposits indicate that the stratigraphy of surficial sediments in the western Asgard Range extends back to at least 15.0 Ma. The preservation of Miocene- and Pliocene-age sediments on valley slopes shows that major bedrock landforms are relict and that little slope evolution has occurred during at least the last 13.6 Ma. Although glaciers played a role in shaping the present western Asgard topography, the main landforms were

probably initiated by denudational processes that are now responsible for scarp retreat in cuesta landscapes elsewhere in the world.

Several phases of glaciation can be recognized. These were (a) a pre-middle Miocene phase of alpine glaciation >15.0 ago (when Sessrumnir and Inland Forts tills were deposited from wet-based alpine glaciers) and (b) a middle-Miocene phase of northeast-flowing ice-sheet overriding between 13.6 Ma and 14.8/ 15.2 Ma ago (when Asgard, Jotunheim, and Nibelungen tills were deposited and ultimately cut beneath thick glacier ice). There is no evidence in the stratigraphic record for notable glacier expansion in the western Asgard Range during the last 13.6 Ma. Instead, in-situ ashfall deposits indicate persistent cold-desert conditions, with only minor expansion of rock glaciers (<2.5 km) at valley heads.

These conclusions from the western Asgard Range have several implications for the Pliocene behavior of the adjacent East Antarctic Ice Sheet. The first is that the deglaciation hypothesis requires overriding of the Transantarctic Mountains (including the western Asgard Range) by a wet-based East Antarctic Ice Sheet sometime after 3.0 Ma ago in order to emplace Pliocene marine diatoms in high-elevation Sirius Group outcrops, including those in the western Dry Valleys region (Webb et al., 1984; Webb and Harwood, 1991; Barrett et al., 1992). But there is no evidence of such post-Miocene ice-sheet overriding of the western Asgard Range by the East Antarctic Ice Sheet. The second implication is that the deglaciation hypothesis requires atmospheric warming of at least 20°C above present values to impose the surface-melting ablation zones necessary for ice-sheet melting (Huybrechts, this volume). The mean atmospheric temperature also must have remained 20° - 25°C warmer than at present for survival of scrub Nothofagus during deposition of Sirius outcrops by an expanded East Antarctic Ice Sheet (Barrett, 1991). Yet the western Asgard Range lacks not only Pliocene till deposited by wet-based glaciers, but also Pliocene outwash, kame terraces, ice-marginal channels, and lacustrine deposits. Rather, the paleoclimatic evidence shows persistent hyper-arid, cold-desert conditions during at least the last 13.6 Ma, with little temperature increase above present-day values. Therefore the geologic and geomorphic record from the western Asgard Range is consistent with long-term stability of the East Antarctic Ice Sheet.

REFERENCES

Ackert, R.P., Jr., 1990: Surficial geology and geomorphology of the western Asgard Range, Antarctica: implications for late Tertiary glacial history. [M.S. thesis]: Orono, University of Maine.

Augustinus, P.C. and Selby, M.J., 1990: Rock slope development in McMurdo oasis, Antarctica, and implications for interpretations of glacial history. *Geografiska Annaler.* 72 A (1), 55-62.

Barrett, P.J., Adams, C.J., McIntosh, W.C., Swisher III, C.C. and Wilson, G.S., 1992: Geochronological evidence supporting Antarctic deglaciation three million years ago. *Nature* 359, 816-818.

Barrett, P.J., 1991. Antarctica and global climatic change: a geological perspective. In *Antarctica and Global Climatic Change (C. Harris and B. Stonehouse eds.)*: 35-50.

Behrendt, J.C. and Cooper, A.K., 1991: Evidence of rapid Cenozoic uplift of the shoulder escarpment of the Cenozoic West Antarctic Rift system and a speculation on possible climate forcing. *Geology* 19, 315-319.

Behrendt, J.C. and Cooper, A.K., 1990: Speculation on the uplift of the shoulder of the Cenozoic West Antarctic rift system and its relation to late Cenozoic climate change. *In Cooper, A.K. and Webb, P.N., Eds., International workshop on Antarctic offshore stratigraphy (ANTOSTRAT) [overview and extended abs.]: U.S. Geological Survey Open-File Report 90-309,* p.63-71.

Berg, T.E. and Black, R.F., 1966: Preliminary measurements of growth of nonsorted polygons, Victoria Land, Antarctica. In *Antarctic soils and soil forming processes (J.C.F. Tedrow, Ed.) American Geophysical Union, Ant. Res. Ser. No. 8,* Washington, DC., 61-108.

Black, R.F., 1976: Periglacial features indicative of permafrost: ice and soil wedges. *Quat. Res. 6, 3-26.*

Bockheim, J.G., 1982: Properties of a chronosequence of ultraxerous soils in the Trans-Antarctic Mountains. *Geoderma* 28, 239-255.

Campbell, I.B. and Claridge, G.G.C., 1975: Morphology and age relationships of Antarctic soils. In *Quaternary studies (R.P. Suggate and M.M. Cresswell, Ed.).* The Royal Society of New Zealand, Wellington, 83-88.

Calkin, P.E., 1974: Subglacial geomorphology surrounding the ice-free valleys of Southern Victoria Land, Antarctica. *Journal of Glaciology* 13(69), 415-429.

Chinn, T.J., 1980: Glacier balances in the Dry Valleys area, Victoria Land, Antarctica. In *Proceedings of the Riederalp Workshop IAHS-AISH Publication no. 125,* 237-247.

Cooke, R.U., Warren, A. and Goudie, A.S., 1993: *Desert Geomorphology.* University College London Press. London.

Denton, G.H., Sugden, D.E., Marchant, D.R., Hall, B.L., and Wilch, T.I., 1994: East Antarctic Ice Sheet sensitivity to Pliocene climatic change from a Dry Valleys perspective. *Geografiska Annaler,* In press.

Denton, G.H., Prentice, M.L., Kellogg, D.E. and Kellogg, T.B., 1984: Late Tertiary history of the Antarctic Ice

Sheet: Evidence from the Dry Valleys. *Geology* 12, 263-267.

Dowsett, H.J., Cronin, T.M., Poore, R.Z., Thompson, R.S., Whately, R.C. and Wood, A.M., 1992: Micropaleontological Evidence for Increased Meridional Heat Transport in the North Atlantic Ocean During the Pliocene. *Science* 258, 1133-1135.

Hall, B.L., Denton, G.H., Lux, D.R. and Bockheim, J.G., 1994: Late Tertiary antarctic paleoclimate and ice-sheet dynamics inferred from surficial deposits in Wright Valley. *Geografiska Annaler*, In press.

Harwood, D. M., 1986: Diatom biostratigraphy and Paleoecology and a Cenozoic history of Antarctic ice sheets. PhD dissertation, Ohio State University, Columbus Ohio.

Holdsworth, G. and Bull, C., 1970: The flow law of cold ice: investigations of Meserve Glacier, Antarctica. In *International Symposium on Antarctic Glaciological Exploration (Hanover, New Hampshire, USA, 3-7 September 1968)*, 204-216: *IAHS Publ.* no. 86.

Howard, A.D. and Kochel, R.C., 1988: Introduction to cuesta landforms and sapping processes on the Colorado Plateau. In *Sapping features of the Colorado Plateau: a comparative planetary geology field guide. NASA special publication SP-491.*

Huybrechts, P., 1992: Glaciological and climatological probabilities and improbabilities of alternative glaciation models of Antarctica. In *LIRA Workshop Landscape Evolution, abstracts, Haarlem, The Netherlands.*

Kennett, J.P., 1982: *Marine Geology.* Prentice-Hall, Englewood Cliffs, New Jersey.

Keys, J.R., 1980: Air temperature, wind, precipitation and atmospheric humidity in the McMurdo region. *Antarctic Data Series. no. 9,* Victoria University of Wellington, No. 17.

Kyle, R., 1990: McMurdo Volcanic Group - western Ross Embayment. In *Volcanoes of the Antarctic plate and southern oceans. American Geophysical Union, Ant. Res. Ser. 48* Washington, DC. 19-25.

Laity, J.E. and Malin, M.C., 1985: Sapping processes and the development of theater-headed valley networks on the Colorado Plateau. *Geol. Soc. Amer. Bull.* 96, 203-217.

Mayewski, P.A., 1975: Glacial geology and late Cenozoic history of the Transantarctic Mountains, Antarctica. *Institute of Polar Studies Report 56,* 168 p.

Miller, K.G., Fairbanks, R.G. and Mountain, G.S., 1987: Tertiary oxygen isotope synthesis, sea level history, and continental margin erosion. *Paleoceanography* 2(1), 1-19.

Mabbutt, J.A., 1977: *Desert Landforms.* MIT Press, Cambridge, Ma.

Marchant, D.R., Denton, G.H. and Swisher III, C.C., 1994: Miocene-Pliocene-Pleistocene glacial history of Arena Valley, Quartermain Mountains, Antarctica. *Geografiska Annaler,* In press.

Marchant, D.R., Swisher III, C.C., Lux, D.R., West, Jr., D.P. and Denton, G.H., 1993a: Pliocene paleoclimate and East Antarctic ice-sheet history from surficial ash deposits. *Science* 260, 667-670.

Marchant, D.R., Swisher III, C.C, Potter, N.P., Jr., and Denton, G.H., 1993b: Antarctic paleoclimate and ice-

sheet dynamics reconstructed from volcanic ashes in the Dry Valleys. *Palaeo. Palaeo. Palaeo.*, submitted.

McKelvey, B.C., Webb, P.N., Gorton, M.P. and Kohn, B.P., 1972: Stratigraphy of the Beacon Supergroup between the Olympus and Boomerang Ranges, Victoria Land. In *Antarctic Geology and Geophysics. (Raymond J Adie, Ed.)* Universitetsforlaget, Oslo p. 345-352.

Nye, J.F., 1973: Water at the bed of a glacier. In *Symposium on the Hydrology of Glaciers,* Cambridge, 9-13 September 1969, *Inter. Assoc. Sci. Hydrol.* 95, 189-194.

Oberlander, T.M., 1977: Origin of segmented cliffs in massive sandstones of southeastern Utah. *In Geomorphology in Arid Regions (D.O. Doehring, Ed.),* 79-114.

Oerlemans, J., 1982: A model of the Antarctic Ice Sheet. *Nature* 297, 550-553.

Péwé, T.L., 1959: Sand-wedge polygons (tesselations) in the McMurdo Sound, region, Antarctica - a progress report. *Am. Jour. Sci.* 257 (8), 545-552.

Péwé, T. L., 1966: Paleoclimatic significance of fossil ice wedges. *Biuletyn Peryglacjalny 15,* 65-73.

Prentice, M.L., Bockheim, J.C., Wilson, S.C., Burckle, L.H., Hodell, D.A., Schluchter, C. and Kellogg, D.E., 1993: Late Neogene Antarctic Glacial History: Evidence from Central Wright Valley, *American Geophysical Union, Ant. Res. Ser.* In press.

Robin, G. de Q., 1988: The Antarctic ice sheet, its history and response to sea level and climatic changes over the past 100 million years. *Palaeo, Palaeo., Palaeo.* 67, 31-50.

Rothlisberger, H.A., 1972: Water pressure in intra- and subglacial channels. *Jour. Glaciology* 11, 177-203.

Savin, S.M., Douglas, R.G., and Stehli, F.G., 1975: Tertiary marine paleotemperatures. *Geol. Soc. Amer. Bull. 86, 1499.*

Schwerdtfeger, W., 1984: Weather and climate of the Antarctic. In *Developments in Atmospheric Science 15,* Elsevier Publishing Company, Amsterdam.

Schmidt, K.H., 1989: The significance of scarp retreat for Cenozoic landform evolution on the Colorado Plateau, USA. *Earth Surf. Proc. Land 14*, 93-105.

Selby, M.J., 1974: Slope evolution in an Antarctic oasis. *New Zealand Geographer* 30, 18-34.

Selby, M.J., 1971: Slopes and their development in an ice-free, arid area of Antarctica. *Geogrrafiska Annaler* 53(A), p. 235-245.

Selby, M.J. and Wilson, A.T., 1971: The origin of the Labryinth, Wright Valley, Antarctica. *Geol. Soc. Amer. Bull.* 82, 471-476.

Shackleton, N.J. and Kennett, J.P., 1975: Paleotemperature history of the Cainozoic and the initiation of Antarctic glaciation: oxygen and carbon analysis in DSDP sites 277, 279 and 281. In *Initial Reports of the Deep Sea Drilling Project (Kennett, J.P. and Houtz, R. Eds.)* 29, 743-755.

Shaw, J. and Healy, T.R., 1977: Rectilinear slope formation in Antarctica. *Annals of the American Association of Geographers* 67(1).

Shreve, R.L., 1985: Esker characteristics in terms of glacier physics, Katahdin esker system, Maine. *Geol. Soc. Amer. Bull.* 96, 131-146.

Shreve, R.L., 1972: Movement of water in glaciers. *Journal of Glaciology* 11(62), 205-14.

Sugden, D.E. and John, B.S., 1976: *Glaciers and Landscape*. Arnold, 372 p.

Sugden, D.E., Denton, G.H., and Marchant, D.R., 1991: Subglacial meltwater channel systems and ice sheet overriding, Asgard Range, Antarctica. *Geografiska Annaler* 73 (A), 109-121.

Sugden, D.E., Denton, G.H. and Marchant, D.R., 1994: Landscape evolution of the Dry Valleys, Transantarctic Mountains. *Journal of Geophysical Research,* submitted.

Webb, P.N. and Harwood, D.M., 1991: Late Cenozoic glacial history of the Ross Embayment, Antarctica. *Quat. Sci. Rev.* 10, 215-223.

Webb, P.N. and Harwood, D.M., 1987: Terrestrial flora of the Sirius Formation: Its significance for late Cenozoic glacial history. *Ant. Jour. of the U.S.* 22(4), 7-11.

Webb, P.N., Harwood, D.M., McKelvey, B.C., Mercer, J.H. and Stott, L.D., 1984: Cenozoic marine sedimentation and ice-volume variation on the East Antarctic craton. *Geology* 12, 287-291.

Weed, R. and Norton, S.A., 1991: Siliceous crusts, quartz rinds and biotic weathering of sandstones in the cold desert of Antarctica. In *Proceedings of the International Symposium on Environmental Biogeochemistry,* 327-339. Elsevier Publishers.

Wilson, A.T., 1973: The great antiquity of some Antarctic landforms - Evidence for an Eocene temperate glaciation in the McMurdo region. In *Palaeoecology of Africa, the surrounding islands of Antarctica (E.M. van Zinderen Bakker Sr. Ed.), VIII,* Balkema, Cape Town.

Young, A.R.N., 1985: Geomorphic evolution of the Colorado Plateau margin in west-central Arizona: a tectonic model to distinguish between the causes of rapid, symmetrical scarp retreat and scarp dissection. In *Tectonic Geomorphology (M. Morisawa and J.T. Hack, Eds.).* Allen and Unwin, Boston.

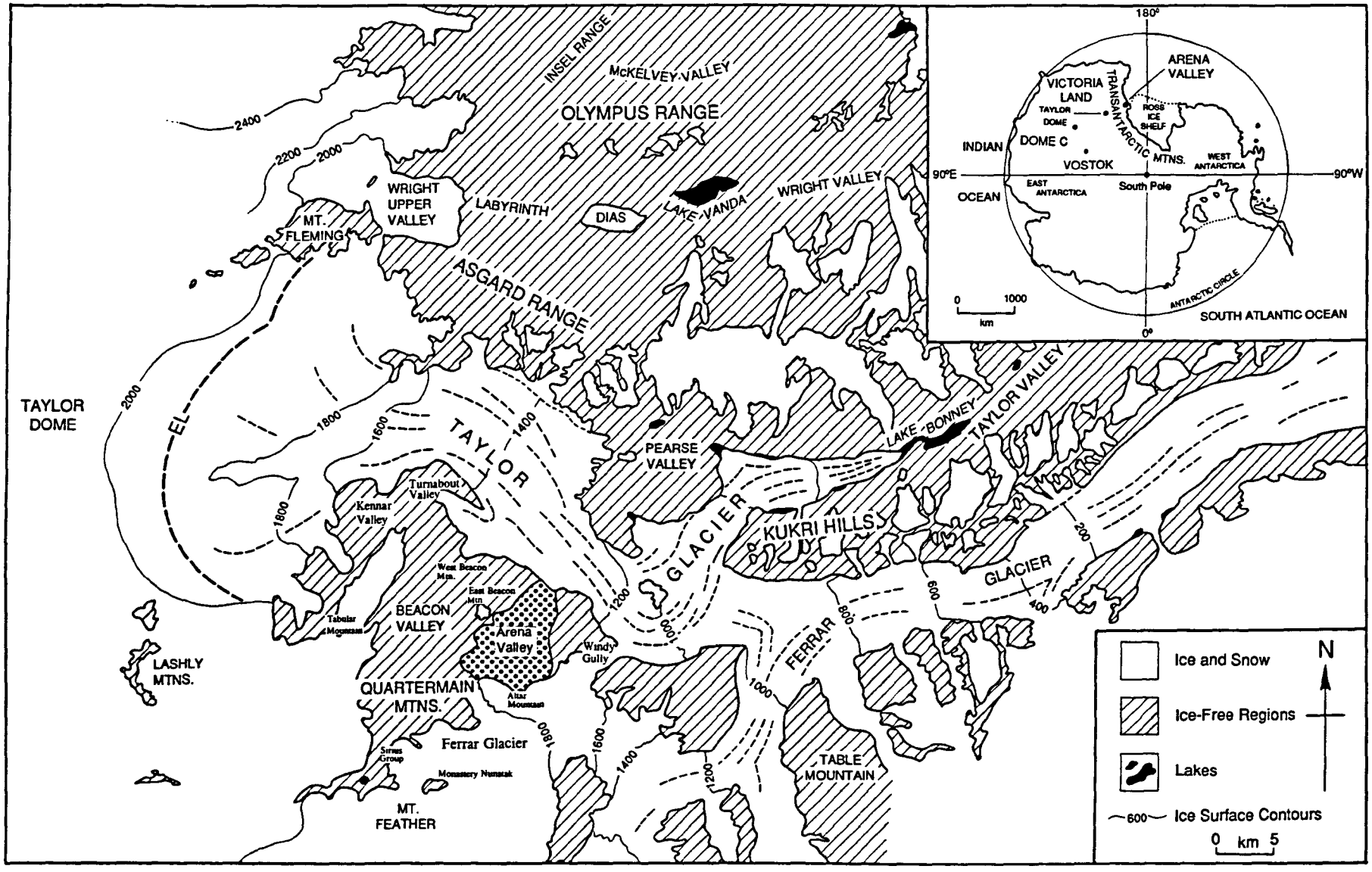

Figure 1. Location map of the Dry Valleys region.

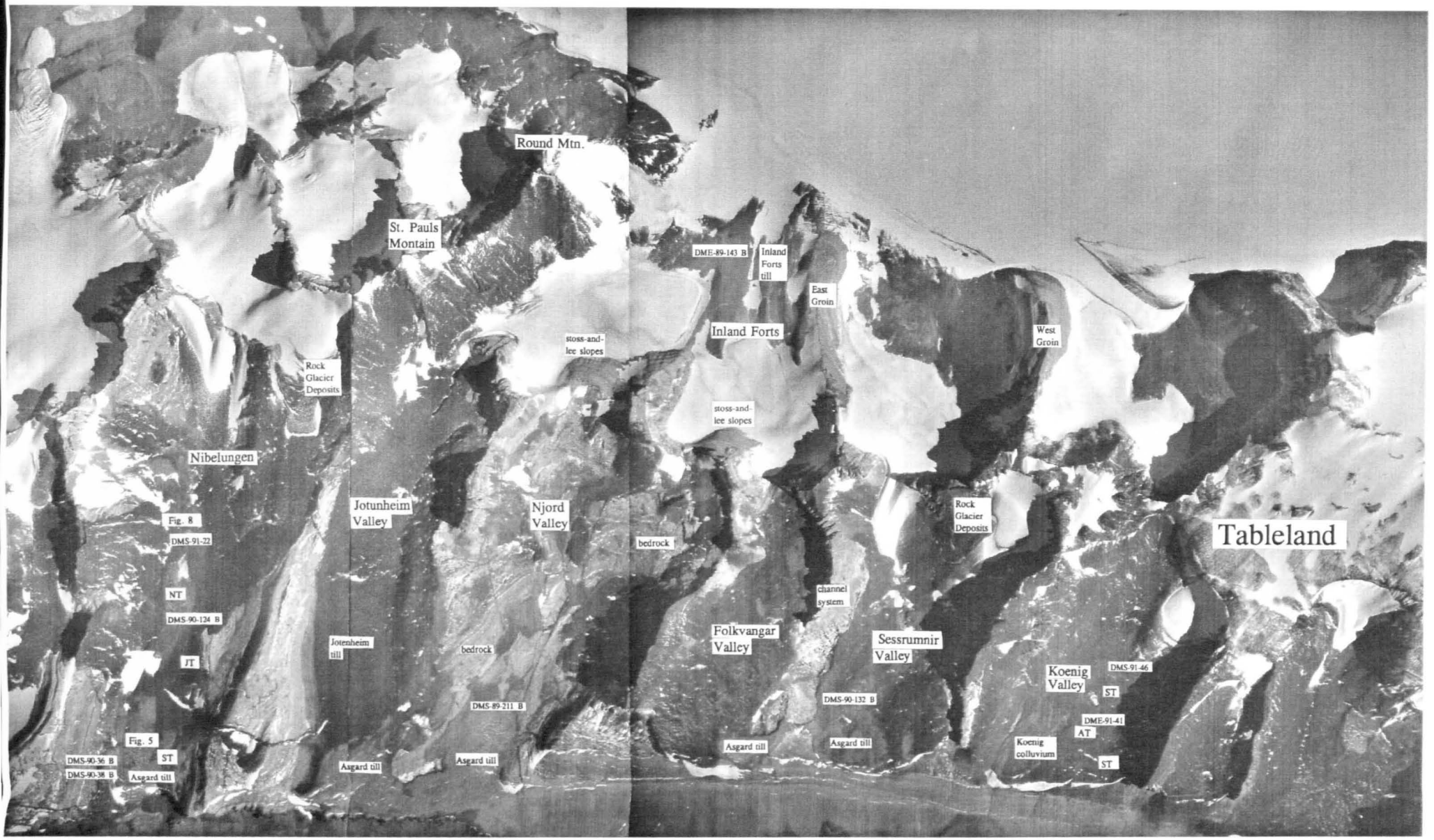
Round Mtn.
St. Pauls Montain
DME-89-143 B
Inland Forts till
East Groin
Inland Forts
West Groin
stoss-and-lee slopes
Rock Glacier Deposits
stoss-and-lee slopes
Nibelungen
Jotunheim Valley
Njord Valley
bedrock
Rock Glacier Deposits
Tableland
Fig. 8
DMS-91-22
channel system
NT
DMS-90-124 B
Folkvangar Valley
Sessrumnir Valley
Jotenheim till
bedrock
JT
Koenig Valley
DMS-91-46
ST
DMS-89-211 B
DMS-90-132 B
DME-91-41
AT
Fig. 5
Asgard till
Asgard till
Koenig colluvium
ST
DMS-90-36 B
ST
DMS-90-38 B
Asgard till
Asgard till
Asgard till

Figure 3. Oblique aerial view of western Asgard Range. View from west to east. Individual valleys grade from well-developed, box canyons (with theater-shaped headwalls) in the western portion of the range to elongate through-valleys farther to the east. North-facing valleys show hanging outlets unmarked by transverse bedrock lips. Smooth rectilinear bedrock slopes extend from valley lips to the top of the Labyrinth in upper Wright Valley. Sample numbers show ash locations described in text.

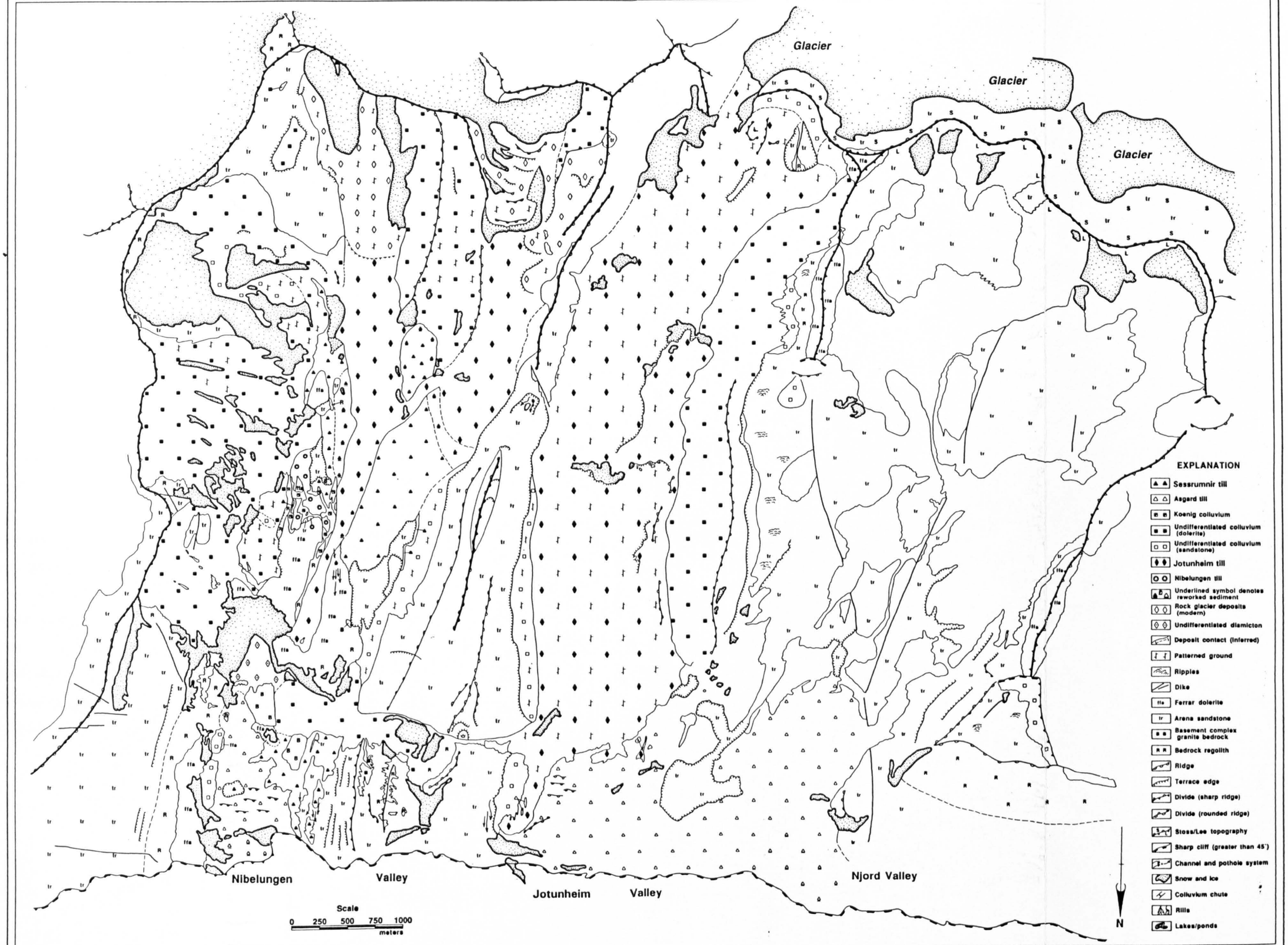
Glacier
Glacier
Glacier
Nibelungen
Valley
Jotunheim
Valley
Njord Valley
Scale
0 250 500 750 1000
meters
N
EXPLANATION
Sessrumnir till
Asgard till
Koenig colluvium
Undifferentiated colluvium (dolerite)
Undifferentiated colluvium (sandstone)
Jotunheim till
Nibelungen till
Underlined symbol denotes reworked sediment
Rock glacier deposits (modern)
Undifferentiated diamicton
Deposit contact (inferred)
Patterned ground
Ripples
Dike
Ferrar dolerite
Arena sandstone
Basement complex granite bedrock
Bedrock regolith
Ridge
Terrace edge
Divide (sharp ridge)
Divide (rounded ridge)
Stoss/Lee topography
Sharp cliff (greater than 45°)
Channel and pothole system
Snow and ice
Colluvium chute
Rills
Lakes/ponds

EXPLANATION

- Sessrumnir till
- Asgard till
- Koenig colluvium
- Undifferentiated colluvium (dolerite)
- Undifferentiated colluvium (sandstone)
- Jotunheim till
- Nibelungen till
- Underlined symbol denotes reworked sediment
- Rock glacier deposits (modern)
- Undifferentiated diamicton
- Deposit contact (inferred)
- Patterned ground
- Ripples
- Dike
- Ferrar dolerite
- Arena sandstone
- Basement complex granite bedrock
- Bedrock regolith
- Ridge
- Terrace edge
- Divide (sharp ridge)
- Divide (rounded ridge)
- Stoss/Lee topography
- Sharp cliff (greater than 45°)
- Channel and pothole system
- Snow and ice
- Colluvium chute
- Rills
- Lakes/ponds

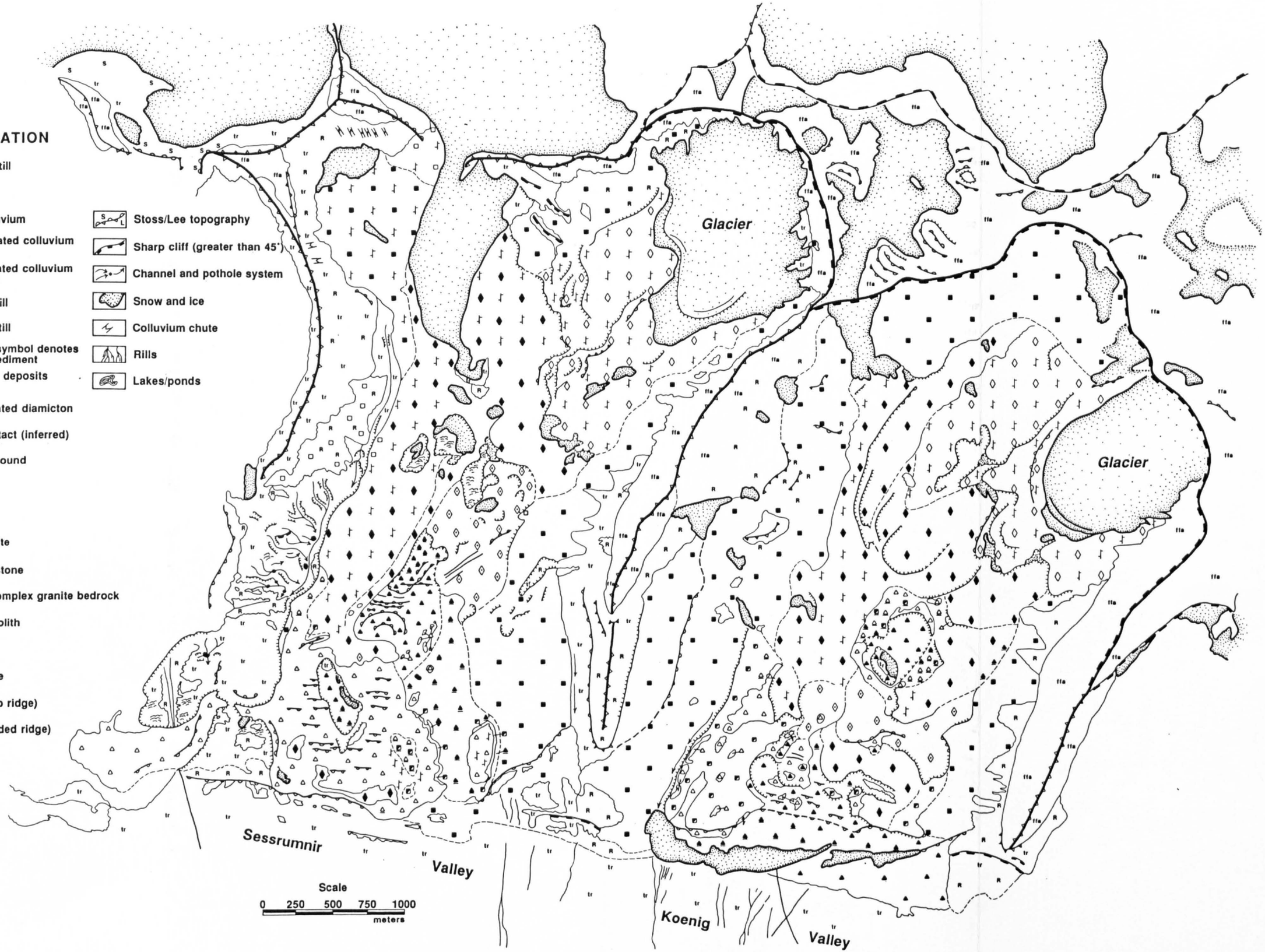

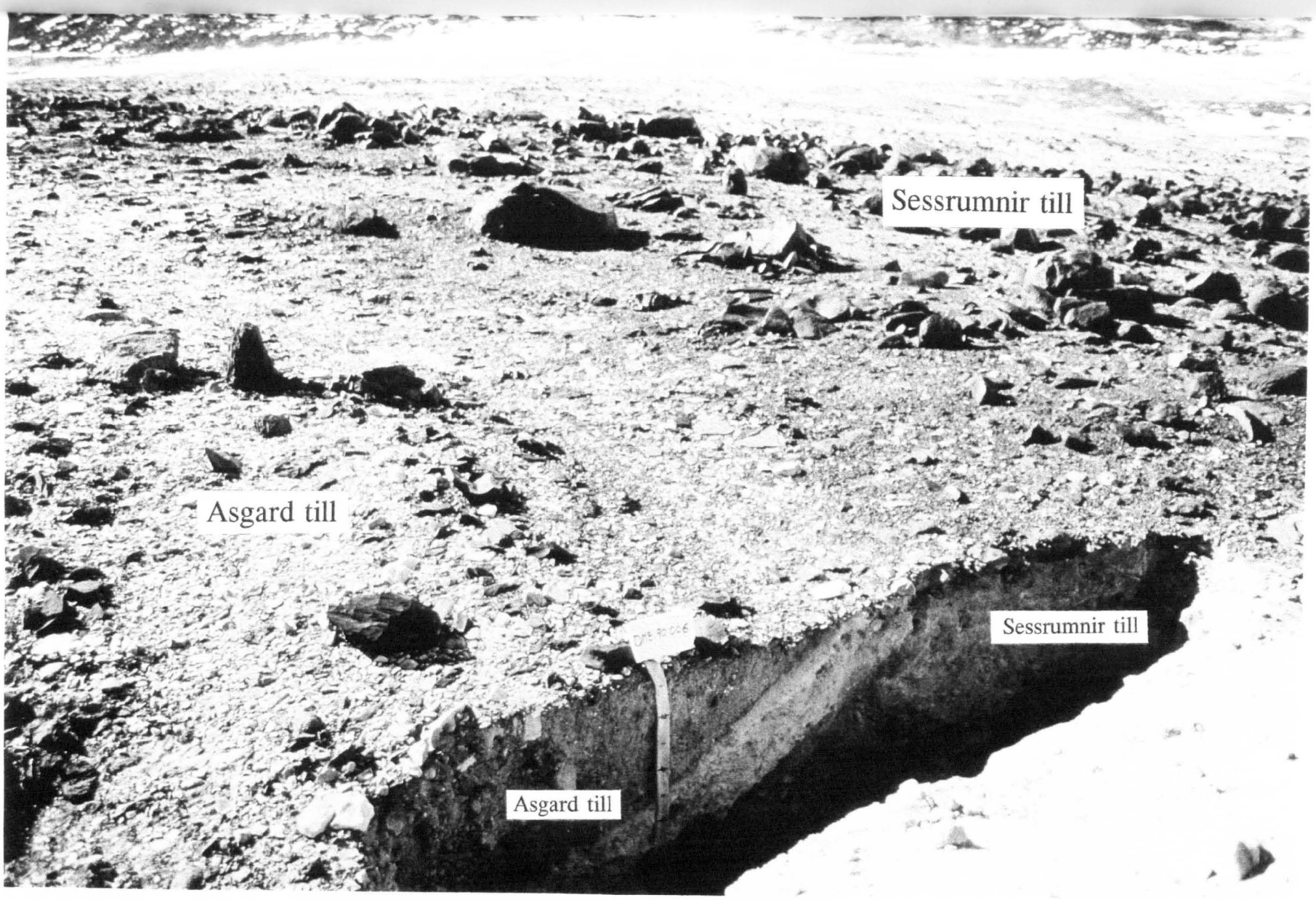

Figure 6. Photograph of hand-dug section cut across surface contact of Sessrumnir and Asgard till at point indicated in Figure 7. Note inclined strata within the Asgard till (light colored unit) truncated at the present ground surface.

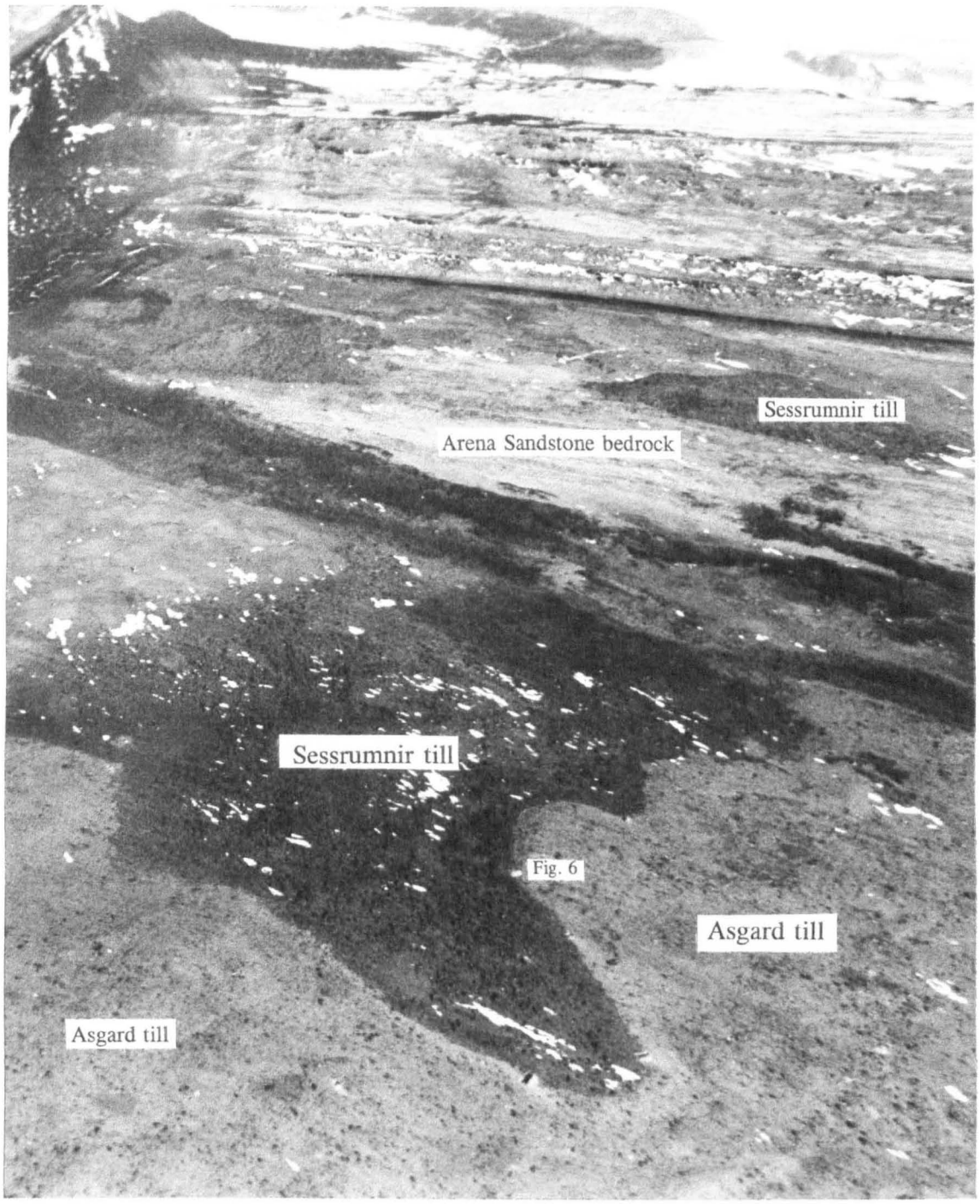

Figure 7. Low-elevation aerial photograph looking southwest across lower Nibelungen Valley, showing disjointed and eroded outcrop patterns of Sessrumnir and Asgard tills, and aligned boulders in lower Nibelungen Valley. The boulders trend diagonally across the photograph, from the upper left corner to the lower right corner.

Figure 8. Oblique aerial view looking northeast down Nibelungen Valley. Foreground shows the Nibelungen till and upvalley basin. A second basin, which cuts through Sessrumnir till, occurs at the western edge of the valley. Inselbergs of Sugden et al. 1994 and Denton et al. 1994 cap the Olympus Range

(a)

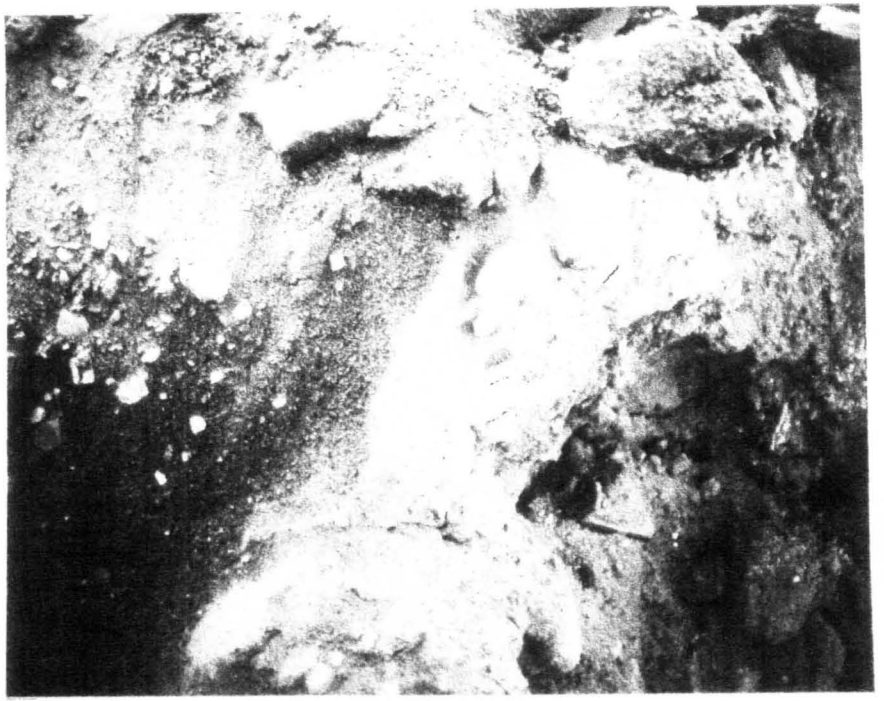

(b)

Figure 9. (a) Oblique view of a hand-dug section cut across an active sand wedge in lower Wright Valley. Top surface of wedge has been removed. Small lenses of ice shown at right side of photograph. Note vertical stratification of sand and gravel. Scale, 17 cm long, is on open axis of active wedge. Photograph and caption from Black (1976). (b) Close-up view of volcanic ash (center stripe) filling relict sand-wedge deposit in central Koenig Valley (Fig. 2). Note vertical stratification of sand and gravel. Ash vein is about 10 cm wide. $^{40}Ar/^{39}Ar$ analyses indicate that the ash (DME-91-41) is 13.6 Ma old. This relict sand-wedge deposit truncates Asgard till. Hence the isotopic date of 13.6 Ma represents a minimum age for deposition of Asgard till (see also Table 2 and Appendix I).

Table 1. Stratigraphy, sedimentology, and isotopic age of mapped surficial deposits in the western Asgard Range

DEPOSIT	DISTRIBUTION	AGE MA	STRATIGRAPHIC POSITION	STRAT. CONTACT	THICKNESS	TEXTURE	CLAST	ERR.	GLAC.	CL.
Rock glaciers	< 2 km from valley headwalls	< 12.5	overlies Asgard till and undifferentiated colluvium	sharp	thickens downvalley to >3 m	boulders	85% dolerite 15% sandstone	none	none	10YR 6/4
Undifferen. colluvium	on or near valley walls	> 12.0	overlies Asgard till	sharp	<1.5 m	sandy gravel	50% dolerite 50% sandstone	none	none	10YR 6/4
Jotunheim till	on valley floors; particularly in Jotunheim valley	> 10.5	overlies Sessrumnir till and Asgard till	sharp	thins down-valley to <30 cm	gravelly sand	95% dolerite 5% sandstone	none	none	10YR 5/6
Nibelungen till	downvalley from bedrock hollow in upper Nibelungen V.	< 15.2 > 13.6*	overlies ash on top of Koenig colluvium pavement	very sharp; preserves underlying pavement	<75 cm	sandy gravel	85% sandstone 15% granite locally >35% granite	none	none	2.5Y 6/4
Asgard till	at valley mouths, especially in Sessrumnir Valley	<15.2* >13.6	overlies Sessrumnir till in Nibelungen Valley; elsewhere overlies Koenig colluvium	very sharp above 1500 m elevation; otherwise gradational	1.0 to 1.5 m	gravelly sandy mud	85% sandstone 13% dolerite 2% granite	yes	5 to 10%	2.5Y 6/4
Koenig colluvium	near base of valley walls and along valley floors	>15.2	overlies Sessrumnir till in Nibelungen Valley	sharp	60 to 95 cm	sandy gravel	75% dolerite 25% sandstone locally >75% granite	none	none	5YR 8/4
Inland Forts till	on the floor of south-facing valleys in Inland Forts	>13.5	overlies striated and molded bedrock; southward ice flow (downvalley)	Arena Sandstone bedrock	10 cm to 1.0 m	gravelly sandy mud	90% sandstone 10% dolerite	none	6%	10YR 7/4
Sessrumnir till	on valley floors; in Sessrumnir valley, extends from mouth to < 1 km from headwall	>15.2	overlies striated and molded bedrock; northward ice flow (downvalley)	Ferrar Dolerite and granite bedrock	>1.25 m, particularly in Nibelungen Valley	gravelly sandy mud	99% dolerite 1% siltstone	Aztec siltstone?	10%	2.5Y 7/4

* Indicates inferred upper or lower age limit based on stratigraphic relations (see text); otherwise deposit age based directly on $^{40}Ar/^{39}Ar$ analyses of individual volcanic crystals or multiple glass shards from overlying/ underlying in-situ volcanic ashfall deposits. Sedimentary textures and clast composition based on field observations. The abbreviation Err. indicates abundance of glacial erratics; Glac. indicates abundance of glacially molded/ striated clasts; Cl. indicates average Munsel Color based on field observations.

Table 2. Summary of volcanic ash data from text and appendix I.

SAMPLE NUMBER	DESCRIPTION	STRATIGRAPHIC POSITION	MATERIAL DATED	$^{40}Ar/^{39}Ar$ AGE	SIGNIFICANCE
		ASH-FILLED SAND WEDGES			
DMS-90-36 B	Stringers (2 to 3 cm thick) of black, vesicular ash buried to 25 cm depth in U-shaped sand-and-gravel deposit that truncates undifferentiated colluvium in lower Nibelungen Valley.	Ash is surrounded by ventifacts; many clasts coated with ash. Undifferentiated colluvium and ash deposit overlie Asgard till with sharp stratigraphic contacts.	glass	10.0 Ma	Ash is inferred to have been deposited in an ancient sand wedge. Ash postdates (or is concurrent with) deposition of undifferentiated colluvium. Isotopic date provides a minimum age for Asgard till. Cold desert at 10.0 Ma.
DMS-90-38 B	Stringers of black vesicular ash buried between 25 and 50 cm depth in sandy, undifferentiated colluvium in lower Nibelungen Valley. Ash occurs imbedded in ice cement at 50 cm depth.	Ash is surrounded by ventifacts; many clasts coated with ash. Undifferentiated colluvium and ash overlie Asgard till with sharp stratigraphic contacts.	sanidine	12.0 Ma	Ash is inferred to have been deposited in an ancient sand wedge. Ash postdates (or is concurrent with) deposition of undifferentiated colluvium. Isotopic date provides a minimum age for Asgard till. Cold desert at 12.0 Ma.
DMS-89-132 B	Pods (10 cm^3) and stringers (2 to 5 cm) of black, vesicular ash buried to 35 cm depth in sandy outcrop of Jotunheim till in central Sessrumnir Valley.	Ash occurs in association with gravel-sized ventifacts and vertical beds of oxidized sand-and-gravel layers that cut Jotunheim till.	sanidine	10.5 Ma	Ash is inferred to have been deposited in an ancient sand wedge. Ash postdates (or is concurrent with) deposition of Jotunheim till. Isotopic date provides a minimum age for Jotunheim till. Cold desert at 10.5 Ma.
DMS-89-143 B	Vertically oriented stringer (3 to 8 cm thick) of black, vesicular ash.	Ash stringer truncates Inland Forts till with sharp stratigraphic contacts. Ventifacts occur in the upper 5 cm of the ash stringer.	glass	13.5 Ma	Ash is inferred to have been deposited in an ancient sand wedge. Isotopic date provides a minimum age for Inland Forts till. Glaciers at head of Inland Forts have remained cold-based since ash deposition. Cold desert at 13.5 Ma.
DME-91-41	Thick, vertical lens of gray, vesicular ash (10 to 15 cm) that tapers to V-shaped point at 30 cm depth. Ash is sandwiched between well-oxidized, vertically stratified sand-and-gravel layers.	V-shaped wedge of ash and stratified sand-and-gravel truncates Asgard till with sharp stratigraphic contacts in central Koenig Valley.	sanidine glass	13.6 Ma 14.7 Ma	Ash was deposited in ancient sand-wedge deposit that truncates Asgard till. Ash dates provide minimum age for deposition of Asgard till and initial buildup of overriding ice. Cold desert at 13.6/ 14.7 Ma.
DMS-91-22	Extensive pod/stringer of gray, vesicular ash buried 10 to 35 cm depth at the margin of a large (>1.25 m deep), relict sand wedge deposit. Ash occurs banked up against ventifacts that line the margin of the sand-wedge deposit.	V-shaped wedge of ash and stratified sand-and-gravel truncates Sessrumnir till with sharp stratigraphic contacts in upper Nibelungen Valley.	crystal	15.0 Ma	Ash was deposited in ancient sand-wedge deposit that truncates Sessrumnir till. Ash dates provide minimum age for deposition of Sessrumnir till and a minimum age for wet-based alpine glaciation in the western Asgard Range. Initial valley cutting and development of rectilinear slopes in western Asgard Range antedates 15.0 Ma. Cold desert at 15.0 Ma.

Table 2 (cont.). Summary of volcanic ash data from text and appendix I.

SAMPLE NUMBER	DESCRIPTION	STRATIGRAPHIC POSITION	MATERIAL DATED	$^{40}Ar/^{39}Ar$ AGE	SIGNIFICANCE
		ASH IN ROCK GLACIER DEPOSIT			
DMS-91-46	Thin, horizontal stringers of black, vesicular ash (1 to 2 cm thick) interbedded with coarse-grained sand and fine-grained gravel. Rock glacier deposit occurs 2.5 km north of valley headwall.	Ash occurs within the upper 25 cm of the outermost, well-preserved rock glacier deposit in Koenig Valley. Rock glacier deposit overlies Asgard till with sharp stratigraphic contacts.	sanidine glass	12.5 Ma 13.5 Ma	Indicates maximum expansion of rock glaciers in the last 12.5 Ma. Suggests that temperate alpine glaciation of western Asgard Range antedates 12.5 Ma.
		WATERLAIN ASH DEPOSIT			
DMS-89-211 B	Thick bed of gray, stratified ash (35 cm) that shows folded laminations, flame structures, faults, and small dropstones.	Ash occurs at the margin of a bedrock hollow in central Njord Valley. Ash overlies a silty diamicton that rests on weathered bedrock.	sanidine glass	14.5 Ma 15.0 Ma	Present morphology of western Asgard Range antedates 14.5/ 15.0 Ma. Small, seasonally ice-covered pond/ lake existed in central Njord Valley at 14.5/ 15.0.
		ASH OVERLYING BURIED DESERT PAVEMENT			
DMS-90-124 B	Thin stringers of black, vesicular ash that fill voids between buried gravel-and-cobble ventifact pavement in Nibelungen Valley. Ash coats the upper surface of gravel ventifacts.	Ash and associated ventifact pavement occur buried at 60 cm depth and overlie Koenig colluvium in stratigraphic section. Nibelungen till rests on top of ash and pavement with a sharp stratigraphic contact.	sanidine glass	14.8 Ma 15.2 Ma	Present morphology of western Asgard Range antedates 14.8/ 15.2 Ma. Dry, desert conditions favorable for development/ preservation of desert pavement at 14.8/ 15.2 Ma. Koenig colluvium antedates 14.8/ 15.2 Ma; Nibelungen till postdates 14.8/ 15.2 Ma. The latter places a maximum age for glacial overriding of the western Asgard Range at 14.8/ 15.2 Ma.

APPENDIX 1 $^{40}Ar/^{39}Ar$ Data

Sample	$\%^{39}Ar$	$^{37}Ar/^{39}Ar$	$^{36}Ar/^{39}Ar$	$^{40}Ar^*/^{39}Ar$	$\%^{39}Ar$	Age (Ma)	SD
ASH-FILLED SAND WEDGES							
DMS90-36B (Glass / 61B)							
5111-01A	8.4	0.0780	0.06607	2.0449	9.5	10.237	1.595
5111-01B	26.6	0.0767	0.07810	2.0312	8.1	10.169	0.739
5111-01C	26.8	0.0759	0.00852	1.9960	44.3	9.993	0.224
5111-01D	13.6	0.0809	0.02101	1.9841	24.2	9.934	0.979
5111-01E	16.0	0.0760	0.00116	2.0296	85.8	10.161	0.278
5111-01F	8.7	0.0720	0.00083	2.0563	89.5	10.294	0.516
					Plateau Age =	**10.08 ± 0.17 SE**	
DMS90-38B (Sanidine / 61A)							
5095-01		0.0218	0.00031	2.4285	96.5	12.151	0.193
5095-02		0.0438	0.00086	2.3712	90.4	11.865	0.277
5095-03		0.0370	0.00072	2.4049	92.0	12.033	0.290
5095-04		0.0304	0.00021	2.4401	97.6	12.209	0.380
5095-05		0.0182	0.00249	2.4570	76.8	12.137	0.927
					Weighted Mean =	**12.07 ± 0.13 SE**	
DMS89-132B (Sanidine / 41B)							
3180-01		0.0100	0.00034	0.9170	89.9	9.767	0.063
3180-02		0.0240	0.00040	0.9418	88.7	10.031	0.069
3180-04		0.0136	0.00034	0.9453	90.2	10.068	0.069
3180-05		0.0106	0.00019	0.9721	94.4	10.353	0.066
3180-06		0.0128	0.00010	0.9817	97.0	10.454	0.072
					Weighted Mean =	**10.12 ± 0.03 SE**	
3180-03		0.0110	0.00023	1.3997	95.2	14.887	0.075
DMS89-143B (Glass / 61A)							
5091-01A	10.3	1.2967	0.02850	2.6739	24.3	13.684	3.140
5091-01B	41.6	0.6636	0.00721	2.6413	55.9	13.518	0.724
5091-01C	15.7	1.8044	0.01330	2.5902	40.6	13.257	1.893
5091-01D	10.9	2.3462	0.02053	3.1109	34.5	15.910	4.014
5091-01E	16.1	9.0472	0.02986	1.1159	12.0	5.723	2.036
5091-01F	6.0	631.3426	0.21296	48.4444	65.4	233.129	17.320
					Plateau Age =	**13.56 ± 0.69 SE**	
DME91-41 (Sanidine / 98A)							
7174-02		0.0213	0.00145	15.8278	97.4	13.589	0.197
7174-07		0.0582	0.00040	15.9122	99.3	13.661	0.147
7174-08		0.0000	0.00126	15.8924	97.7	13.644	0.095
7174-09		0.0000	0.00146	15.9245	97.4	13.672	0.187
7174-10		0.0000	0.00052	15.9054	99.0	13.655	0.119
					Weighted Mean =	**13.65 ± 0.06 SE**	
DME91-41 (Glass / 98A)							
7185-01A	14.5	0.1593	0.00498	17.4518	92.3	14.978	0.302
7185-01B	1.0	0.6002	0.00247	16.9513	96.1	14.550	0.243
7185-01C	0.5	0.4866	0.00540	16.5883	91.4	14.240	0.417
7185-01D	1.3	0.1247	0.00141	16.9101	97.6	14.515	0.175
7185-01E	9.6	0.1654	0.00166	17.3040	97.3	14.851	0.061
7185-01F	15.9	0.1388	0.00185	17.2699	97.0	14.822	0.072
7185-01G	9.5	0.1292	0.00155	17.1905	97.5	14.754	0.065
7185-01H	6.4	0.1485	0.02264	17.1369	72.0	14.709	0.090
7185-01I	18.2	0.0829	0.04104	17.1700	58.6	14.737	0.093
7185-01J	8.3	0.0841	0.00216	17.1869	96.5	14.751	0.057
7185-01K	15.1	0.1364	0.00365	17.1088	94.1	14.685	0.055
					Plateau Age =	**14.75 ± 0.03 SE**	

APPENDIX 1 $^{40}Ar/^{39}Ar$ Data (continued)

Sample	$\%^{39}Ar$	$^{37}Ar/^{39}Ar$	$^{36}Ar/^{39}Ar$	$^{40}Ar^{*}/^{39}Ar$	$\%^{39}Ar$	Age (Ma)	SD
ASH-FILLED SAND WEDGES (continued)							
DMS91-22 (Sanidine / 98A							
7183-01		0.0984	0.00201	18.0002	96.8	15.446	0.045
7183-02		0.1368	0.00151	17.2810	97.5	14.832	0.145
7183-04		0.1135	0.00039	17.4501	99.4	14.976	0.187
7183-05		0.1176	0.00199	17.6940	96.8	15.185	0.063
7183-06		0.1050	0.00224	17.7621	96.5	15.243	0.073
7183-07		0.0998	0.00197	17.5596	96.8	15.070	0.064
7183-09		0.1086	0.00108	17.2757	98.2	14.827	0.059
7183-10		0.0798	0.00475	17.4196	92.6	14.950	0.148
7183-11		0.0734	0.00269	17.2758	95.6	14.827	0.144
7183-12		0.1071	0.00148	17.3039	97.6	14.851	0.110
					Weighted Mean	**= 15.01**	**± 0.02 SE**
Analyses not used in mean calculation							
7183-03		13.0090	0.00516	13.2935	96.6	11.420	0.071
7183-08		0.1086	0.00112	20.3787	98.4	17.478	0.077
7183-13		0.1126	0.00354	23.1014	95.7	19.800	0.102
DMS91-22 (Glass / 98A)							
7179-01A	9.3	0.8831	0.10562	16.0059	33.9	13.741	0.290
7179-01B	21.8	0.1235	0.05125	16.5810	52.3	14.233	0.122
7179-01C	33.2	0.1314	0.02563	16.5815	68.7	14.234	0.090
7179-01D	22.4	0.1285	0.01316	16.6009	81.1	14.250	0.079
7179-01E	4.7	0.1347	0.01435	15.9215	79.0	13.669	0.193
7179-01F	1.9	0.1069	0.02336	18.3097	72.6	15.711	0.494
7179-01G	1.4	0.0600	0.03174	15.0362	61.6	12.912	0.686
7179-01H	1.1	0.1751	0.04576	13.5650	50.1	11.653	0.823
7179-01I	2.4	0.2166	0.04351	15.1982	54.2	13.050	0.442
7179-01J	1.5	0.1167	0.02872	17.0089	66.7	14.599	0.538
7179-01K	0.4	4.4100	0.08557	12.3835	33.1	10.641	2.378
					Plateau Age	**= 14.24**	**± 0.05 SE**
ASH IN ROCK GLACIER DEPOSIT							
DMS91-46 (Sanidine / 98A)							
7175-02		0.0189	0.00027	14.7757	99.5	12.689	0.279
7175-06		0.0719	0.00288	14.5970	94.5	12.536	0.120
					Weighted Mean	**= 12.56**	**± 0.11 SE**
DMS91-46 (Glass / 98A)							
7177-01A	1.5	0.2294	0.00676	14.9106	88.3	12.804	0.279
7177-01B	4.5	0.1440	0.00217	15.8432	96.2	13.602	0.106
7177-01C	4.8	0.1485	0.00095	16.1503	98.4	13.865	0.116
7177-01D	5.7	0.1439	0.00159	16.4794	97.3	14.146	0.100
7177-01E	5.3	0.1802	0.00138	16.5823	97.7	14.234	0.063
7177-01F	6.1	0.2328	0.00182	15.8270	96.8	13.588	0.075
7177-01G	10.4	0.2332	0.00089	15.8382	98.5	13.598	0.079
7177-01H	13.6	0.1704	0.00211	15.7264	96.3	13.502	0.057
7177-01I	46.2	0.1960	0.00189	15.7201	96.7	13.497	0.045
7177-01J	1.7	4.0515	0.00755	15.5585	89.1	13.359	0.184
7177-01K	0.2	3.2314	0.00935	16.0022	86.5	13.738	1.911
					Plateau Age	**= 13.56**	**± 0.69 SE**

APPENDIX 1 $^{40}Ar/^{39}Ar$ Data (continued)

Sample	$\%^{39}Ar$	$^{37}Ar/^{39}Ar$	$^{36}Ar/^{39}Ar$	$^{40}Ar^*/^{39}Ar$	$\%^{39}Ar$	Age (Ma)	SD
WATERLAIN ASH DEPOSIT							
DMS89-211B (Sanidine / 41B)							
3184-03		0.0146	0.00056	1.3377	89.0	14.231	0.109
3184-02		0.0137	0.00068	1.3567	87.0	14.432	0.105
3184-04		0.0131	0.00049	1.3967	90.5	14.856	0.091
Weighted Mean = 14.55 ± 0.06 SE							
Analyses not used in mean calculation							
3184-01		0.0192	0.00125	2.1253	85.2	22.557	0.120
3184-05		0.0274	0.00085	12.4483	98.0	128.279	0.373
DMS89-211B (Glass / 41B)							
3176-01		0.0824	0.00006	1.4128	99.1	15.026	0.043
3176-02		0.0827	0.00006	1.4168	99.1	15.068	0.045
3176-03		0.0837	0.00008	1.4246	98.7	15.151	0.050
Weighted Mean = 15.08 ± 0.03 SE							
ASH OVERLYING BURIED DESERT PAVEMENT							
DMS90-124B (Sanidine / 61B)							
5099-01		0.0490	0.00151	3.0117	87.2	15.057	0.652
5099-02		0.0344	0.00003	2.9972	99.8	14.985	0.851
5099-03		0.0291	0.00021	2.9350	98.0	14.675	0.380
5099-04		0.0304	0.00002	3.0147	99.8	15.073	0.740
Weighted Mean = 14.84 ± 0.28 SE							
DMS90-124B (Glass / 61B)							
5098-01A	1.8	0.0478	0.00720	3.5246	62.4	17.609	2.047
5098-01B	43.9	0.0738	0.00422	3.0609	71.1	15.302	0.113
5098-01C	49.8	0.0923	0.00046	3.0407	95.9	15.202	0.082
5098-01D	2.2	0.0516	0.00143	2.9147	87.4	14.574	3.043
5098-01E	0.1	0.0000	0.00391	1.2365	51.7	6.197	50.949
5098-01F	2.1	0.0150	-0.00282	3.9130	127.1	19.539	1.655
Plateau Age = 15.24 ± 0.08 SE							

All sanidine $^{40}Ar/^{39}Ar$ ages are total fusion analyses
Irradiation Data
41B J = 0.005920 ± 0.0000090
61A J = 0.002847 ± 0.0000036
61B J = 0.002783 ± 0.0000024
98A J = 0.000478 ± 0.0000006

CHAPTER FIVE

Miocene-Pliocene-Pleistocene Glacial History of Arena Valley, Quartermain Mountains, Antarctica

ABSTRACT

An $^{40}Ar/^{39}Ar$ chronology of in-situ to near in-situ volcanic ashfall deposits indicates that the surficial stratigraphy of Arena Valley extends back at least to middle-Miocene time. Wet-based glacial ice occupied part of Arena Valley more than 11.3 Ma ago. Thick, northeast-flowing ice subsequently engulfed Arena Valley, again more than 11.3 Ma ago. Only minor glacier expansion occurred during Pliocene and Pleistocene time. The maximum Pliocene thickening of Taylor Dome, 35 km inland of Arena Valley, was certainly less than 475 m and probably less than 250 m. Maximum thickening of Taylor Dome was less than 160 m during the Pleistocene.

The preservation of Miocene- and Pliocene-age ashes on steep valley slopes indicates that the major bedrock landforms of Arena Valley are relict and that little slope evolution/ colluviation has occurred during the last 11.3 Ma. The geologic record of Arena Valley glaciation and landscape evolution shows persistent cold-desert conditions and hence implies stability of the adjacent East Antarctic Ice Sheet for at least the last 11.3 Ma.

INTRODUCTION

The Dry Valleys region of southern Victoria Land contains one of the longest and most complete terrestrial glacial records in Antarctica. In places, glaciogenic surficial deposits extend back at least to middle-Miocene time. Here, we describe a surficial stratigraphic and geomorphic record of the Quartermain Mountains that extends back to at least 11.3 Ma. The Quartermain massif is a sandstone-and-dolerite capped mountain range situated at the western margin of the Dry Valleys region (Figs. 1 and 2). Our goal is to produce a detailed geologic record of late Cenozoic glacial and non-glacial sedimentation and paleoclimate change.

The Quartermain Mountains are ideal for recording ice-sheet fluctuations and paleoclimate change because they are adjacent to the East Antarctic Ice Sheet and exhibit a suite of glacial erosional features, semi-arid landforms, and widespread drift and colluvium. The drifts include an outcrop of the Sirius Group on Mt. Feather at 2650 m elevation. This deposit, a semi-lithified glacial till that overlies southwest-trending bedrock striations, is inferred to represent deposition beneath a temperate ice-sheet that overrode the Dry Valleys region after 3.0 Ma in late Pliocene/early Pleistocene time (Barrett et al., 1992; Webb et al., 1984; Webb and Harwood, 1991; see also Marchant et al., 1994a; Denton et al., 1994).

PHYSICAL SETTING

Dry Valleys region. The Dry Valleys region in the Transantarctic Mountains includes 4000 km^2 of predominantly ice-free desert topography between the Ross Sea and the Taylor Dome on the edge of the East Antarctic Ice Sheet (Fig. 1). This region exposes part of the uplifted and tilted shoulder of the West Antarctic Rift System, which extends more than 3000 km from northern Victoria Land to the Ellsworth Mountains (Behrendt and Cooper, 1990; 1991). Cenozoic volcanism, which occurs both in and adjacent to the Dry Valleys region, is associated in part with active crustal thinning and extension (Kyle, 1990). Exposed bedrock in the Dry Valleys region includes a basement complex of lower Paleozoic igneous and metamorphic rocks overlain by very gently dipping Devonian-to-Triassic sandstones, siltstones, and conglomerates of the Beacon Supergroup, all of which are intruded by Jurassic-age Ferrar Dolerite and Cenozoic volcanics. The main valleys (Wright, Victoria, and Taylor) are bounded by the Asgard and the Olympus Ranges, and by the Quartermain Mountains.

Taylor Dome and East Antarctic Ice Sheet. The East Antarctic Ice Sheet (26×10^6 km^3) comprises several interior ice domes that exceed 3000 m in elevation (Dome Argus, 4000 m, Valkyrejedomen, 3700 m, and Dome Circe, 3200 m). A number of smaller ice domes, generally $<$ 2800 m in elevation, occur near the ice-sheet periphery. The Taylor Dome, which rises about 100 m elevation above the ice-sheet surface about 35 km inland of the Dry Valleys region, is one such peripheral dome (Fig. 1). This dome merges with a broad ice divide that extends far inland to Dome Circe (Drewry, 1982) (Dome C on Fig. 1). Such an ice configuration means that far-travelled, inland East Antarctic ice flowing outward toward McMurdo Sound is currently deflected around the Dry Valleys region. In fact, the main drainage for inland East Antarctic ice in this region is now through the Mawson and Mulock Glaciers, which flow north and south of the Dry Valleys into the Ross Sea. In contrast, Taylor Dome feeds several small glaciers that drain into the Dry Valleys region, including Taylor, Wright Upper, Victoria Upper, and Ferrar Glaciers. Although advance and retreat of these glaciers primarily reflect the ice-surface rise and fall of Taylor Dome, they also record large-scale interior East Antarctic Ice Sheet fluctuations that are sufficient to overwhelm the Taylor Dome (Drewry, 1982).

The sandstone- and dolerite-capped Quartermain Mountains are situated near the confluence of the Ferrar and Taylor Glaciers in the western Dry Valleys, about 35 km southeast of Taylor Dome. Ferrar Glacier delimits the western mountain margin, whereas Taylor Glacier flows along the eastern margin. Lobes of Taylor Glacier with surface blue-ice zones flow southward into north-facing Quartermain valleys. Alpine glaciers and permanent snow banks within the Quartermain Mountains are essentially restricted to topographic areas favorable for the collection of windblown snow. Under the present hyper-arid, cold-desert Dry Valleys climate, such alpine glaciers are slow moving, cold-based, and non-erosive (Holdsworth and Bull, 1970); flow rates are probably less than 3.0 m per year and perhaps as low as 0.1 to 0.5 m per year (Chinn, 1980). All glaciers lack surface-melting ablation zones. There

are no outwash plains, kame terraces, lacustrine sediments, or ice-marginal channels associated with any present-day glaciers in the Quartermain Mountains.

Records of present-day mean annual temperature are not available for the high-elevation western Dry Valleys. To estimate the mean annual atmospheric temperature in the Quartermain Mountains, we must refer to measurements taken beside Lake Vanda at 123 m elevation in central Wright Valley. Here mean annual temperature is -19.8°C (Schwerdtfeger, 1984) and annual precipitation is equivalent to less than 10 mm of water (Keys, 1980). Assuming an average rate of 1°C/100 m elevation rise (Robin, 1988), mean annual temperature in the Quartermain Mountains is about -30°C to -35°C. Precipitation levels may slightly exceed 10 mm of water equivalent in some parts of the Quartermain Mountains (Bockheim, 1982).

MORPHOLOGY OF THE QUARTERMAIN MOUNTAINS

The morphology of the Quartermain Mountains is typical of sandstone-and-dolerite ranges of the western Dry Valleys region. It shows a suite of north- and south-facing valleys that are cut back into a high-elevation plateau, leaving a prominent escarpment, butte-and-mesa erosional remnants, high-level valley benches, and flat-topped divides, all cut by smooth rectilinear slopes. Individual valleys lie between 1500 m and 1000 m elevation and are incised into Beacon Supergroup sandstones and Ferrar Dolerite intrusions, although granite bedrock of the basement complex crops out at about 950 m elevation along the north flank of New Mountain adjacent to Windy Gully (Hamilton and Hays, 1963).

The high-elevation tableland at the western margin of the Quartermain Mountains shows two distinct plateaux (Figs. 2 and 3). Mt. Feather, a flat-topped mesa reaching 2985 m elevation, forms the high-level plateau. It lies above a lower, dissected, snow- and ice-covered surface that rises to an average elevation of 2350 m and nearly encircles the southern margin of Beacon Valley. A small (0.6 km^2), narrow bench at 2650 m elevation occurs on the northeastern flank of Mt. Feather between the high- and low-elevation plateaux. This narrow bench is cut by steep, rectilinear slopes that descend eastward 700 m to Ferrar Glacier and drop more than 1000 m to the floor of Beacon Valley. A small remnant of the Sirius Group crops out on the surface of this bench (Brady and Mckelvey, 1979, 1983; Harwood, 1986); it is the only place where the Sirius Group occurs in the Quartermain Mountains (Fig. 3). Similar benches (some > 2 km^2) occur elsewhere between 1600 and 1700 m elevation along the tops of drainage divides that separate individual Quartermain valleys. These benches slope northeastwards of about 5°, which is opposite to the general westward sandstone bedrock dip of 2° to 4° in the Dry Valleys region (Hamilton and Hays, 1963). The largest such bench occurs between lower Beacon and Arena Valleys, where a broad sandstone platform separates East and West Beacon Mountains.

The main north-facing valleys of the Quartermain Mountains are Kennar, Turnabout, Beacon, Arena, and an unnamed valley east of Arena Valley (Fig. 2). These valleys are now predominantly free of glacial ice, although a lobe of Taylor Glacier dams the mouth of each valley. In sharp contrast, most south-facing valleys in the Quartermain Mountains are filled with glacier ice that flows into the upper Ferrar Glacier. Arena Valley, the focus of this paper, is about 8 km long. Its width varies from 2.5 km in the lower valley to about 5 km in the center. Topographic relief averages about 600 m from valley floor to adjacent divides (Fig. 4). Altar Mountain (2200 m elevation) occurs at the valley head and divides upper Arena Valley into two troughs, here called East and West Forks. These forks merge in central Arena Valley and form a single trunk that extends to the valley mouth. A series of high-elevation sandstone and dolerite cliffs nearly enclose the valley. These cliffs are punctuated by pyramid-shaped erosional remnants (East Beacon, South Beacon, and Slump Mountains) and are breached in several places to form low-lying, smooth bedrock cols and saddles. Two such saddles occur at the headwalls of East and West Forks. In West Fork, the saddle lies only 30 m above the surface of the Ferrar Glacier; in East Fork, the saddle is about 100 m above Ferrar Glacier. The floor of upper Arena Valley shows a series of flat-lying, stepped terraces that descend northward in staircase fashion from the valley headwall. Alpine glaciers (< 3 km long) occur in the lee of stepped bedrock terraces in West Fork. Finally, two stubby east-facing tributaries (each 3 to 4 km long and 1 to 2 km wide) occur along the western margin of central Arena Valley.

Superimposed on valley floors, headwalls, divides, and rectilinear slopes in Arena Valley is an integrated landform system comprised of small-scale basins (2 to 4 m deep), stoss-and-lee forms, and eroded unconsolidated sediments. From south to north, these morphologic forms grade from stoss-and-lee slopes (at the valley headwall and drainage divides) to sinuous bedrock channels and ultimately to wide areas of etched and eroded unconsolidated sediments with intervening bare-bedrock terrain.

Stoss-and-lee slopes are best developed on east-west trending ridges that lie below 1800 m elevation. Stossed saddles in upper West Fork and in central Arena Valley are at 1630 m and 1750 m elevation, respectively. Stossed ridge crests do not occur at the heads of north-facing valleys that cut into the high-elevation, western tableland. The tops of saddles at the head of Arena Valley (and along the main tributary divide in central Arena Valley) show smooth, south-facing slopes and roughened north-facing slopes (Fig. 5). The resultant bedrock form is similar to that of a roche moutonnée. Bedrock overhangs, narrow chutes, jointed bedrock cliffs, and semi-circular depressions (2 to 4 m deep and 10 m wide) occur at saddle crests and on the rough north-facing slopes. Bedrock striations trending roughly northeast-southwest occur beneath a small patch of coarse- grained till (Brawhm till) on the stossed headwall crest in upper West Fork.

Ridge crests, saddles, and the tops of headwalls that show well-developed stoss-and-lee topography are generally bare without thick colluvium or till. They all grade downvalley into elongate tracts of exposed sandstone bedrock.

For example, in the West Fork of Arena Valley, weathered and nearly bare Arena Sandstone bedrock extends 3 km downvalley from the headwall crest.

Sinuous channels. Bedrock channels in bare bedrock terrain occur downvalley from saddles with stoss-and-lee topography in the upper East and West Forks of Arena Valley (Fig. 6). These channels are as much as 3 km in length, sinuous in plan view, and incised in Arena Sandstone bedrock to a depth of 1 to 4 m. In East Fork, the channels are anastomosing and thus diverge around sandstone platforms/ terraces before merging downvalley to form a single trunk on the floor of central Arena Valley.

Basins. Basins that average 2 to 3 m deep are incised into unconsolidated deposits in upper and central Arena Valley. These basins, which may be oblong, elongate, or spherical in shape, expose underlying corrugated Altar Mountain and Arena Sandstone bedrock. Basin edges are sharp. Unconsolidated deposits that extend to the edge of basins have not slumped appreciably down basin walls. The largest single basin in Arena Valley is about 500 m long, 200 m wide, and 3 m deep; it occurs in the lee of the pinnacle of Altar Mountain along the 1600-1700 m elevation bench that separates East and West Forks. In places, individual basins converge laterally to form wide areas of exposed bedrock, for example along the floor of central Arena Valley. Margins of such composite basins are irregular in plan view, showing serrated deposit edges and narrow bedrock salients. Basins also occur near the outlet of the main bedrock channel at the mouth of West Fork.

STRATIGRAPHY OF SURFICIAL DEPOSITS

Figures 6 and 7 display the areal distribution of unconsolidated deposits in Arena Valley. Tables 1 and 2 present the physical characteristics, geographic setting, stratigraphic position, and isotopic age of drift and colluvium units. We separate the drift units into three groups on the basis of lithology, areal distribution, and moraine pattern. Group 1 encompasses all drifts deposited by glacier ice that flowed northeastward down Arena Valley; it includes Slump Mountain diamicton and Altar, Arena, and Brawhm tills. All drifts of Group 1 are restricted to upper and central Arena Valley, lack erratics, and in the case of Arena and Brawhm tills overlie striated and molded bedrock. In contrast, Group 2 drifts represent deposition from ice lobes that flowed southwestward up Arena Valley from Taylor Glacier. This group includes Quartermain I and II tills, and Taylor II, III, IVa, and IVb drifts. Group 2 drifts are restricted to central and lower Arena Valley, contain 3-5% granite erratics, and in the case of Taylor II-IVb drifts show arcuate moraines that open towards Taylor Glacier. Finally, Group 3 drifts were deposited at the margins of expanded alpine glaciers in upper Arena Valley. These drifts show arcuate moraines that open toward current alpine glaciers. The other surficial map units in Arena Valley are colluvium, which occurs on valley slopes and walls, and in-situ and near in-situ volcanic ash deposits.

The drift units in Arena Valley show marked differences in terms of surface morphology and preservation. Taylor II, III, IVa, and IVb drifts, along with all alpine drifts, are well preserved and feature numerous distinct and nearly intact moraine ridges. In sharp contrast, all other drift units, as well as old colluvial units, are exposed only as eroded remnants with little remaining surface morphology. These remnants mantle less than 50% of the bedrock floor and walls of central and upper Arena Valley. They crop out together in intricate areal patterns because units of differing stratigraphic and isotopic ages are all truncated at the ground surface. In places, such remnants stand out as isolated mesas that rise abruptly 1 to 2 m above the surrounding weathered bedrock.

Group 1 Drifts

Altar till. Altar till is a silt-rich and highly oxidized (5YR 7/6) diamicton. It reaches a maximum thickness of 75 cm, overlies weathered sandstone bedrock, and crops out in a discontinuous sheet along the northeast flank of Altar Mountain (Figs. 6 and 7). It terminates abruptly halfway down the mountain flank, which has a constant slope of 28°. The till displays near-horizontal layers of medium-to-coarse-grained gravel set within a sandy matrix. The gravel consists predominantly of dolerite, about 3% of which shows well-developed striations and glacial molding. The till matrix is disaggregated Arena Sandstone bedrock, along with green-and-maroon fragments of the Altar Mountain Sandstone. These green-and-maroon fragments in association with striated dolerite clasts are diagnostic of Altar till.

The striated and glacially molded clasts and overall poor sorting of Altar till indicate a glacial origin. Because molded and striated bedrock pavements have not been observed, we cannot determine the direction of ice flow. However, Altar till lacks granite erratics, a component of all drifts deposited by southward-flowing ice in Arena Valley, and we therefore postulate that glacier ice responsible for Altar till flowed downvalley.

Arena till. Arena till is a sandstone-rich and poorly sorted diamicton that crops out in central Arena Valley in six discontinuous patches, each elongated in a northeast direction. The largest of these till patches is nearly 0.75 km long and 0.4 km wide, with a maximum thickness of 1.5 m. All Arena till patches thin downvalley from basins that expose weathered Altar Mountain Sandstone and fine-grained basalt dikes (Figs. 7 and 8). The till has a complex internal stratigraphy with well-sorted sand-and-gravel layers interbedded with a massive silt-rich diamicton. Recumbent folds occur in about 2% of the excavations; these folds commonly plunge to the northeast. Flame structures mark the contact between fine-sand and silt layers. The till is composed predominantly of Altar Mountain Sandstone (90%), with lesser amounts of Ferrar Dolerite and basalt. Narrow trains of basalt rocks can be traced southward to source areas along individual dikes exposed at the margin of individual basins. About 27% of the clasts within Arena till shows well-developed striations and/or glacial molding.

At some locations, Arena till overlies striated sandstone and dolerite bedrock. Striations, which were measured at over 50 localities, trend from about northeastward 5° to 15° and are consistent with trends derived from bullet boulders at the till surface. At several localities the steep side of crescentic gouges faces to the southwest, indicating an ice-flow direction down the valley axis to the northeast. Typical stoss-and-lee forms that occur along with striated bedrock also show ice flow toward the northeast.

The striated and molded clasts, poor sorting, and underlying striated and molded bedrock pavement all suggest a glacial origin for Altar till. We explain the areal pattern of Arena till and associated upvalley basins by a combination of subglacial quarrying/plucking and deposition. We postulate that glacier ice eroded the basins/ hollows and deposited the material so acquired in linear till patches that extend downvalley from these basins/ hollows. The folded stratification, flame structures, bedrock striations, and glacially molded and striated clasts all indicate that wet-based ice deposited Arena till.

Slump Mountain diamicton. Slump Mountain diamicton is a silt-rich and unconsolidated deposit that mantles the floor of upper-central Arena Valley. The outcrop pattern varies from narrow interconnected debris patches separated by weathered sandstone bedrock in the south, to wide sheets draped uniformly over sandstone bedrock/ residuum in the north (Figs. 6 and 7). Slump Mountain diamicton terminates abruptly at the margins of bedrock hollows/ basins (which occur upvalley from linear Arena till patches) and Arena till (Fig. 8). There are no clear stratigraphic contacts between Slump Mountain diamicton and Arena till; rather, they appear to grade together. The diamicton is structureless and massive. It shows a weathered matrix composed of dissaggregated Altar Mountain Sandstone bedrock. The clast fraction, a minor component of this deposit, is composed of angular dolerite (70% of the total clast fraction) and sandstone gravel. About half of these clasts bear desert varnish and/or siliceous crusts. Slump Mountain diamicton lacks erratic lithologies, glacially molded/ striated clasts, and moraines.

The origin of this diamicton is poorly understood. However, because it is texturally and lithologically similar to Arena till, and shows no clear stratigraphic contacts with the Arena till, we postulate that Slump Mountain diamicton was deposited during the same glacial event as Arena till. Our favored hypothesis is that Slump Mountain diamicton represents deposition from ice tongues during the buildup of the ice that deposited Arena till.

Brawhm till. Brawhm till is a poorly sorted and unoxidized gravel-rich diamicton that occurs between 1550 and 1650 m elevation along the stossed bedrock headwall of upper West Fork (Figs. 3, 6, and 7). Brawhm till crops out in five discrete patches, each < 100 m^2 in area and < 75 cm thick. Individual till patches thin to feather edges and commonly fill bedrock joints that pass across Arena Saddle. The till is composed of a chaotic mixture of gravel- and cobble-sized clasts of Ferrar Dolerite (90%) and Beacon Supergroup sandstones. About 25% of the clasts show

well-developed desert varnish; 50% show extensive fractures and impact chips (fractures that cut across desert varnish and expose unweathered-rock cores); less than 1% show glacial striations. Clasts in Brawhm till all come from local bedrock.

Brawhm till overlies striated Arena Sandstone bedrock. At two localities, the striations show an array of trends, but most trend northeast, parallel with the axis of Arena Valley. At the westernmost locality, the array of striations fans out over a range of 45°. Prominent striations etched deep into the Arena Sandstone trend about N 10° E. The steep sides of associated crescentic fractures face to the southwest, indicating ice flow across Arena Saddle into upper Arena Valley from southwest to northeast.

Brawhm till is nearly continuous with unoxidized and undifferentiated colluvium on adjacent rectilinear slopes (Figs. 3, 6, 7). The colluvium is similar in texture and lithology to Brawhm till, although gravels within the colluvial deposits lack impact chips. This undifferentiated colluvium shows irregular boundaries and thins to a feather edge along weathered Arena Sandstone bedrock.

The areal distribution and irregular outcrop pattern of Brawhm till, the array of underlying bedrock striations, and the crescentic bedrock fractures together suggest northeast-flowing glacier ice. The lack of erratic lithologies and the limited number of striated and molded clasts, together with the preponderance of angular dolerite and sandstone gravels (partially coated with desert varnish), strongly suggest that Brawhm till was not transported far beneath wet-based glacier ice. Till deposition could have occurred beneath expanded Ferrar ice that spilled over the West Fork saddle and flowed northeastward into Arena Valley. Because Brawhm till is lithologically and texturally similar to nearby colluvial deposits, we suggest that the Brawhm till patches represent dolerite-rich colluvium that was retransported subglacially for only a short distance.

Group 2 Drifts

Quartermain II till. Quartermain II till is a granite-bearing diamicton that occurs in patches along the lower valley wall and floor of central Arena Valley (Figs. 6 and 7). These patches are elongate in a northeast-southwest direction. They have sharp, near-vertical edges that stand 1 to 1.5 m in relief above weathered Arena Sandstone bedrock. The upper limit of Quartermain II till decreases upvalley from north to south. Quartermain II till underlies the largest patch of Arena till with gradational stratigraphic contacts. It is composed predominantly of angular, gravel- and cobble-sized clasts of Ferrar Dolerite (60%), with fewer Beacon Supergroup sandstones and granite erratics. In places, it displays lenses of moderately sorted quartz sand interbedded with alternating layers of dolerite grus and coarse-grained gravels. Nearly 60% of the clasts show desert varnish; none shows glacial molding and/or striated facets. Stage 5 salt pans of Bockheim (1990) occur between 10 and 15 cm depth.

The granite erratics, poor sorting, and areal distribution of Quartermain II till suggest glacial deposition from an ancestral lobe of Taylor Glacier that projected into Arena Valley. The absence of glacially molded and striated clasts, associated outwash, and underlying striated bedrock pavements suggests that Quartermain II ice failed to reach the pressure melting point in Arena Valley.

Quartermain I till. Quartermain I till crops out in two isolated moraines and in eight small patches along the floor of east-central Arena Valley. The larger of the two moraines, which is about 250 m long and 6 m high, trends northeast-southwest along the valley axis (Figs. 6, 7 and 9). The smaller moraine, 50 m long and 2 m high, is slightly arcuate in plan view and opens toward the east valley wall. The surface of Quartermain I till lacks relief and merges smoothly with the surface of surrounding Slump Mountain diamicton. The till is composed of angular gravel- and cobble-sized clasts of Ferrar Dolerite (85%), with lesser amounts of Beacon Supergroup sandstone (12%) and granite (3%). Stage 5 salt pans of Bockheim (1990) occur between 15 and 25 cm depth.

The till overlies Arena till and Slump Mountain diamicton with sharp contacts. In stratigraphic section, a buried in-situ desert pavement separates Quartermain I till from underlying Arena till (Fig. 9). This buried pavement consists of ventifacted sandstone cobbles, which are identical in size, shape, and lithology to clasts that now armor nearby outcrops of Arena till exposed at the surface. Thick siliceous crusts and quartz rinds (5 to 10 mm) on the surface of these buried clasts indicate long exposure to a desert environment (Weed and Norton, 1991) prior to burial by overlying Quartermain I till.

The moraine morphology and granite erratics suggests an upvalley glacial origin for Quartermain I till. In-situ desert pavements beneath Quartermain I till indicate that overriding ice was cold-based and non-erosive.

Taylor drifts. The Taylor drifts are composed of angular, unweathered gravel- and cobble-sized clasts of Beacon Supergroup sandstones, Ferrar Dolerite, and granite erratics. They include 39 arcuate moraines that project southward from the present Taylor Glacier lobe into lower Arena Valley (Figs. 6, 7, and 10). The moraines and drift rest without disturbance on the surface of relict soil horizons and delicate in-situ desert pavements. The outcrop pattern, surface morphology, cross-cutting relations, and soil development allow separation of four distinct drifts. From oldest to youngest, these are Taylor IVb, IVa, III, and Taylor II (Denton et al., 1989; Bockheim, 1977, 1982; Marchant et al., 1994). ^{3}He and ^{10}Be exposure ages of surface clasts from moraine crests afford chronologic control (Brook and Kurz, 1993; Brook et al., 1993). The results indicate that the oldest Taylor IVb moraines antedate 2.2 Ma. Taylor drifts overlie Quartermain till, undifferentiated colluvium, and Arena till. The sedimentology and morphology of Taylor drifts is described in Marchant et al. (1994b), and details are shown in Table 2.

The lobate moraine morphology, granite erratics, and proximity of Taylor II, III, IVa, and IVb drifts to the present Taylor Glacier margin at the mouth of Arena Valley indicate southward incursions of Taylor Glacier into lower Arena Valley (Marchant et al., 1994b). The lack of striated clasts and fine-grained matrix, along with the presence of in-situ desert pavements, relict soil horizons, and undisturbed morphologic forms beneath Taylor drifts, all indicate that deposition was from cold-based ice.

Group 3 drifts

Small boulder-rich moraines, each between 0.5 and 1.0 m high, occur alongside margins of two small alpine glaciers in upper and lower East Fork. These moraines are arcuate and rest unconformably on older unconsolidated deposits and on weathered Arena Sandstone bedrock. They are composed of a chaotic assemblage of angular, gravel- and cobble-sized clasts of local sandstone and Ferrar Dolerite that is clast supported, although in hand-dug stratigraphic sections some show coarse-grained sand lenses interbedded with gravel and cobble layers. These moraines lack erratics, glacially molded/ striated clasts, associated outwash, or underlying striated bedrock pavements.

The best-developed alpine moraine sequence occurs in upper East Fork, where 10 arcuate ridges crop out between 1700 and 1850 m elevation along the west wall of East Fork (Fig. 11). These moraines extend up to 0.5 km from the western margin of an alpine glacier (about 1 km long and 0.75 km wide) that rests on a north-facing, rectilinear sandstone bedrock slope in the lee of the stossed valley headwall. This glacier reaches a maximum elevation of 1950 m and nearly overtops the bedrock headwall. The outcrop pattern, ridge morphology, and soil development within individual moraines allow separation into four drifts informally designated, from oldest to youngest, Alpine D, C, B, and A. Details are presented in Table 2.

The areal distribution and arcuate pattern of the moraines show that Alpine A, B, C, and D moraines were deposited by expansions of the adjacent alpine glacier. The absence of striated clasts and glacial outwash indicates deposition by cold-based ice without significant basal and/or surface-ice melting. On the basis of morphology and weathering characteristics (depth of oxidation and salt pan development, Bockheim, 1990), we correlate Alpine A, B, C, and D drifts in upper Arena Valley with Taylor II, III, IVa, and IVb drifts in lower Arena Valley.

Colluvium

Undifferentiated colluvium. About 60% of the bedrock walls in Arena Valley is covered with a thin veneer of unoxidized (10YR 6/4), poorly sorted, gravel-rich colluvium (Figs. 6 and 7). This undifferentiated colluvium thickens towards the base of valley walls, reaching a maximum of about 1.5 m on the west wall of lower Arena Valley. It extends downslope from narrow bedrock couloirs, bedrock regolith, or bedrock cliffs. Undifferentiated

colluvium is composed entirely of local sandstone and dolerite bedrock, although on the west wall of lower Arena Valley granite erratics derived from underlying Quartermain I or Quartermain II till occur within extensive colluvial sheets. The surface of undifferentiated colluvium lacks rills, channels, levees, and gullies.

In hand-dug stratigraphic section, the a-axes of gravel- and cobble-sized clasts are parallel with the present surface slope. Most clasts within undifferentiated colluvium bear desert varnish and/or ventifacted facets. The matrix fraction is composed of coarse- and medium-grained quartz sand and weathered dolerite grus. There are no striated and/or glacially molded clasts within undifferentiated colluvium. Layers of concentrated volcanic ash 5 to 10 cm thick occur interbedded with undifferentiated colluvium along the west wall of lower Arena Valley. Here, undifferentiated colluvium is inferred to reflect minor hillslope erosion.

Monastery colluvium. Monastery colluvium is a highly oxidized (7YR 6/4) and poorly sorted diamicton. It crops out in two localities in upper and central Arena Valley. One locality is along the rectilinear, northeast flank of Altar Mountain between 1500 and 1700 m elevation (Fig. 4). A second is along the gentle (5 to 10°) footslope of the main tributary valley in east-central Arena Valley (Figs. 6 and 7). At both localities, Monastery colluvium is composed predominantly of well-developed sandstone and dolerite ventifacts set within a sandy matrix. Ventifacts faceted on all sides account for about 25% of the clast fraction of Monastery colluvium. Sandstone ventifacts show thick quartz rinds and siliceous crusts ($>$ 2 mm), indicating long-term exposure in a desert environment (Weed and Norton, 1991). In cleared sections, Monastery colluvium shows alternating layers of coarse-grained dolerite grus, oxidized quartz sand, and gravel-sized ventifacts. The long axes of such ventifacts are parallel with the present surface slope.

Monastery colluvium overlies highly oxidized Altar till on the northeast flank of Altar Mountain. The contact is gradational. In stratigraphic section, the transition from overlying Monastery colluvium to underlying Altar till occurs over a vertical distance of 15 to 20 cm. Where it crops out in west-central Arena Valley, Monastery colluvium shows a well-developed pavement of interlocking gravel- and cobble-sized ventifacts of Beacon Heights Orthoquartzite, Ferrar Dolerite, and Arena Sandstone.

Monastery colluvium represents the products of minor hillslope erosion and subaerial weathering in a desert climate. Altar till, which underlies Monastery colluvium in stratigraphic section, still mantles the rectilinear wall along the north flank of Altar Mountain. Hence, most of the morphology of Arena Valley antedates Monastery colluvium.

Volcanic Ash Deposits

Volcanic ash, both in-situ and reworked, occurs in Arena Valley. Volcanic ash is mixed into lobate avalanche

deposits; is buried in thin layers within undifferentiated colluvium; is disseminated within Quartermain I till (moraines and drift patches); and overlies a tightly knit desert pavement that armors Monastery colluvium in central Arena Valley. In-situ volcanic-ash deposits contain < 1% non-volcanic contaminants and have glass shards with delicate spires and intact bubble vesicles. Ashes that have been reworked after initial deposition show abraded glass shards that hold detrital silts within broken vesicles. Most reworked ashes show >50% non-volcanic contaminants. None of the volcanic ashes in Arena Valley shows extensive weathering. All surficial ash deposits in Arena Valley contain less than 5% secondary clays (see also Table 3). Most of the ashes are phonolitic in composition. Likely source areas include Mt. Discovery and Mt. Morning offshore of the Dry Valleys region; both are composite stratovolcanoes with phonolitic lava flows and are part of the nearby Erebus Volcanic Province (Kyle, 1990).

Ash-avalanche deposits. Two ash-avalanche deposits occur in Arena Valley. Both emanate from cliffed bedrock couloirs at the heads of rectilinear slopes, are lobate in plan view, convex in cross-profile, and contain at least 30% volcanic ash in the matrix (< 2 mm) fraction. In hand-dug sections, ash-avalanche deposits overlie slightly stratified, undifferentiated colluvium.

The lower Arena Valley ash-avalanche deposit is 350 m long and 50 m wide. It occurs on the east-facing rectilinear wall near the valley mouth. The deposit extends downslope from a narrow bedrock couloir at about 1650 to 1625 m elevation, overlies undifferentiated colluvium, and terminates two-thirds of the way down the valley wall at about 1100 m elevation (Fig. 12). Lateral contacts between the avalanche deposit and adjacent colluvium are sharp and are marked by an abrupt change in surface slope. In cross profile, the central core of the avalanche deposit rises about 3 m above adjacent undifferentiated colluvium. The avalanche deposit thickens downslope to a maximum of slightly more than 1.5 m. Thin Taylor IVa drift overlies this avalanche deposit between 1325 and 1100 m elevation, without any modification of the lobate morphology of the deposit (Fig. 12).

In hand-dug sections, the lower Arena Valley ash-avalanche deposit shows a chaotic admixture of unweathered sandstone gravel (about 10%), dolerite ventifacts (about 15%), quartz sand and dolerite grus (about 35%), granite erratics (<1%), and coarse-grained (1.0 to 1.5 mm) volcanic ash (about 45%). The ash is phonolitic in composition and includes fibrous glass shards and euhedral anorthoclase crystals. Granite erratics within the avalanche deposit extend up to 1600 m elevation. This is about 325 m above the upper limit of Taylor IVa moraines and about 100 m above the upper limit of Taylor IVb moraines on the east wall of lower Arena Valley opposite the ash-avalanche deposit. The lower Arena Valley avalanche deposit lacks internal stratification and clasts do not show preferred orientation. Stage 5/6 salt pans of Bockheim (1990) occur between 15 and 25 cm depth. A small cone-shaped deposit composed of undifferentiated colluvium without volcanic ash overlies the avalanche head with sharp stratigraphic contacts. The colluvium, which reaches a maximum thickness of 45 cm, covers about 10% of the ash-

avalanche deposit. The long axis of dolerite and sandstone clasts within this colluvium are parallel with the present surface slope.

A second ash-avalanche deposit occurs on the east-facing wall of upper West Fork. This deposit shows multiple lobes that branch from a central tongue (200 m long and 20 m wide). The central tongue extends downslope from narrow couloirs incised in cliffed Beacon Heights Orthoquartzite and terminates just above the bedrock floor of central West Fork. The base of the avalanche deposit is physically separated from the central tongue by steep bedrock cliffs (32° to 40°); it rests at 1380 m elevation on the floor of a bare-bedrock sandstone basin in upper West Fork (Fig. 7). The central avalanche tongue shows an asymmetric cross profile with the steep side facing upvalley. Sandstone boulders occur at the margins of individual lobes.

The avalanche deposit exhibits a chaotic internal assortment of dolerite ventifacts and grus, quartz sand, pitted sandstone gravel, and volcanic ash (35% to 45% of the matrix fraction). Stage 5/6 salt pans of Bockheim (1990) occur between 15 and 25 cm depth; sandstone pseudomorphs occur to 65 cm depth. The upper Arena Valley avalanche deposit overlies eroded remnants of undifferentiated colluvium with gradational stratigraphic contacts; this colluvium crops out in discontinuous patches that stand 1 to 1.5 m in relief above weathered Arena Sandstone bedrock.

The geomorphic setting, morphology, and poor sorting together suggest rapid emplacement of ash-avalanche deposits over pre-existing undifferentiated colluvium. We suggest that the avalanche deposits originated from collapse of unstable accumulations of volcanic ash (either trapped in bedrock couloirs or resting on oversteepened valley slopes) that incorporated pre-existing unconsolidated deposits. Both ash-avalanche deposits in Arena Valley probably formed at or near times of volcanic eruptions because high-velocity winds would have dispersed unprotected surficial volcanic ash, and because ash probably would have become unstable and avalanched shortly after initial buildup in steep bedrock couloirs. Certainly ash could not remain in bedrock couloirs during parallel retreat of cliff faces (see Selby, 1971, 1974), simply because the couloirs would have been destroyed and avalanche deposits would have been buried or flushed downslope; therefore, development of rectilinear valley walls must antedate ash deposition. The cone-shaped undifferentiated colluvial deposit, which overlies about 10% of the lower Arena Valley ash-avalanche deposit, indicates that here some minor colluviation postdated deposition of the avalanche deposit.

Ash layers within colluvium. Thin layers (10 to 15 cm) of concentrated volcanic ash are interbedded within undifferentiated colluvium at 1500 m elevation on the west valley wall about 0.5 km south of the lower Arena Valley ash-avalanche deposit. These ash layers occur about halfway down the colluvial slope, about 100 m below couloirs incised in overlying Arena Sandstone and Beacon Heights Orthoquartzite. Ash layers extend to 60 cm

depth and show sharp basal contacts with interbedded colluvium; colluvial layers fine upwards. The ash layers show fine-grained (<0.5 mm), dark-gray (5Y 2/4), vesicular pumice and clear volcanic crystals. We postulate that volcanic ashfall was mixed with colluvium at or near the time of eruption. Otherwise high-velocity winds would have dispersed unprotected surficial ashfall deposits.

Ash in Quartermain I till. Quartermain I till contains 5 to 10% volcanic ash disseminated in the matrix fraction (< 2 mm). The ash is composed of coarse-grained (1.0 mm), light-gray pumice (5Y 6/4) and clear volcanic anorthoclase crystals. Glass shards are abraded and hold detrital silts in pipe vesicles. Crystals are angular and lack evidence of chemical etching. The ash disseminated in Quartermain I till probably reflects either primary ashfall onto the glacier accumulation surface (with subsequent dispersal during englacial or basal transport) or basal entrainment of pre-existing ash deposits by glacier ice.

Ashfall on a desert pavement. A pale-white (10YR 8/2) ash layer (Arena Valley Ash, Marchant et al., 1993a) crops out at the surface of Monastery colluvium along the gentle footslope (15° to 20°) of the main tributary in west-central Arena Valley (Fig. 13). This ash deposit, which is about 25 cm thick, shows a basal unit (0.5 to 1.0 cm thick) that lacks non-volcanic contamination and an upper ash-rich diamicton that contains about 5% detrital quartz sand, dolerite grus, and gravel ventifacts. The basal unit overlies with a sharp stratigraphic contact a tightly knit desert pavement that armors underlying Monastery colluvium. This pavement consists of gravel-sized ventifacts of local Arena Sandstone, Beacon Heights Orthoquartzite, and Ferrar Dolerite. Sandstone ventifacts bear siliceous crusts and quartz rinds 5 to 10 mm thick, suggesting that the pavement was long exposed at the ground surface in a desert climate (Weed and Norton, 1991). The Arena Valley Ash is unweathered, containing less than 2.5% secondary clays. Volcanic crystals (anorthoclase, aegerine, subcalcic augite, and magnetite) lack evidence of chemical etching when viewed at high magnification (SEM analyses, Marchant et al., 1993a, 1993b).

The sharp stratigraphic contact with the underlying ventifact pavement and the absence of non-volcanic contaminants indicate that the basal layer of the Arena Valley Ash is a primary ashfall deposit (Marchant et al., 1993a). We postulate that desert conditions favorable for the development/ preservation of ventifact pavements existed in Arena Valley at the time of volcanic eruption.

Chronology of Surficial Deposits

Relative Chronology. Any interpretation of the glacial history of the Quartermain Mountains rests on a detailed relative chronology of surficial deposits in Arena Valley. The relative chronology presented here is based on the map patterns of surficial deposits displayed in Figures 6 and 7, along with the sedimentologic and stratigraphic data for individual units given in the previous section and in Tables 1 and 2.

Eroded patches of Altar till and Monastery colluvium are the most oxidized and probably the oldest deposits in Arena Valley (5Y 7/6). Monastery colluvium overlies (and therefore postdates) Altar till with gradational stratigraphic contacts along the northeast flank of Altar Mountain.

Dissected patches of Quartermain II till, Arena till, and Slump Mountain diamicton show the next-highest degree of weathering and depth of oxidation in Arena Valley (10YR 5/6), but are still significantly less weathered than either Altar till or Monastery colluvium. This contrast marks the largest break in soil development within Arena Valley. Hence, Quartermain II till, Arena till, and Slump Mountain diamicton are probably significantly younger than Monastery colluvium and Altar till. At two localities in central Arena Valley, Quartermain II till underlies Arena till with gradational stratigraphic contacts. In turn, Arena till shows no contrast in soil morphologic development, and grades laterally into Slump Mountain diamicton. Therefore, we consider these two units to be of the same relative age. Hence, Quartermain II till antedates both Arena till and Slump Mountain diamicton.

Quartermain I till overlies Arena till and Slump Mountain diamicton in several hand-dug stratigraphic sections. Figure 9 shows that a buried sandstone ventifact pavement separates the two tills. Thick siliceous crusts and quartz rinds (5 to 10 mm) on the surface of buried ventifacts indicate long exposure in a desert environment (Weed and Norton, 1991) prior to burial by overlying Quartermain I till.

Undifferentiated colluvium, which is widespread on valley slopes, postdates Slump Mountain diamicton and perhaps Quartermain I till. This relative age assignment is based on the fact that undifferentiated colluvium overlies both Slump Mountain diamicton and Quartermain II till in hand-dug sections near the base of the east wall of central Arena Valley. Undifferentiated colluvium in Arena Valley everywhere shows identical surface and internal weathering and therefore is probably of the same relative age.

The lower Arena Valley ash-avalanche deposit overlies undifferentiated colluvium. The ash-avalanche deposit and the underlying colluvium both contain granite erratics that extend up to 1600 m elevation. These granite erratics must have been brought into Arena Valley during former Taylor Glacier expansion(s). Because they occur as much as 100 m above the upper limit of Taylor II-IVb drifts, these granite erratics probably reflect either the Quartermain I or Quartermain II glacial events. If so, the lower Arena Valley ash-avalanche deposit postdates either Quartermain I or Quartermain II till, or both.

Taylor II-IVb drifts in lower Arena Valley postdate Quartermain I till, undifferentiated colluvium, and the lower Arena Valley ash-avalanche deposit (Fig. 12). On the basis of similar moraine morphology and weathering characteristics (depth of oxidation and salt pan development, Bockheim, 1990), we correlate Taylor II, III, IVa, and IVb drifts in lower Arena Valley with Alpine A, B, C, and D drifts in upper Arena Valley.

Finally, Brawhm till, which forms isolated patches on the saddle in upper West Fork, shows moderate oxidation and surface weathering. Because it does not occur in stratigraphic association with unconsolidated deposits in Arena Valley, Brawhm till cannot be placed into a fixed relative age framework. However, from soil morphologic development (Stage 5 salt pans of Bockheim, 1990) and surface weathering characteristics (highly pitted dolerite cobbles), we postulate that Brawhm till postdates Quartermain II till and antedates Taylor IVb drift.

Absolute chronology. Our absolute chronology of surficial sediments in Arena Valley is based on the isotopic dating of associated in-situ and near in-situ ash deposits, as well as on exposure-age analyses of surface clasts on Taylor drifts. Isotopic dating of volcanic ashes was carried out at the Berkeley Geochronology Center (BGC). Volcanic crystals (anorthoclase and sanidine) and glass shards extracted from the matrix of ashfall deposits were dated at BGC using a fully automated laser-fusion $^{40}Ar/^{39}Ar$ dating system that allows analysis of single volcanic crystals (<1.0 mm in size) and individual pumice shards. Exposure ages are from Brook and Kurz, (1993), Brook et al. (1993), and Brown et al. (1991). Table 3 and in-situ and near in-situ ash layers afford minimum ages for the surfaces on which they rest, ash disseminated in glacial tills affords maximum ages for these deposits. An overall chronology of the surficial deposits of Arena Valley is based on linking the isotopic ages listed in Appendix I/ Table 3 with the relative chronology.

Altar till, Monastery Colluvium, Quartermain II till, Arena till, Slump Mountain diamicton, and undifferentiated colluvium all predate 11.3 Ma. These age assignments are based on the isotopic date of the lower Arena Valley ash-avalanche deposit (11.3 Ma; DME-86-113), which unconformably overlies undifferentiated colluvium. In turn, undifferentiated colluvium overlies Monastery colluvium, Quartermain II till, and Slump Mountain diamicton/ Arena till.

The maximum and minimum ages for Quartermain I till are 11.6 Ma and 4.4 Ma, respectively. The maximum age is based on $^{40}Ar/^{39}Ar$ analyses of volcanic crystals disseminated in Quartermain I till (11.3 Ma, DMS-87-26 and 11.6 Ma, DMS-87-27 Ma); the minimum age of 4.4 Ma comes from ^{10}Be exposure-age analyses on a clast from the surface of Quartermain I till (SCW-87-1-1-HF5, Brown et al., 1991; and Table 3). Undifferentiated colluvium in upper West Fork antedates 6.4/ 7.4 Ma, an age based on $^{40}Ar/^{39}Ar$ analyses of volcanic crystals disseminated in the upper Arena Valley ash-avalanche deposit (DMF-86-141/ DMS-86-131), which unconformably overlies remnants of eroded undifferentiated colluvium on the east-facing wall of upper West Fork. For reasons given above, we suggest that erosion of this colluvium probably occurred during the Brawhm glacial event. If this is so, Brawhm till antedates 6.4/ 7.4 Ma.

Taylor drifts, along with correlative alpine drifts in East Fork, postdate deposition of the lower Arena Valley ash-avalanche deposit and Quartermain I till. Exposure-age analyses (cosmogenic ^{3}He and ^{10}Be, Table 2) on clasts from moraine crests indicate that Taylor IVb drift is > 2.2 Ma; Taylor IVa drift is > 1.0 Ma; Taylor III drift is > 200 Ka; and Taylor II drift is > 117 Ka (data from Brook and Kurz, 1993; Brook et al., 1993).

DISCUSSION

Glacial History

In-situ and near in-situ Miocene- and Pliocene-age volcanic ashes, relict colluvial sheets, and moraine ridges on steep valley walls (28° to 36°) point to the great antiquity of surficial deposits in Arena Valley and indicate that the overall morphology of the Quartermain Mountains existed before middle-Miocene time (>11.3 Ma). The implication is that rectilinear slopes, terraces, and benches in Arena Valley are inherited landforms that predate the onset of hyper-arid, cold-desert conditions.

Taylor and alpine drifts. Taylor and alpine drifts represent advances of south- and north-flowing glaciers into the lower and upper reaches of Arena Valley, respectively. These advances were relatively minor, so that central Arena Valley remained free of glacial ice. Taylor II-IVb drifts record four successive expansions of a cold-based Taylor Glacier lobe into lower Arena Valley. Figure 14 depicts the present longitudinal ice-surface profile of Taylor Glacier at the mouth of Arena Valley, along with reconstructions related to the elevations of individual drift sheets in lower Arena Valley. Along with exposure-age data given above, these profiles show that the maximum thickening of Taylor Glacier during at least the last 2.2 Ma (represented by Taylor IVb drift) was 475 m above the present-day ice-surface. Similarly, the maximum Pleistocene thickening of Taylor Glacier (represented by Taylor IVa drift) was about 325 m above the present-day surface of adjacent Taylor Glacier.

Alpine drifts in upper East Fork of Arena Valley show four successive expansions of a cold-based alpine glacier. From weathering data given above, we correlate Alpine A, B, C, and D drifts in upper East Fork with Taylor II, III, IVa, and IVb drifts in lower Arena Valley. The outermost and oldest alpine drift (Alpine D) occurs only 3 km from the present alpine glacier in upper East Fork. Such restricted areal expansion carries with it the implication that Ferrar Glacier failed to spill over the valley head threshold and merge with local alpine glaciers during Alpine A-D/ Taylor II-IVb time. This conclusion is consistent with the evidence for limited Pliocene and Pleistocene expansion of Taylor Glacier into lower Arena Valley and the evidence of the Arena Valley Ash deposit, which shows that ice has not advanced into central Arena Valley for at least the last 4.3 Ma. In fact, the youngest evidence for glacial ice flowing over Arena Saddle and down into Arena Valley is at least late Miocene in age (>7.4 Ma), and comes from the Brawhm till and underlying striated bedrock at Arena Saddle (Fig. 7).

Quartermain I till, Brawhm till, and through-valley glaciation. Quartermain I till and Brawhm till represent expansion of south- and north-flowing glaciers into lower and upper Arena Valley, respectively. Quartermain I till is dated at between 11.6 Ma and 4.4 Ma ago, and Brawhm till has a minimum inferred age of >7.4 Ma. We explain the unusual areal distribution of Quartermain I moraines (roughly parallel with and at the center of the valley axis) by deposition along the margin of an ancestral Taylor Glacier that merged with ice flowing northeast down the valley axis. We suggest that the Quartermain I ice tongue merged with Brawhm ice. If this is correct, then ice flowed through Arena Valley during the Brawhm/Quartermain I glacial event sometime between 7.4 and 11.6 Ma ago.

Highly dissected, undifferentiated colluvial deposits on the west wall of upper Arena Valley are inferred to represent partial erosion beneath the Brawhm ice tongue. This dissected undifferentiated colluvium occurs up to about 1700 m elevation on the east-facing wall of West Fork, where a continuous, non-dissected sheet of undifferentiated colluvium shows an abrupt lower boundary. We postulate that the upper limit of dissected colluvium in West Fork approximates the upper limit of Brawhm glacial ice. If so, the maximum ice-surface elevation of the Brawhm ice tongue in upper Arena Valley was probably about 1700 m. Although Brawhm and Quartermain I ice merged at the valley center, we conclude that ice expansion fell short of glacial overriding.

Arena till, Slump Mountain diamicton, Quartermain II till, and ice-sheet overriding. Arena till, Slump Mountain diamicton, and Quartermain II till represent glacier expansion into Arena Valley in excess of that which occurred during Taylor II-IVb/ Alpine A-D time. Unlike Taylor/ Alpine drifts, these deposits patchy and lack surface morphology. Therefore, we rely on the areal distribution of Arena till, Slump Mountain, and Quartermain II till, along with the associated meso-scale erosional forms (basins, channels, stripped bedrock and stoss-and-lee topography), to reconstruct ice extent and thickness in Arena Valley.

Arena till was quarried from shallow sandstone basins and drawn-out downvalley beneath northeast-flowing ice. These sandstone basins, in turn, merge upvalley with extensive tracts of bare bedrock, which are cut by sinuous channels in East and West Fork. This integrated system of basins, channels, and tracts of bare bedrock is contiguous with stoss-and-lee topography along the crest of low-lying saddles in upper East and West Forks. The entire suite of meso-scale erosional forms is thus interconnected and ultimately associated with deposition of the basal Arena till, which grades laterally into Slump Mountain diamicton. The implication is that Arena till, Slump Mountain diamicton, and the suite of meso-scale bedrock erosional forms are all basal features produced beneath northeast-flowing glacier ice. This flow direction comes from the striated pavement beneath Arena till patches and from the headwall stoss-and-lee forms.

We explain the origin and areal distribution of stoss-and-lee topography, erosional basins, channels, bare-bedrock tracts, and unconsolidated deposits by variations in the basal thermal regime of overriding ice. In this regard, abrasion is associated with wet-melting ice, stripping and plucking with wet-freezing ice, and the preservation of unconsolidated sediments with frozen ice. We postulate that wet-melting conditions occurred on south-facing headwalls and where ice velocity was greatest. Thus, extensive abrasion would be concentrated along low-lying saddles at the head of East and West Forks, which channeled northeast-flowing ice. Following mechanisms described by Nye (1973), Rothlisberger (1972), Shreve (1972, 1985), and Sugden and John (1976), we infer that the channels of lower East and West Forks reflect erosion from meltwater produced at the upglacier side of the Arena Valley headwall. Bedrock basins at the north end of these channels and at the valley center probably reflect stripping of unconsolidated sediments beneath wet-freezing ice. Such stripping would explain the unusually patchy areal distribution of unconsolidated sediments in Arena Valley.

A key problem is whether the interconnected array of erosional and depositional features reflect basal conditions beneath an overriding ice sheet or a local alpine glacier. We favor an origin beneath thick overriding ice for several reasons. One is that stoss-and-lee topography along the crest of upper East and West Forks indicates ice flow across the Arena Valley headwall. A second is that high-elevation (1750 m) stoss-and-lee topography along the tributary divide in west-central Arena Valley implies submergence beneath thick glacier ice. Third, bedrock basins that truncate Monastery colluvium at 1700 m elevation on the divide between East and West Forks imply that ice overrode the pinnacle of Altar Mountain at 2200 m elevation.

In summary, we infer massive overriding of the eastern Quartermain Mountains from deposition of basal till tied to subglacial bedrock erosional features that can be mapped continuously high into the saddles and peaks of upper Arena Valley. We infer that Quartermain II till represents initial buildup of glacier ice which culminated in the submergence of Arena Valley by northeast-flowing ice. Ice-sheet overriding of Arena Valley occurred prior to 11.3 Ma ago. This age is based on $^{40}Ar/^{39}Ar$ analyses of volcanic ash within the lower Arena Valley ash-avalanche deposit, which postdates Quartermain II till, Arena till, and Slump Mountain diamicton according to our relative chronology.

Altar till. The origin of Altar till, the oldest glacial deposit exposed in Arena Valley, is poorly understood. Striated and molded dolerite clasts within Altar till indicate transport beneath wet-based ice. We infer that this ice flowed northeastward, downvalley, but we do not yet know ice thickness in Arena Valley. Altar till antedates 11.3 Ma, but it is here assumed to predate ice-sheet overriding by a considerable length of time because it shows significantly greater oxidation than Quartermain II till, Arena till, and Slump Mountain diamicton. The preservation of rectilinear slopes beneath Altar till indicates that glacier ice did not significantly modify pre-existing bedrock

landforms.

Regional Correlations

The surficial stratigraphy of Arena Valley and the western Asgard Range (Marchant et al., 1994a; Fig. 2) show nearly identical records of relative sequences of glacial and non-glacial deposits. On the basis of similar weathering and stratigraphic positions, we correlate Altar till in Arena Valley (>11.3 Ma) with Inland Forts and Sessrumnir tills (>15.0 Ma) in the western Asgard Range. All of these tills rest on striated sandstone bedrock and represent the stratigraphically lowest deposit in the valleys in which they occur. On the basis of similar soil development (depth of oxidation) and stratigraphic position with underlying Altar and Sessrumnir tills, we correlate Monastery colluvium (>11.3 Ma) in Arena Valley with Koenig colluvium (>14.8/ 15.2 Ma) in the western Asgard Range. Likewise, on the basis of similar surface and internal weathering, outcrop pattern, and stratigraphic position, we correlate Asgard till (>13.6 Ma and <14.8/ 15.2 Ma), Jotunheim till (> 10.5 Ma and <14.8/ 15.2 Ma), and Nibelungen till (< 14.8/ 15.2 Ma) in the western Asgard Range with Quartermain II till (>11.3 Ma), Slump Mountain diamicton (>11.3 Ma), and Arena till (>11.3 Ma) in Arena Valley, respectively. Finally, on the basis of stratigraphic position, well-preserved surface morphology, and soil development, we correlate Brawhm/Quartermain I tills, together with Taylor/ Alpine drifts in Arena Valley, with the suite of well-preserved rock glacier deposits at the heads of the western Asgard Range.

The evidence in Arena Valley and the western Asgard Range indicates that both areas were filled with wet-based alpine glaciers prior to 15.0 Ma ago. Following this early glacial episode, deposition of Monastery colluvium and Koenig colluvium marks a return to ice-free conditions (semi-arid?) in both Arena Valley and the western Asgard Range. Subsequently, both regions were inundated by thick northeast-flowing glacier ice sometime between 13.6 Ma ago and 14.8/ 15.2 Ma ago. This ice represents the most extensive late Cenozoic glacial event recorded in the western Dry Valleys region. Initial buildup of overriding ice involved expansion of trunk glaciers that filled Taylor and Wright Valleys and sent peripheral lobes of glacier ice southward into the Quartermain Mountains and the western Asgard Range, respectively. During overriding unconsolidated sediments and bedrock were stripped and eroded, creating dissected till and colluvium outcrops, and stoss-and-lee slopes, subglacial channels, and basins. Nibelungen and Arena tills were deposited from material quarried in upvalley basins during overriding. Deposition of undifferentiated colluvium in both regions marks a return to ice-free conditions by 11.3 Ma ago. With the exception of small rock glaciers at the heads of the Asgard Valleys, which expanded a maximum of 2.5 km in the last 12.5 Ma (Marchant et al., 1994a), surficial sedimentation in the western Asgard Range effectively ceased by 12.5 Ma ago. Although colluviation in Arena Valley also effectively ceased by this time, thin cold-based glaciers continued to invade lower Arena Valley intermittently throughout the Pliocene and Quaternary, just as the current Taylor Glacier does today.

Paleoclimate

Late Cenozoic paleoclimate of Arena Valley can be inferred from slope stability and from the physical characteristics of surficial deposits. The results all point to persistent cold-desert conditions in Arena Valley since deposition of Monastery colluvium >11.3 Ma ago.

Polar glacier thermal regime. Taylor and Alpine drifts (<3.0 Ma) were deposited in a cold-desert climate. This conclusion comes from the inferred thermal regime of expanded Taylor and alpine glaciers and from the stability of in-situ moraine ridges on steep valley walls. Taylor and Alpine drifts have physical characteristics that indicate deposition by cold-based glaciers. Because the Taylor lobes in lower Arena Valley were less than 475 m thick and the alpine glacier at the head of East Fork was less than 200 m thick, these basal thermal conditions almost surely indicate polar conditions during drift deposition. The striking absence of outwash sediments, lacustrine deposits, kame terraces, ice-marginal channels, or other glacio-fluvial/waterlain sediments in the lower Arena Valley points to a lack of surface-melting ablation zones, which now occur only at or near the 0°C atmospheric isotherm. The presence of in-situ Taylor IVb, IVa, and Taylor II moraine ridges on steep valley walls (28° to 33°) implies little or no slope development for at least the last 2.2 Ma. Such slope stability is consistent with persistent cold-desert conditions since at least late Pliocene time. Therefore, we suggest that the maximum atmospheric temperatures in lower Arena Valley remained well below 0°C, promoting cold-based glaciers and inhibiting slope development for at least the last 2.2 Ma.

An estimate of Arena Valley paleoclimate during middle Miocene time (> 11.3 Ma) comes from the glacier thermal regime during buildup and demise of overriding ice. Because ice buildup involved expansion of thin, peripheral ice tongues into lower and upper Arena Valley, thermal conditions at the base of these ice tongues represent a crude estimate of atmospheric temperature. Evidence for melting at the base of thin, slow-moving ice tongues would favor a climate warmer and wetter than today. In contrast, evidence for cold-based ice would indicate that atmospheric temperatures were well below 0°C.

Quartermain II till represents the initial buildup of overriding ice in lower Arena Valley. It was deposited beneath an expanded, ancestral Taylor Glacier that filled Taylor Valley and sent peripheral lobes of glacial ice up into Arena Valley. Because Quartermain II till lacks striated/ molded clasts, it probably was deposited from cold-based ice. From this we infer that mean annual atmospheric temperatures remained below 0°C during buildup of overriding ice in Arena Valley.

The lack of glacial outwash, kame terraces, ice-marginal channels, and lacustrine deposits in Arena Valley implies dissipation of overriding ice under cold-desert climate conditions. A simple observation shows the maximum

allowable mean annual atmospheric temperature during dissipation of overriding ice from Arena Valley. Small ice-marginal lakes and surficial geomorphic features characteristic of liquid water (rills, levees, gullies, mudflows, and stream channels) are common below 800 m near the Quartermain Mountains, where mean annual temperature is now about -27°C. This estimate is based on a recorded mean annual temperature of -19.8° C at Lake Vanda at 123 m elevation in central Wright Valley (Schwerdtfeger, 1984), along with an average lapse rate of 1°C/100 m elevation rise (Robin, 1988). Surficial sediments in Arena Valley are unmarked by rills, levees, stream channels, lacustrine deposits or other geomorphic features indicative of liquid water. We therefore conclude that mean annual atmospheric temperatures during dissipation of overriding ice from Arena Valley (prior to 11.3 Ma ago) probably did not rise above -27°C. An important point is that the demise of overriding was not caused by climatic amelioration sufficient to introduce surface-melting ablation zones.

Slope stability. The preservation of Miocene-age ash-avalanche deposits (11.3 Ma, DMS-86-113 and 6.4/ 7.4 Ma, DMF-86-141/ DMS-86-131) and relict colluvium on steep valley walls (28° slope) with thin layers of volcanic ash (8.5 Ma, DMS-86-110 C) buried <50 cm from the present ground surface indicate minimal slope development and colluviation in Arena Valley since middle-Miocene time. This is consistent with cold-desert climate conditions since at least 8.5 to 11.3 Ma ago.

Buried desert pavements and ice-free terrain. Isotopically dated ash and drift on buried desert pavements that are similar in all respects to modern desert pavements in Arena Valley indicate intervals of arid climate conditions. The buried sandstone-ventifact pavement that separates Quartermain I till from underlying Arena till indicates desert climate conditions prior to 4.4 Ma, and most likely prior to 7.4 to 11.6 Ma (range of minimum isotopic ages for Quartermain I till). Similarly, the buried ventifact pavement beneath the in-situ Arena Valley Ash deposit indicate desert climate conditions at 4.3 Ma (see also Marchant et al., 1993a). Finally, buried ventifacts at the stratigraphic contact between Taylor III and Taylor IVa drift indicate arid conditions in Arena Valley at about 200 Ka ago.

Chemical stability of volcanic ashes. Volcanic glass is unstable at the ground surface and alters to clay at a rate dependent on atmospheric temperature and the abundance of pore water (rates are increased at high atmospheric temperatures and high pore-water pressures; Lowe, 1986; Lowe et al., 1983). For example, under humid temperate conditions in New Zealand, which are compatible with growth of Nothofagus, volcanic ashes older than about 50,000 years have weathered to >60% clay (Birrell and Pullar, 1973; Lowe et al., 1983; Lowe, 1986). In-situ and near in-situ volcanic ash deposits in Arena Valley contain less than 5% clay-sized grains (Marchant et al., 1993a, 1993b). The absence of significant clay-sized grains in Miocene and Pliocene surficial ash deposits in Arena Valley suggests that the warm climate conditions in the Transantarctic Mountains could not have existed in the western Dry Valleys region during Pliocene time. Rather, the chemical stability of surficial ashes is consistent with

persistent cold desert climate conditions in Arena Valley for at least the last 11.3 Ma.

Implications For Pliocene Dynamics of the East Antarctic Ice Sheet

Two divergent hypotheses have been developed with regard to Pliocene paleoclimate and East Antarctic Ice Sheet dynamics. The deglaciation hypothesis is based on the ecology and source of reworked marine diatoms and on Nothofagus (Southern Beech) fossil wood within Sirius Group glacial deposits in the Transantarctic Mountains. It postulates Pliocene East Antarctic Ice-Sheet deglaciation and subsequent ice-sheet overriding of the Transantarctic Mountains sometime after 3.0 Ma (Webb et al., 1984; Webb and Harwood, 1991; Barrett et al., 1992). The deglaciation hypothesis relies on a fundamental assumption; namely, that reworked marine diatoms within the Sirius Group originated in marine basins in the interior of East Antarctica and were subsequently stripped from these basins and transported into the Transantarctic Mountains (which then supported Nothofagus) by an expanded, wet-based East Antarctic Ice Sheet (Webb and Harwood, 1987). In sharp contrast, the stability hypothesis postulates that the East Antarctic Ice Sheet has been relatively stable under persistent cold-desert conditions since around 14 Ma. The stability hypothesis is based on interpretations of the marine-oxygen isotope record, which show a major, sustained increase in $d^{18}O$ values beginning about 14 Ma (Shackleton and Kennett, 1975; Savin et al., 1975; Miller et al., 1987).

One key test of the deglaciation hypothesis is to determine from glacial-geologic reconstructions whether Pliocene marine diatoms could have been emplaced in the Sirius Group outcrop at 2650 m elevation on Mt. Feather by East Antarctic ice that thickened to override the Quartermain Mountains after 3.0 Ma ago (Barrett et al., 1992). This requires reconstruction of the maximum Pliocene-Pleistocene ice-surface elevations of upper Taylor and Ferrar Glaciers. If this ice surface was below 2650 m, then it is difficult to envision how the Sirius Group outcrop could have been deposited during Pliocene/ Pleistocene time by East Antarctic ice. On the other hand, if the ice-surface elevation exceeded 2650 m elevation, then the Sirius Group outcrop at Mt. Feather could have been deposited by East Antarctic ice during Pliocene/ Pleistocene time. The maximum Pliocene thickening of Taylor Glacier in Arena Valley is 475 m, yielding an upper limit of Taylor Glacier in Arena Valley of 1475 m elevation. We conclude that East Antarctic ice could not have emplaced the Sirius Group outcrop at 2650 m elevation at Mt. Feather during Pliocene time. Rather, marine diatoms must have been incorporated within this outcrop by some mechanism other than East Antarctic glacier ice.

Our major assumption is that the present topography of the Quartermain Mountains, and therefore the present ice-flow configuration of the Taylor and Ferrar Glaciers, existed during the Pliocene when the Sirius Group was postulated to have been deposited on Mt. Feather (Fig. 3). The critical point here is not the absolute elevation of the Quartermain Mountains, but rather the local relief between the Sirius Group outcrop at 2650 m elevation at Mt. Feather and the floor of Arena Valley at 1400 m elevation. This assumption is verified by $^{40}Ar/^{39}Ar$ laser-fusion

analyses of in-situ and near in-situ ashfall deposits in Arena Valley which indicate that the present morphology (and hence local relief) of the Quartermain Mountains antedates 11.3 Ma.

A second test of the deglaciation hypothesis concerns Pliocene paleoclimate in the Dry Valleys region. The deglaciation hypothesis requires atmospheric temperatures 20°C above present values at 3.0 Ma to accommodate ice-sheet collapse (Huybrechts, 1994). This is inconsistent with the paleoclimate record of Arena Valley, which shows persistent hyper-arid, cold-desert conditions since at least 11.3 Ma.

CONCLUSIONS

1. The last major ice-sheet expansion through Arena Valley was middle Miocene or older in age. A suite of unconsolidated sediments and meso-scale glacial erosional forms indicate that Arena Valley was inundated by a northeast-flowing ice sheet prior to 11.3 Ma ago. Subsequent glacier expansions into Arena Valley were of limited extent. Maximum Pliocene and Pleistocene thickening of Taylor Glacier in Arena Valley was 475 m and 325 m, respectively. These data for limited glacier expansion are inconsistent with deposition of high-elevation Sirius Group outcrops at Mt. Feather from a greatly expanded East Antarctic Ice Sheet. Rather, the data indicate that the overall Pliocene configuration of the East Antarctic Ice Sheet in this sector of the Transantarctic Mountains was very similar to the present ice-sheet configuration and hence strongly favor the Pliocene stability hypothesis.

2. Paleoclimate interpretations from glacier thermal regimes, slope stability, and the physical characteristics of surficial deposits indicate persistent cold-desert and hyper-arid environmental conditions in Arena Valley during the last 11.3 Ma. Mean annual atmospheric temperatures in Arena Valley during the last 11.3 Ma remained well below 0°, and probably did not rise above -27°C. This does not support Pliocene ice-sheet deglaciation, which requires development of surface-melting ablation zones at the ice sheet margin. Rather, the persistent polar environments favor the existence of a robust polar East Antarctic Ice Sheet throughout Pliocene time.

3. Present erosional processes have not been particularly effective in shaping the topography of the Quartermain Mountains in the last 11.3 Ma. If denudation by salt weathering, wind deflation, and frost shattering had been effective over the last 11.3 Ma, we would not expect to find in-situ to near in-situ Miocene- and Pliocene age ashes, tills, and relict colluvial deposits on steep valley slopes. One estimate of the degree of erosion by salt weathering and wind deflation in Arena Valley since late Miocene time comes from the relative erosion of sandstone bedrock within basins related to ice-sheet overriding and adjacent unconsolidated deposits. This indicates that the maximum erosion of exposed sandstone bedrock during at least the last 11.3 Ma was probably on the order of 2 to 3 m.

REFERENCES

Barrett, J., Adams, C.J., McIntosh, W.C., Swisher III, C.C. and Wilson, G.S., 1992: Geochronological evidence supporting Antarctic deglaciation three million years ago. *Nature* 359, 816-818.

Behrendt, J.C. and Cooper, A.K., 1991: Evidence of rapid Cenozoic uplift of the shoulder escarpment of the Cenozoic West Antarctic Rift system and a speculation on possible climate forcing. *Geology* 19, 315-319.

Behrendt, J.C. and Cooper, A.K., 1990: Speculation on the uplift of the shoulder of the Cenozoic West Antarctic rift system and its relation to late Cenozoic climate change. In *Cooper, A.K. and Webb, P.N., Eds., International workshop on Antarctic offshore stratigraphy (ANTOSTRAT) [overview and extended abs.]: U.S. Geological Survey Open-File Report* 90-309, p. 63-71.

Birrell, K.S. and Pullar, W.A., 1973: Weathering of paleosols in Holocene and late Pleistocene tephras in central North Island, New Zealand. *New Zealand Jour. of Geol. and Geophys.* 16, 687-702.

Bockheim, J.G., 1990: Soil development rates in the Transantarctic Mountains. *Geoderma*, 47, 59-77.

Bockheim, J.G., 1982: Properties of a chronosequence of ultraxerous soils in the Transantarctic Mountains. *Geoderma* 28, 239-255.

Bockheim, J.G., 1977: Soil development in Taylor Valley and McMurdo Sound area. *Ant. Jour. of the United States* 12(4), 105-108.

Brady, H. and McKelvey, B., 1983: Some aspects of the Cenozoic glaciation of southern Victoria Land, Antarctica. *Jour. of Glac.* 29 (102), 343-349.

Brady, H. and McKelvey, B., 1979: The interpretation of a Tertiary tillite at Mount Feather, southern Victoria Land, Antarctica. *Jour. Glac.* 22 (86), 189-193.

Brook, E.J., and Kurz, M.D., 1993: Using in-situ ^{3}He in Antarctic quartz sandstone boulders for surface-exposure chronology. *Quat. Res.* 39, 1-10.

Brook, E.J., Kurz, M.D., Ackert, R., Jr, Denton, G.H., Brown, E.T., Raisbeck, G.M. and Yiou, F., 1993: Chronology of Taylor Glacier advances in Arena Valley, Antarctica, using in-situ cosmogenic ^{3}He and ^{10}Be. *Quat. Res.* 39, 11-23.

Brown, E.T., Edmund, J.M., Raisbeck, G.M., Yiou, F., Kurz, M.D. and Brook, E.J., 1991: Examination of surface exposure ages of Antarctic moraines using in-situ produced ^{10}Be and ^{26}Al *Geochim. et Cosmo. Acta* 55 (8), 2269-2284.

Chinn, T.J., 1980: Glacier balances in the Dry Valleys area, Victoria Land, Antarctica. In *Proceedings of the Riederalp Workshop IAHS-AISH Publication no. 125*, 237-247.

Denton, G.H., Sugden, D.E., Marchant, D.R., Hall, B.L., and Wilch, T.I., 1994: East Antarctic Ice Sheet sensitivity to Pliocene climatic change from a Dry Valleys perspective. *Geografiska Annaler*, In the press.

Denton, G.H., Bockheim, J.G., Wilson, S.C. and Stuiver, M., 1989: Late Wisconsin and early Holocene glacial history, inner Ross Embayment, Antarctica. *Quat. Res.* 31, 151-182.

Drewry, D.J., 1982: Ice flow, bedrock, and geothermal studies from radio-echo sounding inland of McMurdo Sound, Antarctica. In *Antarctic Geoscience (C. Craddock, Ed.) University of Wisconsin Press, Madison,* 977-983.

Hamilton, W. and Hays, T., 1963: Type section of the Beacon Sandstone, Antarctica. *US Geological Survey Professional Paper* 456-A., Washington, D.C.

Harwood, D. M., 1986: Diatom biostratigraphy and Paleoecology and a Cenozoic history of Antarctic ice sheets. PhD dissertation, Ohio State University, Columbus Ohio.

Holdsworth, G. and Bull, C., 1970: The flow law of cold ice: investigations of Meserve Glacier, Antarctica. In *International Symposium on Antarctic Glaciological Exploration (Hanover, New Hampshire, USA, 3-7 September 1968),* 204-216: *IAHS Publ.* no. 86.

Huybrechts, P. 1994: Glaciological and climatological aspects of a stabilist versus a dynamic view of the late Cenozoic glacial history of East Antarctica. *Geografiska Annaler,* In the press.

Keys, J.R., 1980: Air temperature, wind, precipitation and atmospheric humidity in the McMurdo region. *Antarctic Data Series* 9, Victoria University of Wellington, No. 17.

Kyle, R., 1990: McMurdo Volcanic Group - western Ross Embayment. In *Volcanoes of the Antarctic plate and southern oceans. American Geophysical Union, Ant. Res. Ser. 48* Washington, DC. 19-25.

Lowe, D.J., 1986: Controls on the rates of weathering and clay mineral genesis in airfall tephras: a review and New Zealand case study. In *S.M. Colman and D. Dethier ed., Rates of chemical weathering of rocks and minerals.* Academic Press, Inc., New York., 265-330.

Lowe, D.J. and Nelson, C.S., 1983: *Occas. Rep. 11.* Department of Earth Sciences, University of Waikato, Hamilton, New Zealand.

Marchant, D. R., Denton, G.H. Sugden, D.E. and Swisher III, C.C., this volume: Miocene glacial stratigraphy and landscape evolution of the western Asgard Range, Antarctica.

Marchant, D.R., Denton, G.H., Bockheim, J.G., Wilson, S.C. and Kerr, A.R., 1994: Quaternary ice-level changes of upper Taylor Glacier, Antarctica: Implications for Paleoclimate and ice-sheet dynamics. *Boreas,* in Press.

Marchant, D.R., Swisher III, C.C., Lux, D.R., West, Jr., D. and Denton, G.H., 1993a: Pliocene paleoclimate and East Antarctic ice-sheet history from surficial ash deposits. *Science* 260, 667-670.

Marchant, D.R., Swisher III, C.C., Potter, N.P, Jr. and Denton, G.H., 1993b: Antarctic Paleoclimate and ice-sheet dynamics reconstructed from volcanic ashes in the Dry Valleys. *Paleo., Paleo., Paleo.* submitted.

Miller, K.G., Fairbanks, R.G. and Mountain, G.S., 1987: Tertiary oxygen isotope synthesis, sea level history, and continental margin erosion. *Paleoceanography* 2(1), 1-19.

Nye, J.F., 1973: Water at the bed of a glacier. In *Symposium on the Hydrology of Glaciers,* Cambridge, 9-13

September 1969, *Inter. Assoc. Sci. Hydrol.* 95, 189-194.

Robin, G. de Q., 1988: The Antarctic ice sheet, its history and response to sea level and climatic changes over the past 100 million years. *Palaeo., Palaeo., Palaeo.* 67, 31-50.

Rothlisberger, H.A., 1972: Water pressure in intra- and subglacial channels. *Jour. of Glac.* 11, 177-203.

Savin, S.M., Douglas, R.G., and Stehli, F.G., 1975: Tertiary marine Paleotemperatures. *Geol. Soc. Amer. Bull.* 86, 1499.

Schwerdtfeger, W., 1984: Weather and climate of the Antarctic. In *Developments in Atmospheric Science 15.* Elsevier Publishing Company, Amsterdam.

Selby, M.J., 1974: Slope evolution in an Antarctic oasis. *New Zealand Geographer* 30, 18-34.

Selby, M.J., 1971: Slopes and their development in an ice-free, arid area of Antarctica. *Geografiska Annaler,* 53(A), 235-245.

Shackleton, N.J. and Kennett, J.P., 1975: Paleotemperature history of the Cainozoic and the initiation of Antarctic glaciation: oxygen and carbon analysis in DSDP sites 277, 279 and 281. In *Initial Reports of the Deep Sea Drilling Project,* (Kennett, J.P., and Houtz, R. Eds.) 29, 743-755.

Shreve, R.L., 1985: Esker characteristics in terms of glacier physics, Katahdin esker system, Maine. *Geol. Soc. Amer. Bull.* 96, 131-146.

Shreve, R.L., 1972: Movement of water in glaciers. *Jour. of Glac.* 11(62), 205-14.

Sugden, D.E. and John, B.S., 1976: *Glaciers and Landscape.* Arnold, 372 p.

Webb, N. and Harwood, D.M., 1991: Late Cenozoic glacial history of the Ross Embayment, Antarctica. *Quat. Sci. Revs.* 10, 215-223.

Webb, N. and Harwood, D.M., 1987: Terrestrial flora of the Sirius Formation: Its significance for late Cenozoic glacial history. *Antarctic Journal of the U.S.* 22(4), 7-11.

Webb, N., Harwood, D.M., McKelvey, B.C., Mercer, J.H. and Stott, L.D., 1984: Cenozoic marine sedimentation and ice-volume variation on the East Antarctic craton. *Geology* 12, 287-291.

Weed, R. and Norton, S.A., 1991: Siliceous crusts, quartz rinds and biotic weathering of sandstones in the cold desert of Antarctica. In *Proceedings of the International Symposium on Environmental Biogeochemistry,* 327-339. Elsevier Publishers.

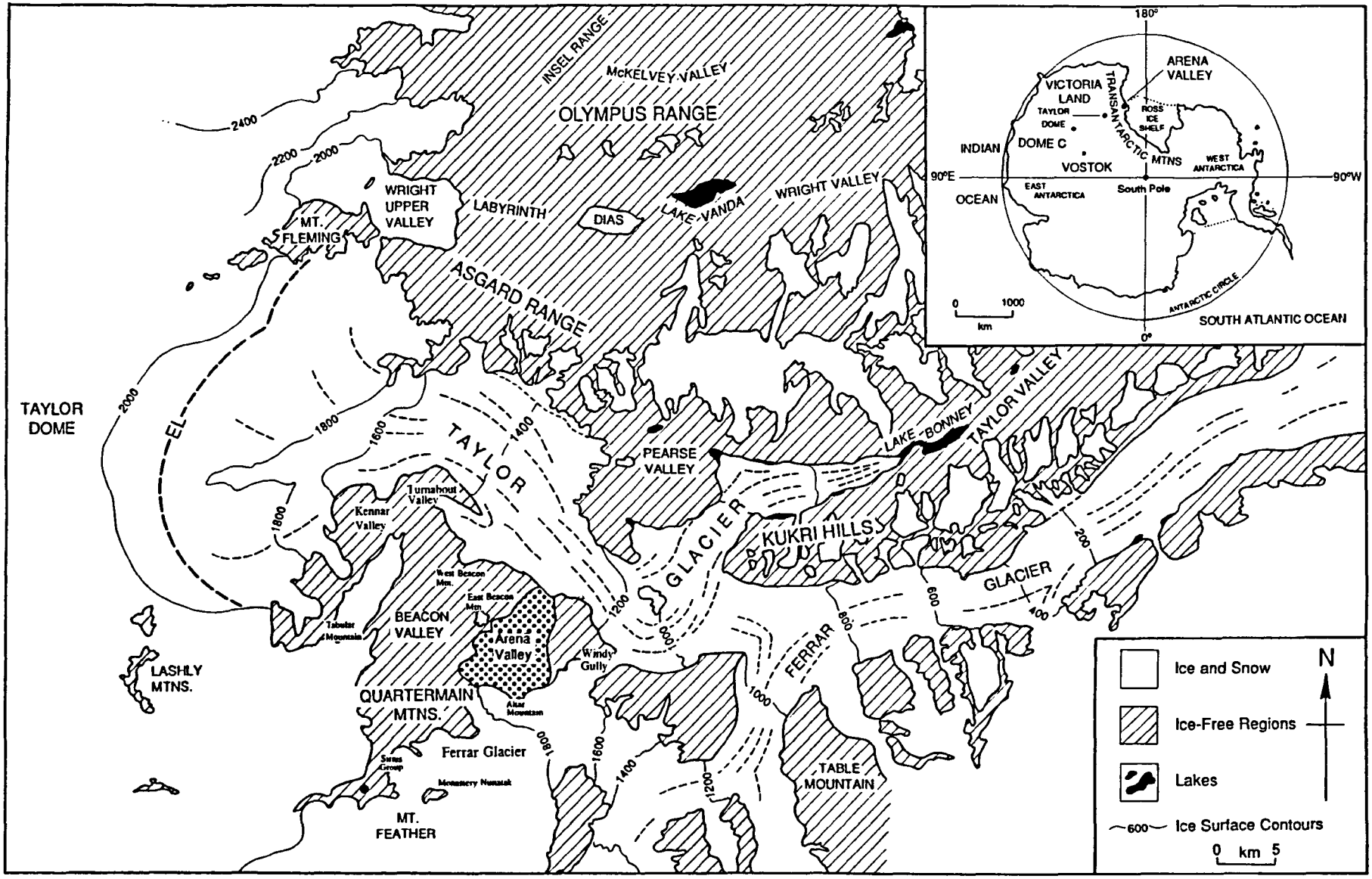

Figure 1. Location map of the Dry Valleys region.

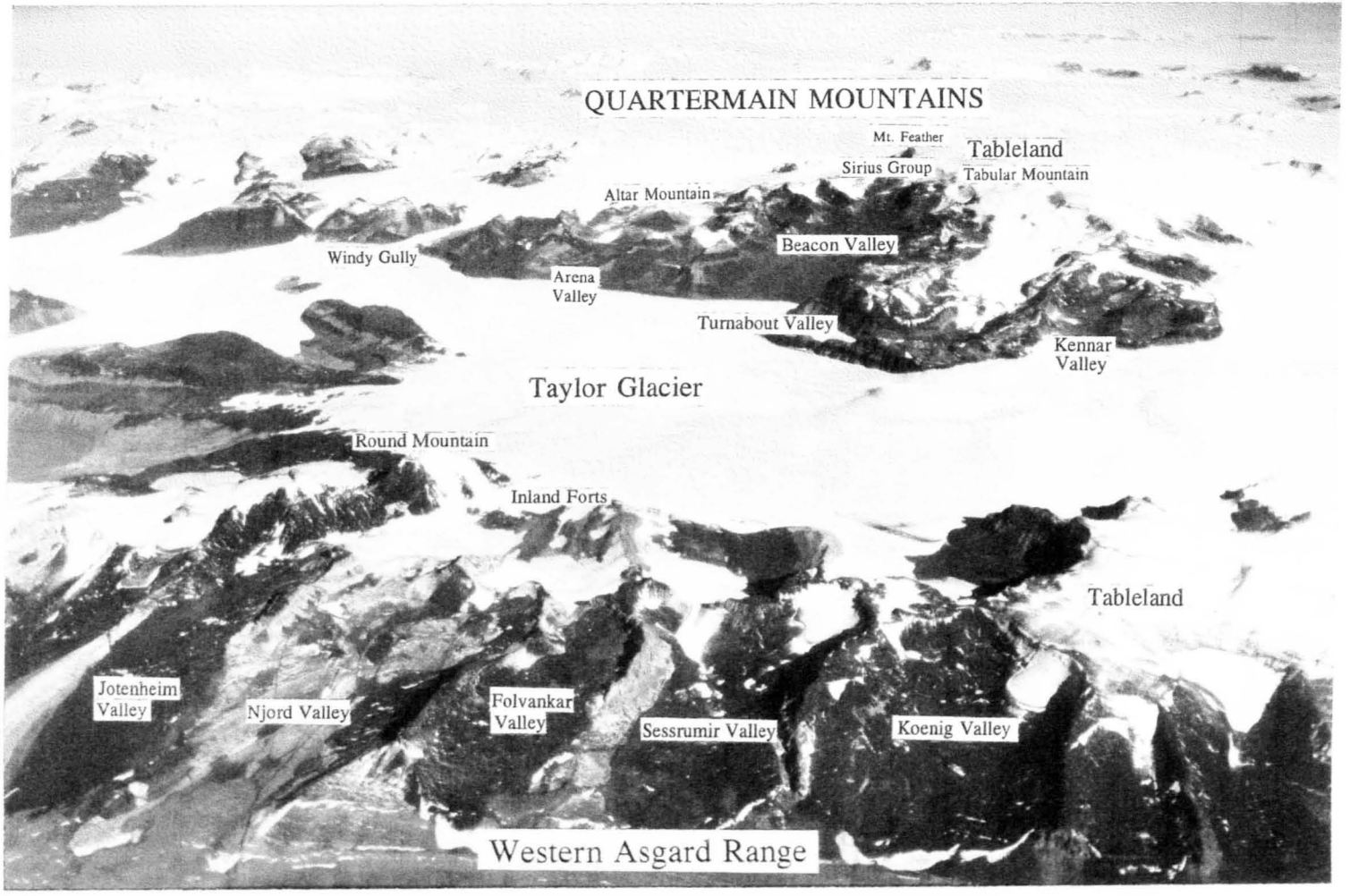

Figure 2. Oblique aerial view (looking south) across the western Asgard Range to the Quartermain Mountains. See Marchant et al. (this volume) for additional details of the western Asgard Range. The Quartermain Mountains are situated about 30 km to the south of the Asgard Range.

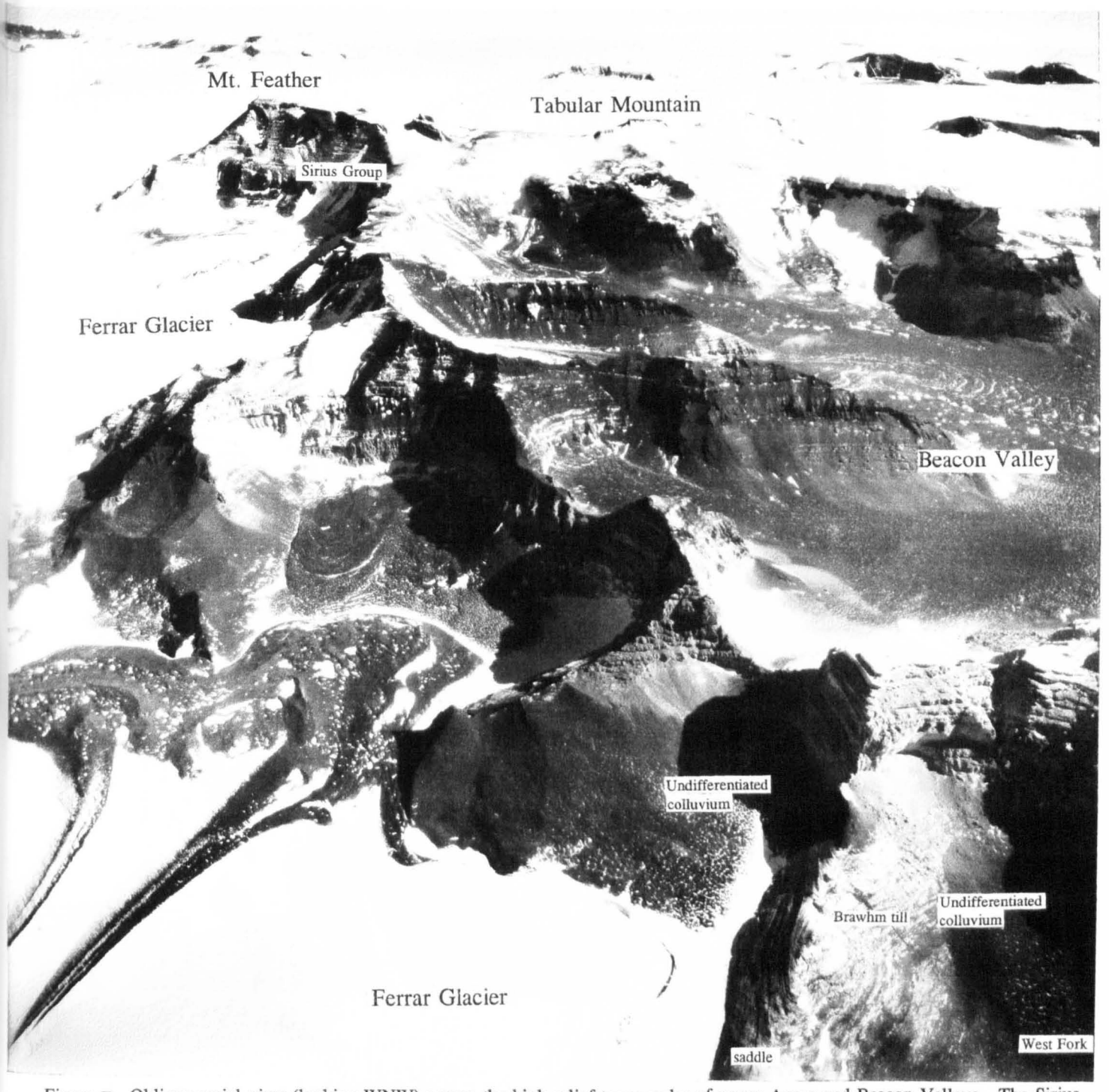

Figure 3. Oblique aerial view (looking WNW) across the high-relief topography of upper Arena and Beacon Valleys. The Sirius Group occurs on the surface of a small erosional terrace at 2650 m elevation. Brawhm till occurs on the stossed headwall of West Fork, shown at the bottom right of the photograph.

Figure 4. Oblique aerial view (looking southeast) across the Quartermain Mountains. Note prominent 1600-to-1700-m elevation benches between East and West Beacon Mtns., in the lee of Altar Mountain, and on the east divide of lower Arena Valley. Snow banks and small

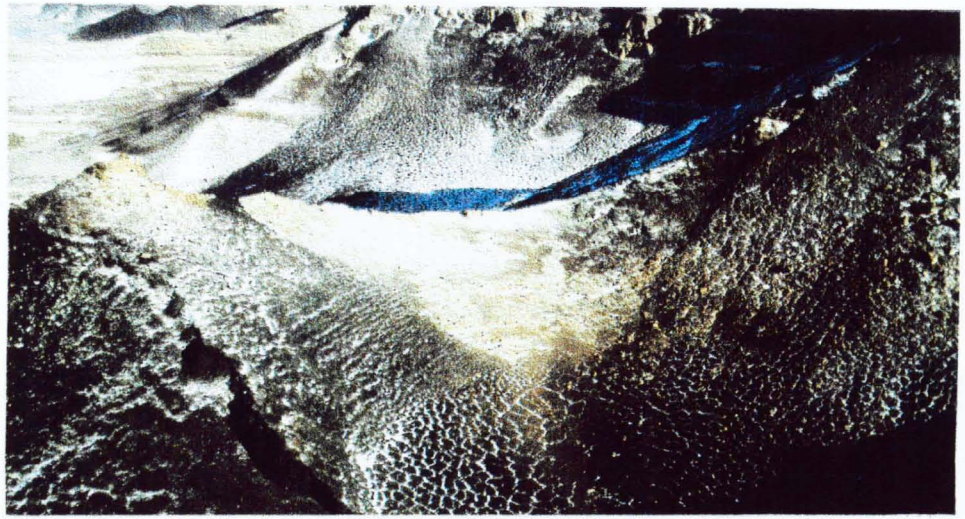

(a)

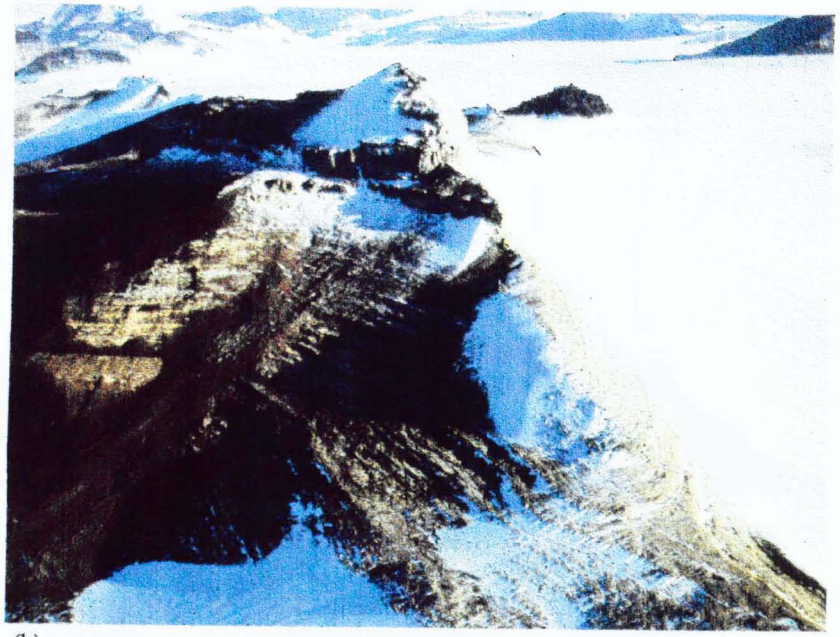

(b)

Figure 5. (a) Oblique aerial view (looking south) showing selective erosion of undifferentiated colluvium in the lee of the stossed divide in central Arena Valley. (b) Stoss-and-lee topography along East Fork saddle and the south face of Altar Mountain. Note that stoss slopes are bare. Glacial striations occur beneath Brawhm till (not shown, but just off the lower right corner of the photograph).

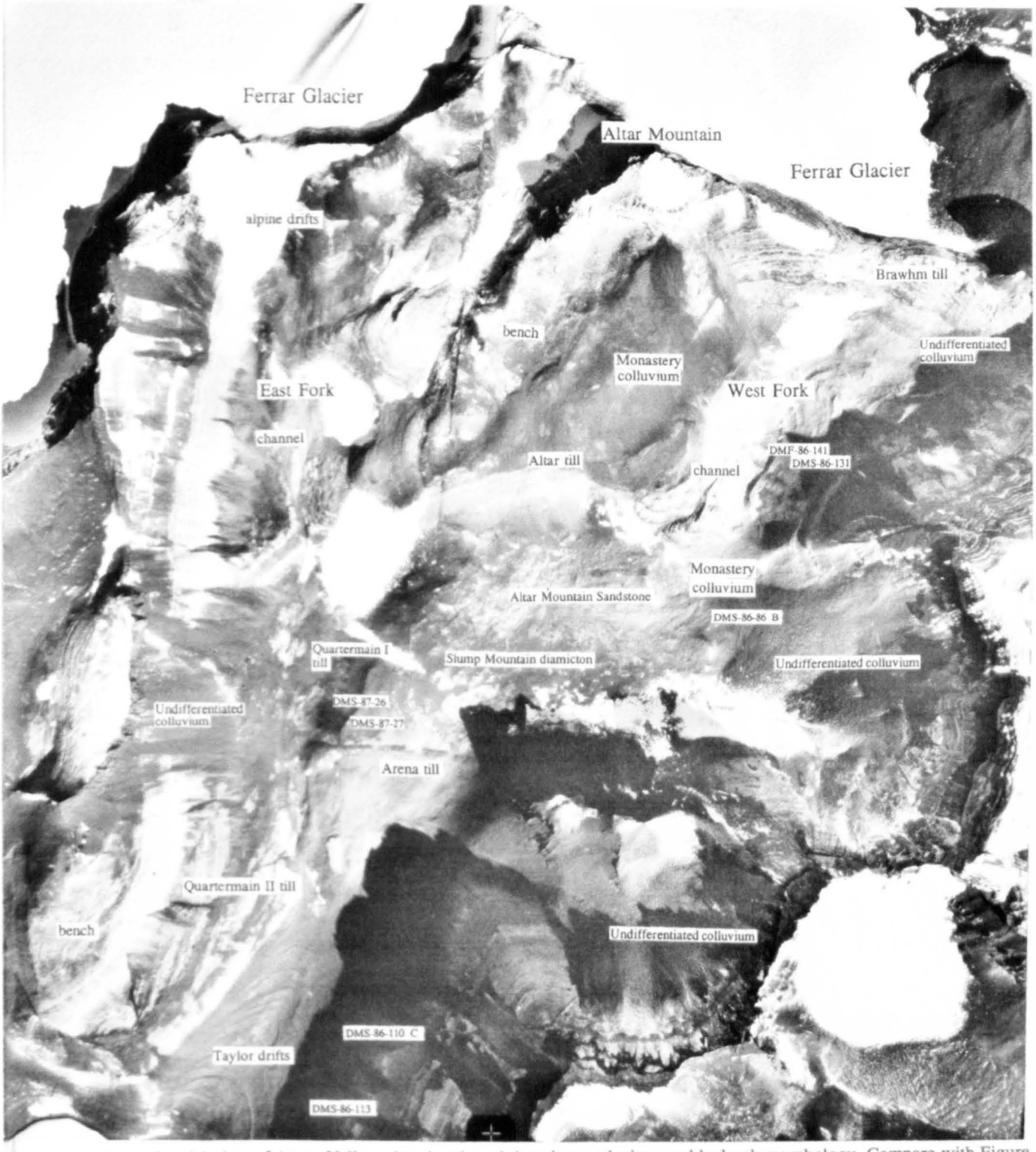

Figure 6. Vertical aerial view of Arena Valley, showing deposit locations, ash sites, and bedrock morphology. Compare with Figure 7.

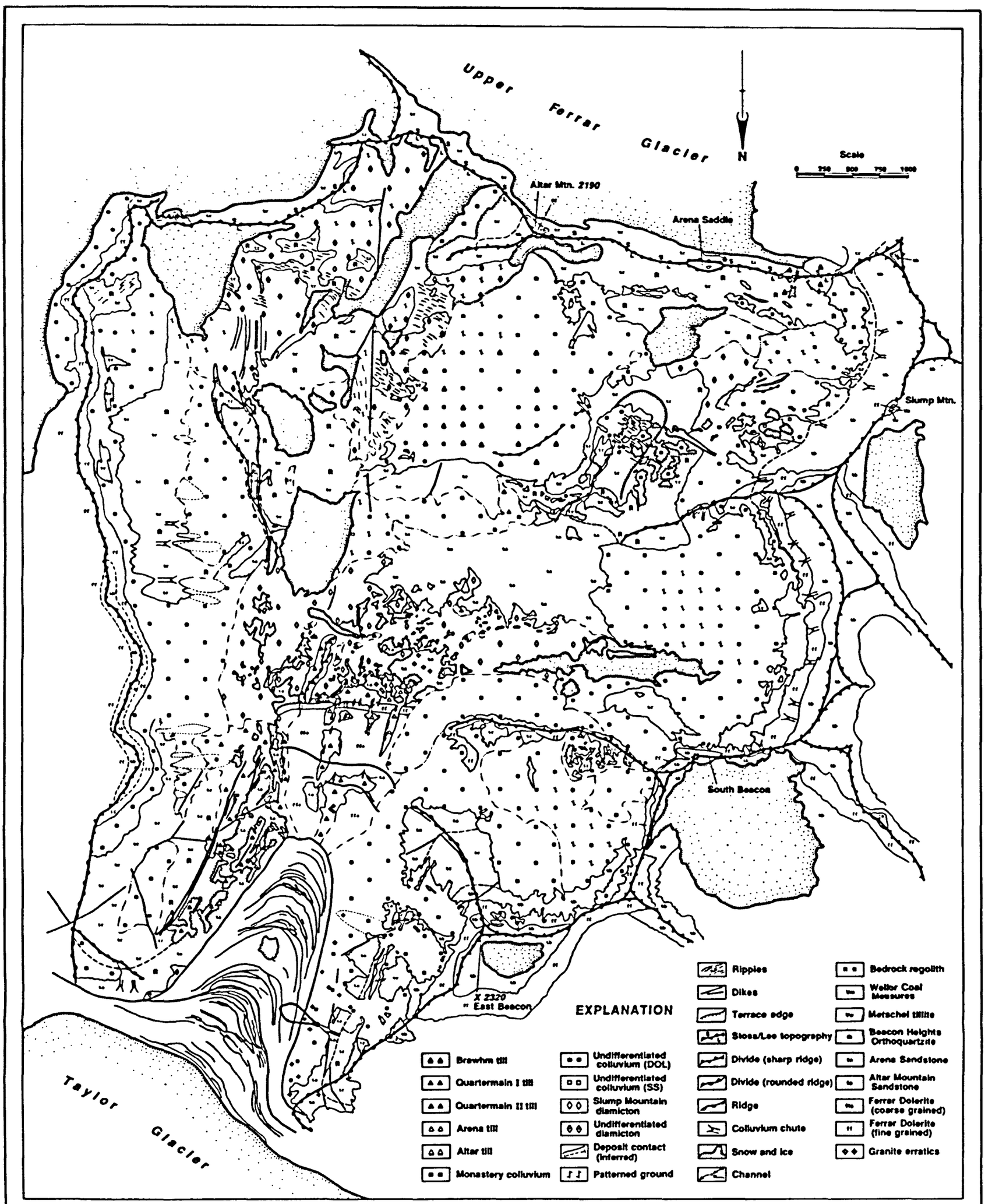
Upper Ferrar Glacier
N
Scale
0 250 500 750 1000
Altar Mtn. 2190
Arena Saddle
Slump Mtn.
South Beacon
X 2320
" East Beacon
Taylor Glacier
EXPLANATION
Brawhm till
Quartermain I till
Quartermain II till
Arena till
Altar till
Monastery colluvium
Undifferentiated colluvium (DOL)
Undifferentiated colluvium (SS)
Slump Mountain diamicton
Undifferentiated diamicton
Deposit contact (inferred)
Patterned ground
Ripples
Dikes
Terrace edge
Stoss/Lee topography
Divide (sharp ridge)
Divide (rounded ridge)
Ridge
Colluvium chute
Snow and ice
Channel
Bedrock regolith
Weller Coal Measures
Metschel tillite
Beacon Heights Orthoquartzite
Arena Sandstone
Altar Mountain Sandstone
Ferrar Dolerite (coarse grained)
Ferrar Dolerite (fine grained)
Granite erratics

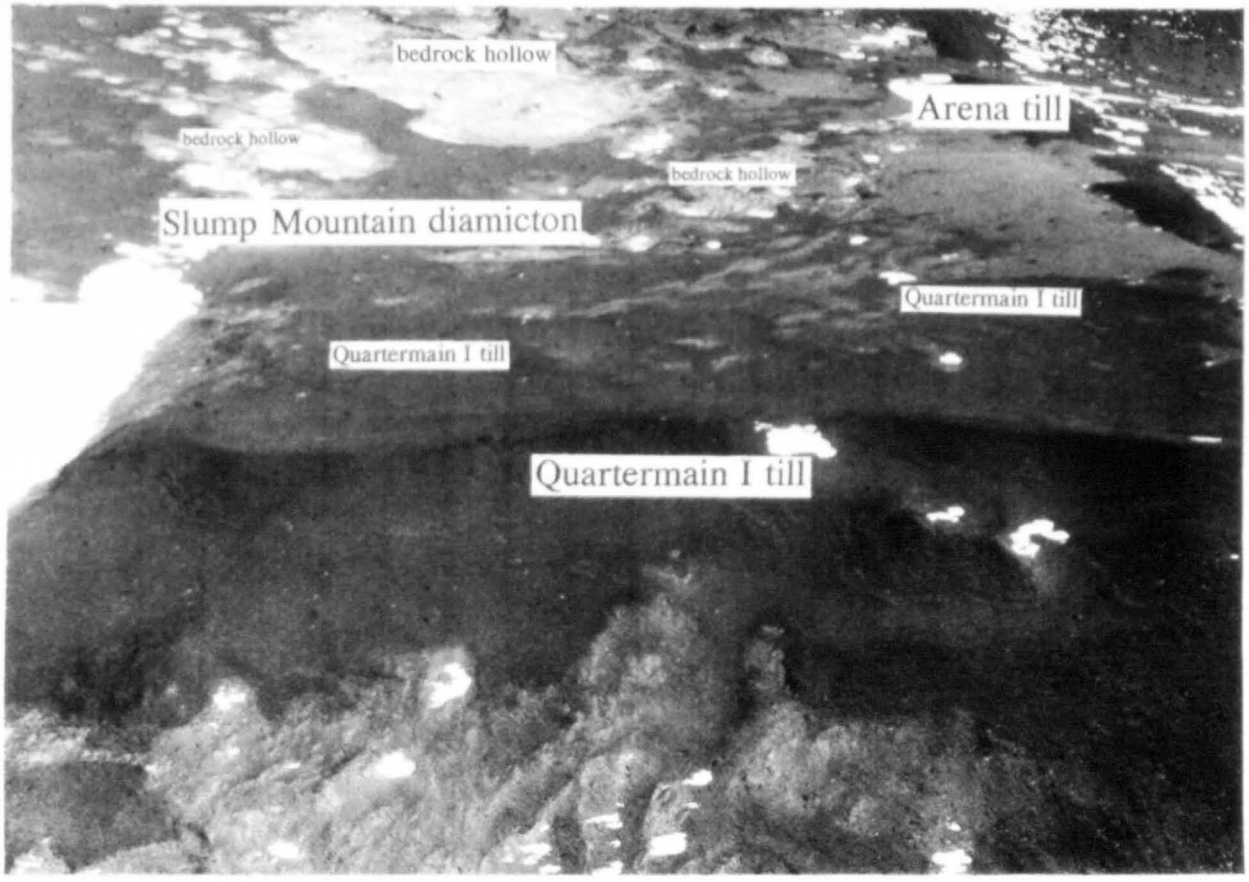

Figure 8. Oblique aerial view of central Arena Valley (looking west) showing closed-bedrock hollows, Slump Mountain diamicton and Arena till. Large moraine of Quartermain I till in foreground (see also Figure 9).

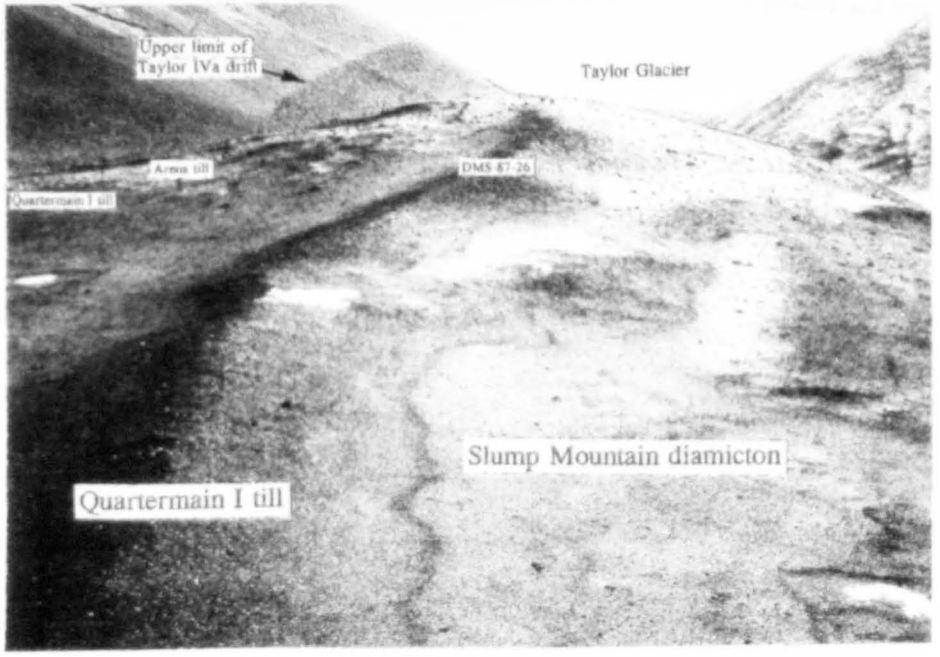

(a)

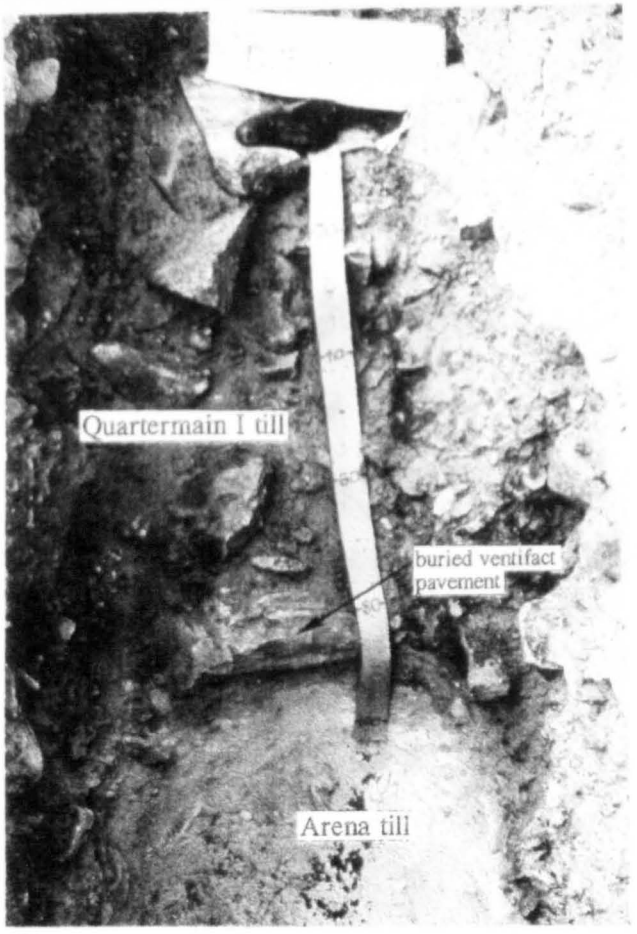

(b)

Figure 9. (a) Oblique aerial view of central and lower Arena Valley. Largest Quartermain I moraine (with location of ash site DMS-87-26) shown in foreground. In background, upper limit of Taylor IVa moraines is clearly visible along the west valley wall. (b) Hand-dug section showing the sharp stratigraphic contact of Quartermain I till and underlying Arena till. A buried sandstone ventifact pavement separates the two tills.

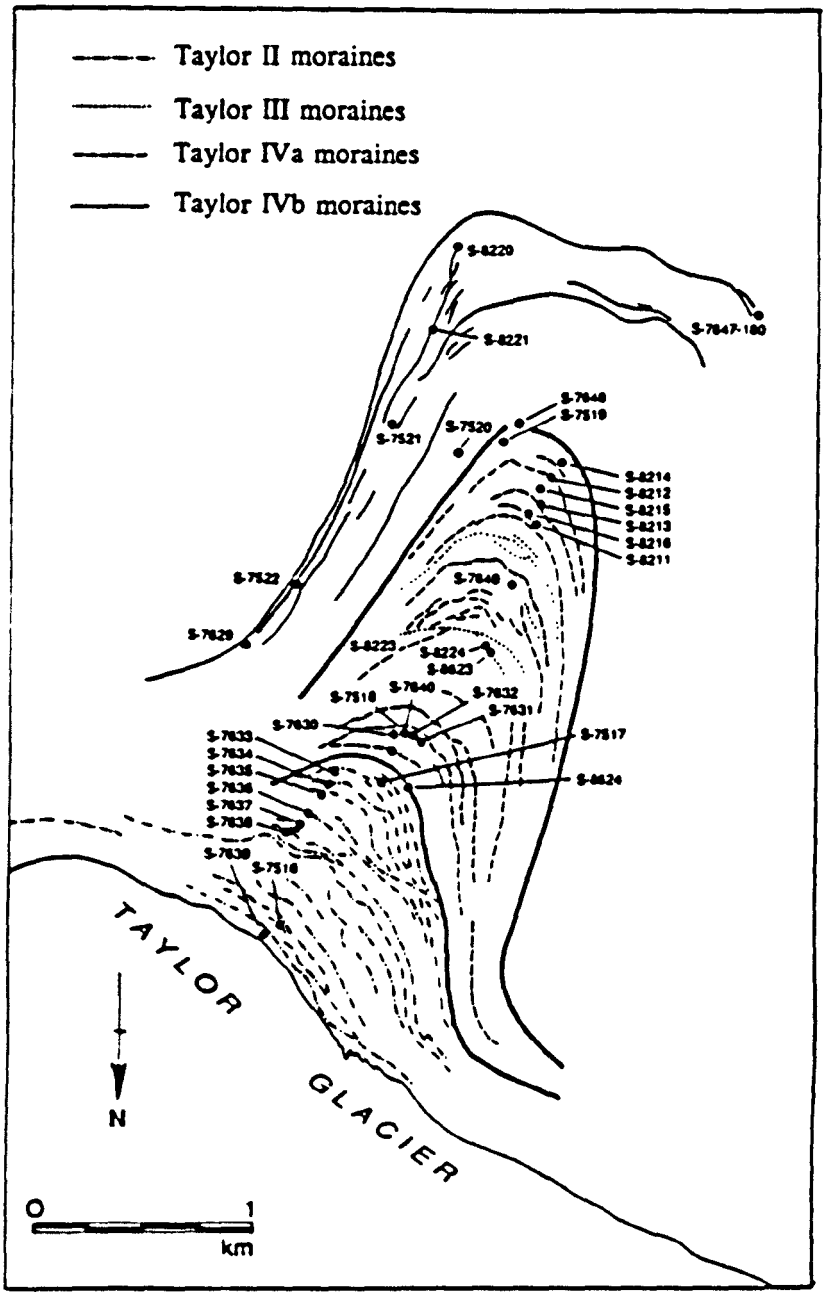

Figure 10. Taylor moraines in lower Arena Valley. S-82-20 and other numbers refer to soil pit localities (see Marchant et al. (1994) for details of soil excavations). Bold lines on map mark upvalley limit of Taylor II and Taylor IVa moraines. Taylor III moraines are superimposed on Taylor IVa drift and moraines.

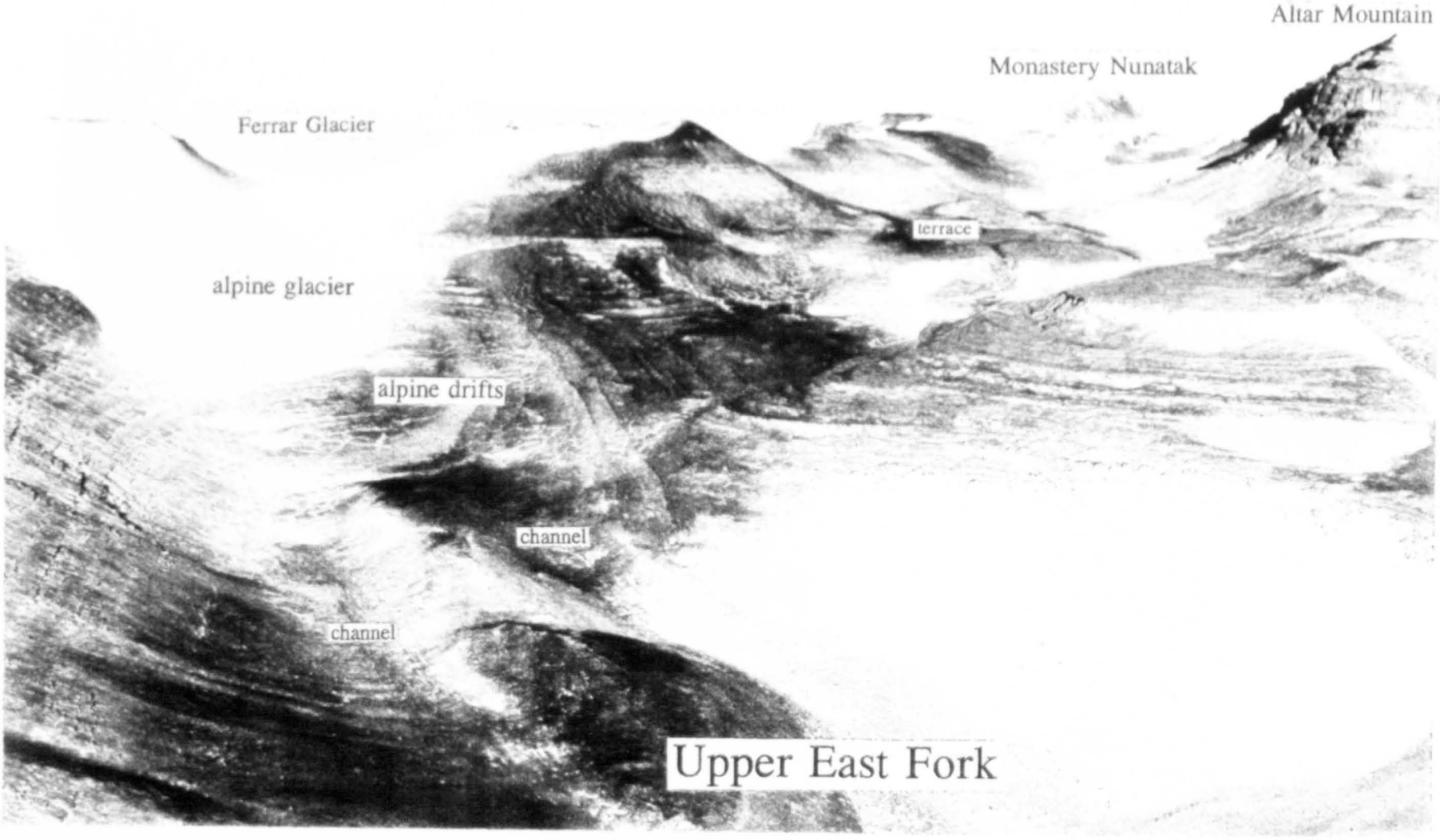

Figure 11. Oblique aerial view of upper East Fork (looking south), showing alpine drifts, channels, terraces, and Altar Mountain. Monastery Nunatak, situated about 10 km south of Arena Valley) occurs in background.

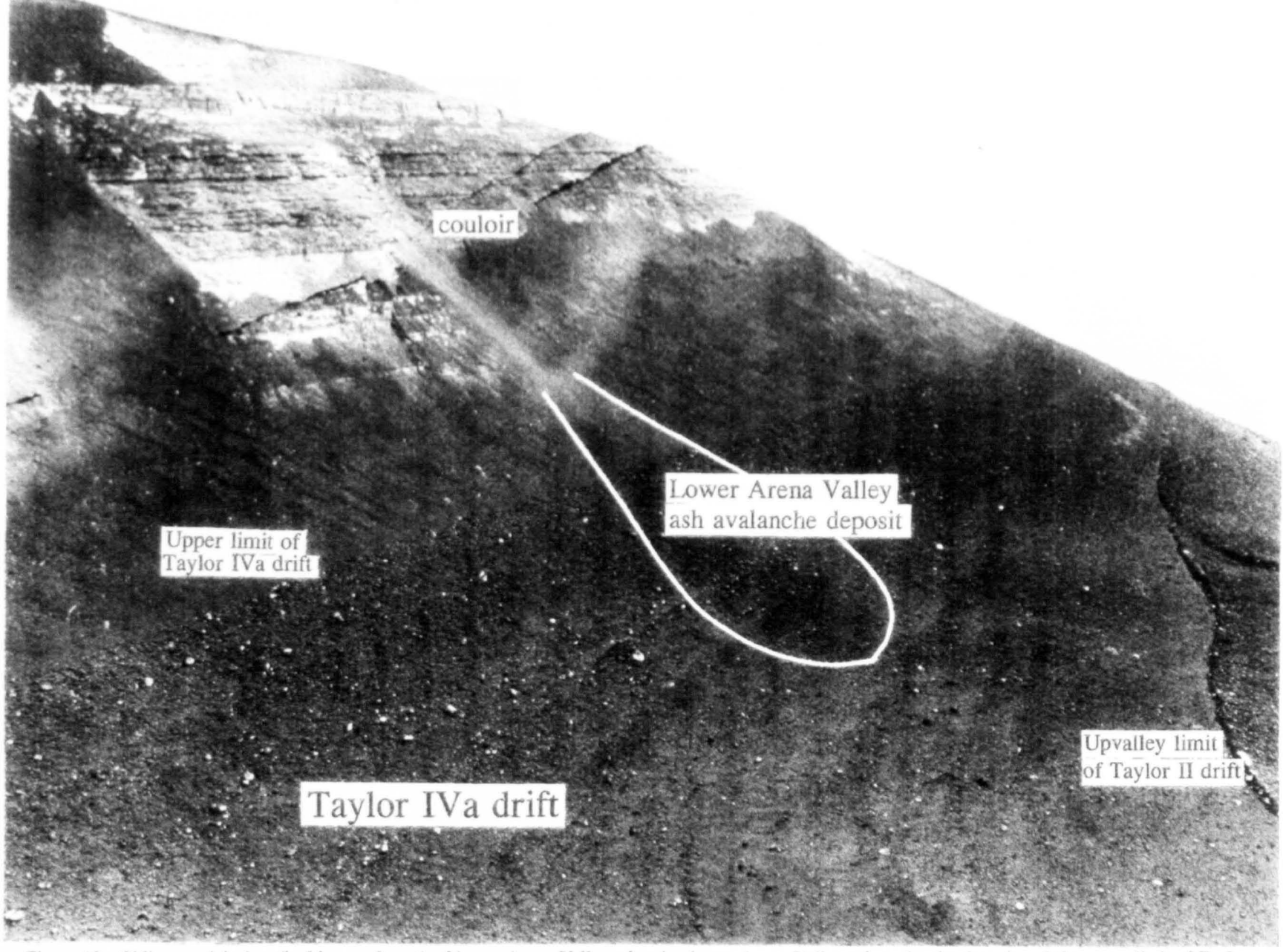

Figure 12. Oblique aerial view (looking northwest) of lower Arena Valley, showing lower Arena Valley ash avalanche deposit and the upper limit of Taylor IVa and Taylor II drift. Avalanche deposit unconformably overlies undifferentiated colluvium. $^{40}Ar/^{39}Ar$ analyses of volcanic crystals and glass shards within the avalanche deposit indicate an age of 11.3 and 12.9 Ma, respectively. The preservation of the avalanche deposit morphology and the lack of overlying colluvium indicates slope stability for the last 11.3 Ma (see text for description).

(a)

(b)

Figure 13. Photographs of the Arena Valley Ash (DMS-86-86 B), which overlies a buried desert pavement. (a) Excavation shows the sharp stratigraphic contact of the Arena Valley Ash and underlying Monastery colluvium. (b) Same excavation but with the ash cut back to expose the underlying ventifact pavement. $^{40}Ar/^{39}Ar$ analyses of individual volcanic crystals removed from the Arena Valley Ash indicate an age of 4.34 Ma $\pm$ 0.025.

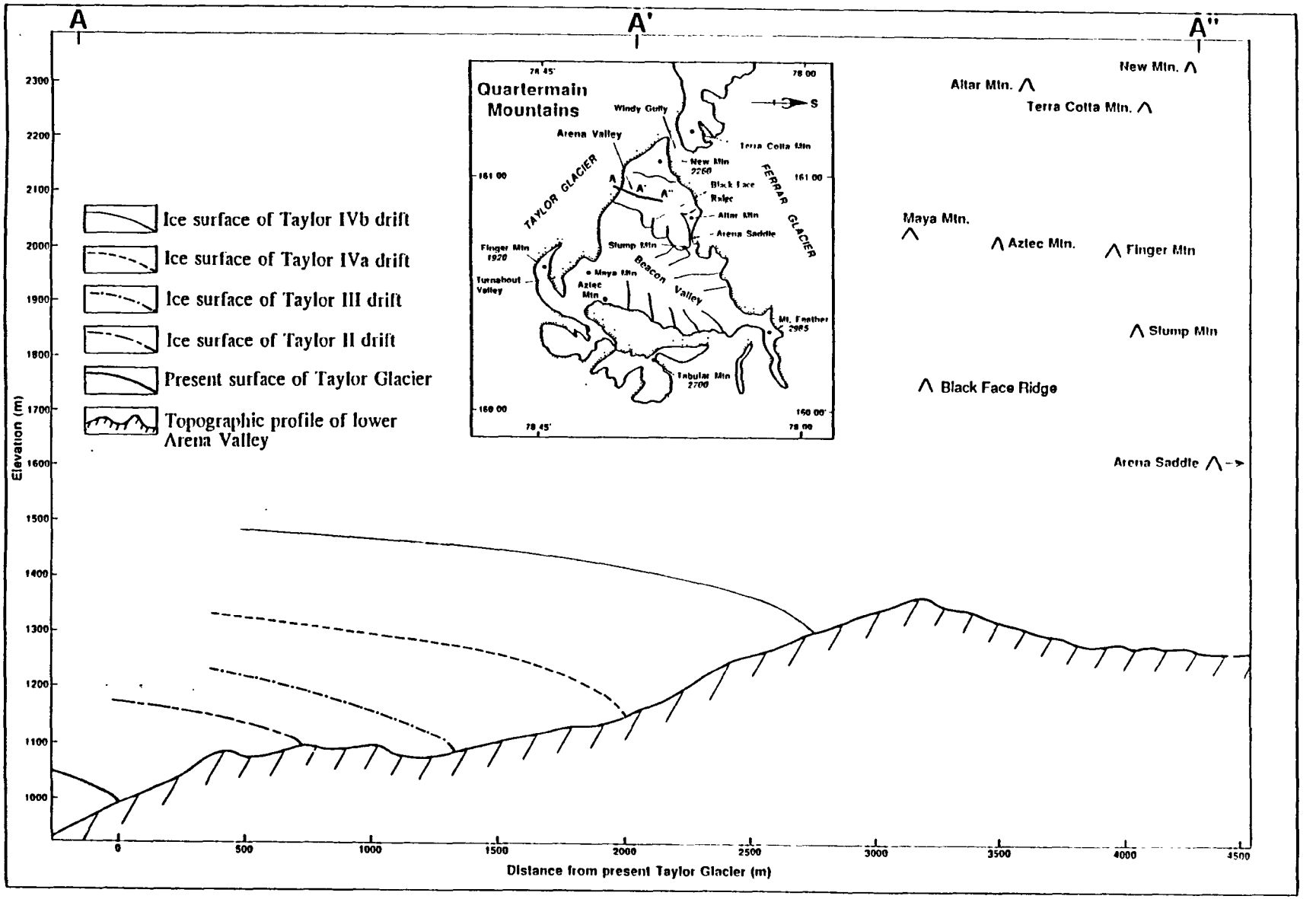

Figure 14. Longitudinal profile of lower Arena Valley and former Pliocene- and Quaternary age ice-surface elevations of Taylor Glacier. Inset shows location of cross section. Ice-surface profiles reflect outcrop elevations of individual drift sheets and outer moraine ridges.

Table 1. Stratigraphy, sedimentology, and isotopic age of Miocene-age deposits in Arena Valley.

DEPOSIT	DISTRIBUTION	AGE[1] Ma	STRATIGRAPHIC POSITION	STRAT. CONTACT	THICKNESS	TEXTURE	CLAST	ERR.	GLAC.	CL.
Quartermain I till	moraines and till patches in central Arena Valley	<11.6 > 7.4[2] > 4.4[3]	overlies Arena till and Slump Mountain diamicton	very sharp; preserves desert pavement	1.0 to 3.0 m	gravelly sand	85% dolerite 12% sandstone 3% granite	granite	none	10YR 5/6
Brawhm till	in five patches along the stossed headwall of upper East Fork	<11.6[4] > 7.4	overlies bedrock striations; northeast ice flow	Arena Sandstone bedrock	<75 cm	gravelly sand	90% dolerite 10% sandstone	none	none	10YR 5/6
Undifferen. colluvium	on valley walls, particularly beneath dolerite free faces	>11.3 > 8.5	overlies Monastery colluvium, Quarter-main II till, and Slump Mountain diamicton	gradational	<1.75 m	gravelly sand	50% dolerite 50% sandstone	reworked granite at v. mouth	none	10YR 6/4
Arena till	downvalley from bedrock hollows in central Arena Valley	>11.3	overlies striated/ molded bedrock and erosional remnants of Quartermain II till	gradational with underlying Quart-ermain II till	thins downvalley from a max. of 1.5 m	gravelly mud	90% sandstone 10% dolerite	reworked granite above Q. II till	27%	2.5Y 6/4
Slump Mountain diamicton	on floor of central Arena Valley; cut by bedrock hollows	>11.3	overlies weathered Altar Mountain Sandstone bedrock/ residuum	gradational; merges with Arena till	thins downvalley from a max. or 1.5 m	gravelly mud	70% dolerite 30% sandstone	none	none	2.5Y 6/4
Quartermain II till	along the east wall of central and lower Arena Valley	>11.3	overlies weathered sandstone bedrock/ sandstone residuum; underlies Arena till	gradational	<1.5 m	sandy gravel	60% dolerite 35% sandstone 5% granite	granite	none	10YR 5/6
Monastery colluvium	along the north flank of Altar Mtn. and at the base of valley walls	>11.3	overlies Altar till	gradational	<1.0 m	gravelly sand	90% dolerite 10% sandstone	none	none	5YR 7/6
Altar till	on north flank of Altar Mtn.	>11.3	overlies weathered sandstone bedrock/ residuum	Arena Sandstone	<1.0 m	gravelly mud	85% dolerite 15% siltstone	none	5%	5YR 7/6

[1] See also Table 3 and Appendix I for details. [2] Inferred lower-age limit of Quartermain I till based on correlation with Brawhm till (see text and Table 3 for details). [3] Minimum age of Quartermain I till based on ^{10}Be exposure-age analyses of sample SCW87-1-1HF5 (Brown et al., 1991). This sample has a lower limit of 3.4 Ma and an upper limit of 6.4 Ma. [4] Maximum age of Brawhm till based on correlation with Quartermain I till. Sedimentary textures and clast composition based on field observations. ERR., abundance of glacial erratics; GLAC., abundance of glacially molded/ striated clasts; CL., average Munsell Color of oxidized horizon.

Table 2. Stratigraphy, sedimentology, and isotopic age of Pliocene- and Pleistocene-age deposits in Arena Valley.

DEPOSIT	DISTRIBUTION/ ELEVATION[1]	AGE[2, 3]	STRAT. POSITION	STRAT. CONTACT	THICKNESS	TEXTURE	CLAST	ERR.	GLAC.	CL.
Taylor II	15 moraines about 0.1 to 0.75 km south of present Taylor Glacier margin; 200 m in elevation above Taylor Glacier	>117 Ka	overlies Taylor IVa drift	sharp	3.0 to 4.0 m	boulders with a gravel/sand matrix	90% dolerite 8% sandstone 2% granite	gran.	none	10YR 6/4
Alpine A	3 moraines 0.1 to 0.2 km west of alpine glacier	>117 Ka	overlies undif. diamicton	not exposed in section	1.5 m	boulders with a gravel/sand matrix	75% sandstone 25% dolerite	none	none	10YR 6/4
Taylor III	3 moraine segments about 1.0 to 1.7 km south of present Taylor Glacier margin; 250 m in elevation above Taylor Glacier	>200 Ka	overlies Taylor IVa drift	in-situ ventifact pavement preserved under Taylor III drift	1.2 to 2.0 m	boulders with a gravel/sand matrix	90% dolerite 7% sandstone 3% granite	gran.	none	10YR 6/4
Alpine B	5 moraines about 0.2 to 0.3 km west of alpine glacier	>200 Ka	overlies undif. diamicton	not exposed in section	1.0 to 1.2 m	cobbles with a gravel/sand matrix	60% sandstone 40% dolerite	none	none	10YR 6/4
Taylor IVa	16 moraines about 0.75 to 2.25 km south of present Taylor Glacier margin; 325 m in elevation above Taylor Glacier	>1.0 Ma	overlies colluvium and lower ash avalanche deposit	sharp	1.0 m	boulders and cobbles with a gravel/sand matrix	70% dolerite 27% sandstone 3% granite	gran.	none	10YR 5/6
Alpine C	2 moraines about 0.35 km west of alpine glacier	>1.0 Ma	cuts across East Fork channel	sharp	1.0 m	cobbles with a gravel/sand matrix	65% dolerite 35% sandstone	none	none	10YR 5/6
Taylor IVb	8 moraines about 1.0 to 3.0 km south of present Taylor Glacier margin; 475 m in elevation above Taylor Glacier	>2.2 Ma <7.4 Ma[4]	overlies Arena till and dissected Quartermain II till	sharp	0.5 to 1.0 m	boulders	95% dolerite 4% sandstone 1% granite	gran.	none	7.5YR 6/4
Alpine D	1 moraine 0.5 km west of alpine glacier	>2.2 Ma <7.4 Ma	overlies weathered sandstone bedrock/ residuum	Arena Sandstone	< 60 cm	coarse-grained gravels and sand	70% dolerite 30% sandstone	none	none	10YR 5/6

[1] Elevations based on height of moraines above the present ice-surface elevation of Taylor Glacier at the mouth of Arena Valley. [2] Isotopic age of Taylor drifts based on exposure age data from Brook and Kurz (1993) and Brook et al. (1993). [3] Inferred age of alpine drifts based on correlation with Taylor drifts. [4] Maximum age of Taylor IVb/ Alpine D drifts based on minimum age of Quartermain I till, which antedates Taylor IVb drift. Textures based on field observations; ERR. and GLAC. indicate abundance of glacial erratics and glacially polished and striated clasts, respectively; CL., average Munsell color of oxidized horizon.

Table 3. Summary of volcanic ash data from text and in Appendix I.

SAMPLE NUMBER	DESCRIPTION[1]	STRATIGRAPHIC POSITION	MATERIAL DATED	$^{40}Ar/^{39}Ar$ AGE	SIGNIFICANCE
		ASH ON DESERT PAVEMENT			
DMS-86-86 B	A pale-white (10YR 8/2) ash deposit that shows an upper ash-rich diamicton and a basal ashfall layer (1.0mm thick). The phonolitic ash contains euhedral crystals of anorthoclase, aegerine, subcalcic augite, and magnetite. This deposit contains < 2.5% clay.	Ash layer rests on in-situ ventifact pavement near the mouth of the stubby tributary in west-central Arena Valley. This pavement caps Monastery colluvium. A second ventifact pavement overlies the ash deposit.	anorthoclase	**4.34 Ma**	The preservation of the in-situ ash and underlying ventifact pavement indicates minimal slope development at the tributary headwall in the last 4.3 Ma. This suggests that mean annual temperatures have remained well below 0°C during this time. We postulate that dry conditions favorable for the development/ preservation of ventifact pavements have existed continuously in Arena Valley since ash deposition (see also Marchant et al., 1993a). Date provides a minimum age for Monastery colluvium.
		ASH LAYER IN COLLUVIUM			
DMS-86-110 C	Fine-grained (<0.5 mm), dark-gray (5YR 2/4), vesicular pumice with euhedral volcanic crystals. Dated ash occurs buried in a horizontal layer (10 cm thick) at about 25 cm below the present ground surface. This ash layer contains about 30% non-volcanic sands and gravel.	Ash layer occurs interbedded with undifferentiated colluvium at 1500 m elevation, on the west wall of lower Arena Valley (28° slope). Interbedded colluvial layers grade upward from cobble ventifacts to coarse-grained sand.	sanidine	**8.49 Ma**	Because the ash layer is buried beneath only 25 cm of non-volcanic colluvium, we postulate that all but the uppermost 25 cm of colluvium at this site predates 8.49 Ma. Hence, the overall rectilinear slope morphology predates 8.49 Ma. Such slope stability is best explained by persistent hyper-arid, cold-desert conditions (similar to the present) for the last 8.49 Ma.
		UPPER ARENA VALLEY ASH AVALANCHE DEPOSIT			
DMF-86-141	Ash within the central avalanche lobe at about 1500 m elevation. Ash consists of coarse-grained, vesicular glass shards and angular volcanic crystals and is protected from wind deflation by a thin pavement composed of a single layer of interlocking gravel-sized ventifacts. Avalanche deposit overlies dissected outcrops of undifferentiated colluvium.	Disseminated ash is admixed with unweathered sandstone gravel, dolerite grus, and coarse-grained sands. Salt pans (stage 5/6 of Bockheim, 1990) occur between 15 and 25 cm depth.	crystal glass	**6.42 Ma** **7.38 Ma**	The preservation of the upper ash avalanche deposit indicates little, if any, slope development at this site during the last 6.4 to 7.3 Ma. Deposition and dissection of undifferentiated colluvium here predate 6.4 to 7.3 Ma ago. We postulate that dissection of this colluvium occurred beneath the ice that deposited Brawhm till in upper West Fork. Hence Brawhm till most likely antedates 6.4 to 7.3 Ma ago.
DMS-86-131	Ash removed from soil pit about 50 m downslope from DMF-86-141, otherwise similar description as DMF-86-141.	Same stratigraphic position as DMF-86-141	sanidine	**7.4 Ma**	The isotopic age and depositional setting indicate little, if any, slope development at this site in the last 7.4 Ma. From considerations given above, deposition of Brawhm till most likely antedates 7.4 Ma.

Table 3 (cont). Summary of volcanic ash data from text and in Appendix I.

SAMPLE NUMBER	DESCRIPTION[1]	STRATIGRAPHIC POSITION	MATERIAL DATED	$^{40}Ar/^{39}Ar$ AGE	SIGNIFICANCE
		LOWER ARENA VALLEY ASH AVALANCHE DEPOSIT			
DMS-86-113	Ash disseminated within the lower Arena Valley ash avalanche deposit at about 1425 m elevation. Coarse-grained ash (1.5 mm) is admixed with a chaotic assortment of unweathered sandstone gravel, dolerite ventifacts and grus, granite erratics, and quartz sand. Ash is protected from wind deflation by a thin pavement composed of a single layer of interlocking gravel-sized ventifacts.	Ash avalanche deposit rests on the west wall of lower Arena Valley. Ash deposit overlies undifferentiated colluvium. A small cone-shaped colluvial deposit (<45 cm thick) overlies the head of the ash avalanche deposit. This colluvial deposit covers about 10% of the total area of the ash avalanche deposit.	crystal glass	**11.3 Ma** **12.9 Ma**	The isotopic age and depositional setting suggest little slope evolution at this site during at least the last 11.3 Ma. Deposition of undifferentiated colluvium at this site predates 11.3 Ma. Rectilinear slope development here antedates 11.3 Ma as well. The preservation of the lobate avalanche deposit morphology indicates that wet-based glaciers have not occupied lower Arena Valley during the last 11.3 Ma. It also indicates that mean annual atmospheric temperatures during this time remained well below 0°C, otherwise the deposit form would have been eroded or cut by rills, channels, and gullies.
		ASH DISSEMINATED IN QUARTERMAIN I TILL			
DMS-87-26	Coarse-grained, vesicular ash disseminated in the large Quartermain I moraine. This ash constitutes about 5 to 10% of the matrix (< 2mm) fraction of Quartermain I till.	Disseminated ash occurs down to base of moraine. Quartermain I till overlies Arena till and Slump Mountain diamicton with sharp stratigraphic contacts.	crystal	**11.27 Ma**	The ash disseminated in Quartermain I till probably reflects either primary ashfall onto the glacier accumulation surface (with subsequent dispersal during englacial or basal transport) or basal entrainment of pre-existing ash deposits. As such Quartermain I till is most probably younger than (or equal to) 11.27 Ma.
DMS-87-27	Coarse-grained, vesicular ash disseminated in the small Quartermain I moraine.	This Quartermain I moraine overlies Arena till with sharp stratigraphic contacts. A buried desert pavement separates Quartermain I and Arena tills.	crystal	**11.59 Ma**	The isotopic age of this ash provides a maximum age of 11.59 Ma for deposition of this Quartermain I moraine. We correlate Quartermain I till with Brawhm till. The minimum age of Brawhm till is 6.4 to 7.4 Ma (see DMF-86-141). Hence, Quartermain I and Brawhm tills were most likely deposited between 7.4 and 11.59 Ma.

[1] All ash deposits are unweathered. Crystals lack evidence of chemical etching and glass shards are not altered to clays. Surficial ash deposits in Arena Valley contain less than 5% clay-sized grains (Marchant et al., 1993a, 1993b). The chemical stability of surficial ash deposits is consistent with persistent cold-desert conditions in Arena Valley since middle-Miocene time (about 11.5 Ma). This is because at the ground surface glass is unstable and quickly alters to clay. The rate of alteration is largely dependent on atmospheric temperature and the abundance of pore water [rates are increased at high atmospheric temperatures and high pore-water pressures (Lowe, 1986)]. For example, under humid temperate conditions in New Zealand, tephras older than about 50,000 years old are > 60% clay (Lowe and Nelson, 1983; Birrell and Pullar, 1973; Lowe, 1986).

Table 4. Correlation of the surficial stratigraphy of the Arena Valley, Quartermain Mountains and of the western Asgard Range (Marchant et al., this volume).

ARENA VALLEY, QUARTERMAIN MTNS.		WESTERN ASGARD RANGE		SIGNIFICANCE
Altar till	> 11.3 Ma	Sessrumnir till Inland Forts till	> 15.0 Ma > 13.8 Ma	Alpine glaciation (with wet-based glaciers) in the western Dry Valleys region sometime prior to 15.0 Ma ago.
Monastery colluvium	> 11.3 Ma	Koenig colluvium	> 14.8 Ma	Ice-free conditions > 14.8 Ma ago, during which time surficial sediments were deeply oxidized and weathered. Such extensive weathering implies deposition and oxidation under a warmer-than-present climate.
Quartermain II till Slump Mountain diamicton Arena till	> 11.3 Ma > 11.3 Ma > 11.3 Ma	Asgard till Jotunheim till Nibelungen till	> 13.6 Ma > 10.5 Ma > 13.6 Ma < 15.2 Ma	Initial buildup of the present East Antarctic Ice Sheet and glacial overriding of the western Dry Valleys region sometime between 13.6 and 15.2 Ma.
Undifferentiated colluvium	> 11.3 Ma	Undifferentiated colluvium	> 12.0 Ma < 13.6 Ma	Minor colluviation (under cold-desert conditions) after the demise of middle-Miocene ice-sheet overriding.
Brawhm/ Quartermain I tills	< 11.6 Ma > 7.4 Ma	Rock glacier deposits	< 12.5 Ma	Modest expansion of glacial ice. Thickening insufficient to allow penetration of inland ice into the western Asgard Range. The western Asgard Range valleys have remained free of inland ice for at least the last 12.5 Ma. However, because of the unique configuration and geographic position of Arena Valley with respect to Taylor and Ferrar Glaciers, modest expansion of these outlet glaciers resulted in overflow into upper and lower Arena Valley and deposition of Brawhm and Quartermain I tills. Cold-based glaciers in Arena Valley and in the western Asgard Range indicate persistent cold-desert conditions.
Taylor IVb / Alpine D Taylor IVa / Alpine C Taylor III / Alpine B Taylor II / Alpine A	< 7.4 Ma > 2.1 Ma[1] > 1.0 Ma[1] > 200 Ka[1] > 117 Ka[1]	Rock glacier deposits	< 12.5 Ma	Continued ice-free conditions in the western Asgard Range. Maximum Pliocene thickening of Taylor Glacier at the mouth of Arena Valley was only 475 m. Maximum Pliocene thickening of inland Taylor Dome (35 km west of Arena Valley) was most likely less than 250 m. Maximum Quaternary thickening of Taylor Dome was less than 160 m. Inland East Antarctic ice did not override the western Dry Valleys region during Pliocene-Pleistocene time.

[1] Ages of Taylor drifts based on exposure-age analyses in Brook and Kurz (1993) and Brook et al. (1993).

APPENDIX 1 $^{40}Ar/^{39}Ar$ Data

Sample	%^{39}Ar	$^{37}Ar/^{39}Ar$	$^{36}Ar/^{39}Ar$	$^{40}Ar^{*}/^{39}Ar$	%^{39}Ar	Age (Ma)	SD
ASH ON BURIED DESERT PAVEMENT							
DMS-8686B (Sanidine / 61A2)							
5075-01		0.0302	0.00023	0.8177	92.4	4.191	0.203
5075-02		0.0381	0.00020	0.8257	93.3	4.232	0.237
5075-03		0.0485	0.00001	0.8672	99.7	4.444	0.250
5075-04		0.0189	0.00032	0.8201	89.4	4.203	0.239
5075-05		0.0266	0.00052	0.8277	84.3	4.242	0.278
5075-06		0.0305	0.00019	0.8824	94.1	4.522	0.554
5075-07		0.0259	0.00005	0.8697	98.2	4.457	0.422
5075-08		0.0200	0.00015	0.8524	94.9	4.368	0.283
5075-09		0.0335	0.00027	0.8278	91.1	4.242	0.418
5075-10		0.0370	0.00031	0.8320	90.0	4.264	0.528
5075-11		0.0388	0.00013	0.8648	96.0	4.432	0.271
5075-12		0.0349	0.00023	0.8406	92.5	4.308	0.293
5075-13		0.0407	0.00018	0.8540	94.1	4.377	0.334
5075-14		0.0214	0.00021	0.8272	93.1	4.239	0.495
5075-15		0.0444	0.00003	0.8844	99.3	4.532	0.366
5075-16		0.0314	0.00009	0.8578	97.0	4.396	0.169
5075-17		0.0307	0.00008	0.8538	97.2	4.375	0.359
5075-18		0.0118	0.00025	0.8482	91.9	4.347	0.409
					Weighted Mean =	**4.33**	**± 0.07 SE**
UPPER ARENA VALLEY ASH AVALANCHE DEPOSIT							
DMF86-141 (Sanidine / 41B)							
3174-11		0.0312	0.00012	0.5948	94.3	6.341	0.188
3174-10		0.0177	0.00022	0.6052	90.3	6.452	0.316
3174-17		0.0602	0.00021	0.5854	90.8	6.241	1.009
					Weighted Mean =	**6.37**	**± 0.16 SE**
3174-14		0.4619	0.13965	29.1394	41.4	287.106	59.507
3174-22		0.5528	0.18004	43.5671	45.0	413.959	119.478
3174-21		0.0000	0.02415	383.9334	100.0	2139.044	44.623
DMF86-141 (Glass / 41B)							
5088-01A	4.2	0.1069	0.00612	1.4407	44.4	7.437	1.544
5088-01B	23.2	0.0873	0.00208	1.4215	70.0	7.338	0.260
5088-01C	33.4	0.0882	0.00121	1.4568	80.4	7.520	0.288
5088-01D	18.5	0.0899	0.00112	1.4396	81.5	7.266	0.287
5088-01E	17.8	0.0933	0.00288	1.4074	62.5	7.266	0.287
5088-01F	2.9	5.0740	0.00278	1.2476	74.0	6.442	1.517
					Plateau Age =	**7.38**	**± 0.14 SE**
DMS86-131 (Sanidine / 61B)							
5113-02		0.0448	0.00000	1.4809	100.0	7.444	0.676
5113-03		0.0378	0.00009	1.4396	98.1	7.237	1.051
5113-05		0.0435	0.00086	1.4823	85.4	7.451	0.489
5113-06		0.0322	0.00140	1.5301	78.7	7.691	0.761
5113-07		0.0413	0.00070	1.4200	87.3	7.138	0.787
					Weighted Mean =	**7.42**	**± 0.04 SE**
5113-04		0.0004	0.00013	1.7669	97.8	8.878	0.637
5113-01		0.0096	0.00012	1.9729	98.2	9.910	0.335

APPENDIX 1 $^{40}Ar/^{39}Ar$ Data (continued)

Sample	$\%^{39}Ar$	$^{37}Ar/^{39}Ar$	$^{36}Ar/^{39}Ar$	$^{40}Ar^*/^{39}Ar$	$\%^{39}Ar$	Age (Ma)	SD
LOWER ARENA VALLEY ASH AVALANCHE DEPOSIT							
DMS87-113 (Sanidine / 20)							
1794-01		0.1144	0.00175	4.2405	89.2	10.894	0.104
1794-08		0.0432	0.00078	4.4076	95.1	11.322	0.088
1794-02		0.1265	0.00102	4.4810	93.8	11.510	0.085
					Weighted Mean =	**11.28**	**± 0.05 SE**
1794-04		0.0643	0.00416	57.5321	97.9	142.476	0.576
1794-06		0.0340	0.00262	57.7051	98.7	142.888	0.440
1794-03		0.0174	0.00738	75.8994	97.2	185.690	0.334
1794-09		0.0176	0.00358	87.4462	98.8	212.337	0.365
1794-05		0.0365	0.00238	98.9741	99.3	238.553	0.799
1794-07		0.0313	0.01340	102.5835	96.3	246.683	0.846
DMS86-113 (Glass / 41B)							
5089-01A	0.5	0.2980	0.00081	2.8567	92.9	14.718	3.439
5089-01B	22.1	0.1209	0.00079	2.4965	91.7	12.369	0.146
5089-01C	54.4	0.1142	0.00031	2.5066	96.8	12.920	0.060
5089-01D	20.8	0.1366	0.00005	2.4822	99.7	12.795	0.141
5089-01E	2.0	0.4047	0.00079	2.3834	92.0	12.287	2.688
					Plateau Age =	**12.90**	**± 0.06 SE**
DMS86-110C (Sanidine / 41B)							
5107-01		0.0047	0.00037	1.6919	94.0	8.474	0.827
5107-02		0.0417	0.00050	1.6969	92.2	8.499	0.740
5107-03		0.0232	0.00061	1.6843	90.4	8.436	0.612
5107-04		0.0254	0.00030	1.7140	95.2	8.585	0.601
5107-05		0.0299	0.00032	1.6850	94.8	8.440	1.397
					Plateau Age =	**8.50**	**± 0.33 SE**

APPENDIX 1 $^{40}Ar/^{39}Ar$ Data (Continued)

Sample	$\%^{39}Ar$	$^{37}Ar/^{39}Ar$	$^{36}Ar/^{39}Ar$	$^{40}Ar^{*}/^{39}Ar$	$\%^{39}Ar$	Age (Ma)	SD
ASH DISSEMINATED IN QUATERMAIN 1 TILL							
DMS87-26 (Sanidine / 20)							
1789-01	0.0612	0.00340	4.0970	80.3	10.527	0.444
1789-04B	0.0594	0.00246	4.2367	85.4	10.885	0.244
1789-08	0.0306	0.00100	4.4163	93.8	11.345	0.156
1789-10	0.1089	0.00715	4.4398	67.8	11.405	0.904
1789-04	0.0325	0.00076	4.6559	95.4	11.958	0.309
				Weighted Mean	**= 11.27**	**± 0.12 SE**
1789-03	0.0251	0.02461	3.5761	33.0	9.192	1.038
1789-06	0.0415	0.00114	5.2939	94.0	13.590	0.577
1789-05	0.0159	0.00334	57.7469	98.3	142.987	0.478
1789-02	0.0254	0.00699	94.4336	97.9	228.273	0.679
1789-07	0.0391	0.00305	103.7365	99.1	249.273	0.521
1789-09	0.0415	0.00376	125.2737	99.1	296.973	0.570
1789-02B	0.0184	0.00276	125.6885	99.4	297.880	0.728
DMS87-27 (Sanidine / 20)						
1793-03	0.0490	0.00129	4.3313	91.9	11.127	0.138
1793-09	0.0707	0.00962	4.3942	60.8	11.288	0.266
1793-02	0.0351	0.00063	4.4788	96.0	11.504	0.138
1793-01	0.0538	0.00583	4.5054	72.4	11.573	0.267
1793-01B	0.0411	0.01545	4.6069	50.2	11.833	0.288
1793-05	0.0525	0.00032	4.6103	98.0	11.841	0.334
1793-03B	0.0895	-0.00023	4.6292	101.6	11.889	0.615
1793-04	0.0653	0.00054	4.6436	96.7	11.927	0.398
1793-10	0.0873	-0.00002	4.7163	100.2	12.112	0.143
				Weighted Mean	**= 11.59**	**± 0.07 SE**
1793-07	0.1241	0.00233	5.1453	88.3	13.210	0.197
1793-06	0.0522	0.28648	11.2848	11.8	28.847	1.788
1793-08	0.2024	3.23002	126.3656	11.7	299.358	504.924

All sanidine $^{40}Ar/^{39}Ar$ ages are total fusion analyses

Irradiation Data

20 J = 0.001428 ± 0.000001
41B J = 0.005920 ± 0.000009
61B J = 0.002783 ± 0.000002
61A2 J = 0.002844 ± 0.000004
98A J = 0.000478 ± 0.000001

CHAPTER SIX

Quaternary changes in level of the upper Taylor Glacier, Antarctica: implications for paleoclimate and East Antarctic Ice Sheet dynamics

ABSTRACT

Glacial drifts perched alongside outlet glaciers that drain through the Transantarctic Mountains constrain inland polar plateau ice elevations. The Taylor Glacier, which heads in the Taylor Dome (a peripheral dome of the East Antarctic Ice Sheet), drains East Antarctic ice into the Dry Valleys sector of Transantarctic Mountains and terminates in central Taylor Valley, about 24 km west of the Ross Sea. Five gravel-rich drifts (including 39 distinct moraine ridges) fringe a lateral lobe of the Taylor Glacier in the lower Arena Valley, Quartermain Mountains, southern Victoria Land. ^{3}He and ^{10}Be exposure age dating (from Brook *et al.* 1992), together with Arena Valley stratigraphy and soil morphologic data, provide chronologic control for these drifts and constrain maximum Quaternary thickening of the inland Taylor ice dome to less than 160 m. These minor Quaternary expansions of Taylor Glacier were out-of-phase with outlet glaciers that pass through the Transantarctic Mountains and terminate in the Ross Sea north and south of the Dry Valleys region. Textural analyses suggest that drift deposition occurred from cold-based ice, even though Taylor Glacier advances most likely occurred during global interglaciations. The thermal regime of former Taylor Glacier ice lobes, the character of geomorphic features superimposed on individual drifts, the chemical composition of soils developed on Taylor drifts, and the stability of in-situ moraine ridges on steep valley walls suggest that the present cold-desert climate in Arena Valley has persisted for at least the last 2.2 Ma.

INTRODUCTION

Quaternary East Antarctic Ice Sheet dynamics and paleoclimate are central to interpretations of coeval eustatic sea level and marine oxygen isotopes. Glacial drifts perched alongside outlet glaciers that drain through the Transantarctic Mountains limit changes in East Antarctic ice-surface elevation inland of the Transantarctic Mountains. Here we describe glacial drifts in the Arena Valley adjacent to the Taylor Glacier, an outlet glacier that drains Taylor Dome (a peripheral dome of the East Antarctic Ice Sheet) and terminates in the ice-free region of southern Victoria Land. Arena Valley is unique in the Transantarctic Mountains because it is adjacent to the western margin of the East Antarctic Ice Sheet and contains an extraordinarily complete sequence of glacial drifts representing former ice-sheet fluctuations.

Throughout late Quaternary time, Taylor Glacier terminated on land and did not merge with ice masses that periodically grounded in the Ross Sea (Denton *et al.* 1989a). Therefore, it is one of the few Transantarctic outlet glaciers that record fluctuations of East Antarctic ice independent of ice grounded in the Ross Sea. Thus, Quaternary fluctuations of Taylor Glacier reveal the relative timing of ice-level changes of Taylor Dome and ice

grounding in the Ross Sea (Denton *et al.* 1989a), constrain glacial overriding of the Transantarctic Mountains (Denton *et al.* 1984), monitor major East Antarctic Ice Sheet fluctuations along an ice divide that extends inland from Taylor Dome to Dome Circe (Drewry 1982), and bear on questions of regional paleoclimate. Our results are based on pedologic examination of 150 soil profiles along with geomorphic and glacial geologic mapping of 39 well-preserved moraines adjacent to a peripheral lobe of the present Taylor Glacier in Arena Valley. ^{3}He and ^{10}Be exposure age dating (Brook *et al.* 1992; Brown *et al.* 1991), along with Arena Valley stratigraphy and soil weathering data, provide chronologic control.

Physical Setting

The ice-free Dry Valleys region of southern Victoria Land feature about 4000 km^2 of high-relief desert topography on the east flank of the Transantarctic Mountains between the McMurdo Sound sector of the Ross Sea and the East Antarctic polar plateau (Fig. 1).

The Glaciers

The polar glaciers of southern Victoria Land are cold and predominantly dry based (Chinn 1980). They lack well-defined accumulation zones, show little to no surface melting, and are nowhere associated with widespread outwash sediments. Most of the Dry Valleys glaciers are strikingly free of surficial and basal debris and are nearly everywhere frozen to their bed. They occur in a cold-desert climate, where mean annual temperatures are well below -20°C and precipitation values are less than 45 mm water equivalent per year (Schwerdtfegger 1984). Robin (1988) calculated that the 0°C isotherm in the Dry Valleys region lies about 600 m below sea level. As a result, ablation in the present cold-desert climate occurs almost entirely by sublimation, with less than 10% derived from surface meltwater run-off (Chinn 1980). Thus, the geographic distribution of glacier accumulation and ablation zones is governed solely by local wind patterns and the resulting concentration of transient snow drifts in topographically favored areas and sporadic blue-ice sublimation patches in windswept zones (Chinn 1980). This is different from the situation on temperate glaciers where excess precipitation and extensive surface-melting zones control glacier accumulation and ablation (Sugden & John 1976). Hence, polar glaciers lack well defined equilibrium lines and, if present, such lines reflect only local wind patterns. They are not related to the position of the 0°C isotherm. In fact, the Taylor Glacier equilibrium line, as defined by the irregular geographic boundary between dry snow and blue ice on the glacier surface (Muller 1962; Robinson 1984), lies at about 2000 m elevation (Fig. 1), 2600 m above the 0°C isotherm, where mean annual temperatures approach -35°C.

The polar Taylor Glacier, which today drains an ice-surface of about 750 km^2 (Robinson 1984) originates in the peripheral Taylor Dome on the East Antarctic Plateau (Fig. 1). The bedrock-controlled Taylor Dome rises 100

m above the surrounding ice-sheet surface and merges with a broad ice divide that extends far inland to Dome Circe (Drewry 1982). Such an ice configuration indicates that Taylor Glacier monitors local ice-surface fluctuations of the Taylor Dome and suggests that it may also monitor major ice-sheet fluctuations along the ice divide between Dome Circe and Taylor Dome. The present Taylor Glacier is about 100 km long. Ablation on the upper Taylor Glacier is entirely from sublimation and averages about 0.18 m water equivalent $year^{-1}$ (measured at 1000 m elevation) (Robinson 1984). Dry based conditions exist at the base of the upper Taylor Glacier ablation zone, although about 50% of the lower ablation zone may be at the pressure melting point (Robinson 1984). Such pressure-melting zones are concentrated towards the Taylor Glacier center, where horizontal ice velocity and ice thickness are greatest (maximum Taylor Glacier horizontal velocity is 14.4 m $year^{-1}$. This figure is based on measured dislocation of surface stakes positioned along the Taylor Glacier center adjacent to Arena Valley (Robinson 1984)). Peripheral Taylor Glacier lobes that project outward from the main glacier trunk into tributary valleys are today entirely cold-based (Robinson 1984).

Arena Valley

Arena Valley, which lies in the Quartermain Mountains alongside the southern edge of the upper Taylor Glacier, is a small (2.5-5.0 km wide and 8 km long) and predominantly ice-free valley (Figs. 1 & 2). Its walls are well-developed rectilinear slopes cut in Beacon Supergroup sandstones and Ferrar Dolerite intrusives. Average valley floor elevations range between 1000 m and 1400 m. Mean annual temperatures approach -30° C. A cold-based peripheral lobe of the present Taylor Glacier extends about 0.5 km southward into the lower Arena Valley and terminates in a steep ice cliff about 25 m high. A remarkably well-preserved sequence of drifts with numerous arcuate moraines occurs alongside this Taylor Glacier lobe. The present ice-surface of Taylor Glacier at the mouth of Arena Valley is at about 1050 m elevation.

Glacial Deposits in the Lower Arena Valley

General Description

Two very different drift types crop out in the lower Arena Valley. Quartermain II drift, the oldest, is a highly dissected and eroded granite-rich drift that crops out in a mosaic of 1-1.5 m high patches separated by intervening sandstone bedrock hollows (Fig. 3, Marchant *et al.* 1993a). This unit pre-dates Quaternary time (see below) and may represent regional expansion of the East Antarctic Ice Sheet with possible glacial overriding of the Transantarctic Mountains (Marchant *et al.* 1993a). The second drift type, the subject of this paper, occurs as a series of loose and unconsolidated gravel-rich drifts that, in places, are superimposed on Quartermain II drift. These drifts, which contain numerous granite erratics, crop out between 1000 and 1500 m elevation in the lower Arena Valley. They include 39 arcuate moraines that project southward from the present Taylor Glacier lobe into the lower Arena Valley (Figs. 2 & 4). Moraines vary in size and shape from

continuous ridges up to 4 m high to narrow boulder-belt moraines composed of only a single arc of perched cobbles and boulders. The drifts rest cleanly on pre-existing morphologic features and unconsolidated sediments. They lack striated clasts and silt-sized matrix sediments. Instead, moraine ridges are composed predominantly of unsorted medium-to-coarse-grained sands and angular cobble and gravel-sized clasts of local Ferrar Dolerite and Beacon Supergroup sandstone. Many clasts within the drifts show desert varnish and/or well-preserved ventifacted facets, suggesting an episode(s) of previous subaerial exposure. There are no ice-marginal channels, kame terraces, or outwash trains associated with these drifts in lower Arena Valley.

Relative Chronology

The outcrop pattern, surface morphology, cross-cutting relations, and soil development within moraines allow separation of four distinct drifts. The four drifts are termed Taylor II, III, IVa, and IVb drifts (Fig. 4) (Denton *et al.* 1989a; Bockheim 1977, 1982; Brook *et al.* 1993; Brook & Kurz 1993). Below we describe first the general morphology of lower Arena Valley drifts and then outline soil development within each unit.

Geomorphological Data

The Taylor II drift crops out within 0.75 km of the present Taylor Glacier lobe in the lower Arena Valley and includes 15 well-preserved and continuous arcuate moraines between 1000 and 1200 m elevation (100-200 m above the edge of the present Taylor Glacier surface at the Arena Valley mouth). Sharp-crested moraines of the Taylor II drift stand 2-4 m in relief and are among the largest in the Arena Valley. Moraines nearest the Taylor ice lobe reflect the present outline of the glacier margin. The up-valley limit of Taylor II drift is delineated by a well-defined moraine ridge that rises over 4 meters above the valley floor (Fig. 5).

The Taylor III drift is comprised of only three discontinuous moraine segments that occur distal and parallel to Taylor II drift (Fig. 6). These three moraines, which crop out on the valley floor at between 100 m and 250 m elevation above the present Taylor Glacier surface at the Arena Valley mouth, show sharp ridge crests but have only 1-2 m of relief. Moraines drape across pre-existing topography and rest without modification on top of older Taylor IVa drift. In stratigraphic section, the contact between Taylor III drift and Taylor IVa drift is sharp. In one hand-dug excavation a buried in-situ desert pavement (composed of an interlocking mosaic of gravel and cobble-sized ventifacts) and relict soil horizon stratigraphically separates the Taylor III drift from underlying Taylor IVa drift (Bockheim, 1977, 1982).

Taylor IVa drift blankets most of the floor and walls of the lower Arena Valley and includes 16 low-relief moraines that crop out between 100 and 325 m elevation above the present Taylor Glacier surface at the Arena Valley mouth (Fig. 6). Taylor IVa drift rests without disturbance on pre-existing morphology of unconsolidated

colluvial deposits on the west wall of the lower Arena Valley. At one locality, the lobate morphology of an unconsolidated and silt-rich debris lobe in these colluvial deposits is clearly preserved beneath six separate moraines of Taylor IVa drift (Fig. 7). Granulometric analyses of matrix sediments from within Taylor IVa drift superimposed on this silt-rich debris lobe show only coarse-sandy textures (Table 1), and indicate that the advancing ice failed to erode and incorporate the underlying silt-rich sediments.

The Taylor IVb drift consists of eight linear boulder moraines that crop out in lower and central Arena Valley between 125 m and 475 m elevation above the Taylor Glacier (Figs. 3 & 6). These bouldery moraines lack matrix and each is comprised of only a single row of aligned boulders and cobbles. The up-valley limit of the Taylor IVb drift, which forms the outermost intact moraine loop in the lower Arena Valley, lies about 3.0 km south of the present Taylor Glacier (Fig 8). The Taylor IVb drift overlies eroded patches of Quartermain II drift and intervening hollows in sandstone bedrock along the east wall of the lower Arena Valley (Fig. 3). Quartermain II drift patches show a highly irregular outcrop pattern that represents post- or syndepositional erosion. Because continuous moraines of the Taylor IVb drift extend across the Quartermain II drift patches and the intervening sandstone hollows, without any modification of them, we suggest that the Taylor IVb drift postdates the deposition (and selective erosion) of the Quartermain II drift. On the basis of ^{3}He and ^{10}Be exposure-age dates on overlying Taylor IVb drift and on Quartermain II drift in central Arena Valley (Brook *et al.* 1993), we consider the Quartermain II drift to be pre-Quaternary in age (most likely at least 3 to 5 Ma in age, Table 2), and therefore do not address it further here.

In summary, Taylor II, III, IVa, and IVb drifts feature thin bouldery moraines (with a preponderance of gravel clasts exhibiting desert varnish and/or ventifacted facets), and rest without disturbance on the surface of pre-existing morphologic forms, relict soil horizons, and delicate in-situ desert pavements. They lack striated and polished clasts, fine-grained stratification, associated outwash trains, and/or other features indicating the presence of glacial meltwater. As such, these drifts are characteristic of sediments deposited from non-erosive cold-based ice. The lobate moraine morphology and proximity of drifts to the present Taylor Glacier ice lobe in lower Arena Valley suggest glacial deposition from an expanded cold-based lobe of the Taylor Glacier. The ubiquitous granite erratics also support deposition from the Taylor Glacier. For example, though numerous granite clasts occur in the lower Arena Valley, there are no such erratics in upper Arena Valley. This, along with the fact that Taylor Glacier today transports granite clasts (presumably eroded from granite bedrock exposed along the margins of the Taylor Glacier), strongly suggests that the Taylor II, III, IVa, and IVb drifts represent deposition from southward incursions of Taylor Glacier into the lower Arena Valley.

Soil Data

Soil morphological properties are uniform within individual drift sheets but show abrupt changes (in some cases order of magnitude changes) between mapped units.

The following soil morphological properties show major breaks at drift boundaries: depths of staining, coherence and matrix salts, salt stage, and weathering stage (Table 3). The staining is due to release of iron from weathering of mafic minerals present in the drifts. The accumulation of soluble salts enables the soils to become coherent at greater depths with increasing age. The accumulation of these salts is reflected by an increase in morphologic salt stage (Bockheim 1990) from salt encrustations beneath coarse fragments on Taylor II drift, to discrete aggregations of salts in Taylor III drift and eventually to strongly cemented salt pans in Taylor IVa drift.

There are insufficient data to draw any conclusive age-related trends in surface boulder weathering features, but the percentage of surface clasts that show desert varnish, ventifact development, spalling, and pitting appears to increase with relative drift ages (Table 4). The percentage of clasts showing ventifacted facets increases from about 1% on Taylor II drift to greater than 70% percent on Taylor III and older drifts. Clasts exhibiting desert varnish, which forms rapidly on the surface of exposed boulders under the cold desert weathering conditions prevalent in Arena Valley, increase from 80% on Taylor II drift to nearly 100% on Taylor III and older drifts.

Table 1 gives analytical data for representative soil profiles. All soils are slightly acid to neutral (Ph 6.2-7.2) due to the accumulation of soluble salts. Based on electrical conductivity values, the amount of water-soluble salts increases sharply from the Taylor III drift to the Taylor IVa drift. The dominant cation and anion in soil:water extracts from the soils are Na and NO3-, respectively. The presence of sodium nitrate is consistent with the ultraxerous nature of the soils in Arena Valley (Bockheim 1982; Campbell & Clairidge 1969). With the exception of soils in the Taylor II drift, ice cement was seldom observed. The ultraxerous soils of Arena Valley have dry permafrost because there is insufficient moisture to cause cementation (Bockheim 1982). All soils on Taylor II, III, and IVa drifts are skeletal (rock fragments greater than 2.0 mm in diameter comprise 35% or more of the profile by volume) with a loamy sand or sandy matrix.

The sharp breaks in soil development and in moraine morphology across drift boundaries, together with direct evidence for Taylor glacier readvance (Taylor III moraines overlie and cross-cut older Taylor IVa moraines) indicate that lower Arena Valley drifts represent distinct glacial advances and retreats of several Taylor Glacier lobes into the lower Arena Valley, rather than continual retreat of a single lobe.

Numerical Chronology

A numerical chronology for the Taylor II, III, IVa, IVb drifts, based on ^{3}He and ^{10}Be exposure age dates

(Brook *et al.* 1993; Brown *et al.* 1991) on surface clasts removed from the top of individual moraine crests corroborates our relative chronology from soil morphologic data. The numerical ages listed in Table 2 (from Brook *et al.* 1993) differentiate five drifts that range back through the Quaternary to at least late Pliocene time. The results show that Taylor II, III, and IVa are Quaternary-age drifts, whereas the Taylor IVb drift may be late Pliocene or older. (Preliminary age data from analyses of cosmogenic ^{21}Ne from quartz sandstones on Taylor IVb drift are consistent with ages derived from ^{10}Be analyses and indicate an exposure age of at least 2.2 Ma (Staudacher & Allegre 1991) (Table 2)). Quartermain II drift is older than 3 to 5 Ma. Taylor IVa drift, the oldest Quaternary-age drift in Arena Valley, represents the maximum advance of the Taylor Glacier in the last 1.1 Ma (Table 2). An important point is that all the drift sheets in lower Arena Valley predate late Wisconsin time. There are no glacial deposits coeval with the last major global glaciation (Stage 2) in the lower Arena Valley (see discussion below).

Discussion

Ice Dynamics

Taylor Glacier. The outcrop patterns, sediment textures, stratigraphic relationships, and granite erratics within the Taylor II, III, IVa, and IVb drifts suggest glacial deposition from successive expansions of a cold-based Taylor Glacier ice lobe into the lower Arena Valley. Figure 8 shows longitudinal ice-surface profiles of former and present Taylor ice lobes in lower Arena Valley. Such profiles reflect outcrop elevations of individual drift sheets and outer moraine ridges. Measured ice-surface profiles along with exposure-age data indicate that the maximum Quaternary thickening of Taylor Glacier, represented by the Taylor IVa drift, was only about 325 m above the present Taylor Glacier ice-surface at the Arena Valley mouth. Because former Taylor Glacier ice lobes in the lower Arena Valley were situated within the Taylor Glacier ablation zone (where ice-surface thickening in response to glacial advance exceeds coeval ice-thickening in the accumulation area (Nye 1960)), we argue that maximum Quaternary thickening of the *Taylor Dome* (35 km west of Arena Valley) was probably much less than the 325 m rise in the Taylor Glacier in the lower Arena Valley (as measured from the distribution of Taylor IVa moraines in the lower Arena Valley). Following procedures outlined in Nye (1960), we calculate that maximum thickening of Taylor Dome during Quaternary time would be about one-half of that observed in Arena Valley, or about 160 m.

Figure 9 shows numerical reconstructions of the Taylor Glacier and inland Taylor Dome assuming (1) plastic flow and (2) a flow law with n= 4.2 (Robinson 1984). Reconstructions that assume plastic flow closely approximate the present ice-surface profile of Taylor Glacier and show that a 325 m thickening at Arena Valley yields a corresponding ice-surface rise at Taylor Dome of about 160 m. Because Taylor Glacier narrows dramatically as it enters Taylor Valley (Fig. 1), we argue, on the basis of mass conservation (i.e. Furbish &

Andrews 1984), that significant ice thickening in the ablation zone could result from only slight thickening in the accumulation zone. As such, maximum Quaternary thickening of the Taylor Dome was most probably less than our calculated maximum estimate of 160 m. These results are consistent with limited late Quaternary interior ice-sheet fluctuations prescribed by ice-core studies (Lorius *et al.* 1984, 1985) and glacial geologic data (Denton *et al.* 1989a; Bockheim *et al.* 1989).

^{3}He and ^{10}Be exposure ages listed in Table 2 show that Taylor II, III, IVa, and IVb drifts all antedate late Wisconsin time. Accordingly, we argue that during late Wisconsin time Taylor Glacier was no larger, and perhaps even slightly smaller, than its present size. Data from outside the Arena Valley show that Taylor Glacier is now at its maximum position since late Wisconsin time, with the exception of minor fluctuations delineated by small Holocene-age ice-cored moraines that occur sporadically alongside the margin of Taylor Glacier (Denton *et al.* 1971, 1989a).

Correlation of lower Arena Valley drifts with glacial deposits exposed elsewhere in ice-free regions alongside the present Taylor Glacier allow construction of longitudinal ice-surface profiles of former Taylor Glaciers and, in certain instances, reveal the relative phasing of Ross Sea glaciations and Taylor Glacier fluctuations during late Quaternary time (Denton *et al.* 1989a). For example, on the basis of soil morphological properties and isotopic dating, Denton *et al.* (1989a) correlated Bonney Drift (a widespread silt-rich drift that crops out along the floor and walls of central Taylor Valley up to 300 m above the present Taylor Glacier surface) with Taylor II drift in lower Arena Valley. Bonney Drift, in turn, is cut by Ross Sea Drift in lower Taylor Valley (Ross Sea Drift represents expansion of grounded ice in the Ross Sea, with ice tongues flowing westward into dry valleys facing McMurdo Sound (Denton *et al.* 1989a)). On the basis of (1) numerous ^{14}C dates from algae associated with Ross Sea drift, (2) cross-cutting relationships between Bonney and Ross Sea Drift, and (3) U/Th dates on carbonates deposited in lakes dammed alongside the Taylor Glacier during its Bonney advance (Hendy *et al.* 1979), Denton *et al.* (1989a) argued that the most recent expansion of grounded ice in the Ross Sea occurred during the last major global glaciation (Stage 2 of the marine oxygen-isotope record), whereas the most recent advance of Taylor Glacier (represented by Bonney Drift /Taylor II drift) occurred during the last major global interglaciation (Stage 5.5). This age assignment for Bonney Drift/ Taylor II drift is in accord with exposure-age data from Arena Valley (Table 2) (Brook *et al.* 1993) and shows that Taylor Glacier expansion occurred out-of-phase with the last Ross Sea glaciation during late Wisconsin time. By extension, we suggest that the Taylor III, IVa, and IVb drifts represent Taylor Glacier expansion during global interglaciations preceding Stage 5.5 However, our present chronology does not permit detailed correlations with specific global interglaciations.

Other Transantarctic outlet glaciers. Thin and unconsolidated gravel-rich drifts are widespread in ice-free areas alongside the Beardmore, Hatherton, Darwin, and Reedy Glaciers (Mercer 1972; Mayeski 1975; Denton *et al.* 1989b; Bockheim *et al.* 1989). All of these outlet glaciers, which drain East Antarctic polar plateau ice through the Transantarctic Mountains, are different from the Taylor Glacier in that they flow directly into the Ross Ice Shelf and do not terminate on land. Soil data show significant differences in soil morphological properties between the youngest drifts alongside Beardmore, Hatherton, Darwin, and Reedy Glaciers and the youngest drift (Bonney Drift/Taylor II drift) alongside Taylor Glacier (Denton *et al.* 1989a, 1989b; Bockheim *et al.* 1989). Bonney Drift/Taylor II drift show moderate weathering consistent with deposition sometime during Stage 5.5 time, whereas the youngest drifts alongside Beardmore, Hatherton, Darwin, and Reedy Glaciers show only very slight surface and internal weathering and are most probably late Wisconsin in age (Denton *et al.* 1989a, 1989b; Bockheim *et al.* 1989). This suggests that Taylor Glacier fluctuated asynchronously with these outlet glaciers during late Quaternary time. The out-of-phase behavior most likely reflects grounding of a late Wisconsin ice sheet in the Ross Sea that dammed outflow of Beardmore, Hatherton, Darwin, and Reedy Glaciers but failed to effect the fully terrestrial Taylor Glacier (Denton *et al.* 1989a, 1989b; Bockheim *et al.* 1989). The effect of a grounded ice sheet in the Ross Sea would most likely result in thickening along the middle and lower reaches of dammed outlet glaciers (if sufficient time elapsed between ice build-up and ice retreat). Because Taylor Glacier failed to merge with Ross Sea ice during late Quaternary time, it could fluctuate independently of ice-shelf grounding episodes in the Ross Sea. Major changes in eustatic sea level caused by the waxing and waning of Northern Hemisphere ice sheets are the most likely cause of ice-sheet grounding in the Ross Sea (Hollin 1962; Stuiver *et al.* 1981). The exact mechanism for Taylor Glacier expansion and contraction during interglacial and glacial conditions is unknown. One possibility is that expansion occurs during episodes of increased precipitation triggered by diminished ice in the Ross Sea (Denton *et al.* 1989a).

The above data implies that glaciers in the Transantarctic Mountains which failed to merge with expanded Ross Sea ice during late Quaternary time fluctuated out-of-phase with grounded ice in the Ross Sea. However, recent data suggest that alpine and plateau glaciers within the mountains of northern Victoria Land advanced in phase with the most recent episode of ice-sheet grounding in the Ross Embayment (Orombelli *et al.* 1991). Because alpine glacier fluctuations in the Transantarctic Mountains appear originate from changes in local precipitation, the data from northern Victoria Land suggest a more complex interplay among local precipitation changes, grounding episodes in the Ross Sea, and fluctuations of alpine and plateau glaciers in the Transantarctic Mountains than has been previously suggested.

Quaternary Paleoclimate

The climate of the Arena Valley during the Quaternary is inferred from (1) the thermal regime of expanded

Taylor Glacier ice lobes, (2) the character of geomorphic features superimposed on individual drifts and nearby unconsolidated diamictons, (3) the chemical composition of soils developed within Taylor II, III, and IVa drifts and, (4) the stability of in-situ moraine ridges on steep valley slopes.

The preservation of loose and unconsolidated sediments, in-situ desert pavements, and relict soil horizons beneath lower Arena Valley drifts suggests deposition from non-erosive cold-based ice. The persistence of thin, Quaternary cold-based ice tongues precludes significant warmth in the Arena Valley, even though Taylor Glacier expansions most probably occurred during global interglaciations. These data indicate that basal ice temperatures within Taylor Glacier lobes in Arena Valley remained below 0° C.

The striking absence of outwash sediments, lacustrine deposits, kame terraces, ice-marginal channels, or other glacio-fluvial/waterlain sediments in the lower Arena Valley indicates that here Quaternary Taylor Glacier ice lobes failed to develop extensive surface-melting ablation zones. Because such surface-melting ablation zones only develop on glaciers that occur near the 0°C isotherm, the lack of outwash or other meltwater features in the lower Arena Valley indicate that throughout the Quaternary the atmospheric 0°C isotherm failed to advance up to 1000 m elevation in the Quartermain Mountains.

A simple calculation shows the maximum allowable mean-annual atmospheric temperature rise in the Arena Valley during Quaternary time. In order to produce temperate-style surface-melting ablation zones near the mouth of Arena Valley the 0°C isotherm (which now theoretically lies about 600 m below sea level in the vicinity of the Quartermain Mountains (Robin 1988)) would have to rise up to at least 1000 m elevation. A 1600 m rise in the 0°C isotherm (sufficient to initiate Taylor Glacier surface melting-ablation zones at 1000 m elevation near the mouth of Arena Valley) corresponds to a rise in atmospheric temperature between 8°C and 22°C over the entire Dry Valleys region, assuming calculated Antarctic surface lapse rates (Fortuin & Oerlemans 1990) between 0.5°C and 1.4°C per 100 m elevation rise, respectively. These figures greatly exceed estimated Quaternary temperatures prescribed by ice-core data, which show similar (or below present) atmospheric temperatures for East Antarctica during late Quaternary time (Lorius *et al.* 1984, 1985).

Our estimates of maximum allowable Quaternary temperature in the Arena Valley are reduced dramatically if we consider that small ice-marginal lakes and surficial geomorphic features characteristic of liquid water (rills, levees, and stream channels) are common below 800 m elevation in the vicinity of the Quartermain Mountains (where minor surface melting accounts for about 10% of the total ablation (Chinn 1980)). The mean annual temperature near Arena Valley approaches -27°C. This estimate is based on a recorded mean annual temperature of -19.8°C at about 100 m elevation at nearby Lake Vanda (Schwerdtfeger 1984) and an average

lapse rate of 1.0°C/100 m elevation rise (Robin 1988). Landscape analyses show that surficial sediments in lower Arena Valley are unmarked by rills, levees, stream channels, lacustrine sediments, and/or other geomorphic features indicative of liquid water (e.g. Marchant *et al.* 1993a, 1993b). Hence, we conclude that the mean annual temperature in lower Arena Valley failed to rise above about -27°C during the Quaternary. This of course assumes that geomorphic features indicative of liquid water would be preserved in the Arena Valley record. Because the present mean annual temperature in the lower Arena Valley approaches -30°C, we suggest that the maximum allowable Quaternary temperature rise in Arena Valley is about 3°C, although we see no direct evidence in the record for warmer-than-present temperatures during the Quaternary.

The chemistry of soil:water extracts from Taylor II, III, and IVa drifts also bears on the Quaternary climate in the Arena Valley. Soils on all of the moraines are enriched in sodium nitrate, a salt which is common in ultraxerous soils along the polar plateau (Claridge & Campbell 1977). Soils in less arid regions of Antarctica (e.g. xerous and subxerous climatic zones), contain primarily sulfates and chlorides, respectively, that originate from marine sources. The sodium nitrate that is present in ultraxerous soils is derived from sublimation of snow blown in from the polar plateau. The salts infiltrate into the soil during occasional periods of minor snowmelt on the surface of dark-colored rocks (black body radiation) but tend to accumulate in the upper 25 cm of the profile. Therefore, the presence of sodium nitrate and accumulation of salts in the upper 25 cm of the profile in all of the soils examined attest to the persistence of an ultraxerous climate in Arena Valley during Quaternary time.

Finally, the presence of in-situ moraine ridges on steep valley walls (28° to 33°) implies little or no slope development in the lower Arena Valley for at least the last 2.2 Ma (age of Taylor IVb drift). Otherwise, the moraine ridges and boulder belts of Quaternary and late Pliocene age would be eroded or buried beneath younger colluvial deposits, which we show here is not the case. Such slope stability is best explained by persistent cold-desert conditions similar to the present Dry Valleys climate. We suggest that maximum temperatures in the lower Arena Valley (since at least 2.2 Ma) remained well below 0°C, inhibiting talus and slope development from freeze-thaw mechanisms.

Conclusions

Taylor Glacier fluctuations were minor during the Quaternary. The age and upper elevation of Taylor IVa drift indicate that the maximum Quaternary thickening of Taylor Glacier at the mouth of lower Arena Valley was only about 325 m. Our numerical modeling of upper Taylor Glacier (Fig. 10, based in part on reconstructed ice-surface profiles from the Arena Valley) shows that the maximum Quaternary rise of Taylor Dome at the head of Taylor Glacier was considerably less than 325 m, and most likely less than 160 m. This implies that

Taylor Dome was not overwhelmed by inland ice and calls for very restricted Quaternary interior East Antarctic Ice Sheet thickening of Taylor Dome and the inland ice divide. This conclusion is consistent with limited late Quaternary interior ice-sheet fluctuations prescribed by ice-core studies (Lorius *et al.* 1984, 1985).

Late Quaternary Taylor Glacier fluctuations were out-of-phase with Transantarctic outlet glaciers that terminated in the Ross Sea. During late Quaternary time, the Taylor Glacier failed to advance while the Beardmore, Hatherton, Darwin, and Reedy Glaciers thickened along their middle and lower reaches (Denton *et al.* 1989a, 1989b; Bockheim *et al.* 1989). This asynchronous behavior most likely reflects grounding of a late Wisconsin ice sheet in the Ross Sea that dammed outflow of glaciers with marine components but failed to effect the fully terrestrial Taylor Glacier (Denton *et al.* 1989a; 1989b). Emerging data from northern Victoria Land (Orombelli *et al.* 1991) suggest a more complex interplay between grounding episodes in the Ross Sea and thickening of outlet glaciers draining ice across the Transantarctic Mountains. Our data indicates that Taylor Glacier advanced during the last major global interglaciation (probably Stage 5.5) (Taylor II drift/Bonney Drift) and may be expanding during the present interglaciation.

The present cold-desert climate in Arena Valley has persisted throughout the Quaternary. The absence of surficial geomorphic features indicative of liquid water in Arena Valley, which are common below 800 m elevation in the Dry Valleys region, suggest that mean annual air temperatures in the Arena Valley failed to rise above -27°C during the last 2.2 Ma (present mean annual temperature in Arena Valley approaches -30°C). The absence of outwash trains, lacustrine sediments, and ice-marginal channels associated with Taylor Glacier lobes in the Arena Valley and the presence of ubiquitous ultraxerous soils and in-situ moraine ridges on steep valley slopes are consistent with persistent cold-desert climates during the Quaternary. This conclusion is in accord with interpretations for a Pliocene-age volcanic ash overlying an in-situ desert pavement in central Arena Valley (3 km south of the Taylor IVb drift limit) suggesting persistent cold-desert conditions in Arena Valley for the last 4.3 Ma (Marchant *et al.* 1993b).

REFERENCES

American Public Health Association, American Water Works Association, Water Pollution Control Federation. 1975: Standard methods for the examination of water and wastewater, 14th ed.

Bockheim, J.G. 1982: Properties of a chronosequence of ultraxerous soils in the Transantarctic Mountains. Geoderma 28, 239-255.

Bockheim, J.G. 1977: Soil development in Taylor Valley and McMurdo Sound area. Antarctic Journal of the United States 12, 105-108.

Bockheim, J.G., Wilson, S.C. Denton, G.H., Anderson, B.G. & Stuiver, M. 1989: Late Quaternary ice surface fluctuations of Hatherton Glacier, Transantarctic Mountains. Quaternary Research 31, 229-254.

Bockheim, J.G. 1990: Soil development rates in the Transantarctic Mountains. Geoderma 47, 59-77.

Bockheim, J.G. & Ugolini, F.C. 1990: A review of pedogenic zonation in well-drained soils of the southern circumpolar region. Quaternary Research 34, 47-66.

Brook, E.J., Kurz, M.D., Ackert, R.P. Jr, Denton. G.H., Brown, E.T., Raisbeck G.M. & Yiou, F. 1992: Chronology of Taylor Glacier advances in Arena Valley, Antarctica, using in-situ cosmogenic ^{3}He and ^{10}Be. Quaternary Research 39, 11-23.

Brook, E.J. & Kurz, M.D. 1993: Using in-situ ^{3}He in Antarctic quartz sandstone boulders for surface-exposure chronology. Quaternary Research 39, 1-10.

Brown, E.T., Edmond, J.M., Raisbeck, G.M., Yiou, F., Kurz, M.D. & Brook, E.J. 1991: Examination of surface exposure ages of Antarctic moraines using in-situ produced ^{10}Be and ^{26}Al Geochimica Cosmochimica Acta 55, 2269-2284.

Campbell, I.B. & Claridge, G.G.C. 1969: A classification of frigic soils - The zonal soils of the Antarctic continent. Soil Science 107, 75-85.

Campbell, I.B. & Claridge, G.G.C. 1975: Morphology and age relationships of Antarctic soils. In Suggate, R.P. & Cresswell, M.M. (eds.): Quaternary Studies, 83-88. The Royal Society of New Zealand, Wellington.

Claridge, G.G.C. & Campbell, I.B. 1977: The salts in Antarctic soils, their distribution and relationship to soil processes. Soil Science 123, 377-384.

Denton, G.H. Armstrong, R.L. & Stuiver, M. 1971: The late Cenozoic glacial history of Antarctica. In Turekian, K.K. (ed.): The late Cenozoic glacial ages, 267-306. Yale University Press, New Haven CT.

Denton, G.H., Prentice, M.L., Kellogg, D.E. & Kellogg, T.B. 1984: Late Tertiary history of the Antarctic ice-sheet: Evidence from the Dry Valleys. Geology 12, 263-267.

Denton, G.H., Bockheim, J.G., Wilson, S.C. & Stuiver, M. 1989a: Late Wisconsin and early Holocene glacial

history inner Ross Embayment, Antarctica. Quaternary Research 31, 151-182.

Denton, G.H., Bockheim, J.G., Wilson, S.C., Leide, J.E. & Anderson, B.G. 1989b: Late Quaternary ice-surface fluctuations of Beardmore Glacier, Transantarctic Mountains. Quaternary Research 31, 183-209.

Drewry, D.J. 1982: Ice flow, bedrock, and geothermal studies from radio-echo sounding inland of McMurdo Sound, Antarctica. In Cradock, C. (ed.): Antarctic Geoscience, 977-983. University of Wisconsin Press, Madison.

Fortuin, J.P.F. & Oerlemans, J. 1990: Paremeterization of the annual surface temperature and mass-balance of Antarctica. Annals of Glaciology 14, 78-84.

Furbish, D.J. & Andrews, J.T. 1984: The use of hypsometry to indicate long-term stability and response of valley glaciers to changes in mass transfer. Journal of Glaciology 30, 199-211.

Hendy, C.H., Healy, T.R., Rayner, E.M., Shaw, J. & Wilson, A.T. 1979: Late Pleistocene glacial chronology of the Taylor Valley, Antarctica, and the global climate. Quaternary Research 11, 172-184.

Hollin, H.T. 1962: On the glacial history of Antarctica. Journal of Glaciology 4, 173-195.

Lorius, C., Raunaud, D., Petit, J.R., Jouzel, J. & Merlivat, L. 1984: Late glacial maximum Holocene atmospheric and ice thickness changes from Antarctic ice core studies. Annals of glaciology 5, 88-94.

Lorius, C., Jouzel, J., Ritz, C., Merlivat, L., Barxov, N.I., Korotkevich, Y.S. & Kotlyakov, V.M. 1985: a 150,000 year climatic record from Antarctic ice core studies. Nature 316, 591-596.

Marchant, D.R., Denton, G.H., Sugden, D.E. & Swisher, C.C. III. 1993a: Miocene-Pliocene-Pleistocene stratigraphy and landscape evolution of Arena Valley, Quartermain Mountains, Antarctica. Geographiska Annaler, In the press.

Marchant, D.R., Swisher, C.C. III, Lux, D.P., West, D.P. Jr. & Denton, G.H. 1993b: Pliocene paleoclimate and East Antarctic Ice Sheet history from surficial ash deposits. Science 260, 667-670.

Mayewski, P.A. 1975: Glacial geology and late Cenozoic history of the Transantarctic Mountains, Antarctica. Institute for Polar Studies Research Report. no. 56.

Mehra, O.P. & Jackson, M.L. 1960: Iron oxide removal from soils and clays by a dithionite-citrate system buffered with sodium bicarbonate. Clays and Clay Mineralogy 7, 317-327.

Mercer, J.H. 1972: Some observations on the glacial geology of the Beardmore Glacier area. In Adie, R.J. (ed.):Antarctic Geology and Geophysics, 427-433. Universitetsforlaget, Oslo.

Muller, F. 1962. Zonation in the accumulation area of the glaciers of Axel Heiberg Island, N.W.T., Canada. Journal of Glaciology 4, No. 33, 302-311.

Nye, J.F. 1960: The response of glaciers and ice-sheets to seasonal and climatic change Proceedings of Royal Society 256 (A), 559-584.

Orembelli G., Baroni, C. & Denton, G.H. 1991: Late Cenozoic glacial history of the Terra Nova Bay region, Northern Victoria Land, Antarctica. Geografia Fisica e Dinamica Quaternaria 13, 139-163.

Paterson, W.S.B. 1969: The Physics of Glaciers. 385 pp. Pergamon Press, London.

Robin, G. de Q. 1988: The Antarctic Ice Sheet, its history and response to sea level and climatic changes over the past 100 million years. Paleogeography, Paleoclimatology, Paleoecology 67, 31-50.

Robinson, P.H. 1984: Ice dynamics and thermal regime of Taylor Glacier, south Victoria Land, Antarctica. Jour. of Glaciology 30, 153-160.

Schwerdtfeger, W. 1984: Weather and climate of the Antarctic. In Developments in Atmospheric Science 15. Elsevier Publishing Co., Amsterdam.

Staudacher, T. & Allegre, C.J. 1991: Cosmogenic neon in ultramafic nodules from Asia and in quartzite from Antarctica. Earth and Planetary Science Letters 106, 87-102.

Stuiver, M., Denton, G.H., Hughes, T.J. & Fastook, J.L. 1981: History of the marine ice-sheet in West Antarctica during the last glaciation, a working hypothesis. In Denton, G.H. & Hughes, T.J. (eds.): The last great ice sheets, 391-436. Wiley-Interscience, New York.

Wilch, T. 1991: $^{39}Ar/^{40}Ar$ chronology of volcanic rocks interbedded with glacial drifts, Taylor Valley, Antarctica: implications for Pliocene behavior of the East Antarctic Ice Sheet. Unpublished MS thesis, University of Maine, Orono, ME.

Figure captions

Figure 1. Location map showing ice-free Dry Valleys and present Taylor Glacier. The polar equilibrium line (EL), as defined by the irregular geographic boundary between dry snow and blue ice on the glacier surface (Muller 1962), lies at about 2000 m elevation (Robinson 1984).

Figure 2. High-elevation oblique aerial photograph of lower Arena Valley, showing the Taylor and Ferrar Glaciers, the Asgard Range, and the Kukri Hills. (US Navy VXE-6 photograph, TMA 2448, no. 0224, F-33).

Figure 3. East wall of lower Arena Valley showing etched and eroded patches of Quartermain II drift (upper limit arrowed) and intervening sandstone bedrock (Arena Sandstone) hollows. The upper limit of Taylor IVb moraines (arrowed) lies at about 1500 m elevation. Note that Taylor IVb moraines extend across Quartermain II drift patches and intervening bedrock hollows without modification.

Figure 4. Taylor moraines in lower Arena Valley. S-82-20 and other numbers refer to soil pit localities. Bold lines on map mark upvalley limit of Taylor II and Taylor IVa moraines. Taylor III moraines are superimposed on Taylor IVa drift and moraines.

Figure 5. Outer limit of Taylor II moraines in lower Arena Valley. Note figure (circled in black) for scale.

Figure 6. Oblique aerial photograph of the lower Arena Valley, showing distribution of Taylor II, III, IVa, and IVb drifts as well as Quartermain II drift. Arrows define the upper limit of Taylor II and IVb drifts, and point out two of the three moraines that crop out on the floor of lower Arena Valley and comprise Taylor III drift. Most of the moraines shown on the valley floor are composed of Taylor IVa drift.

Figure 7. Oblique aerial view of the lower Arena Valley showing an avalanche deposit overlain by Taylor IVa drift. The geomorphic form of the avalanche deposit is preserved beneath Taylor IVa drift.

Figure 8. Longitudinal profile of the lower Arena Valley and former ice-surface elevations of the Taylor Glacier. Inset shows location of cross-section.

Figure 9. Present and former ice-surface profiles for Taylor Glacier. Glaciological models that assume plastic flow closely approximate the present ice-surface profile of Taylor Glacier and show that a 325 m ice-surface elevation rise of Taylor Glacier at the mouth of Arena Valley yields a corresponding ice-surface rise at Taylor Dome of only about 160 m.

Tables

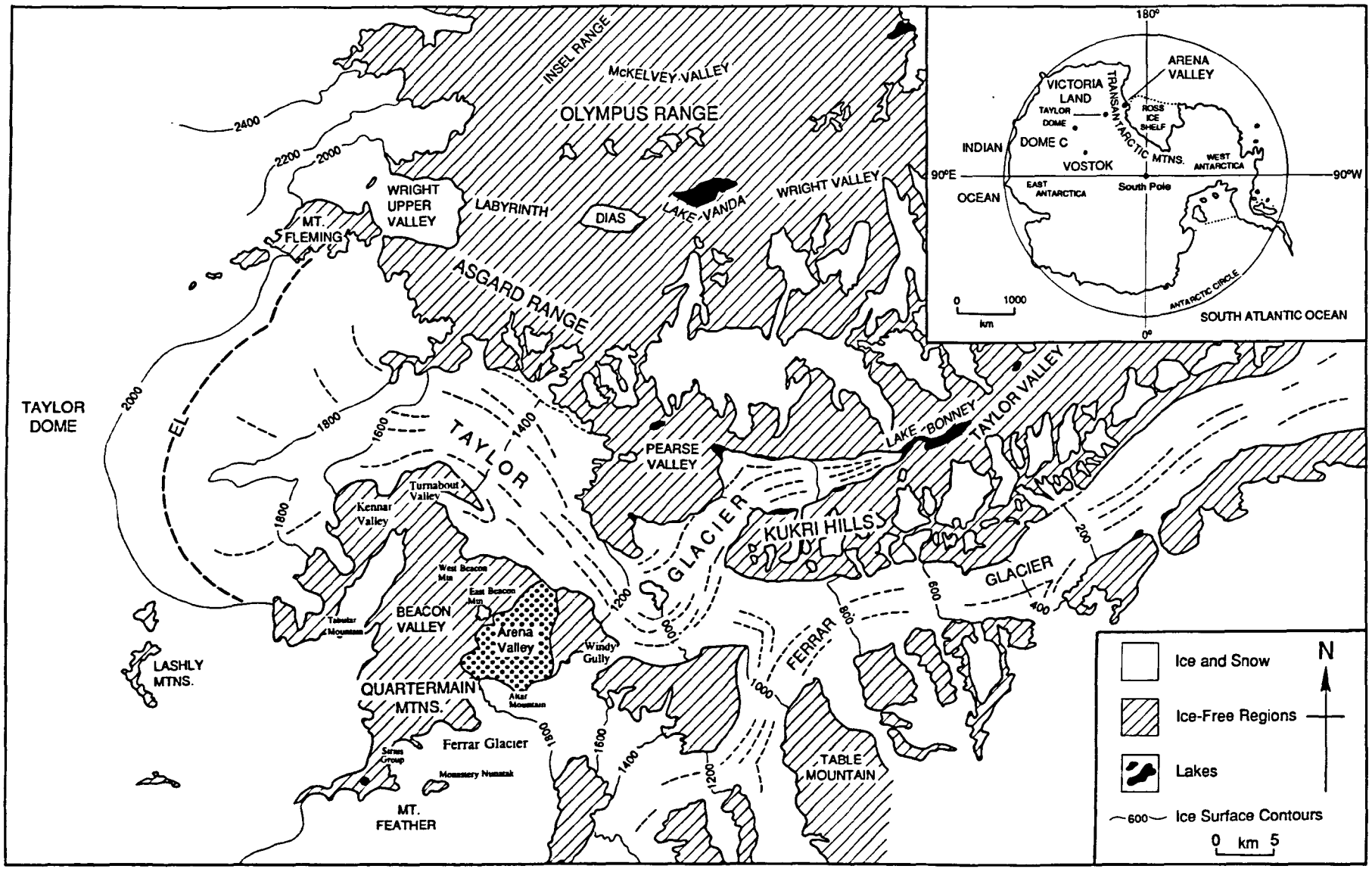

Figure 1. Location map showing ice-free Dry Valleys and present Taylor Glacier. The polar equilibrium line (EL), as defined by the irregular geographic boundary between dry snow and blue ice on the glacier surface (Muller 1962), lies at about 2000 m elevation (Robinson 1984).

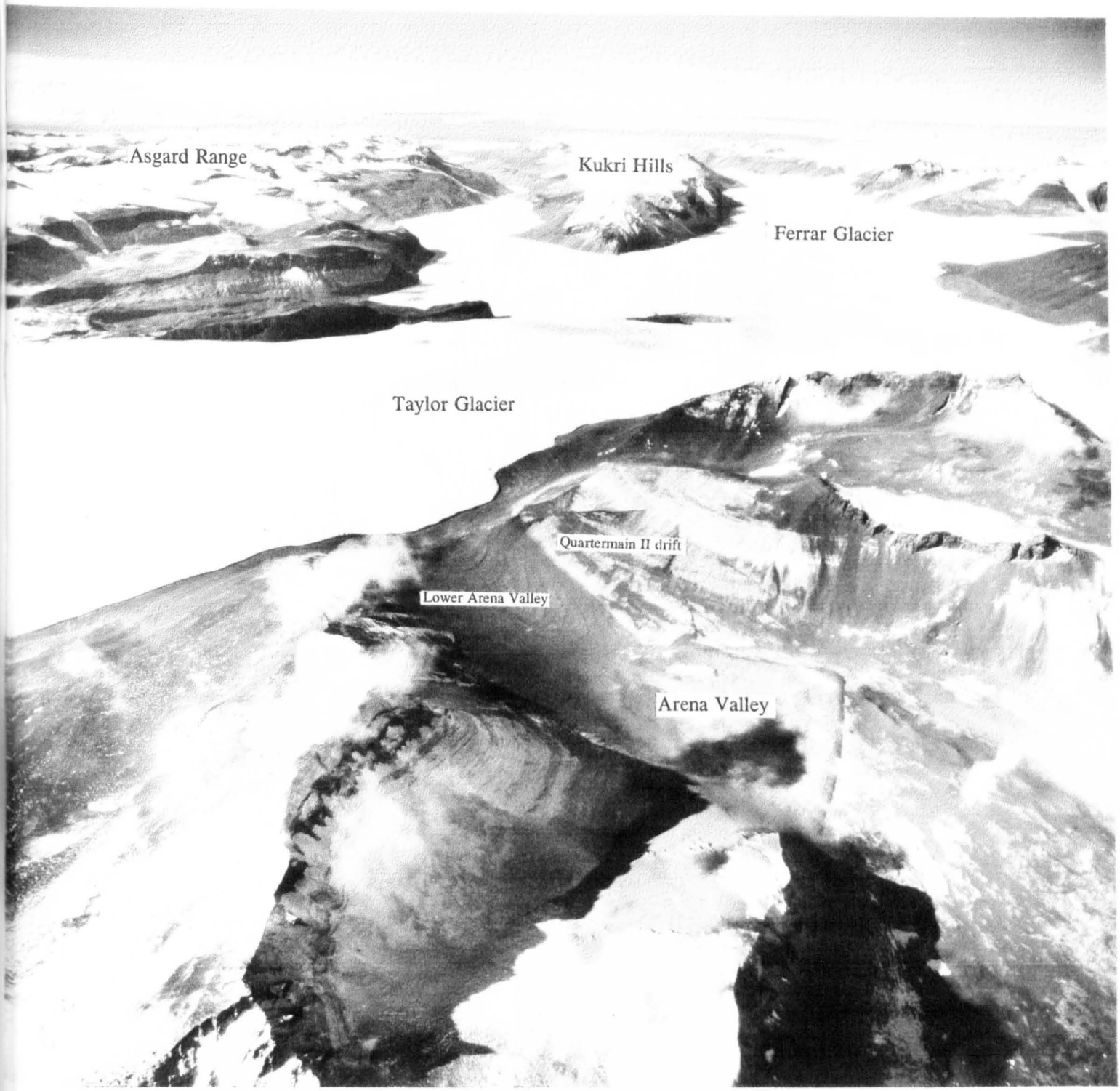

Figure 2. High-elevation oblique aerial photograph of lower Arena Valley, showing the Taylor and Ferrar Glaciers, the Asgard Range, and the Kukri Hills. (US Navy VXE-6 photograph, TMA 2448, no. 0224, F-33).

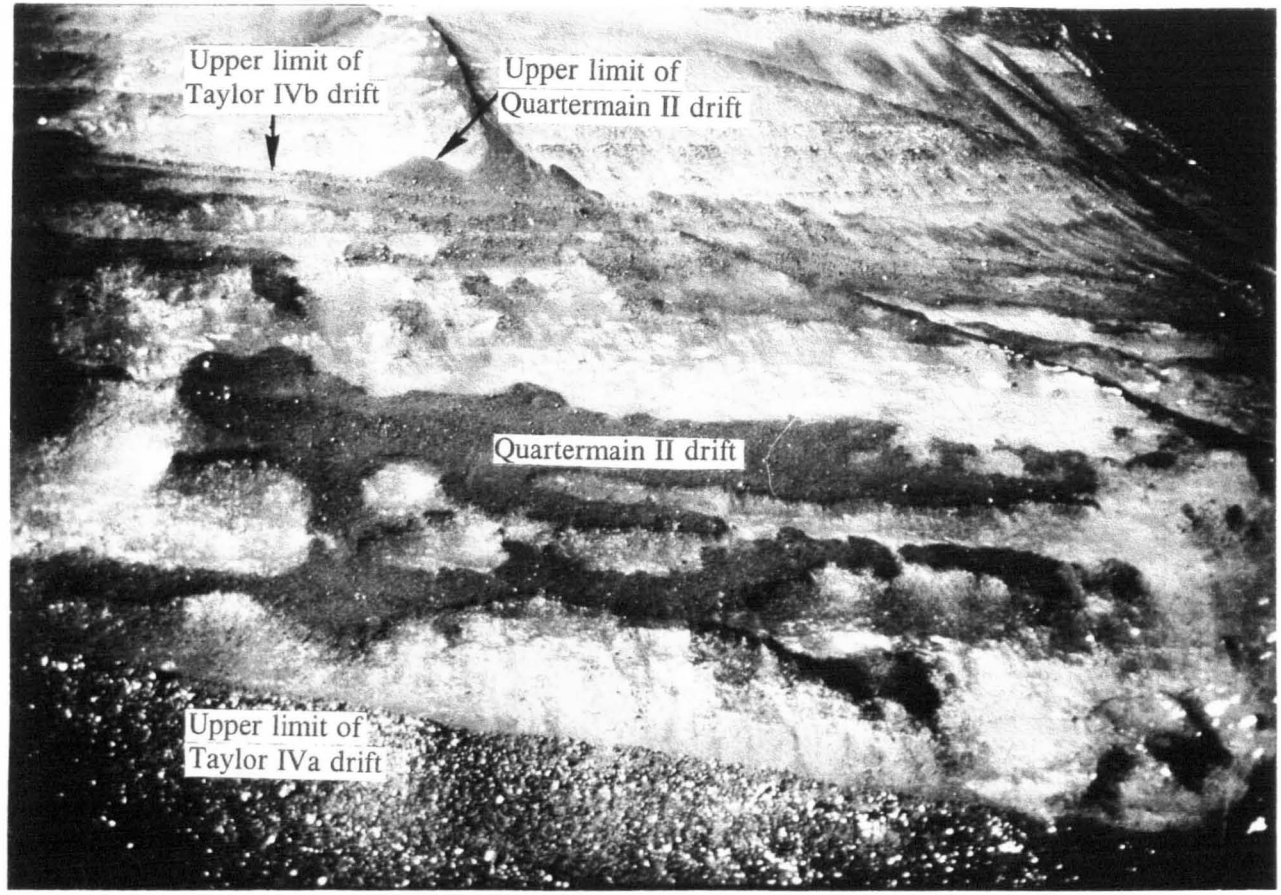

Figure 3. East wall of lower Arena Valley showing etched and eroded patches of Quartermain II drift (upper limit arrowed) and intervening sandstone bedrock (Arena Sandstone) hollows. The upper limit of Taylor IVb moraines (arrowed) lies at about 1500 m elevation. Note that Taylor IVb moraines extend across Quartermain II drift patches and intervening bedrock hollows without modification.

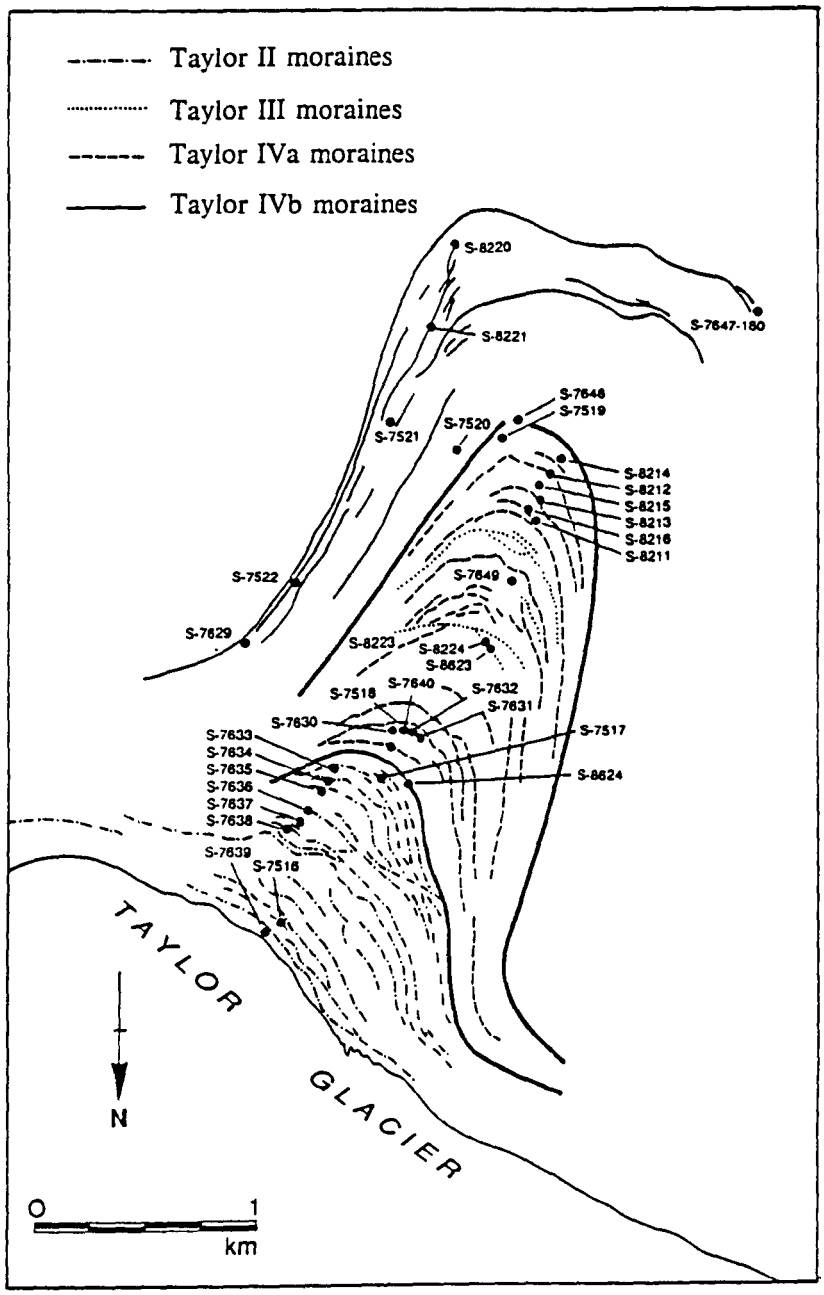

Figure 4. Taylor moraines in lower Arena Valley. S-82-20 and other numbers refer to soil pit localities. Bold lines on map mark upvalley limit of Taylor II and Taylor IVa moraines. Taylor III moraines are superimposed on Taylor IVa drift and moraines.

Figure 5. Outer limit of Taylor II moraines in lower Arena Valley. Note figure (circled in black) for scale.

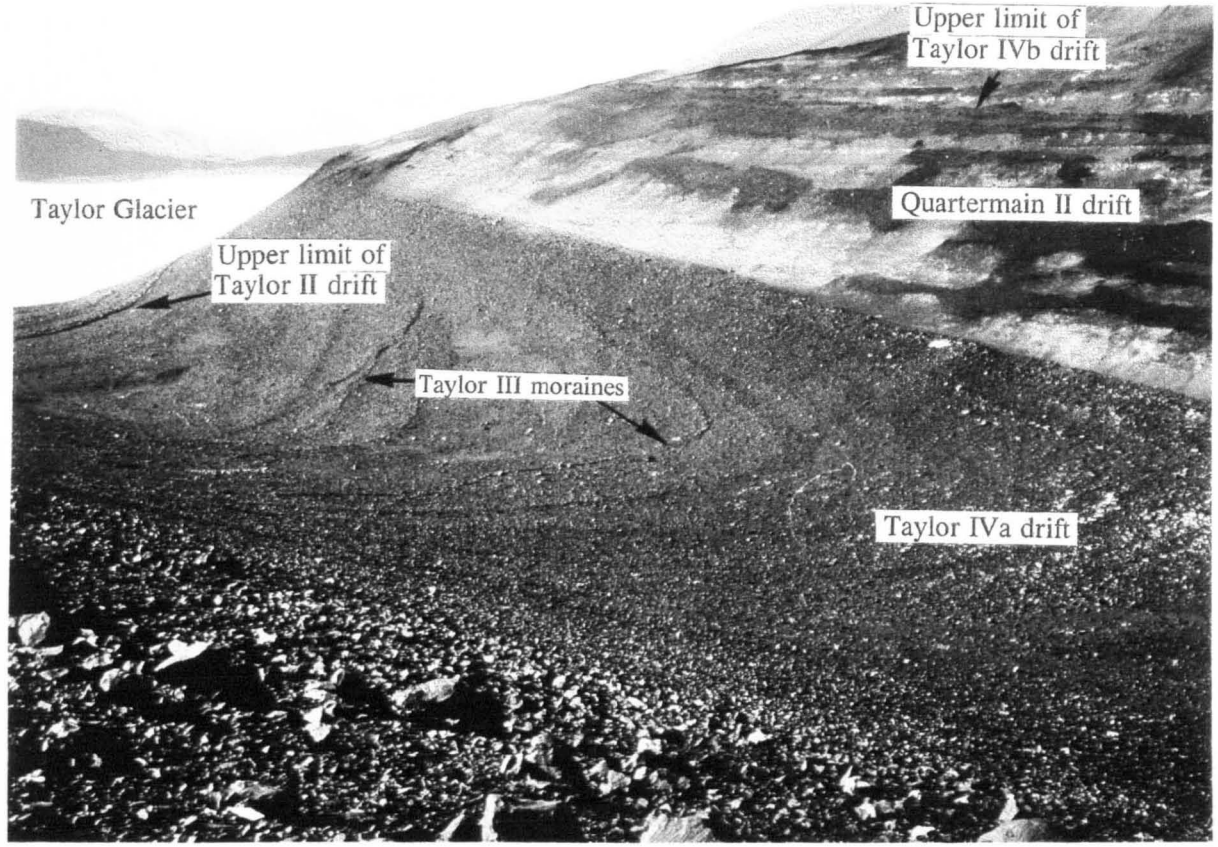

Figure 6. Oblique aerial photograph of the lower Arena Valley, showing distribution of Taylor II, III, IVa, and IVb drifts as well as Quartermain II drift. Arrows define the upper limit of Taylor II and IVb drifts, and point out two of the three moraines that crop out on the floor of lower Arena Valley and comprise Taylor III drift. Most of the moraines shown on the valley floor are composed of Taylor IVa drift.

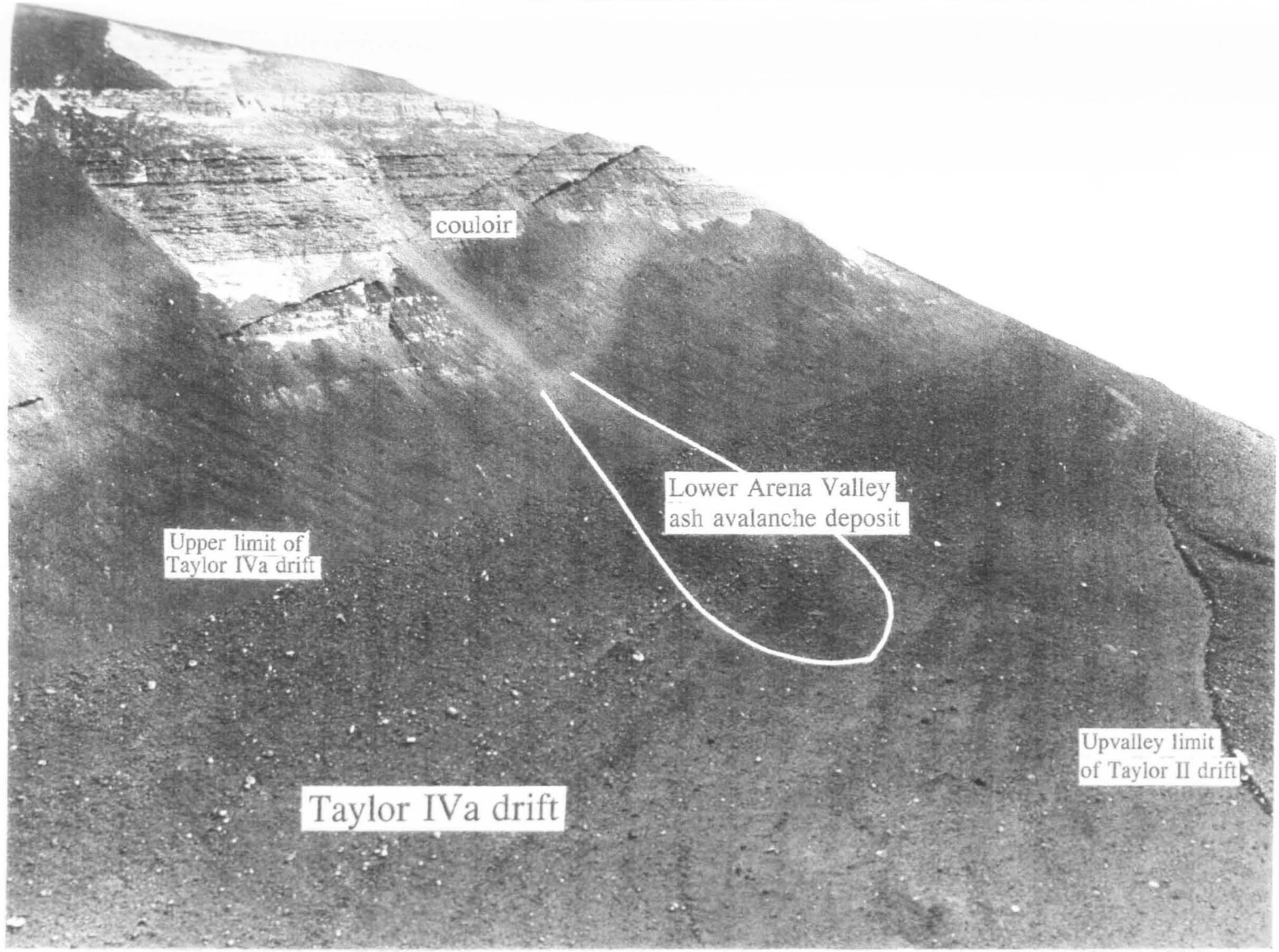

Figure 7. Oblique aerial view of the lower Arena Valley showing an avalanche deposit overlain by Taylor IVa drift. The geomorphic form of the avalanche deposit is preserved beneath Taylor IVa drift.

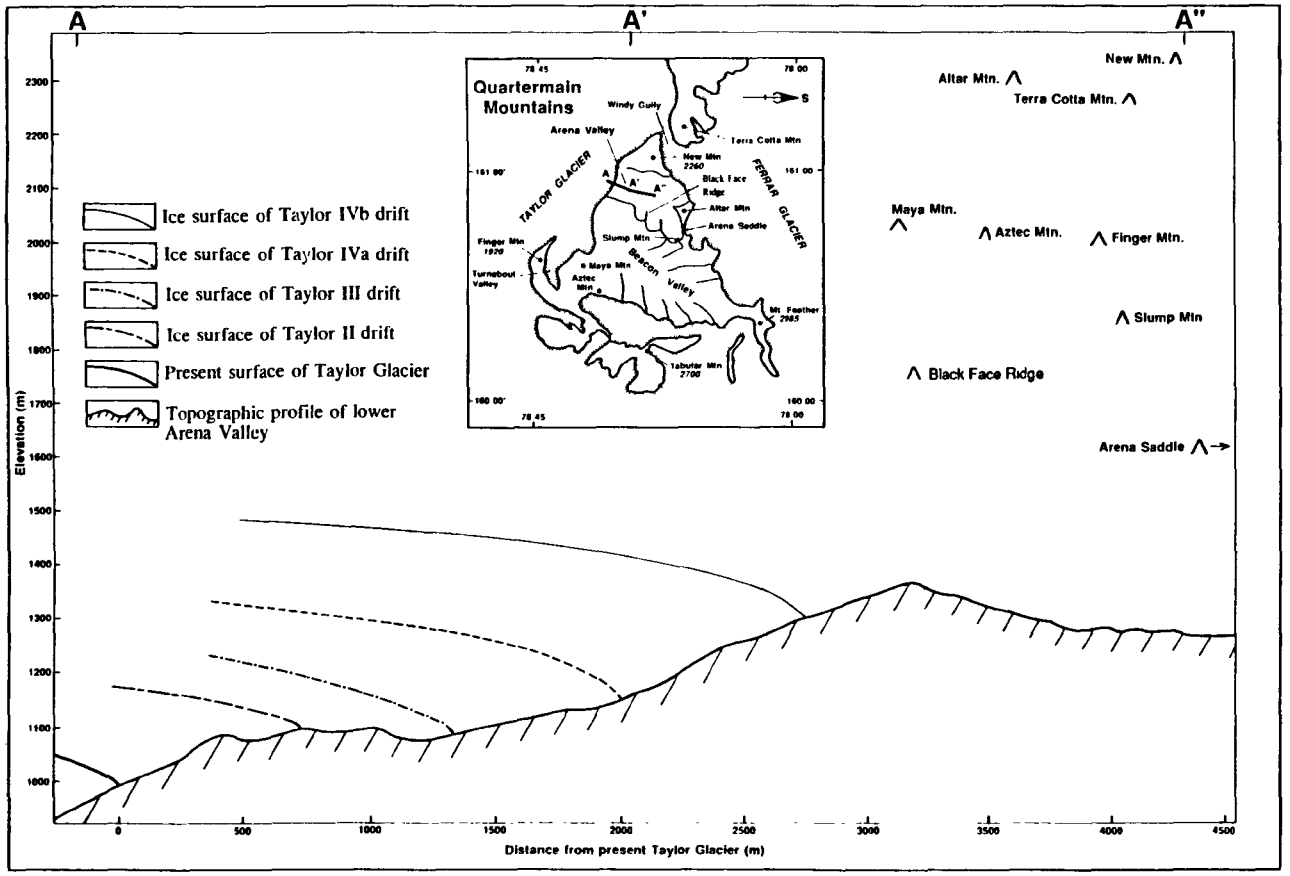

Figure 8. Longitudinal profile of the lower Arena Valley and former ice-surface elevations of the Taylor Glacier. Inset shows location of cross-section.

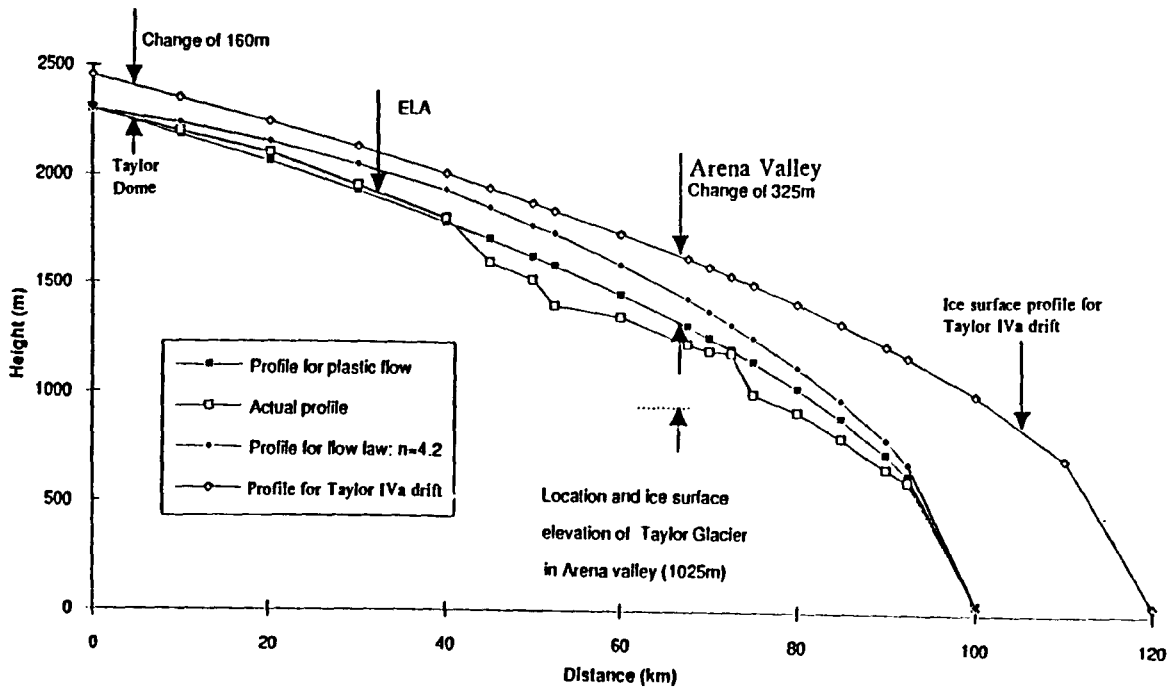

Figure 9. Present and former ice-surface profiles for Taylor Glacier. Glaciological models that assume plastic flow closely approximate the present ice-surface profile of Taylor Glacier and show that a 325 m ice-surface elevation rise of Taylor Glacier at the mouth of Arena Valley yields a corresponding ice-surface rise at Taylor Dome of only about 160 m.

Table 1. Chemical and physical properties of soils on drifts sheets in the lower Arena Valley.

HORIZON[1]	DEPTH (cm)	pH[2]	EC[2] dS/m	WATER-SOLUBLE IONS (mmol/L)[2]							%Fe*	%[3]		
				Na	Ca	Mg	K	SO_4	Cl	NO_3		sand	silt	clay
TAYLOR II DRIFT 76-33														
Bw	0-14	6.2	2.4	4.6	25.6	6.0	0.36	33.7	3.2	0	-	92	5	3
Cu	14-77	6.3	1.0	3.1	6.6	2.1	0.18	7.6	2.3	3.1	-	96	1	3
TAYLOR III DRIFT 82-24														
Bw	0-10	6.9	4.4	33.8	10.3	8.5	0.32	14.3	6.3	31.5	0.34	82	8	10
Cox	10-20	7.2	4.0	25.4	12.5	9.7	0.38	14.3	8.2	32.7	0.28	84	9	7
Cu	20-100	7.0	2.0	5.6	10.2	3.1	0.30	4.3	7.3	10.9	0.23	86	8	6
TAYLOR IVa DRIFT 82-16														
Bw	0-5	6.2	4.0	23.8	18.6	15.4	0.66	44.3	68.4	15.4	0.29	90	3	7
Bsam	5-21	6.2	31.3	417	8.9	115	1.8	144	6.5	414	0.18	89	3	8
BC	21-39	6.6	2.2	11.7	4.0	8.6	0.35	11.2	7.6	8.8	0.27	86	4	10
Cu	39-87	6.3	1.8	8.4	6.6	4.8	0.36	40.5	4.0	5.5	0.24	88	5	7
2Db	87-90	6.2	2.8	7.7	31.0	4.1	0.52	34.3	1.8	4.3	0.21	90	6	4
2Bwb	90-100	6.3	2.0	7.9	14.8	5.5	0.25	20.9	2.5	5.2	0.22	87	6	7

[1] Soil horizon nomenclature follows Birkeland (1984). [2] Methods follow American Public Health Assn. *et al.* (1975). [3] Sand (2.0-0.05 mm), silt (50-2 microns), clay (< 2 microns). * Dithionite-extractable iron from Mehra & Jackson (1960).

Table 2. Exposure-age chronology of the lower Arena Valley drifts

EXPOSURE AGES[1]				MAX DRIFT ELEVATION (m)	
Drift name	Mean ages[2]	Method	N[3]	Above Taylor Glacier[4]	Absolute Elevation
Taylor II	113 ± 45	^{3}He	6	200	1200
	117 ± 51	^{10}Be	5		
Taylor III	208 ± 67	^{3}He	7	250	1250
Taylor IVa	335 ± 18	^{3}He	6	325	1325
	1.0 +0.4 -0.5 Ma	^{10}Be	1		
	1.1 Ma[5]	^{10}Be	1		
Taylor IVb	1.1 ± 0.1 Ma	^{3}He	6	475	1475
	2.1 ± 0.1 Ma	^{10}Be	4		
	2.2 ± 0.1 Ma[6]	^{21}Ne	1		
Quartermain II till	3-5 Ma[7]	^{10}Be		>475	>1474

[1]Data from Brook *et al.* (1993) unless otherwise noted. [2]Mean ages are in 10^3 yr unless otherwise noted. [3]N = number of samples analyzed. [4]Elevations above present Taylor Glacier ice surface adjacent to Arena Valley. [5]This sample has an upper-age limit of about 1.59 Ma and a lower-age limit of 0.823 Ma (Brown et al., 1991). [6]Data from Staudacher & Allegre (1991). [7]Data from Brown *et al.* (1991) suggests a ^{10}Be age of around 4.4 Ma. Actual age of Quartermain II till may be significantly older than 3-5 Ma (Brook *et al.* 1993). Absolute drift elevations differ slightly from elevations given in Brook *et al.* (1993); the above elevation data are based on a new topographic map (unpublished) of Arena Valley at a scale of 1:10,000.

Table 3. Morphological properties on drift sheets in the lower Arena Valley.

	DEPTH (CM)								
PROFILE	COH	STN	SALTS	GHOSTS	ICE CEMENT	SALT STAGE[1]	W[2]	CDE[3]	MAX TEX
					TAYLOR II DRIFT				
75-16	19	33	0	10	>71	0	1	40	s
75-17	10	0	0	15	28	0	1	30	s
76-33	14	14	0	0	>80	1	1	24	vks
76-34	5	5	8	5	>50	1	1	16	sts
76-35	6	6	0	16	>60	1	1	24	gls
76-36	16	16	0	0	>51	1	1	24	ls
76-37	5	5	0	0	>55	1	1	24	gs
76-38	8	8	0	14	>62	1	1	24	gs
76-39	21	21	0	0	21	0	1	24	gs
86-25	7	7	0	0	>100	0	1	16	vgs
AVG.	**12**	**12**	**1**	**6**	**-**	**0.6**	**1.0**	**25**	
					TAYLOR III DRIFT				
82-24	10	20	10	13	>100	2	3	18	s
86-23	14	14	6	0	>100	2	2	9	vgs
AVG.	**12**	**17**	**8**	**7**	**>100**	**2.0**	**2.5**	**14**	
					TAYLOR IVa DRIFT				
82-11	25	25	25	11	>100	5.5	5	18	stscl
82-12	29	29	18	29	>90	5	5	24	sts
82-13	19	19	19	19	>77	5	5	24	ls
82-14	37	45	37	58	>120	5	5	24	s
82-15	40	>100	20	41	>100	5	5	24	s
82-16	39	>100	21	22	>100	5	5	24	s
AVG.	**32**	**>30**	**23**	**30**	**>98**	**5.0**	**5.0**	**23**	

COH = coherence. STN = staining. SALTS = visible salts. GHOSTS = sandstone pseudomorphs. [1]Morphologic salt stage from Bockheim (1990). [2]Weathering stage from Campbell & Claridge (1975). [3]Color-development equivalence (Bockheim 1990).

Table 4. Surface boulder weathering features on drift sheets in the lower Arena Valley.

SITE NO.	BOULDER FREQUENCY[1]	DOLERITE: SANDSTONE[2]	% VARNISHED	% FACETED[3]	% SPALLED	% PITTED
			TAYLOR II DRIFT			
75-16	560	46	80	0	-	-
75-17	856	106	94	1	-	-
AVG.	**708**	**76**	**87**	**1**	**-**	**-**
			TAYLOR III DRIFT			
82-24	1105	173	100	83	39	2
			TAYLOR IVa DRIFT			
82-11	570	>218	100	75	26	12
82-12	771	221	100	63	53	19
82-13	897	>200	100	82	38	16
82-14	615	>235	100	95	43	9
82-15	764	>219	100	74	48	11
82-16	906	202	100	70	37	11
AVG.	**754**	**>218**	**100**	**76**	**41**	**13**
			TAYLOR IVb DRIFT			
75-20	260	64	98	73	-	-
75-21	380	>95	97	67	-	-
75-22	285	13	93	66	-	-
82-20	1083	27	100	76	57	10
82-21	710	8	100	87	46	11
AVG.	**544**	**41**	**98**	**74**	**52**	**10**

[1]Boulder frequency equals the total number of surface clasts greater than 35 cm (as measured along the a-axis) along a transect 100 m long and 3 m wide. [2]Number of dolerite clasts to sandstone clasts. For example, if a total of 700 dolerite and sandstone boulders were counted and all were dolerite, then the ratio would be >700. [3]Percentage of surface clasts showing ventifacted facets.

CHAPTER SEVEN: Conclusions

The preceding chapters give evidence for middle-Miocene-to-Pleistocene paleoclimate change, East Antarctic Ice Sheet dynamics, and landscape evolution of the western Dry Valleys region. This evidence bears critically on the divergent hypotheses of Pliocene ice-sheet deglaciation and Pliocene ice-sheet stability. The fundamental test for the deglaciation hypothesis as outlined in Chapter 1 is to determine if reworked Pliocene marine diatoms in high-elevation Sirius Group outcrops in the western Dry Valleys region could have been emplaced by a greatly expanded East Antarctic Ice Sheet. Likewise, the basic test for the stability hypothesis is to determine if Pliocene climate in the Dry Valleys region remained polar, with mean annual temperatures well below 0°C, or whether atmospheric temperatures rose by as much as 20°C above present values, forcing ice-sheet meltdown. The first and second conclusions of this thesis apply to these fundamental tests. They strongly imply that the East Antarctic Ice Sheet remained polar and robust through the Pliocene. The third and fourth conclusions concern middle-Miocene-to-Pleistocene landscape evolution, paleoclimate change, and glacial history of the Dry Valleys region. They show that most of the bedrock landforms in the western Dry Valleys region are relict and that little slope evolution/ colluviation has occurred under the present hyper-arid cold-desert climate, which began at least 13.6 Ma ago. Overall, conclusions 1-4 indicate that the morphology of bedrock landforms and the configuration of the East Antarctic Ice Sheet in this sector of the Transantarctic Mountains changed very little during the last 13.6 Ma, and thus the geologic data from the western Dry Valleys strongly favours the Pliocene stability hypothesis.

1. Geologic evidence from the Quartermain Mountains and the western Asgard Range (both located in the western Dry Valleys region) shows only minor Pliocene expansion of East Antarctic ice. The maximum thickening of Taylor Glacier in lower Arena Valley (Quartermain Mountains) during late Pliocene time was only about 500 m, which corresponds to an ice-surface rise at Taylor Dome (on the periphery of the East Antarctic Ice Sheet) of less than 250 m. Likewise, expansion of rock glaciers and glacierets at valley heads in the western Asgard Range was only about 2.5 km in the last 12.5 Ma. On the basis of such evidence for minimal Pliocene expansion of East Antarctic ice, I conclude that Sirius Group deposits in the western Dry Valleys region, particularly the deposit at Mt. Feather high in the Quartermain Mountains, could not have been emplaced by the East Antarctic Ice Sheet during Pliocene time. Accordingly, these data from the western Dry Valleys region do not support a major element of the Pliocene deglaciation hypotheses, namely that overriding East Antarctic ice was the agent that emplaced the reworked marine diatoms in Sirius Group outcrops.

2. Paleoclimate interpretations based on the preservation and stratigraphic position of in-situ to near in-situ ashfall deposits favour persistent cold-desert and hyper-arid environmental conditions in the western Dry Valleys region

since at least 15.0 Ma ago. The maximum allowable mean annual atmospheric temperatures in the western Dry Valleys region during the last 13.6 Ma, and most likely during the last 15.0 Ma, were between 3° and 5°C above present values. The implication is that Pliocene ice-sheet deglaciation from surface-melting ablation zones could not have occurred. Rather, the persistent polar environments favor the existence of a robust polar East Antarctic Ice Sheet throughout Pliocene time.

3. The overall morphology of the western Dry Valleys region, including the steep escarpment at the plateau edge, is here attributed to erosion under semi-arid climate conditions prior to the imposition of a cold-desert, hyper-arid environment before 15.0 Ma ago. In this regard, box canyons with theater-shaped heads, gently sloping pediments, buttes, mesas, and spires (all associated with rectilinear slopes) are explained by progressive backwearing and parallel retreat of weathering-limited slopes and scarps. Such landscape development probably began with a renewed phase of intracontinental rifting in the Ross Sea basin about 55 Ma ago (Fitzgerald, 1992). Wet-based alpine glaciers may have occupied the western Dry Valleys periodically before the onset of the present cold-desert, hyper-arid climate prior to 13.6 Ma ago. Wet-based alpine glaciers last occupied the western Asgard Range and the Quartermain Mountains well before 15.0 Ma ago, when the Sessrumnir and Altar tills were deposited. The absence of wet-based glaciers during the last 15.0 Ma in this sector of the Dry Valleys region strongly suggests that the 0°C isotherm never advanced up onto the adjacent East Antarctic Ice Sheet during Pliocene time, and is therefore inconsistent with Pliocene meltdown of the East Antarctic Ice Sheet from extensive surface melting. Rather, the lack of Pliocene wet-based alpine glaciers favours a persistent and robust polar East Antarctic Ice Sheet through the Pliocene.

4. The last major ice-sheet expansion into the western Dry Valleys region is middle Miocene in age. A suite of unconsolidated sediments and glacial erosional forms both in the western Asgard Range and in Arena Valley indicate that mountain ranges of the Dry Valleys region were inundated by a northeast-flowing ice sheet between 13.6 and 15.2 Ma ago. Subsequent glacier expansions were of limited extent. Maximum Pliocene thickening of Taylor Dome, 35 km inland of the Dry Valleys region on the East Antarctic Ice Sheet, was at most 250 m. Similarly, maximum Quaternary thickening of Taylor Dome was probably less than 160 m. These data for limited glacier expansion are inconsistent with deposition of high-elevation Sirius Group outcrops in the western Dry Valleys region from a greatly expanded East Antarctic Ice Sheet. Rather, these data indicate that the overall Pliocene configuration of the East Antarctic Ice Sheet in this sector of the Transantarctic Mountains was very similar to the present ice-sheet configuration and hence strongly favours the Pliocene stability hypothesis.

Wider implications

Sirius Group. The two basic assumptions regarding the current inferred Pliocene date of the Sirius Group revolve around the biostratigraphic ages of its enclosed diatoms and the exact mechansim of diatom emplacement. It now

seems clear that certain critical diatom species in the Sirius Group are indeed Pliocene in age (Barrett et al., 1992), and therefore on the basis of biostratigraphy alone it appears that the Sirius group has a maximum age of 3.0 Ma (Barrett et al., 1992). However it is unclear how the diatoms became incorporated into Sirius Group deposits. It has been postulated that the diatoms were stripped from marine basins in interior East Antarctica and transported to high-elevations in the Tranantarctic Mountains by glacial ice (Webb et al., 1984). If this scenario is correct, then the Sirius Group must be younger than its enclosed diatoms of Pliocene age. However, there are alternative explanations for diatom emplacement. For example, the diatoms could have blown onto the surface of Sirius Group outcrops and filtered down into the deposit any time *after* Sirius Group deposition. If this scenario is correct, one would expect to find a decrease in the concentration of diatoms with increasing depth in Sirius Group outcrops. Such a gradation in diatom concentration is found in some Sirius Group outcrops (Arjien Stroeven, University of Maine, personal communication).

There are no deposits in Arena Valley or in the valleys of the western Asgard Range that correlate with the Sirius Group. The only deposits that could be potential correlatives are the Sessrumnir, Inland Forts, Asgard, Nibelungen, Jotunheim, Altar, and Arena tills (based on textural characteristics and areal distributions), but each of these tills antedates 11.3 Ma. The degree of consolidation of the Sirius Group (here taken to indicate postdepositional alteration) is an order of magnitude greater than any of the deposits in the western Asgard Range valleys or in Arena Valley. Hence, I argue that on the basis of soil consolidation that the Sirius Group is significantly older than all unconsolidated deposits in the western Asgard Range valleys/ Arena Valley and therefore it probably antedates 11.3 Ma.

The association of in-situ fossil Nothofagus with Sirius Group deposits in the Beardmore Glacier region requires atmospheric temperatures of at least 20°C above present values during Sirius Group deposition. However, the Antarctic continent has been thermally isolated by the Cirumantarctic Current since at least 23 Ma ago, when Antarctica finally separated from adjacent continents. Prior to the formation of the Circumantarctic Current, warm marine waters could penetrate far south and provide the warmth necessary for Nothofagus growth in coastal Antarctica. Because we know of no physical process that could warm the Anatarctic continent by 20°C under the present ocean and atmosphere system (that would not *dramatically* alter climate in other parts of the world), and because we have direct physcal evidence of cold polar desert conditions (with mean anual temperatures well-below the minimum requirement for Nothofagus) in the Dry Valleys region since middle Miocene time, we agure that the most recent time Nothogus could have colonized coastal Antarctica occurred prior to 15.0 Ma ago, and almost certainly occurred before Antarctica separated from South America and Australia and the development of the Circumantarctic Current by 23 Ma ago. Hence, we postulate that the Sirius Group is most likely Oligocene in age and that its enclosed diatoms were most likely blown in by the wind.

Tectonics and mountain uplift. The glacial geologic and geomorphic record from the western Dry Valleys region shows that following an early phase of continent rifting (about 55 Ma ago) there was a period of rapid denudation with planation and scarp retreat followed by ice-sheet overriding during middle Miocene time. Surface uplift was greatest during the early Cenozoic with only modest uplift since Miocene time. The evidence for minor post-Miocene surface uplift is afforded by the isotopic date of in-situ and subaerial volcanics that rest within well-developed drainage systems that now open to the sea. For example, in-situ ashfall deposits that rest on desert pavements (or occur in avalanche deposits and sand-wedges) between 1000 and 1400 m elevation in the western Dry Valleys region indicate a maximum potential surface upflift of about 1400 m during the last 15.0 Ma. This figure is sharp contrast with earlier estimates of up to 3000 m of surface uplift of the Transantarctic Mountains since late Pliocene time. Estimates of 3000 m of surface uplift are largely based on the anomalously high-elevations (up to 3000 m) of in-situ Nothofagus and Sirius Group deposits of inferred Pliocene age. However, we show above that Nothofagus and the Sirius Group are probabably Oligocene in age and therefore their presence at high-elevations in the Transantarctic Mountains does not necessarally indicate significant Pliocene mountain uplift.

The occurrence of coarse-grained, middle Miocene tephras in the western Dry Valleys region impies active volcanism near the Dry Valleys region nearly 45 Ma after rifting began in this sector of Antarctica. It is quite possible that this volcanism hearalds past tectonic activity in the Dry Valleys region. The implication is that some surface uplift/ subsidence occurred during middle Miocene time. This implication has important consequences for the cause of middle Miocene ice-sheet overriding of the western Dry Valleys region. Clearly, it opens up the possibility that tectonic subsidence/ uplift of the mountains resulted in ice-sheet overriding/ retreat. In any case, our understanding of ice-sheet dynamics in the western Dry Valleys region may itself turn out to provide important clues on the timing and cause of surface uplift of the Transantarctic Mountains.